Your Maritime Solution Partner SSPA

Report.

No: RE40178202-02-00-A
Dynamic design of Ships



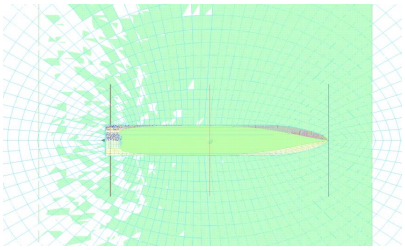

SSPA Sweden AB
Head Office: P.O. Box 24001, SE-400 22 Göteborg, Sweden • Phone: +46 31 772 90 00 • Fax: +46 31 772 91 24
Visiting Address: Chalmers Tvärgata 10, SE-412 58 Göteborg, Sweden
Branch Office: Fiskargatan 8, SE-116 20 Stockholm, Sweden • Phone: +46 31 772 90 00 • Fax: +46 8 31 15 43
Web: www.sspa.se • **E-mail**: postmaster@sspa.se • **Vat No**: SE556224191801

Your Maritime Solution Partner SSPA

Trafikverket
781 89 Borlänge

Reference:
TRV 2017/41844 Ärende-ID 6459

REPORT
Date
2019-10-11
SSPA Report No:
RE40178202-02-00-A
Project Manager:
Jonny Nisbet
Author
Jonny Nisbet
+46 (730) 729052
jonny.nisbet@sspa.se

Dynamic designs of Ships

This report presents the results of the joint research and development project of methods for dynamic designs of ship to increase the knowledge about how dynamic loads on ships affects the structural response.

The project is a cooperation between Chalmers University of Technology (CTH), The Royal Institute of Technology (KTH), SSPA Sweden AB and Stena Teknik AB.

SSPA Sweden AB

Joacim Linder
Vice President
Maritime Consultants

SSPA Sweden AB

Jonny Nisbet
Project Manager
Maritime Consultants

Revision History

Rev.	Publish Date	Description of changes	Signature
A_draft1	2019-07-11	Preliminary	JNI
A	2019-10-11	Final	JNI

Summary and recommendations

The project has been a joint research and development of methods for dynamic designs of ship to increase the knowledge about how dynamic loads on ships affects the structural response.

The project is a cooperation between Chalmers University of Technology (CTH), The Royal Institute of Technology (KTH), SSPA Sweden AB and Stena Teknik AB.

The project was parted into three work packages:

WP	Content	WP-owner
1	**Model manufacturing and model tests:** • Development of model concept, model testing techniques, practices, evaluation techniques and supporting analytical methods. • Detailed design and construction of ship model • Seakeeping model tests and evaluation	**SSPA Sweden**
2	**Feasibility study of measurements of local slamming loads by pressure sensors**	**KTH**
3	**Numerical analysis of hydrodynamics and structure** • Numerical model calibration • Eigen-frequency analysis • Seakeeping simulations	**CTH**

Stena Teknik AB have been supporting the project with drawings and structural properties of the concept ship Stena Electra, as well as contributed with their experience as a shipowner.

A segmented lightweight ship model made of carbon fibre, divinycell and aluminium was designed and built. Dynamics structural loads, forces and moments, as well as deflections of the ship could be measured, making it possible to assess the impact of waves on the ship structure.

The structural properties of the model, such as stiffness, mass distribution and structural damping met the targets of the full-scale ship.

Model test have been performed in order to evaluate the model concept and to compare with corresponding numerical simulations.

Numerical analysis of hydrodynamics and structure have been performed and compared with the model tests. A quasi-static hydrodynamic numerical approach was utilized.

Results of this test series give that

- the model concept works as intended, capturing all the most important physics, including springing and whipping

- Very accurate measurement of forces and moments were obtained, while measurement of deflections may be improved. However, forces and moments are the most important measured entities.
- Results of the numerical simulations show that, even for a slender ship, this quasi-static approach is not accurate enough.
- A combination of model tests and numerical analysis with today's tools seem to be feasible.

For further method development, it is proposed to put forward a method to obtain a minimum test matrix to faithfully represent a ships life, in terms of structural dynamics and fatigue. It is also proposed to put forward numerical tools that can be used to simulate the coupled structural and hydrodynamics of a ship navigating in waves.

Investigation of a novel method, in the current context, for pressure measurement and estimation of pressure distribution over large portions of a ship hull have been performed.

The feasibility study showed that the experimental technique, previously been successfully on high-speed craft, could not be applied on the here studied displacing ship. It has been clarified that application of this modelling technique on this ship would involve significant uncertainties which cannot be sorted out within the limited frames of this project.

Still, this work package has contributed with further valuable understanding regarding the challenges involved in local slamming pressure measurements. The work package report describes the experimental technique that was planned to be used, background to and motifs for not going all the way with this sub-project, and recommendations for further research.

Table of Contents

List of Appendicies

Appendices

Appendix A	SSPA Report RE40168082-00-00-A: “Models for structural dynamics measurements”
Appendix B	SSPA Report RE40178202-01-00-A: “Model manufacturing and model tests”
Appendix C	KTH Report:”Experimentell utvärdering av lokala slammingtryck”
Appendix D	CTH Report, Master Thesis of Javier Pelayo Llop Sayson: “Numerical simulation sssessment of a ship dynamic behavior against SSPA model

Introduction

This report presents the results of a joint research and development of methods for dynamic designs of ship. The project is a cooperation between Chalmers University of Technology (CTH), The Royal Institute of Technology (KTH), SSPA Sweden AB and Stena Teknik AB.

The goal of the project was the following:

- Develop a combined method and model testing setup and perform model tests in order to evaluate the response of the hull beam for a ship hull in waves
- Evaluation of numerical methods for simulation of structural response
- Validate model tests and numerical simulations

The project was parted into three work packages:

WP	Content	WP-owner
1	**Model manufacturing and model tests:** • Development of model concept, model testing techniques, practices, evaluation techniques and supporting analytical methods. • Detailed design and construction of ship model • Seakeeping model tests and evaluation	**SSPA Sweden**
2	**Feasibility study of measurements of local slamming loads by pressure sensors**	**KTH**
3	**Numerical analysis of hydrodynamics and structure** • Numerical model calibration • Eigen-frequency analysis • Seakeeping simulations	**CTH**

Stena Teknik AB have been supporting the project with drawings and structural properties of the concept ship Stena Electra, as well as contributed with their experience as a shipowner.

Parts of the work done in WP1 was funded by SSPAs funds, whereas the main part of WP1, and WP2 and WP3 was funded by Trafikverket.

Figure 0-1 shows an outline of the workflow in the project.

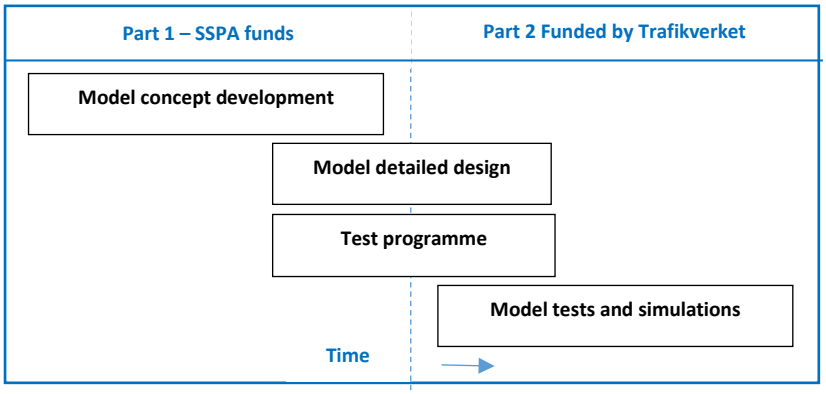

Figure 0-1 Schematic description of project set up and work flow

A short description of each work package is provided in this report.

More details for each work package will be found in each work package report, respectively, which are appended to this report.

1 Background

In order to develop ships for more efficient transport at sea, with reduced specific fuel consumption and emissions, the tendency is to design larger ships (IMO 2015). There is a big potential to develop ships for more efficient transport at sea by optimize the construction to reduce weight and steel to lower the cost for building and operate the ship. In this process it is of first importance to ensure that any changes in the construction is done in a secure way. The effect of less steel and changed construction on the ships damage tolerance against wind and wave loads, and the dynamic response of those external forces, has to be evaluated.

According to a study from IMO (IMO2009) the potential is a 2-20% reduction in greenhouse gases for an optimized hull construction and reduced weight.

To ensure that legislations are fulfilled with respect to structural strength, seakeeping characteristics, environmental requirements and safety at sea more knowledge is required to understand how requirements and solutions affect the complex construction of the ship. Today there is a lack of guidelines and regulations which accounts for the dynamic loads on the ship when it is operating in wind and waves. Studies reports that ships of different types have increased problem due to wave loads leading to resonance (springing) or fading vibrations(whipping) in the hull beam. This has led to that ships have cracked and constructions have broken due to a combination of fatigue and exceedance of global longitudinal strength. A lack of basic understanding may lead to the opposite effect, i.e. the ships are designed to be oversized leading to higher weight and larger displacement, leading to unnecessarily high fuel consumption and increased environmental impact.

The project aimed to conduct joint research and development of refined methods for dynamic design of ships, to increase the knowledge about how dynamic loads on ships affects the structural response.

The project is a cooperation between Chalmers University of Technology (CTH), The Royal Institute of Technology (KTH), SSPA Sweden AB and Stena Teknik AB.

2 WP 1- Model manufacturing and model tests

2.1 Model concept

Several requirements for the model concept have been identified:

Must have:

- Facilitate exact measurements of forces and moments for the most important degree of freedom
- Provide a faithful representation of the lowest global eigen modes in the most important degree of freedom.
- Measurement of motions with good accuracy in the most important degree of freedom
- Exact measurements of forces and moments in all six degrees of freedom.
- Economically feasible.

Good to have:

- Measurement of motions at the other degrees of freedom
- Provide a faithful representation of lowest eigenmodes at other degrees of freedom

A literature study was performed to assess different concepts to design a model for structural dynamic measurements in waves. The literature study is reported in the SSPA report RE40168082-00-00-A5 [Appendix A].

After evaluation of pros and cons for different concepts a so called spring model concept were chosen. The spring model concept consist of a number of rigid segments, put together, with hinged joints combined with adjustable springs to obtained the desired static stiffness and eigenfrequencies

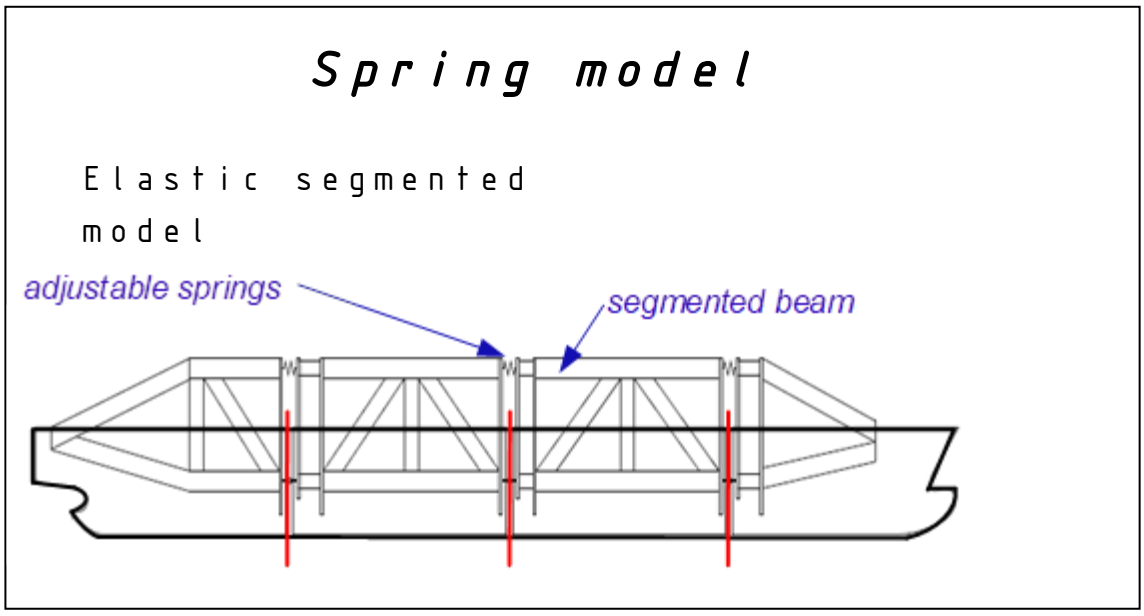

Figure 2-1 Illustration of spring model concept design

The main advantage with the spring model concept is that is somewhat easier to build and calibrate than the other two types. Yet it is a complicated matter to obtain a good design and construction. This model type also has reportedly given relatively exact and well-defined measurements.

2.2 Choice of ship type

Already today several types of container vessels need attention regarding structural dynamics and hydroelasticity.

For future ships, it can be anticipated that there is a desire to decrease deadweight by use of state-of-the-art structural design and modelling tools in combination with high strength and lightweight materials.

Stena Teknik AB, as a project partner, have been expressing a strong belief in lighter and more efficient ship structures in the years to come. They have also expressed a strong wish to investigate how a light structure could be incorporated in their future fleet. Their most recent testbed for innovations and increased efficiency within marine transport, Stena Electra, was hence chosen for the current project.

Figure 2-2. Rendered image of projected design for Stena Elektra.

Normally, a Ro-Ro/Ro-Pax ferry would not suffer significantly from fatigue due to structural dynamics. However, with Stena Teknik's design targets for the future, e.g. lighter ships and more flexible arrangements, life span of such ships will likely to a large extent be determined by hull structural dynamics.

2.3 Model design and construction

Figure 2-3 illustrate the outcome of the extensive design work to obtain a model corresponding to project objectives, carried out at SSPA. In summary requirements on the model were:

- Low structural damping, lower than or equal to 0.5%
- Scaled stiffness virtually identical to full scale ship
- Mass distribution equal to full scale ship
- Very accurate measurement of internal forces and moments in the hull structure
- Possibility to record structural motions with reasonable accuracy.

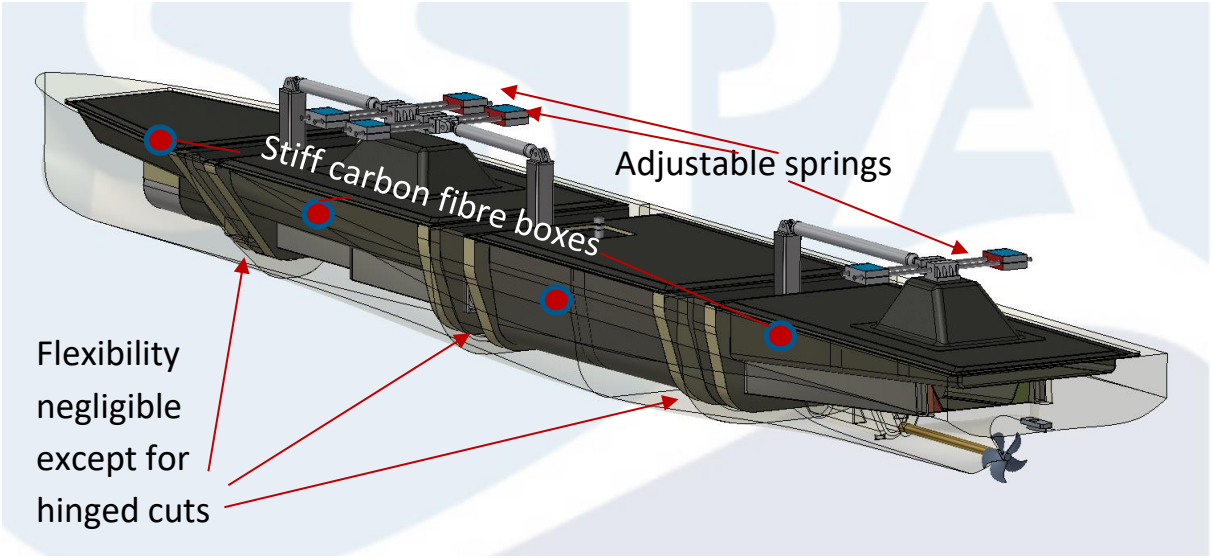

Figure 2-3 Model design and main features

It was considered to model structural dynamics in transverse bending. However, it was judged that the effect of structural dynamics due to lateral bending may be notable but that the design and construction of the model would be significantly more difficult. Further, it was also judged that the accuracy of measurements would be adversely affected and that it would be very uncertain to utilize such a model. The model design, nevertheless contains a number of novelties needed to be tested and evaluated:

- Six degree of freedom force (and moment) measurement integrated into one transducer. One load transducer is mounted in the hinged vertical cuts (in total three load transducers)
- Carbon fibre hull shell construction to be able to obtain the correct longitudinal mass distribution for the chosen lightweight ship
- Utilising optical measurements measure vertical deflection of the hull girder.
- Low friction hinge

2.4 Seakeeping model tests

The seakeeping model tests was carried in the SSPA Maritime Dynamics Laboratory (L= 88 m, B= 39 m, d= 0 – 3.2 m). See http://www.sspa.se/tools-and-facilities/facilities/maritime-dynamics-laboratory.

The Maritime Dynamics Laboratory – MDL – is a versatile facility for the research and development of seakeeping and manoeuvring behavior of ships (and other structures in the sea). MDL can also be used for assessing manoeuvring properties in waves.

The computer controlled multimotion carriage, spanning the whole basin, offers unique possibilities of captive or free sailing manoeuvring tests. In captive manoeuvring tests the facility can be used both to do large-amplitude PMM-tests and rotating arm tests without any change in set-up between the tests.

For free sailing tests the width of the basin allows most manoeuvres to be performed with fairly large models, thus reducing the influence of scale effects. MDL is also a very useful tool when analyzing if a new or existing project fulfils the IMO regulations concerning turning ability as well as yaw checking.

Figure 2-4 *The SSPA Maritime Dynamics Laboratory, MDL*

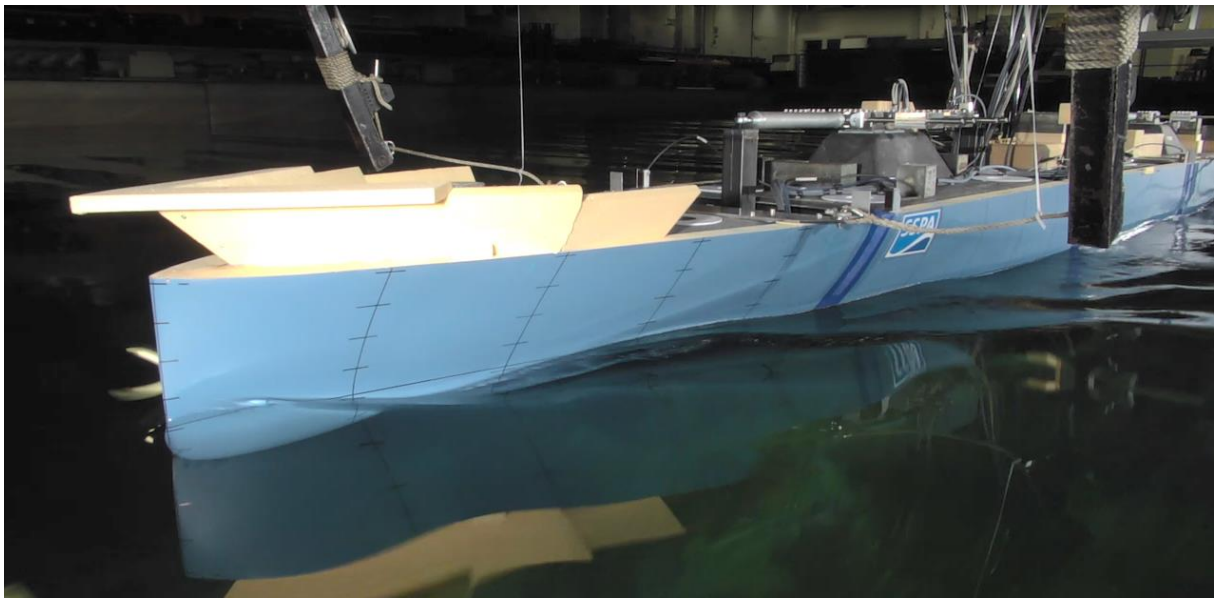

Figure 2-5 Ship model during testing in MDL

2.4.1 Instrumentation and test preparations

The model was first instrumented on the quay for measuring the following parameters:

- Motions, 6 DOF (surge,sway,heave,roll,pitch and yaw)
- Speed
- Position
- Forces and moments in the three vertical cuts between each part of the segmented model (Fx, Fy, Fz, Mx, My, Mz)
- Vertical deflection of the hull girder (for each part of the segmented model)
- Wave height

During the model tests time series are recorded for each quantity.

Static tests were performed in the towing tank trim tank to measure the static moment to check the load transducers. Measured bending moment was compared with theoretically calculated moment.

Resonance tests was then performed in order make a cross check, with static deflection test and measurement of mass distribution, that the stiffness and mass distribution is correct and to be able

to compare resonance frequency in water with resonance frequency on land. The dry resonance frequency and the resonance frequency in water was compared to theoretical relation for their relative values. This comparison is reported in WP3.

The model was ballasted to the relevant center of gravity and radii of gyration for the draught 6.3 m.

The model was then launched into the basin and mounted under the carriage in MDL.

Further, mounted under the carriage an inclining test was performed for verification of the metacentric height of the model.

During the seakeeping tests the model was free-sailing, self-propelled and autopilot controlled and thus free in 6DOF.

2.4.2 Tests program

Several criteria's have been considered when designing the test program:

- The chosen sea states should be representative for the area of operation for the vessel
- Headings and sea states should be chosen to provide large vertical moments and deflections, but still be within the limits of the load balance transducers, in order to provide a database. One of the goals in the project is to compare the measurements with structural numerical simulations
- Test speeds should be chosen so as the actual wave encounter frequencies is within the lower and upper limits of hull girder eigen frequency found in literature for springing experiments

Seakeeping model tests were performed for the following conditions:

Sea state	$H_{1/3}$ (m)	T_{p1} (s)	Tp_2 (s)	Wave direction* [deg]	Speed [kn]
4	1.88	7.6		180, 150	15,18,21
4	1.88		4.0	180	18
5	3.25	9.2		180,150	18,15
5	3.25	9.2		30,0	12
5	3.25		5.0	180	18
6	5.0	10.8		180,150	15, 12

*180 deg equals head sea

The JONSWAP spectrum was chosen to define the wave profile.

2.5 Results

Here are some results presented for illustration.

During the preparation of the model static moments tests were performed in the towing tank. Figure 2-6 show the measured still water bending moment compared to theoretically calculated still water moment together with calculated shear force.

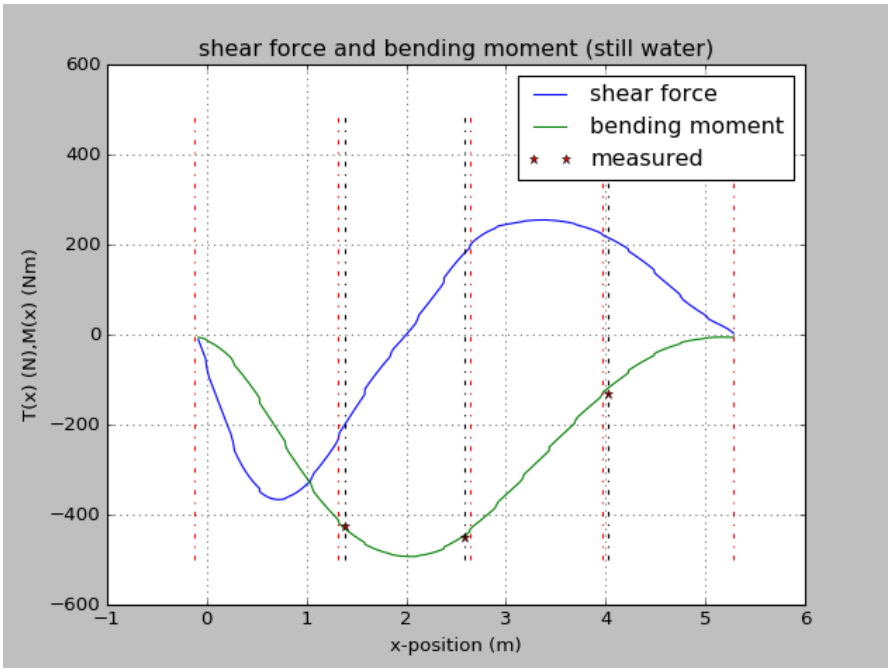

Figure 2-6 Calculated still water shear force and bending moment together with measured still water bending moment

In Figure 2-7, an example of whipping recorded during the current project is shown. Until time=510s, the ship model encounter waves of equal height, then one wave period with large magnitude occur, triggering whipping, which can be seen as the ripple with same frequency as the structural resonance frequency. This oscillations with this frequency decays but persist throughout the measurement due to low structural damping.

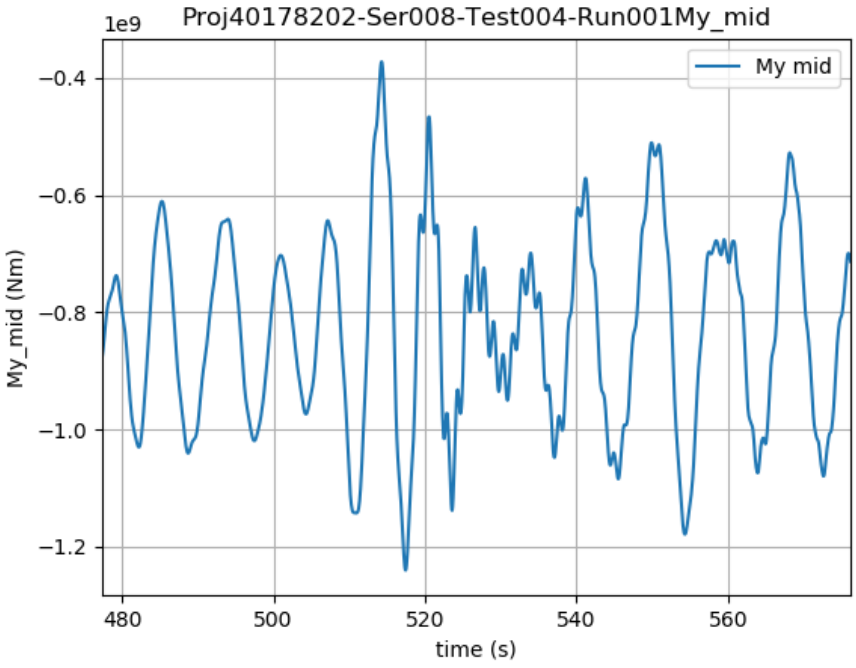

Figure 2-7 Time history of bending moment at test condition 1

Figure 2-8 display a possible use of data from model trials with structural dynamic ship models, where midship bending moment have been used for fatigue cycle counting by the rainflow method. Cycle count have been performed for unfiltered bending moment and for low pass filtered and high pass filtered bending moment. Such data may at a later stage be compared to midship fatigue resistance to calculate fatigue life and fatigue damage.

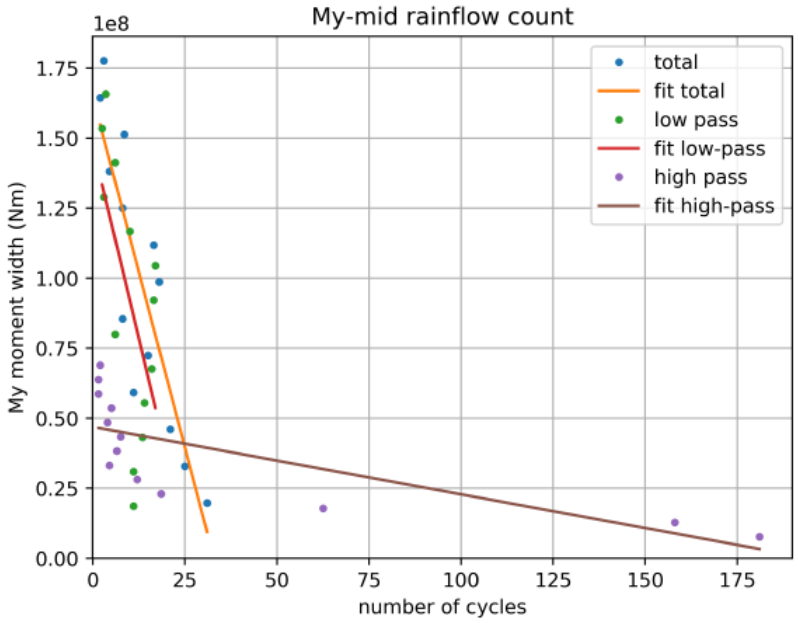

Figure 2-8 Fatigue cycle count of series 4 condition 1.

Figure 2-9 display power spectrum of midship transverse force, vertical force, vertical bending moment and transversal bending moment. For the vertical bending moment (lower, left figure) a main effect of the wave frequency moment and a super posed smaller effect of whipping at the structures' resonance frequency (0.87Hz) can be observed.

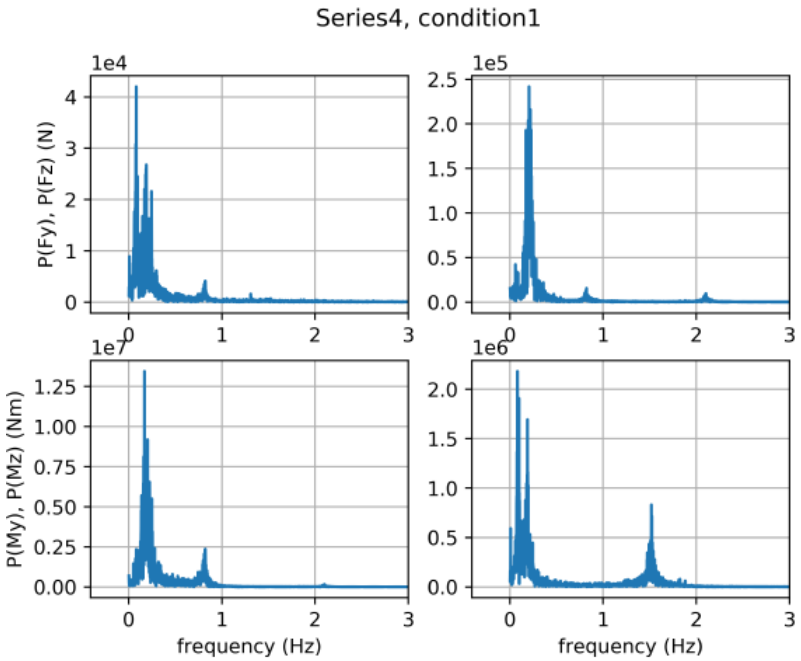

Figure 2-9 Power spectrum of midship transversal force, vertical force, vertical bending moment and transversal bending moment.

A comparison between the measured and simulated sectional forces is presented in WP3 report [Appendix D].

Statistical tables for the measured parameters are presented in the WP1 report [Appendix B].

3 WP 2 - Feasibility study of measurements of local slamming loads by pressure sensors

The feasibility study is reported in the KTH report [Appendix C].

The goal of WP2 project was to develop an experimental setup for measuring local slamming loads on parts of a ship model and from corresponding measurements reconstruct the slamming pressure distribution over a larger area of the bottom of the hull. Tis would enable comparison with global loads measured with the spring model setup developed by SSPA in WP1 and numerical simulations performed by Chalmers in WP3.

The plan for the local loads was to adapt and apply an experimental technique that has previously been applied successfully on high-speed craft. Through the here reported project it has however been clarified that application of this modelling technique on the here studied displacing ship would involve significant uncertainties which cannot be sorted out within the limited frames of this project.

Previous applications where the pressure measuring, and reconstruction technique has been on planing high-speed ships. In these applications the pressure transducers have been installed in parts of the v-shaped hull bottom which are submerged in the water while the ship is idling at zero speed, and at speed through waves the transducers are only occasionally out of the water. Hereby the pressure transducers have been continuously cooled to maintain temperatures close to the water temperatures. However, in the here presented project several pressure transducers would have to be mounted well above the water surface, as pictured in Figure 3-1 and even higher, to enable capturing of the bow flare slamming at the most dramatic wave encounters where the largest global slamming loads were expected to occur.

This rose questions regarding potential problems related to temperature variations of the pressure transducers and initiated a review of previous experiences from this type of measurements.

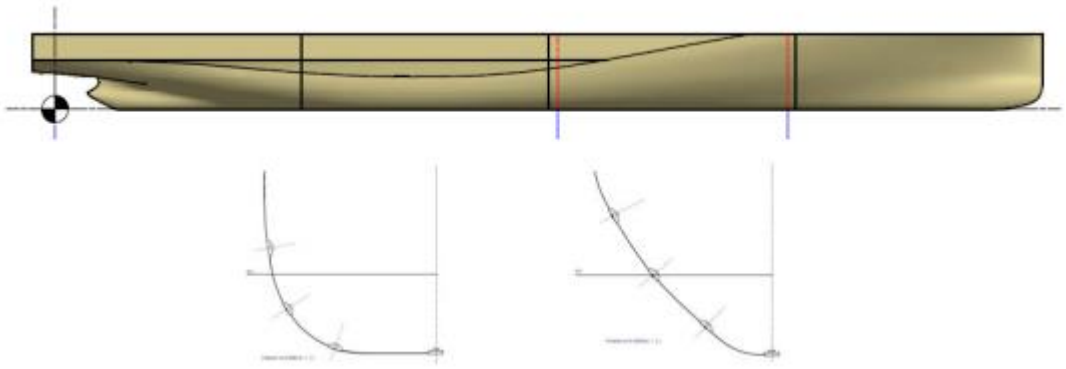

Figure 3-1 Profile view of the Stena Elektra based model showing the four backbone segments and a draft setup with four pressure transducers on two sections in the aft and fore ends of the second foremost hull segment.

It was therefore decided to not go through with buying pressure sensors and building the related part of the experimental setup. It is of course unfortunate that this sub-project could not be performed as planned, still the project has contributed with further valuable understanding regarding the challenges involved in local slamming pressure measurements.

In the WP2 report is the experimental technique that was planned to be used described. Further background to and motifs for not going all the way with this sub-project discussed, and, finally recommendations for further research proposed.

4 WP 3 - Hydrodynamic simulations and finite element analysis

The numerical simulations in this project are composed of “Eigen-frequency Analyses” and “Seakeeping Analyses”, which are corresponding to the “Hammer tests” and the “Seakeeping tests”, respectively. Prior to running the simulations, the finite element (FE) model used in numerical simulations was calibrated to meet the total weight and the mass distribution of the experiment model. The scale difference between the test model and the numerical model has been considered. Figure 4-1 illustrates the flowchart of the numerical analyses as well as their connections to the model experiments. In this chapter, the numerical models are described, and the example numerical results are presented. More detailed analyses are referred to [Appendix D].

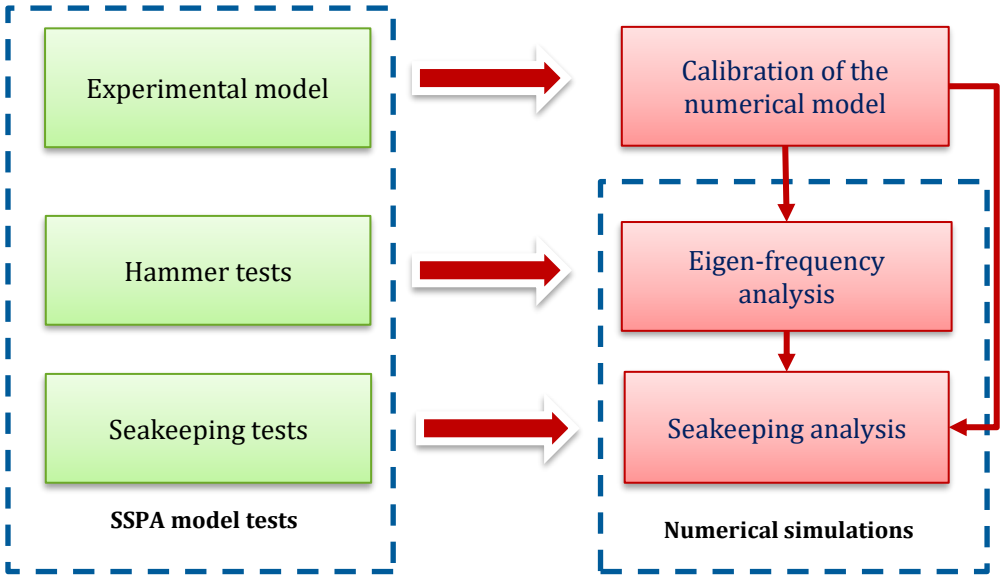

Figure 4-1 Flowchart of the numerical analyses and the relationship to the model experiments

4.1 Numerical model calibration

In contrast to the model tests, the numerical models are in full-scale. The characteristics and results of the model tests are converted to the full scale to be comparable with the numerical results. The scaling was done following the ITTC Recommended Procedures and Guidelines (ITTC 2011); see details of the structural scaling in [Appendix A]. The main particulars of the test model and their corresponding full-scale values are listed in Table 4-1.

Table 4-1 Model characteristics of the experiments and the numerical simulations

Ship particulars	Model tests	Numerical simulations
Length between perpendiculars (m)	5.284	195.5
Waterline length (m)	5.072	187.68
Depth (m)	0.409	15.12
Beam (m)	0.749	27.74
Beam in waterline (m)	0.715	26.46
Draught fore (m)	0.17	6.3
Draught aft (m)	0.17	6.3

Ship particulars	Model tests	Numerical simulations
Displacement (kg)	356.69	18,477,075
LCB, LCG (m)	2.405	88.985
VCG (m)	0.314	11.61

In the original FE model, only the ship hull was modelled. A total of mass points was thus added to represent the ship in full load condition. For each segment mass points are added on the centerline of the upper deck and a lower deck, aiming to reproduce the same VCG as well as the same LCG for that segment. The positions of the mass points are illustrated in Figure 4-2. By this means, the numerical model was calibrated to the same values of weight, center of gravity and moments of inertia as the model vessel. These values in full-scale are listed in Table 4-2.

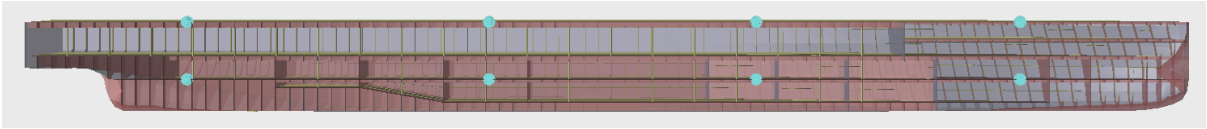

Figure 4-2 Numerical model analysis set up

Table 4-2 Numerical model properties after calibration

Weight (tonnes)	**18477**
Center of Gravity (m)	X=88.895; y=0; z=11.613
$\mathbf{I_{xx}}$ (m^4)	6.469 e+008
$\mathbf{I_{yy}}$ (m^4)	4.590 e+010
$\mathbf{I_{zz}}$ (m^4)	4.568 e+010

4.2 Eigen-frequency analyses

The eigenvalue analyses are carried out using GeniE, a commercial software for marine structural modelling and analysis developed DNV GL (DNV GL, 2015). The eigen-frequency simulations were performed using the FE model described above. The eigen-frequency computation takes in account the hydrostatic pressure surrounding the hull surface when the ship is lying in water, which is termed "Wet" condition. In contrast, if the ship stays in the air, like in a dry-dock, it is termed as "Dry" condition. The resultant frequencies of the analyses are presented in Table 4-3. Rather good agreement between the experimental and numerical results are found. Detailed description of the boundary conditions as well the discussions can be found in Appendix D.

Table 4-3 Results of eigen-frequency analyses

	Numerical [Hz]	Experimental [Hz]	Error
Dry condition	1.56	1.22	27.4%
Wet condition	0.79	0.87	8.8%

4.3 Seakeeping simulations

Seakeeping analyses were carried out using HydroD, a seakeeping software that is based Rankine Panel method (DNV GL, 2016). Figure 4-3 shows the bottom view of an example of the models of the

ship and water. In HydroD, waves are based on linear wave theory, which implies higher order of wave components are neglected. The ship model in HydroD is represented by rigid hull with correct weight distribution. Only wave-frequency responses are calculated in HydroD, while the hydro-elastic effects cannot be captured in HydroD, which is a major limitation of the numerical tools of this study.

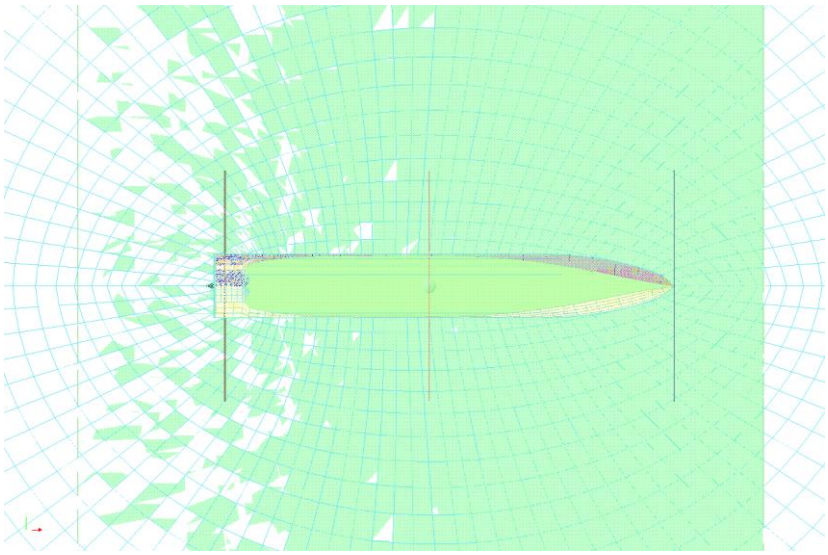

Figure 4-3 the bottom view of ship and water models in HydroD

The JONSWAP spectrum was chosen to define the wave profile, which is consistent with the model tests. For each sea state, the irregular wave is composed of 200 wave components. Each simulation takes 1800s in addition to a transient period of 150s. The timestep was set to 0.1s. The incident waves, ship motions and sectional forces were exacted after the simulations. The time domain results were then transformed into frequency-domain and compared with the experimental results.

The experimental and numerical incident waves were compared for various simulation runs. Figure 4-4 shows the experimental and numerical incident wave spectra of two runs: Sea state S006 (Hs=3.25m) with speed of 18kn, representing a relative calm sea, and Sea state S008 (Hs=5m) with speed of 15kn, representing a tougher sea condition. It is found that when the sea state is relatively low, the numerical wave spectrum takes a similar shape as the experimental wave. At higher sea states, however, the numerical incident wave deviates significantly from the experimental wave. This is nevertheless expected due to the limitation of the linear wave theory.

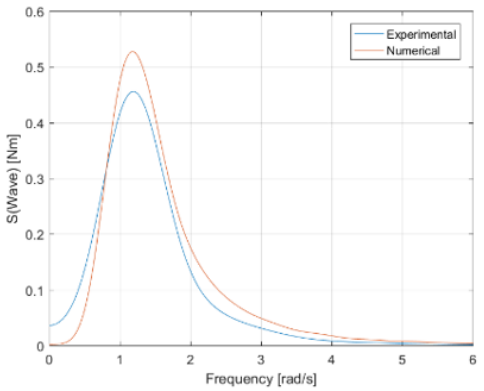

Seastate S006	
Speed (Kts)	18
Wave direction (deg)	180
Significant wave height (m)	3.25
Wave period (s)	9.24

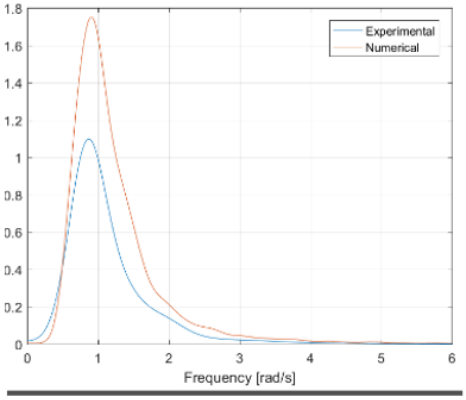

Seastate S008	
Speed (Kts)	15
Wave direction (deg)	180
Significant wave height (m)	5.0
Wave period (s)	10.78

Figure 4-4 experimental and numerical incident wave spectra for two runs.

We also compared the sectional forces. For the two sea states mentioned above, the experimental and numerical records of vertical bending moment at the mid-section of the ship are transformed to power spectra, as illustrated in Figure 4-5. It is found that for the lower sea state, i.e., S006, the numerical spectrum takes similar shape and amplitude as the experimental spectrum. This is expected because the incident waves are rather similar. For the higher sea state, i.e. S008, despite the significant discrepancy in the incident waves, the spectra of the vertical bending moments are rather close to each other. This indicates that the structural responses of sectional forces at the mid-ship are less sensitive to the incident wave.

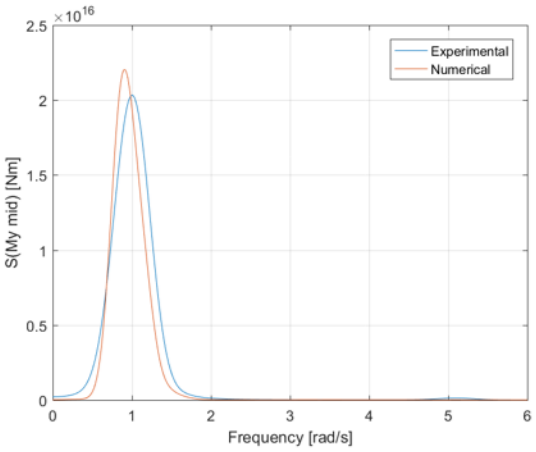

S006	Hs=3.25m, Tp=9.24
Speed (Kts)	18
Wave direction (deg)	180
stand. dev. error	**7%**

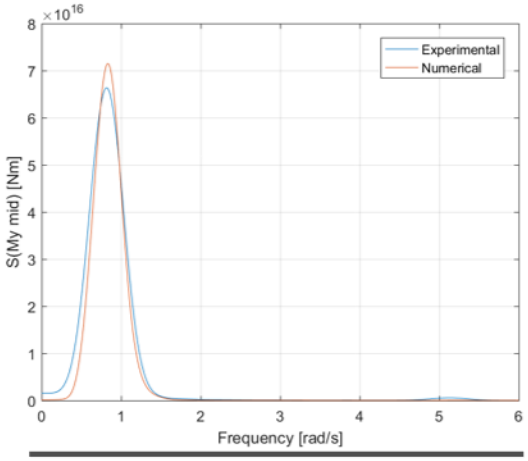

S008	Hs=5m Tp=10.78s
Speed (Kts)	15
Wave direction (deg)	180
stand. dev. error	**7%**

Figure 4-5 vertical bending moment spectra of the two simulations

5 Conclusions

The joint research and development project involving the interdisciplinary research areas hydrodynamics and structural engineering have successfully been completed.

A major part of the project goals has been fulfilled:

- A model test setup to evaluate the structural response of the hull beam for a ship hull in waves, have been designed, manufactured and evaluated by performing seakeeping model tests
- The model design contains several novelties needed that has been tested and evaluated:
    - Six degree of freedom force (and moment) measurement integrated into one transducer
    - Carbon fibre hull shell construction to be able to obtain the correct longitudinal mass distribution
    - Utilising optical measurements measure vertical deflection of the hull girder.
    - Low friction hinge
- The model design offers a flexible, practical and cost-effective test setup allowing for model tests of lightweight ships as well as conventional ships (e.g. container ships)
- The model concept works as intended, capturing all the most important physics, such as measuring forces and moments. It is well suited to capture springing and whipping
- Results show that the optical measurement of structural deflections may be improved.
- Instead a quasi-static hydrodynamic numerical approach was utilised. Results show that, even for a slender ship, this approach is not accurate enough. However, the combination of model tests and numerical analysis with today's tools seem to be feasible.

It was concluded that an experimental technique, applied earlier on high-speed craft, to measure local slamming pressure were not suitable for displacing ships as in this project. The feasibility study performed concluded that a need for further research on slamming pressure measurements is required and recommended for future studies.

5.1 Further research

For further method development, it is proposed to

- put forward, test and evaluate, a method to obtain a minimum test matrix to faithfully represent a ships life, in terms of structural dynamics and fatigue.
- put forward, test and evaluate, numerical tools that can be used to simulate the coupled structural and hydrodynamics of a ship navigating in waves.
- conduct further research on slamming pressure measurements in order to develop small membrane area pressure sensors, that provides measurements suitable for reconstruction of slamming pressure distribution

6 References

DNV GL. 2015. User Manual of GeniE, version 7.2-07. Horvik, DNV GL - Software.

DNV GL. 2016. User Manual of HydroD, version 4.9-02. Horvik, DNV GL - Software.

ITTC. 2011. Recommended Procedures and Guidelines: Global Loads Seakeeping Procedure. 26th ITTC Seakeeping Committee. International Towing Tank Conference.

RAPPORT

Datum:
2017-11-01

SSPA Rapport Nr.:
RE40168082-00-00-A

Projektledare:
Jonny Nisbet

Dynamisk Fartygsdimensionering

Framtagande av modell för Dynamisk Fartygsdimensionering

Referens:

Utdelningsnämnderna för Hugo Hammars Fond för internationell forskning inom sjöfarten

Hugo Hammars Fond för sjöfartsteknisk forskning

Fru Martina Lundgrens fond för sjöfartsteknisk forskning vid SSPA

Författare:
Olov Lundbäck
Olov.lundback@sspa.se
0730729177

Model for structural dynamics measurements

Outline specification for model design and construction

SSPA Sweden AB

Joakim Lundman
Acting Manager of Department
Maritime Consulting

SSPA Sweden AB

Jonny Nisbet
Project Manager
Maritime consulting

Summary and recommendations

Target for the current project is to put forward a model concept for testing structural dynamics in waves at SSPAs Marine Dynamic Laboratoty (MDL). Hitherto a very limited number of model trials have been performed in wave basin with models capturing structural dynamics with respect to fatigue life. Most of them have been purely research oriented. A few of them have given input to actual ship design. E.g. those described in ref. 3 and ref. 7.

The model concept developed in the current project will be tried out and fine tuned at a later stage, as described in *Figure 1*. Hence being able to provide novel services for ship owners and design firms for evolved and increasingly efficient and light hull structural design.

To achieve this, the current project consist of the following parts:

- Litterature study of research within the current matter
- Investigate possibilities and limitations of SSPAs facilities
- Gathering input from SSPAs project partners KTH, Chalmers and Stena Teknik AB
- Sum up the points above to find an optimal concept
- Document and present the model concept as CAD drawings, description of scaling principles and methods for determining model particulars

The proposed concept consist of a model with four rigid segments. The segments are connected by hinged joints with adjustable stiffness by the use of springs. The balance between accuracy and model complexity is achieved by modelling vertical bending stiffness, while the other degrees of freedom can be regarded as rigid. Forces and moments are to be measured in all six degrees of freedom at each cut between the model segments.

A methodology for determining stiffness in joints is also put forward and described in the current report.

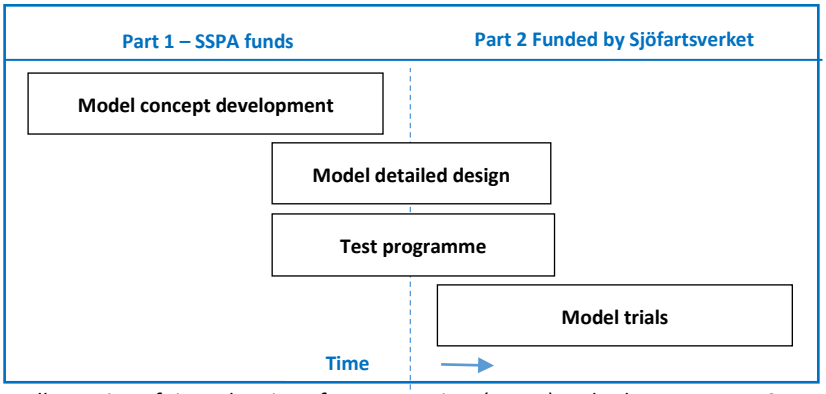

Figure 1 Illustration of time planning of current project (Part 1) and subsequent Part 2.

Table of Contents

1 Introduction

For scantling and verification of ship strength, the effect of wave induced vibrations is most often neglected. Today this practice is more and more challenged by the industry.

Among driving forces for this are:

- Lighter and more efficient hulls
- Increased safety
- Optimised balance of the two points above
- Larger ships
- Desire for increased speeds. However, not in the mainstream development due environmental and economical concern. For some routes and services, development high speed sea transport can be anticipated.

Experience and a number of recent research projects have demonstrated a significant effect of wave induced vibrations (WIV) on extreme loading and fatigue for some ship types. See e.g. ref. 7 and 12.

DNV have introduced class notations for ships evaluated for WIV by procedures outlined in ref. 2.

Model tests, numerical analysis and other alternatives is regarded necessary by DNV (ref. 2) for ships fulfilling one or more of the following:

- Novel design
- Rule length > 330 m
- Breadth > 47 m
- Bow flare angle > 55°
- Vessel contract speed > 25 knots

Increased use of high tensile steel and increase of ship size give a decrease in resonance frequency of hull girder and stiffened plate fields. This lead to an increasing number of ships where wave loads give excitation of hull resonance frequencies. In such cases, vibration can give a significant contribution to hull fatigue damage and risk for exceeding bending moment capacity of hull girder.

Often, wave induced vibrations are divided into:

- Whipping
- Springing

Whipping is transient vibrations induced by impulse loads, as bottom or flare slamming.

Springing is induced by oscillating loads, that excite a natural frequency of the hull girder. The two-node vibration springing mode is considered one the most important dynamic modes for the hull girder stresses for merchant ships. Local whipping effects often result in local loads that create high stresses locally but also conveyed to the hull girder, in some cases reaching the same order of magnitude as springing stress.

Already today several types of container vessels and some types of large tank ships need careful attention regarding structural dynamics and hydroelasticity.

For future ships, it can be anticipated that there is a desire to decrease hull weight by further increased use of state-of-the-art structural design and modelling tools to facilitate ship construction of high strength and lightweight materials e.g. high tensile steel, aluminium.

However there is a need for developing methods within computations and model testing to contribute to the development of more efficient hull structure.

When it comes to design of a scale model compromises are needed. In practice it is not possible to build a scale model that resemble every aspect of a full scale ship regarding hull structural dynamics (and statics). The challenge to do so can be described by the difficulty of making a 5.5m long vehicle by sheets as thick as aluminium foil, as illustrated by Figure 2. One of the main targets of the present project is to propose the right level of simplification and a good compromise to facilitate model testing of hull structural dynamics in MDL.

Figure 2. Illustration of the challenges to model every aspect of full scale hull structure at model scale.

1.1 Methodology and work flow to put forward a model concept

The current subsection describe the methodology and work flow used in the present project to put forward a model concept that is suitable for testing of structural dynamic contribution to fatigue for a ship hull structure at SSPAs facilities in the Marine Dynamic Laboratory (MDL).

In brief, the methodology and wokflow can be described in the following steps:

1. Litterature study
2. Compilation of advantages and disadvantages for different model concepts
3. Weighting of pros and cons with the different model concepts against the possibilities and limitations of SSPAs Marine Dynamics Laboratory (MDL)
4. Based on the outcome of point 1-3 above, choose model concept type.
5. Choose the specific ship to be used for concept design for current project and for detailed design at the subsequent project involving actual model tests in MDL.
6. Put forward and present method for scaling and representing full scale hull structure characteristics in model scale.
7. Specification of which hull characteristics that need to be computed for a detailed model design at the model trial project that will be carried out subsequent to the current project.

Scaling challenges are not present at assessments by computations. On the other hand, the complexity of solving the current matters analytically and/or numerically is on such a high level that a combination of model tests and simulations is very much desirable to complement each other.

1.2 Requirements for model concept

During the project, several requirements for the model concept have been identified. They can be summarised by the points below.

<u>Must have:</u>

1. Facilitate exact measurements of forces and moments for the most important degree of freedom
2. Provide a faithful representation of the lowest global eigen modes in the most important degree of freedom.

3. Measurement of motions with good accuracy in the most important degree of freedom
4. Exact measurements of forces and moments in all six degrees of freedom.
5. Economically feasible.

Good to have:

6. Measurement of motions at the other degrees of freedom
7. Provide a faithful representation of lowest eigenmodes at other degrees of freedom

2 Litterature study

The litterature study was mainly carried out in three steps:

1. Find and choose relevant literature
2. Compile knowledge about the physical foundations on hull structural dynamics at whipping and springing
3. Compile and present knowledge on different model concepts with a focus on putting forward advantages and disadvantages with the different model concepts.

The current section is organised by the type of structural design that is utilised for different works of research. Three main types of structural models have been considered in the current work. In the present report they are denoted: fully flexible model, elastic segmented model and rigid segmented model as described by Figure 3 below. The elastic segmented model type can be divided in two separate categories, “Backbone model” and “Spring model” as also described by Figure 3.

Project objectives include to capture the most important hydro-elastic effects during measurements. Hence the rigid segmented main type of Figure 3 was disregarded early in the literature study, since no structural dynamics is captured by that kind of model.

Instead the three subtypes of Figure 3: Continuous model, “Backbone model” and “Spring model” are the types that have been evaluated against the project objectives.

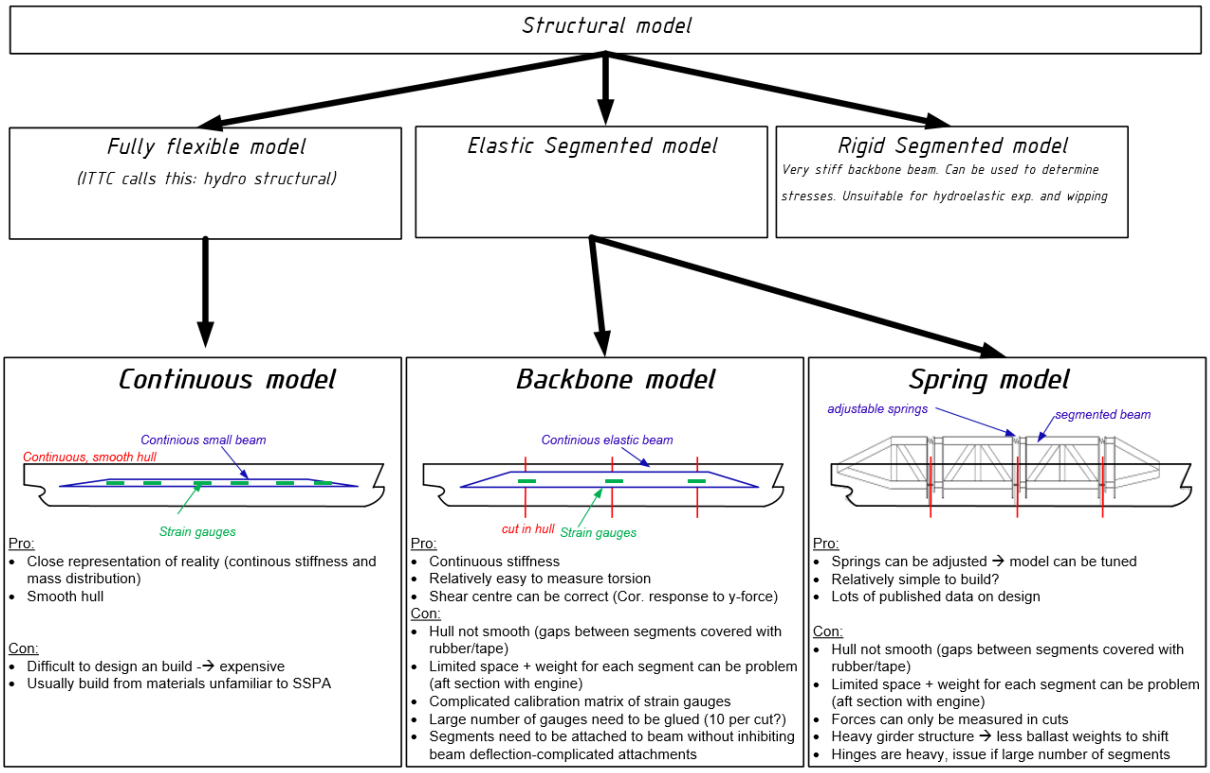

Figure 3. Illustration of main choices regarding model design.

2.1 Continuous model

Models of this type is built with a smooth outer skin with negligible global stiffness. An inner continuous beam, fitted with strain gauges to measure moments in three degrees of freedom, models structural stiffness.

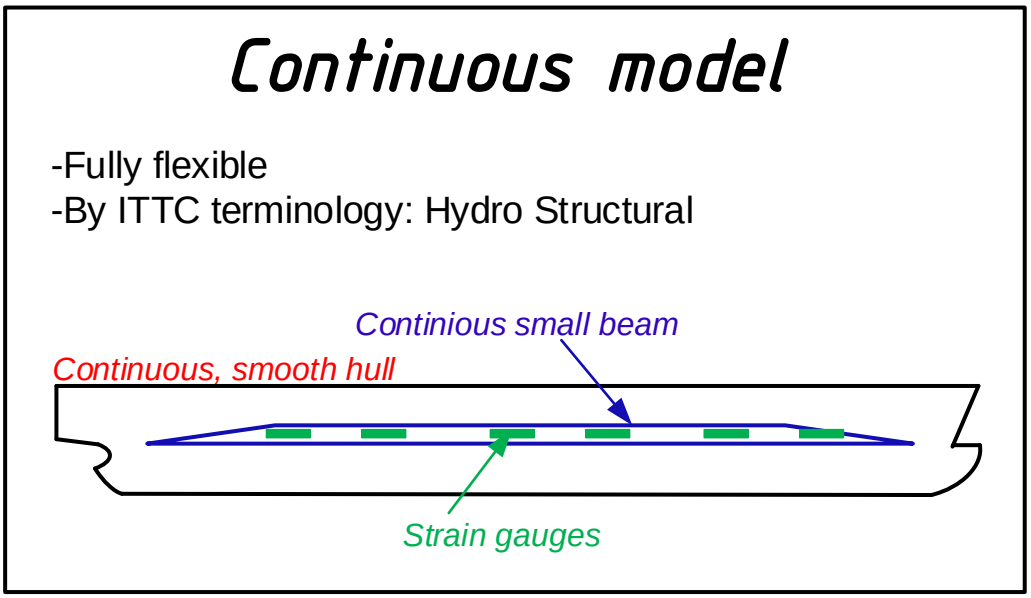

Pros:

- Close representation of reality (continous stiffness and mass distribution)
- Smooth hull

Cons:

- Difficult to design and build -> expensive
- Usually built of materials unfamiliar to SSPA
- Difficult to get measurement results with high accuracy.

In theory, this kind of model can give the best representation of hull structural dynamics. In practice, however a large number of difficulties arise. E.g. having exact measurements in distinct sections, obtaining the right stiffness and damping simultaneously. It would probably require a mix of several materials, many of which are unfamiliar to SSPA. Hence the likelihood is large of having a long and costly development work before a possibly working concept can be achieved.

2.2 Backbone model

The backbone model type consist of a segmented hull with rigid parts joined by a continuous elastic beam, attached to the rigid segments with moment free joints.

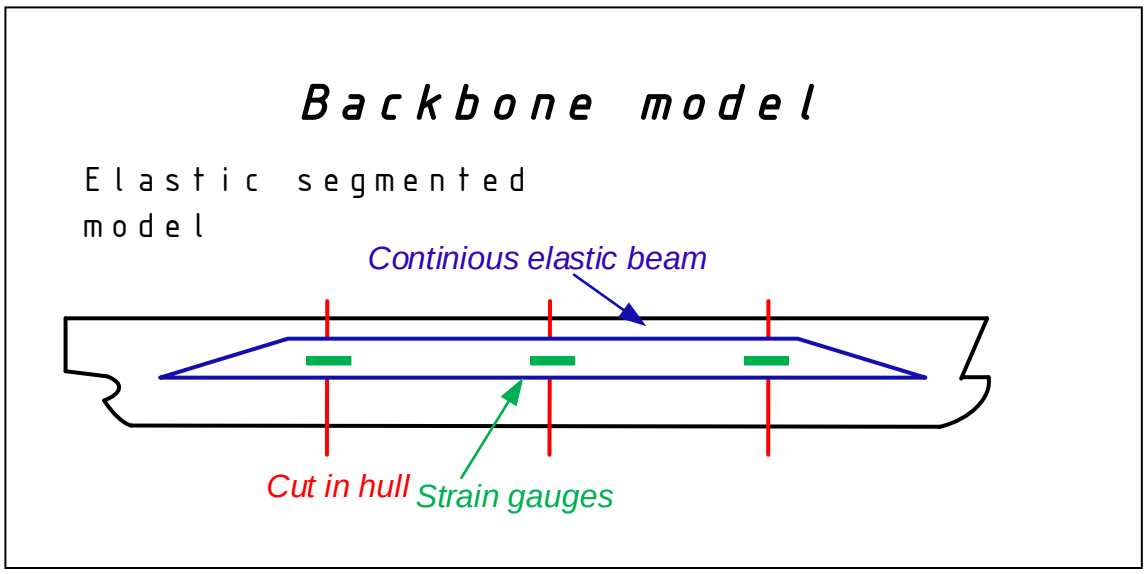

Pro:

- Continuous stiffness
- Relatively easy to scale torsion characteristics
- Shear centre can be correct (correct torsion response when y-force is applied)
- Possible (but difficult) to obtain correct stiffness in both vertical bending, horizontal bending and torsion simultaneously.

Cons:

- Hull not smooth (gaps between segments covered with rubber/tape)
- Limited space + weight for each segment can be problem (aft section with engine)
- Complicated calibration matrix of strain gauges
- Large risk for overhearing (mechanically and electrically) between the different degrees of freedom. This may not be possible to correct completely trough a calibration matrix
- Large number of gauges need to be glued (10 per cut?)
- Segments need to be attached to beam without inhibiting beam deflection-complicated attachments

- Model hull + back bone may be heavy and it may difficult to obtain correct weight distribution

This concept can be described as a mix of the continuous, described in section 2.1 and the spring model described in section 2.3.

Among advantages can be noted that the shear centre is relatively easy to get at the right position, below the keel.

Most important disadvantages are that it is difficult and time consuming to mount and calibrate strain gauges together with the beam combined with relatively large risk for inexact measurements.

If the intention is to utilise the possibility of modelling vertical bending, horizontal bending and torsion simultaneously, the design of the beam and joints will be time consuming and require quite a lot of computational work to obtain the desired characteristics in these three degrees of freedom at every cut.

2.3 Spring model

The spring model concept consist of a number of rigid segments, put together, with hinged joints combined with adjustable springs to obtained the desired static stiffness and eigenfrequencies

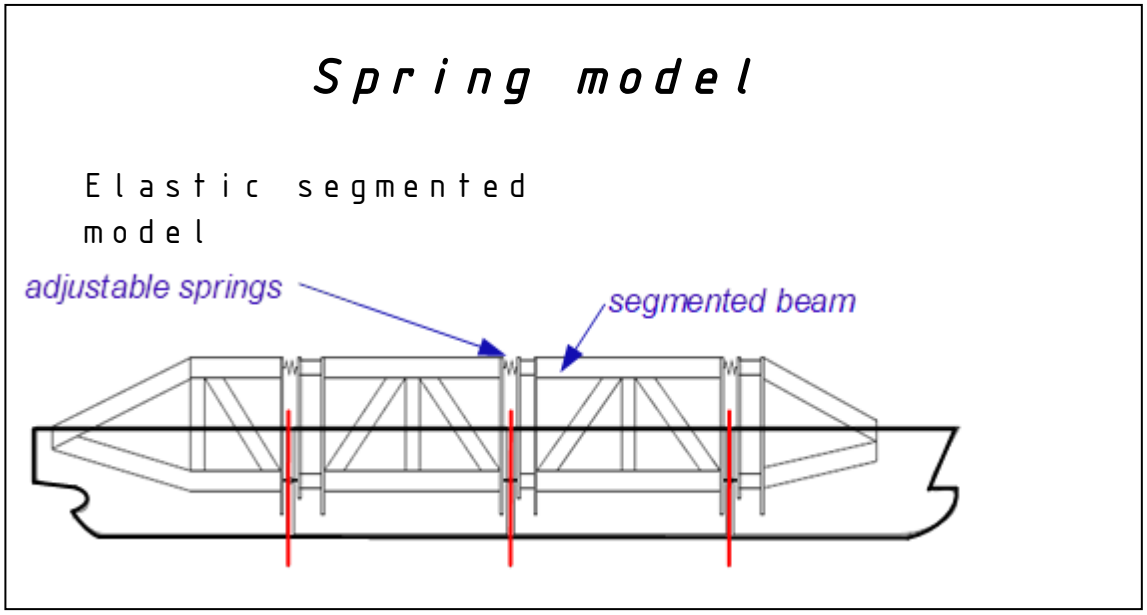

Pro:

- Springs can be adjusted model can be tuned
- Relatively simple to build
- Lots of published data on design
- Calibration relatively straightforward
- Reportedly exact measurements

Con:

- Hull not smooth (gaps between segments covered with rubber/tape)
- Limited space + weight for each segment can be problem (aft section with engine)
- Forces can only be measured in cuts
- Heavy girder structure less ballast weights to shift
- Hinges are heavy, issue if large number of segments

- Springs are heavy - difficult to obtain correct weight distribution
- Complex mechanical design if more than one degree of freedom are to be given the structural dynamic properties of the full scale ship.

The main advantages is that this model concept type is somewhat easier to build and calibrate than the other two types. Yet it is a complicated matter to obtain a good design and construction. This model type also have reportedly given relatively exact and well defined measurements.

2.4 Meetings with Gaute Storhaug

Gaute Storhaug at DNV, formerly NTU/Marintek, is one of the few that have been conducting and participating in model tests that capture the structural dynamics of the ship hull.

Two skype meetings with Gaute Storhaug were held during the project. The first in the initial phase of the project and the second at the final phase to clarify some questions that arose during the project.

At the first meeting a general discussion was held on Storhaugs experience of the different model concepts, from literature and his own experience as a Ph.D.-student on the matter. For the segmented model types the question about the number of segments needed to capture the most important structural dynamics with respect to fatigue. To his knowledge, four segments are enough to capture the most significant mode - two node vertical bending.

There was also a question on the need of a FE-computation in advance to extract the eigenfrequencies of the hull structure. Such a practice is needed to carry out the detailed design but not for the concept work, according to Storhaug. As a result Chalmers was appointed to plan their computational work so that the eigenfrequencies from their computations can be utilised for detailed design of the model.

DNV Gaute Storhaug on scale:

If small model: very little energy in waves, no springing

large model: wall interference, but good for space and weight.

It is important that the eigenfrequency in the force/pressure tranducer is well separated from the (very high) impulse frequency of the slamming pressure.

To capture slamming pressures important for whipping and springing, the total force over the area between the two adjacent web frames where slamming occur is an important measure.

In the evaluation of the loads, the plate field can be allowed to yield, while the stiffeners are not allowed to yield.

Damping is very low. Approximately 0.5% of critical damping. Generally speaking this means that the structural damping of the model shall be kept as low as possible, then there is a good chance that the structural damping of the model hits the target damping.

2.5 Characteristics of others dynamic hull models

In Table 1 characteristics of some ships in the literature on the current matter is noted to have some initial guesses to utilise at early model concept design.

Table 1. Summary of models from previous research

Ref.	Lpp_s (m)	Ship type	α	Model type	f1 (Hz)	Damping	Instru-ment-ation
4	233	Cruise ship	49	2-segm. Spring model	0.83 (wet)	0.007	My, slam
6	~120	Cargo/ Container	1	Non-linear FE	0.77 (wet LT-ship) 0.74 (wet ball.) 0.71 (wet loaded)	N/A	N/A
7	281	Container vessel	43	4-segm Spring model	0.80 (dry) 0.56 (wet loaded)	0.0064	

2.6 Summary and conclusions on choice of model type

When the concept types described in section 2.1 to section 2.3 are weighted against the project requirements in section 1.2, the concept section 2.3 – spring model comes out as the best of the “must have – requirements” i.e. requirement 1-5.

This is especially true when it comes to exactness of measurements and fidelity in structural dynamics for the most important degree of freedom (vertical bending). For the “good to have – requirements” the spring model type is not a practical solution but on the other hand none of the other two model concept types fulfil all the “must have –requirements”. Hence the choice of model type is the spring model described in section 2.3.

3 Choice of ship type

Already today several types of container vessels need attention regarding structural dynamics and hydroelasticity.

For future ships, it can be anticipated that there is a desire to decrease deadweight by use of state-of-the-art structural design and modelling tools in combination with high strength and lightweight materials.

A strong trend within many industrial branches is modularization. Currently there are proposals to utilize advances in technology to increase modularization in ship design by e.g. use one and the same hull structural design for a series of ships with varying number of decks.

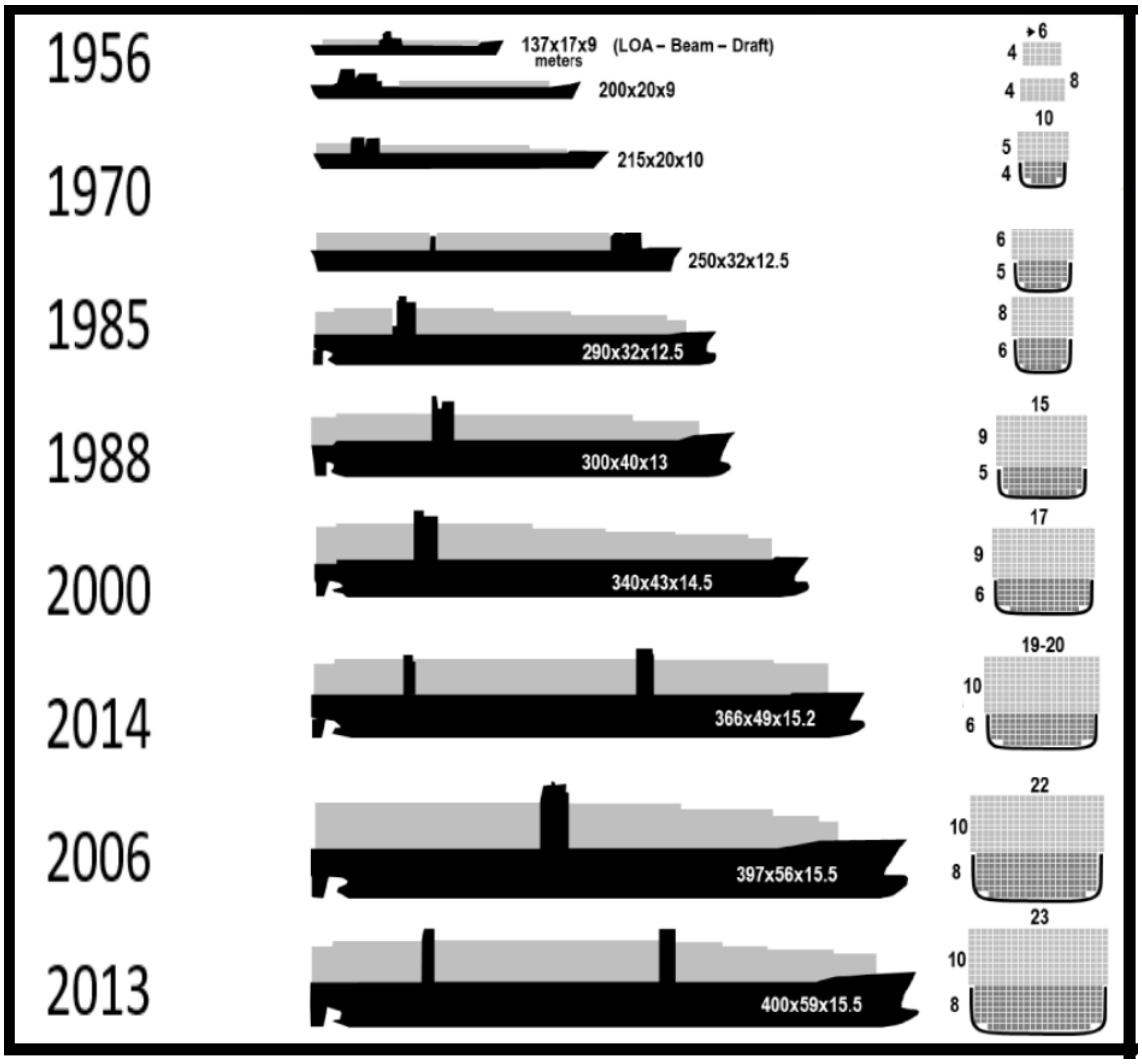

Figure 4 Illustration of development of size for container vessels by the years. From ref. 1.

3.1 Choice of ship and ship particulars

Stena Teknik AB, as a project partner, have been expressing a strong belief in lighter and more efficient ship structures in the years to come. They have also expressed a strong wish to investigate how a light structure could be incorporated in their future fleet. Their most recent testbed for innovations and increased efficiency within marine transport, Stena Electra, was hence chosen for the current project.

Stena Elektra is in an early phase in the design work. Many ship characteristics are still unknown, e.g. the vertical center of gravity (VCG or KG). The VCG value used throughout the current project is an estimation based on similar existing Stena Ships, Stena Electras transverse metacentric height (KM) and SSPAs manoeuvring database, shown as scatter plots in Figure 6-Figure 8. For these scatter plots it is worth to note that some ships are present with several loading conditions.

Figure 5. Rendered image of projected design for Stena Elektra. From ref. 9.

	Elektra, T=6.3	**Jutlandica, T=6.0**	**Germanica, T=6.0**	**Saga, T=6.8**	**Danica, T=6.3**	**Nautica, T=5.86**
Length between perpendiculars [m]	195.5	169.0	221.75	150.0	133.5	126.0
Beam [m]	26.46	27.8	28.7	28.4	28.5	24.0
Displacement [m^3]	17978	18400	28256	16595	15651	11081
Draught [m]	6.3	6.0	6.0	6.8	5.86	6.3
KG [m]	11.91[1]	12.5	11.87	13.4	13.0	10.0
GM [m]	1.8[1]	2.0	1.8	2.0	3.7	2.5
Note 1: Estimated values based on similar Stena Ships, Elektras KM-value of 13.71 and a cut out of SSPAs Manouvring database shown in *Figure 6 - Figure 8*						

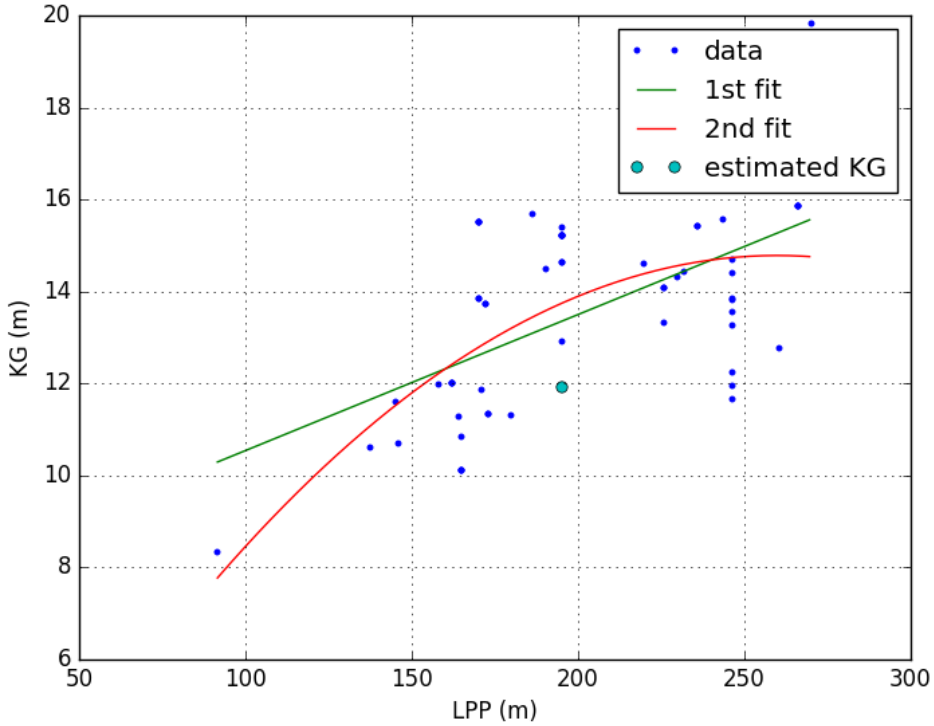

Figure 6. Scatter of VCG vs shiplength for similar ships in SSPAs manoeuvering database

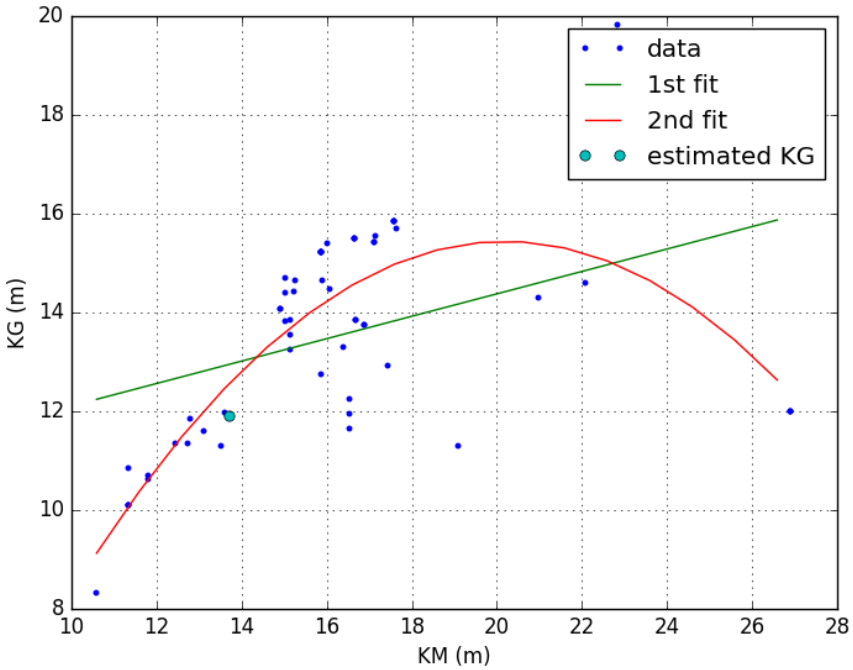

Figure 7. Scatter of VCG vs transverse metacentric height for similar ships in SSPAs manoeuvering database.

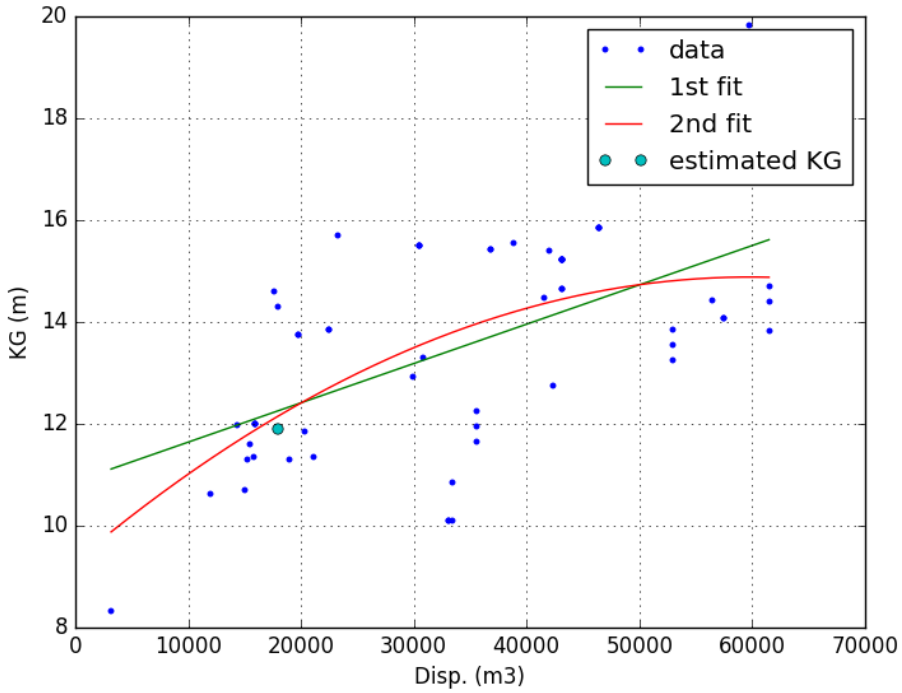

Figure 8. Scatter of VCG vs displacement for similar ships in SSPAs manoeuvering database

3.2 Summary and conclusions on choice of ship type

One of Sweden's leading ship owners, Stena Line/ Stena Teknik, have identified a need to work on several areas to make future sea transport more efficient. One of these areas is lighter and more efficient ship structures.

To achieve this with safety intact, complements to current scantling rules are needed. One such complement is the ability to estimate the fatigue damage due to hull structural dynamics.

Stena Teknik AB have also identified that better knowledge on hull structural dynamics can increase the flexibility of use and increased transport volumes per journey for a ship. This could be facilitated by having a higher degree of hoistable/detachable decks on Ro-Ro/Ro-Pax ferry.

Normally, a Ro-Ro/Ro-Pax ferry would not suffer significantly from fatigue due to structural dynamics. However, with Stena Teknik's design targets for the future, e.g. lighter ships and more flexible arrangements, life span of such ships will likely to a large extent be determined by hull structural dynamics.

Hence, Stena Line/Stena Teknik's projected Stena Electra have been chosen for the current project.

4 Load distribution on hull beam

The chosen ship Stena Elektra is likely to be operated in Skagerrak and Kattegatt. Wave statistics shown in Figure 10-Figure 14 display that common seastates are within WMO Seastate 6 and below.

To ensure some tests to be performed where significant dynamic effects occur seastate 7 from Table 3 may be used.

Table 2. WMO Seastate code

WMO Sea State Code	Wave height	Characteristics
0	0 metres	Calm (glassy)
1	0 to 0.1 metres	Calm (rippled)
2	0.1 to 0.5 metres	Smooth (wavelets)
3	0.5 to 1.25 metres	Slight
4	1.25 to 2.5 metres	Moderate
5	2.5 to 4 metres	Rough
6	4 to 6 metres	Very rough
7	6 to 9 metres	High
8	9 to 14 metres	Very high
9	Over 14 metres	Phenomenal
	Sea states for current study	

4.1 Wave statistics

Expected routes for the current vessel is in the north sea area and skagerrak and coastal waters at Kattegatt.

Wave statistics shown in Figure 10-Figure 14 display that common seastates are within WMO Seastate 6 and below. To ensure some tests to be performed where significant dynamic effects occur seastate 7 from Table 3 is proposed.

It can be seen from Table 3-

Table 5, that the wave heights and wave lengths for Skagerrak and Kattegatt correlate well with those at Ekofisk field in North Sea. It is therefore proposed to utilise data from Table 3 to get the correlation between wave length and wave height, especially for the higher seastates, where little data is available for Skagerrak and Kattegatt.

Table 3. Average of wave heights and wave period including expected frequency of occurrence for Ekofisk field in the North sea.

Sea State	Sign. wave height $H_{1/3}$ [m]		Wave period T_Z [s]	Expected frequency [%]
	range	mean value		
0-2	0-0.5			10.8
3	0.5-1.25	0.88	4.9	30.0
4	1.25-2.5	1.88	5.4	34.3
5	2.5-4.0	3.25	6.6	18.1
6	4.0-6.0	5.00	7.7	5.8
7	6.0-9.0	7.50	9.2	0.9
8	9.0-14	11.50		

Table 4 Average values for wave heights, -periods and -lengths at different Seastates for Väderöarna

	Averages for Skagerrak		
Sea state	**$H_{1/3}$ (m)**	**T_m (s)**	**$L_{wave}(T_m)$ (s)**
SS4	1.57	4.65	33.79
SS5	2.86	5.92	54.77
SS6	4.05	6.65	69.12

Table 5 Average values for wave heights, -periods and -lengths at different Sea states for Trubaduren

	Averages for Kattegatt		
Sea state	**$H_{1/3}$ (m)**	**T_m (s)**	**$L_{wave}(T_m)$ (s)**
SS4	1.57	4.29	28.76
SS5	2.7	5.19	42.10
SS6	4.09	6.09	57.97

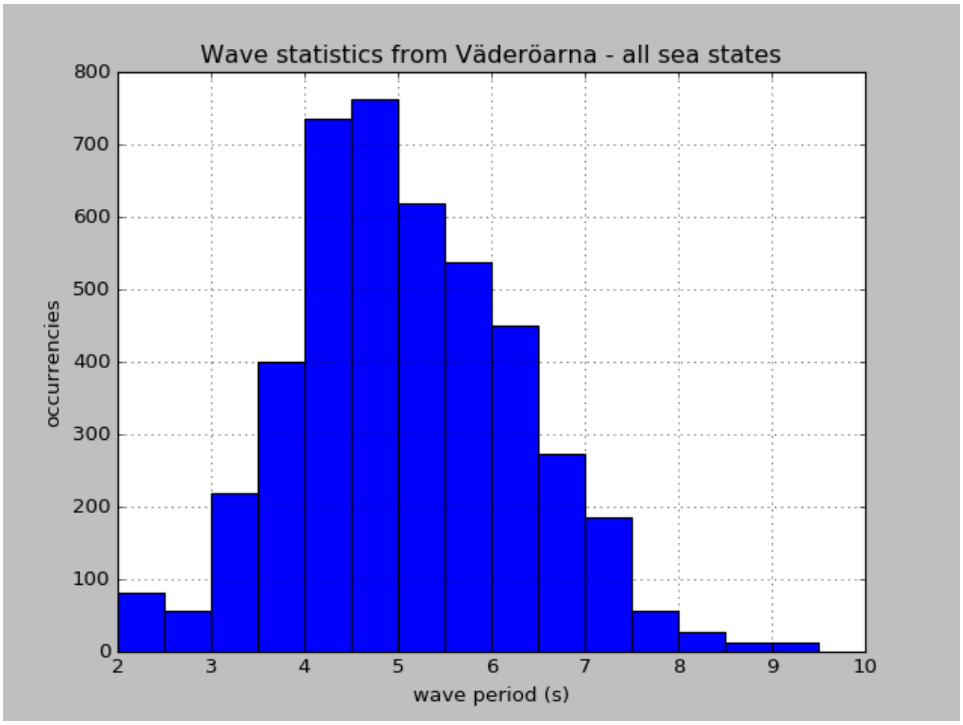

Figure 9. Data for Väderöarna from ref. 8

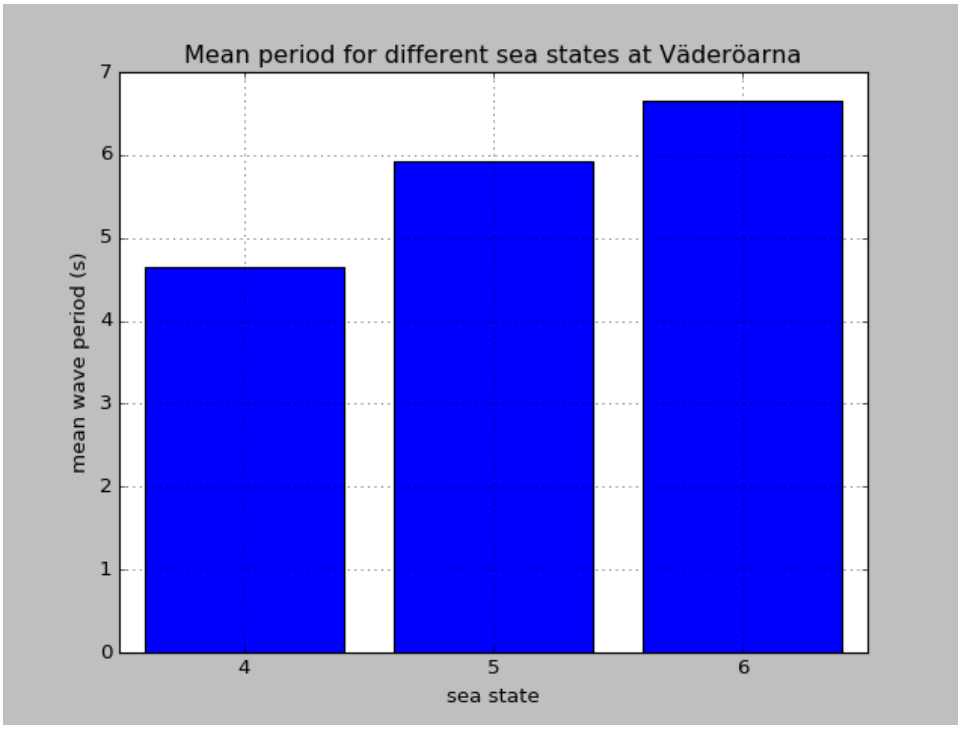

Figure 10.Data for Väderöarna extracted for sea state 4,5 and 6

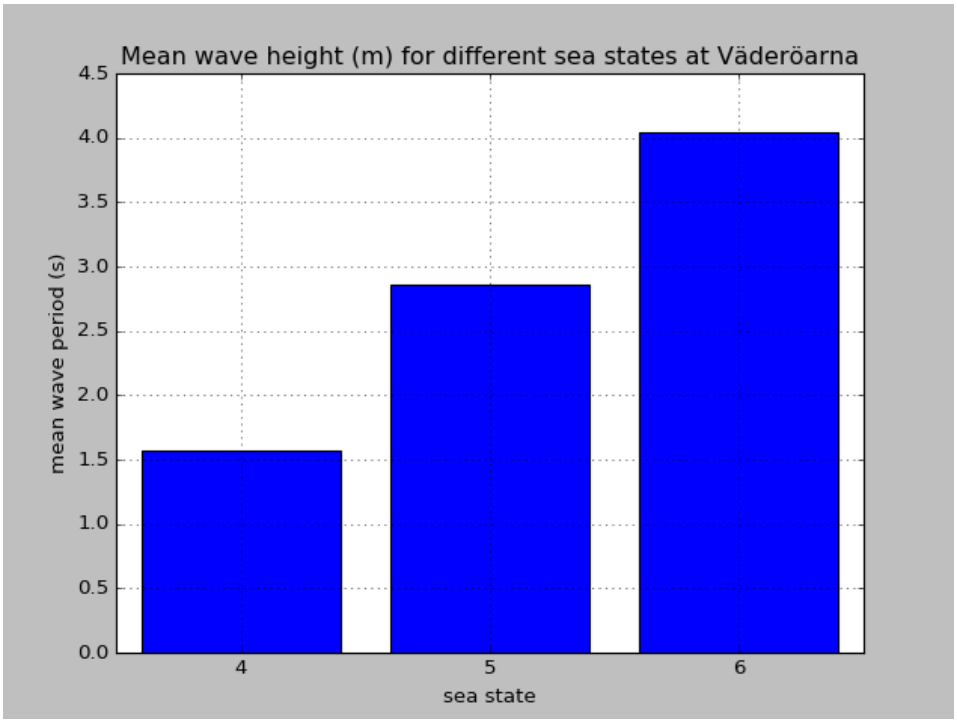

Figure 11. Data for Väderöarna extracted for sea state 4,5 and 6

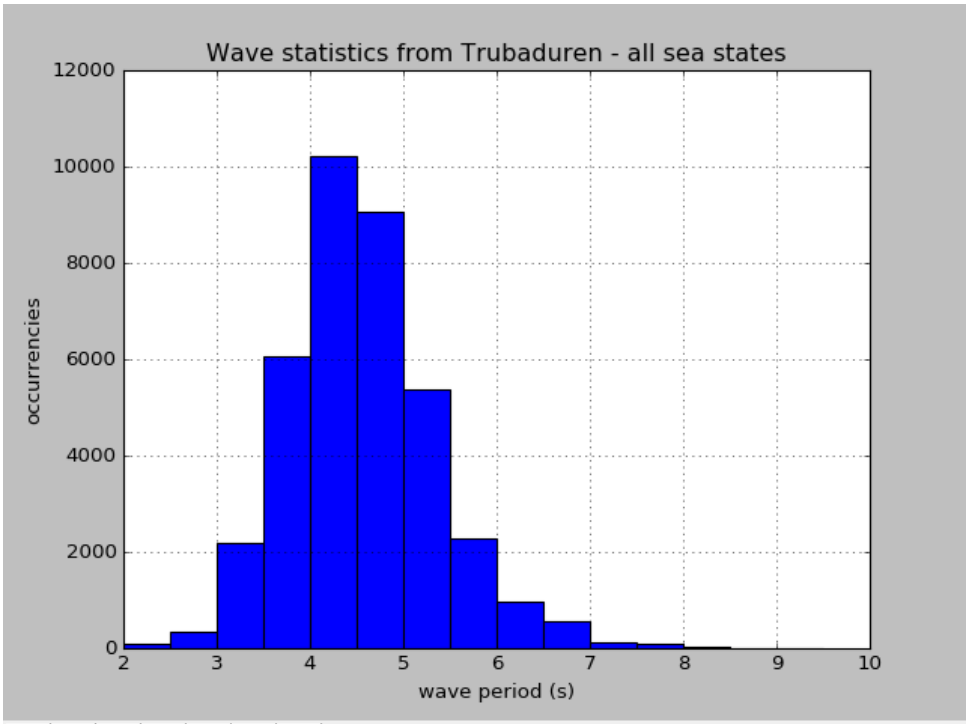

Figure 12 Data for Trubaduren from ref. 8

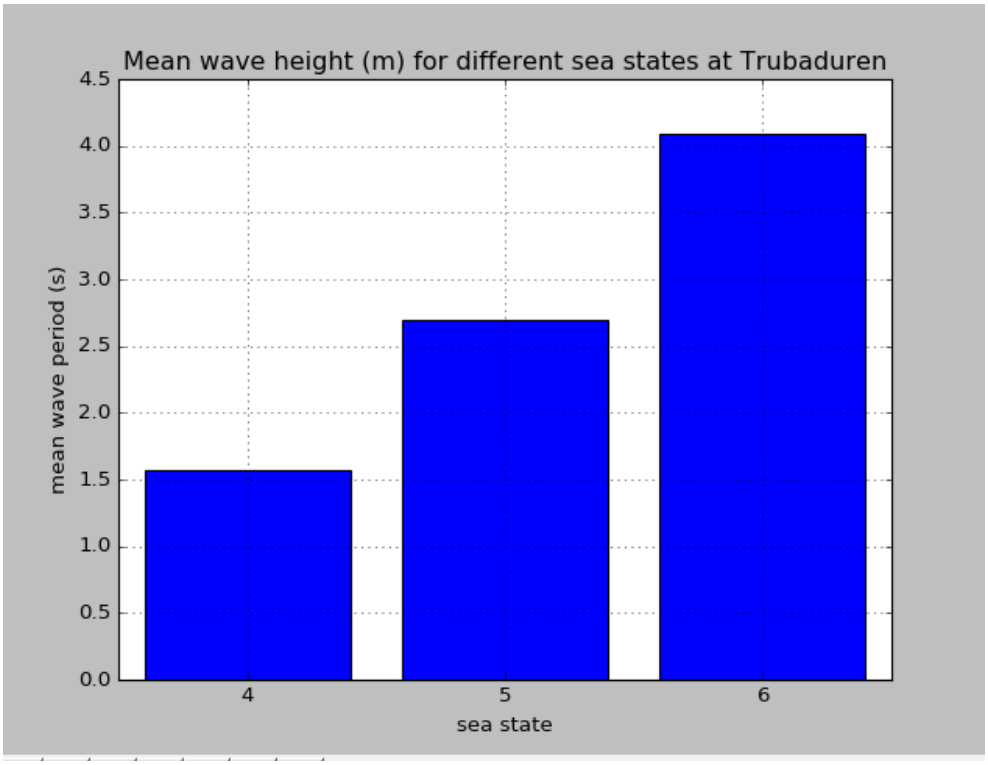

Figure 13. Data for Trubaduren extracted for sea state 4,5 and 6

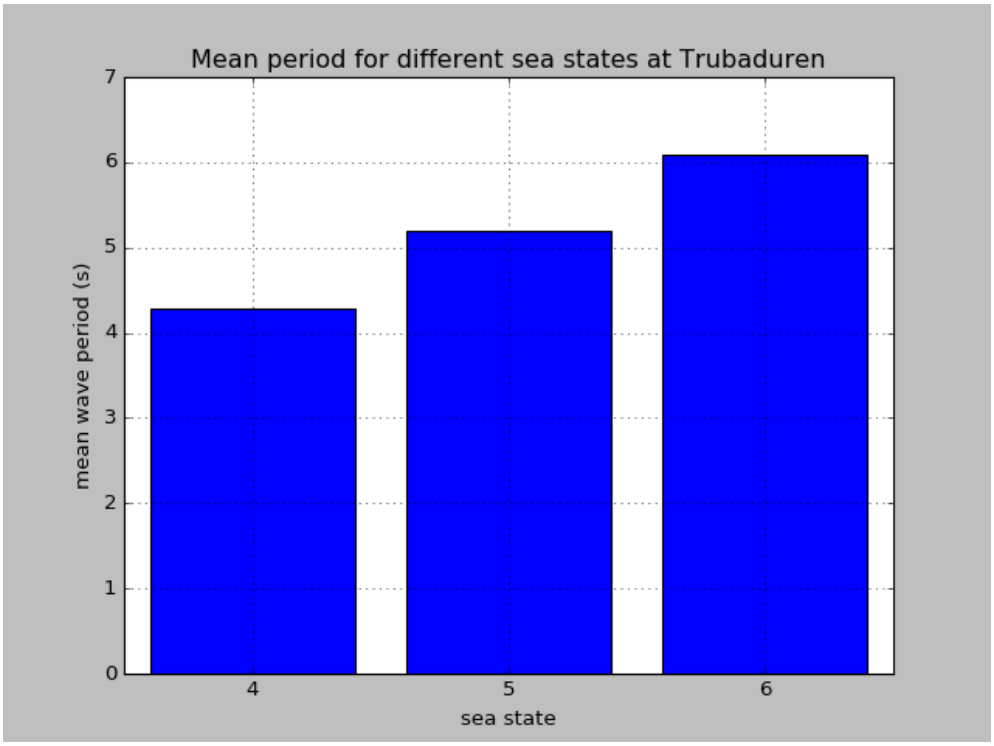

Figure 14. Data for Trubaduren extracted for sea state 4,5 and 6.

4.2 Experiences from NTNU

There is no commercial computational code that capture non-linear springing.

To accurately measure both whipping and springing a minimum of 30 minutes of full scale time should be measured. In summary the following can be assumed:

- Whipping
    - Close 30minutes full scale, since much of the whipping is due to slamming.
- Linear springing
    - Relatively short measurement should be sufficient
- Non-linear springing

4.3 Projected test programme

The test program is intended to consist of seastates that are relatively commonly occurring at the most common waters for Stenas Ro-pax ships as well as those who trigger slamming, whipping and springing.

Proposed test program is described by Table 6-

Table *9*.

Table 6. Conditions to run for measuring bending moments

Sea state\ wave direction (°)	180	150
4	x	x
5	x	x
6	x	x
7	x[1]	
Note 1: May be omitted in order not to destroy equipment. Decision to be taken based on what is noted from tests at the lower seastates		

Table 7. Conditions to run for measuring slamming pressures

Sea state\ wave direction (°)	180
5	x
6	x
7[1]	x

Table 8. Speeds to run

Speeds	Sea states
Reduced	4-6
March	4-6
Full	4-5

Table 9. Proposal for sea states to be tested

Sea state	$H_{1/3}$	T_z/T_P
4	1.88	4.9/6.86
5	3.25	5.4/7.56
6	5.00	7.7/10.78
7[1]	7.5	9.2/12.9

5 Global structural model – Scaling of structural statics and dynamics

Dynamic structural loads are often divided into whipping and springing.

Whipping is transient vibrations induced by impulse loads, such as bottom or flare slamming.

Whipping has hitherto not been faithfully represented by scale models and it is still considered to be practically impossible to build such a scale model. To gather data directed towards whipping the impulse loads (e.g. slamming) are recorded by use of pressure tranducers at selected locations on the hull.

Springing is induced by oscillating loads that excite a natural frequency of the hull girder.

To capture springing in model tests, a scale model with faithful representation of the structure globally is needed. With the chosen model concept, the stiffness is represented by springs at three hinges.

To get a model that represent the full scale ship in the best possible manner, the hinge stiffnesses have been chosen as follow:

1. Stiffness that give equal deflection at hinges for the hinged model and scaled deflections for the full scale ship for a selected test load.
2. Stiffness that give equal 1st and 2nd eigenfrequencies for the scale model and scaled results of full scale ship.

To develop the model concept, criteria 1 above have been used, since much details of the final design and mass distribution are not known.

The subsections below describe a method to be used for finding suitable stiffness to meet criteria 1 above. These procedures can be followed to design the scale model, while more fine tuning accounting for criterion 2 above can be done when the model is built.

To facilitate fine tuning against the two criteria, a model concept with adjustable spring stiffness is chosen.

5.1 Stiffness at hinges

For a hinged model with stiff sections in between, the moment stiffnes at hinges need to be calculated.

To obtain the stiffness distribution, an eavenly distributed load was applied to a hull beam with stiffness distribution from Stena Electra with one deck removed. The deck was removed to meet the requirement of a lighter and more flexible future hull structure.

Figures of sectional moments of inertia was obtained from the structural design of Stena Electra. Hull girder was idealized as illustrated by Figure 15. A continuously varying stiffnes was fed into an in-house beam computation code, which was developed during the project. Figure 17 show stiffness distribution of the hull girder. The fitted stiffness distribution of Figure 17 was fed into the beam computation program together with a constant distributed test load and supports at the end of the beam.

The test load was obtained as an estimated maximum hogging load.

The model scale structural characteristics, M_i, y_i, C_i, were thus calculated for the model concept as illustrated by Figure 19.

M_i is the sectional moment at cut i, y_i, is vertical deflection at cut I, and C_i is angular stiffness at cut i.

To obtain these results an in-house computational program was tailor made for this purpose. The main parts of the computational code is illustrated by *Figure 20*. The PreProcessor and PostProcessor parts were tailor made during the present project, while the BeamMech part was acquired from ref. 15.

Necessary characteristics of force gauges, were obtained, in form of stiffness and measurement range as a subsequent result.

Figure 18 show the resulting vertical deflection when the test load is applied.

Ship model structural design was idealised as illustrated by *Figure 19*. The angular stiffness coefficients for the ship model that give the same deflection in the pivot points for the ship model as the continous hull girder were calculated.

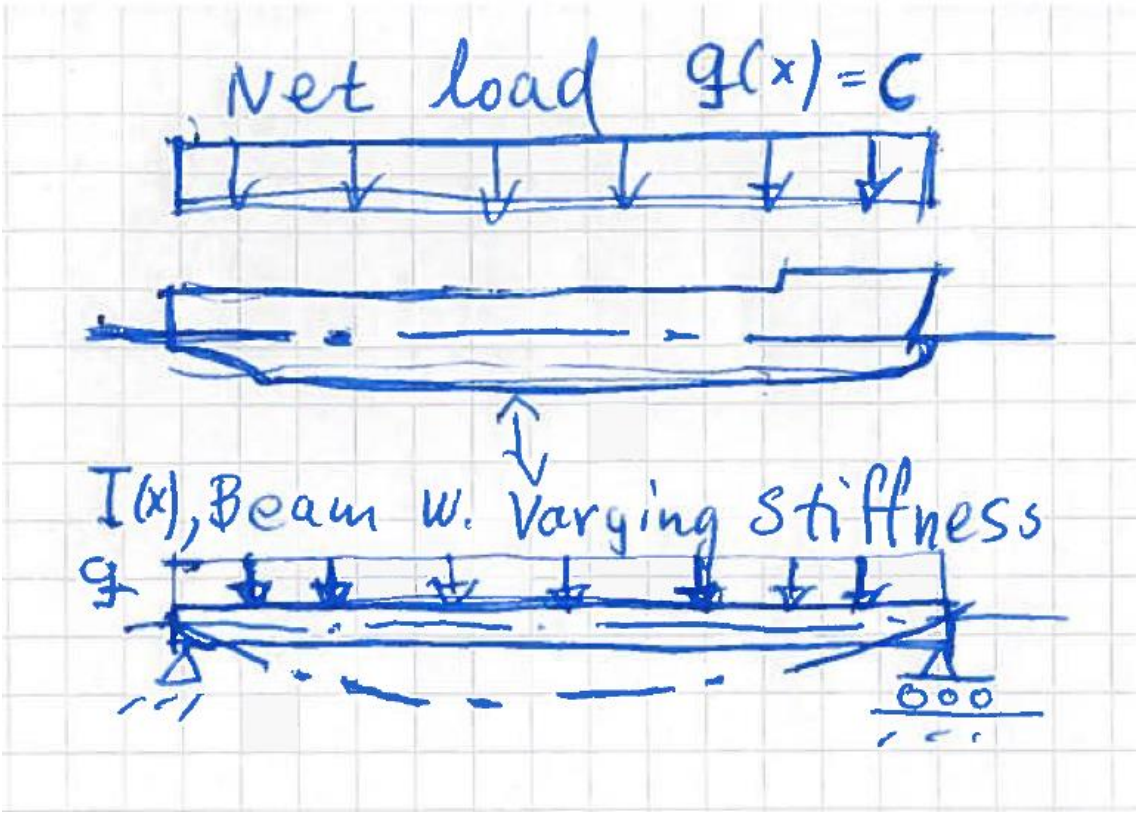

Figure 15 Idealisation of hull girder

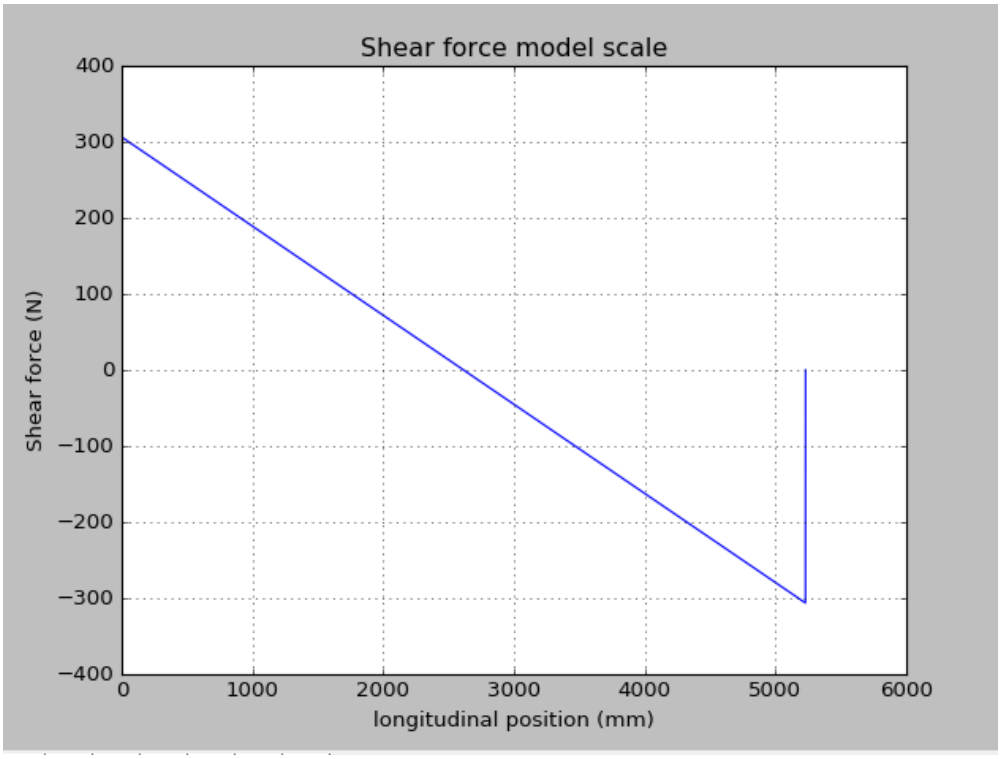

Figure 16. Shear force as a result of the test load

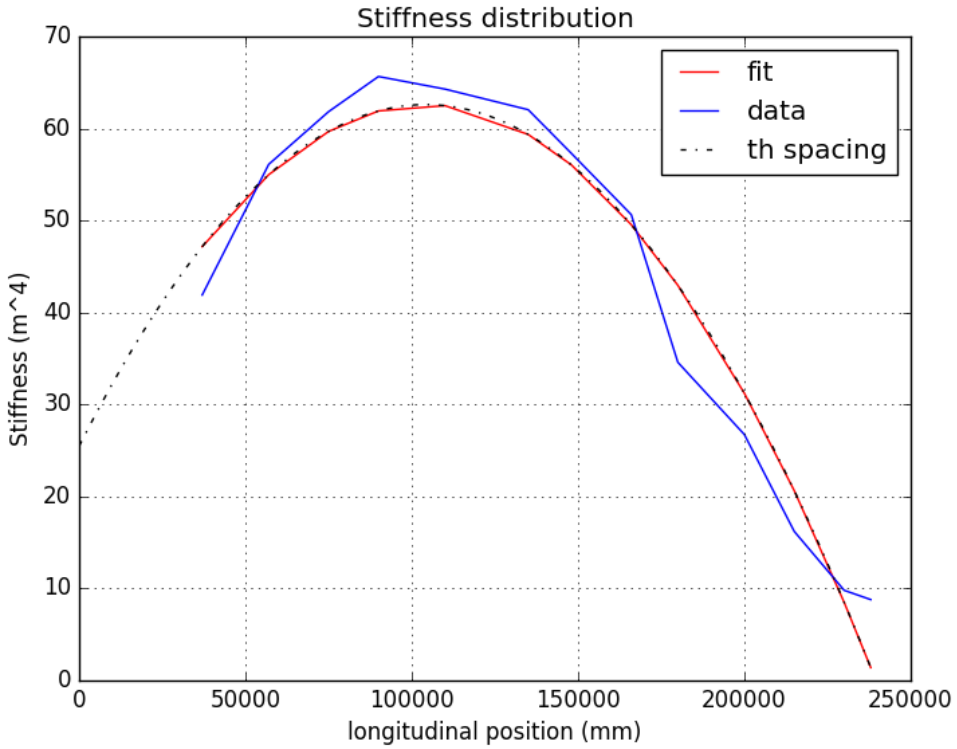

Figure 17 Stiffness distribution

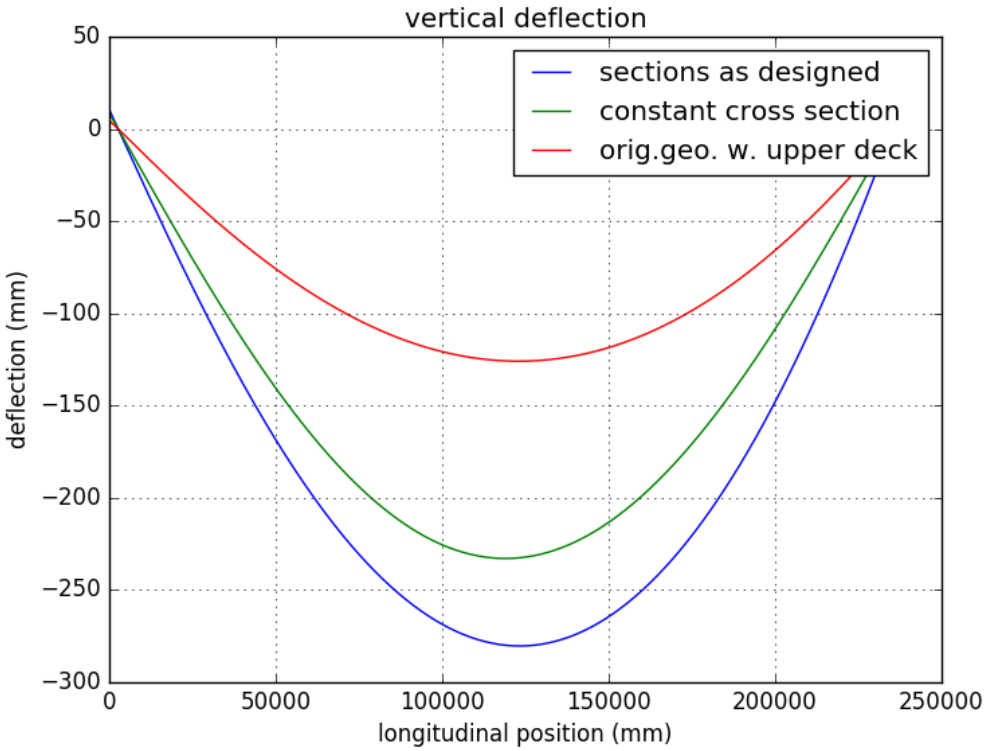

Figure 18 Vertical deflection of idealised hull girder

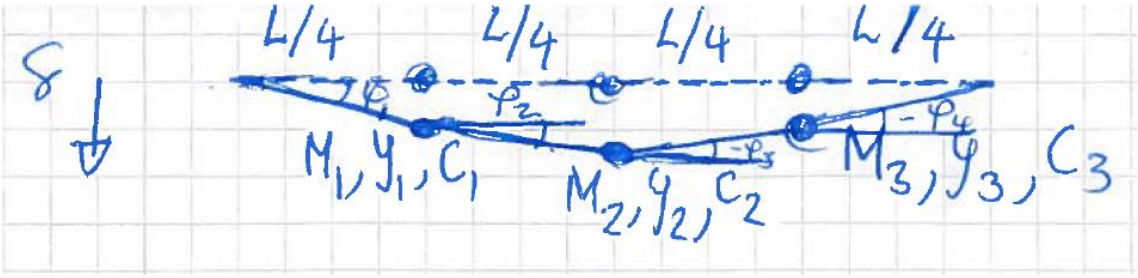

Figure 19 Idealisation of model design

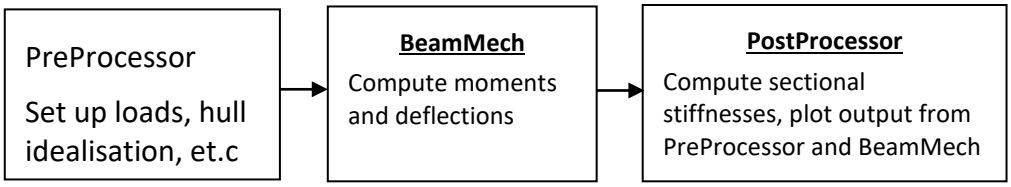

Figure 20. Description of the computational program for determining scale model characteristics

5.2 Scaling to model scale-general notes

For model tests of ships, Froude scaling is applied. Thus forces and moments are scaled with the scale factor to the power of three and four respectively.

Model tests addressing structural design for bending require that the Cauchy scaling law is satisfied, which is done by scaling moment *coefficients* by the scale factor to the power of four.

Full scale coefficients were hence scaled by the scale factor to the power of 4 and they are displayed in Figure 21. To prove that this scaling was correct all quantities were rescaled according to the Cauchy Scaling law. Hence lengths were scaled to the scale factor, forces were scaled to the power of 3 to the scale factor, moments to the power of four and Young's modulus to the scale factor.

The results are shown by Figure 22-Figure 26.

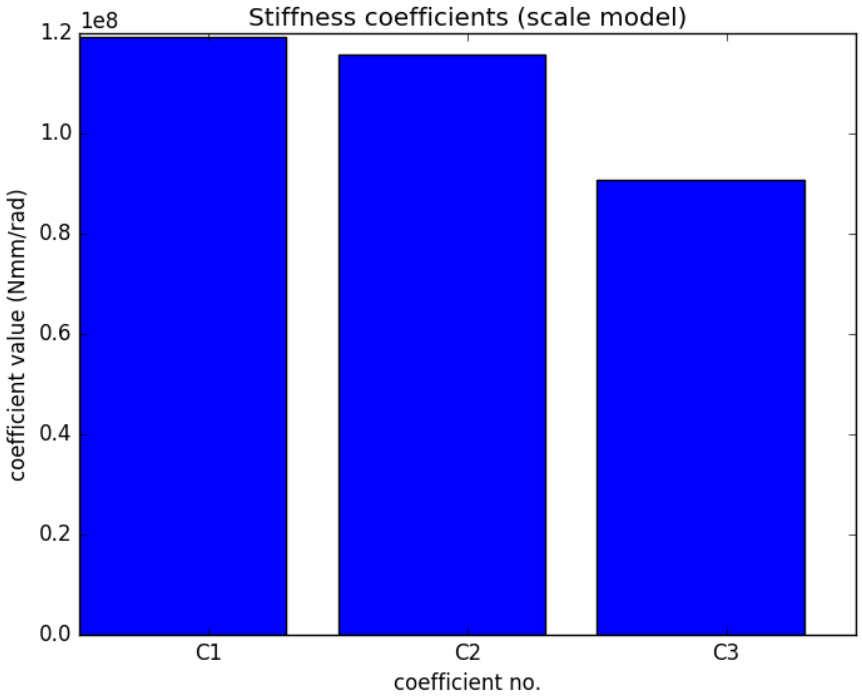

Figure 21 Stiffness at hinges rescaling full scale coefficients to model scale

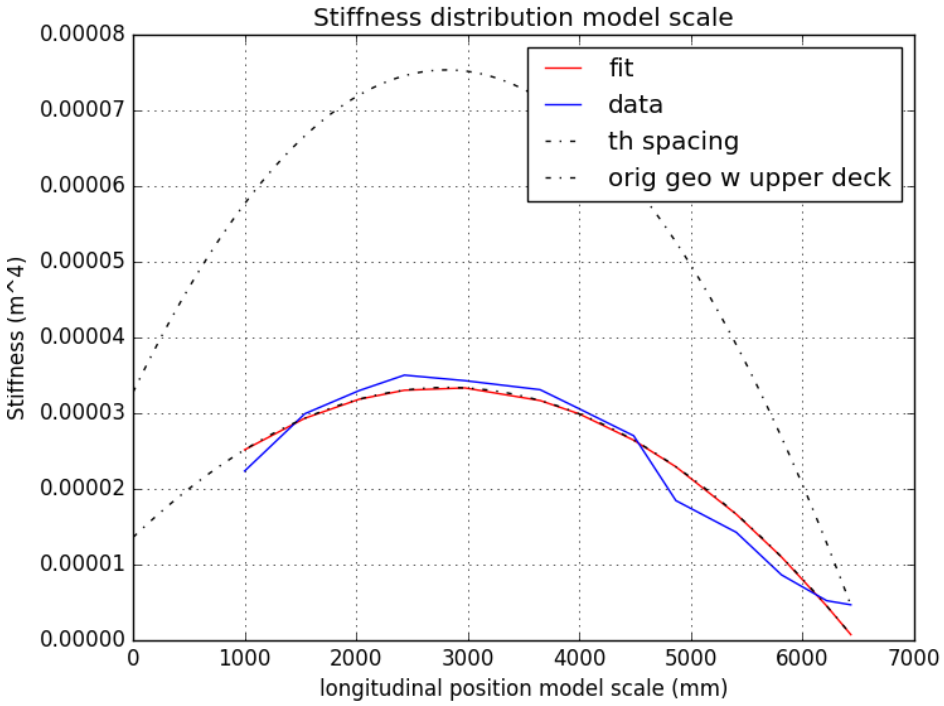

Figure 22 Stiffness distribution in model scale

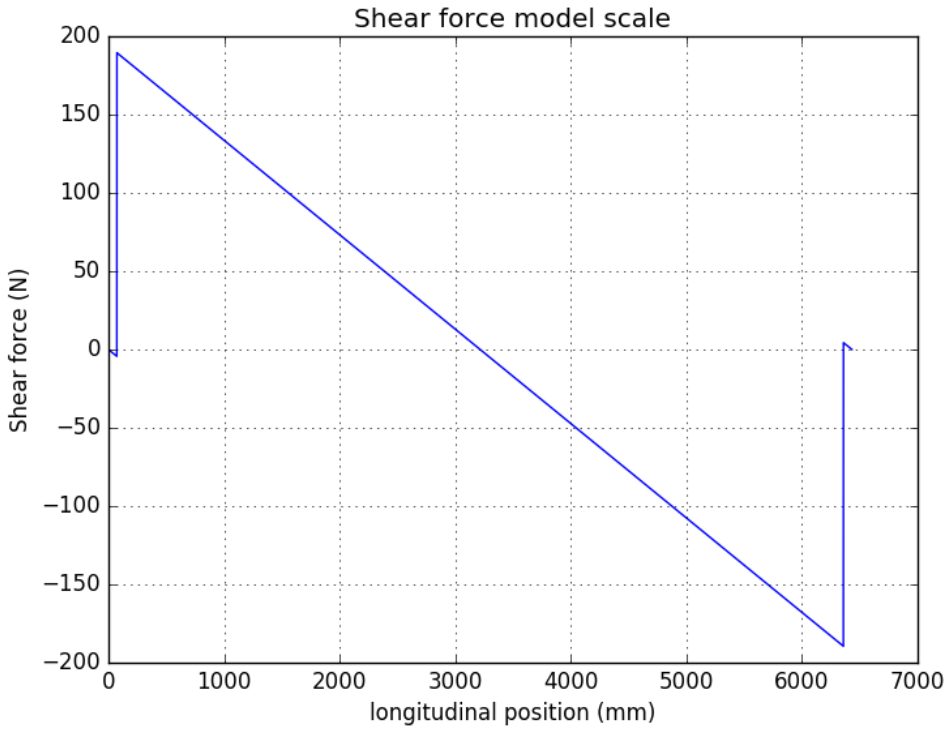

Figure 23 Shear force of test load

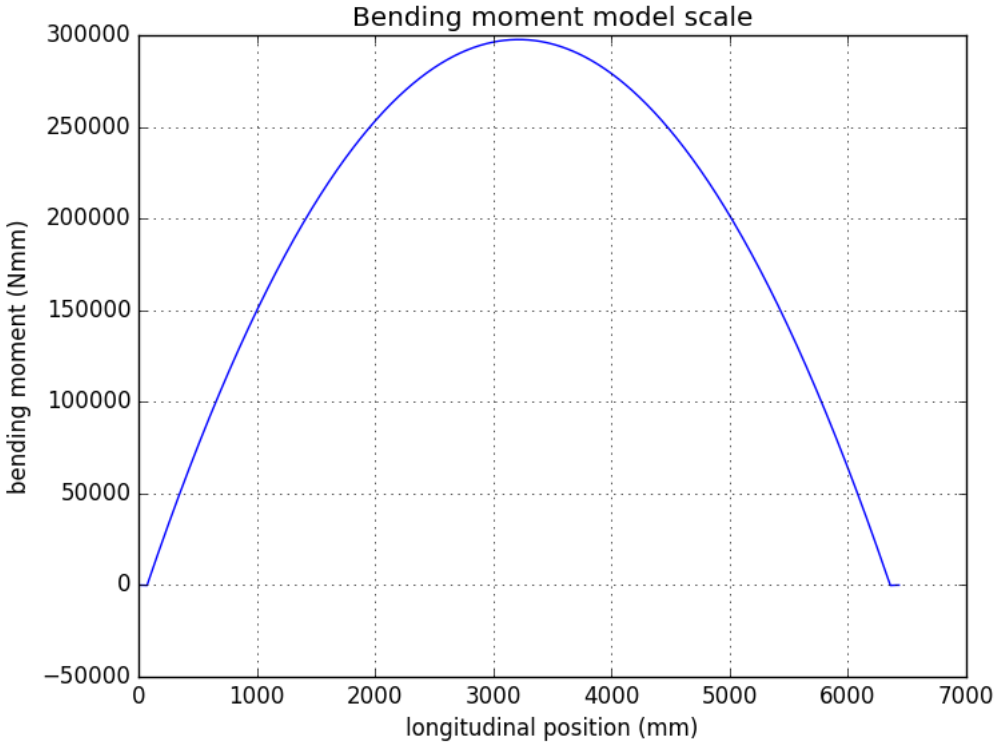

Figure 24 Bending moment model scale of test load

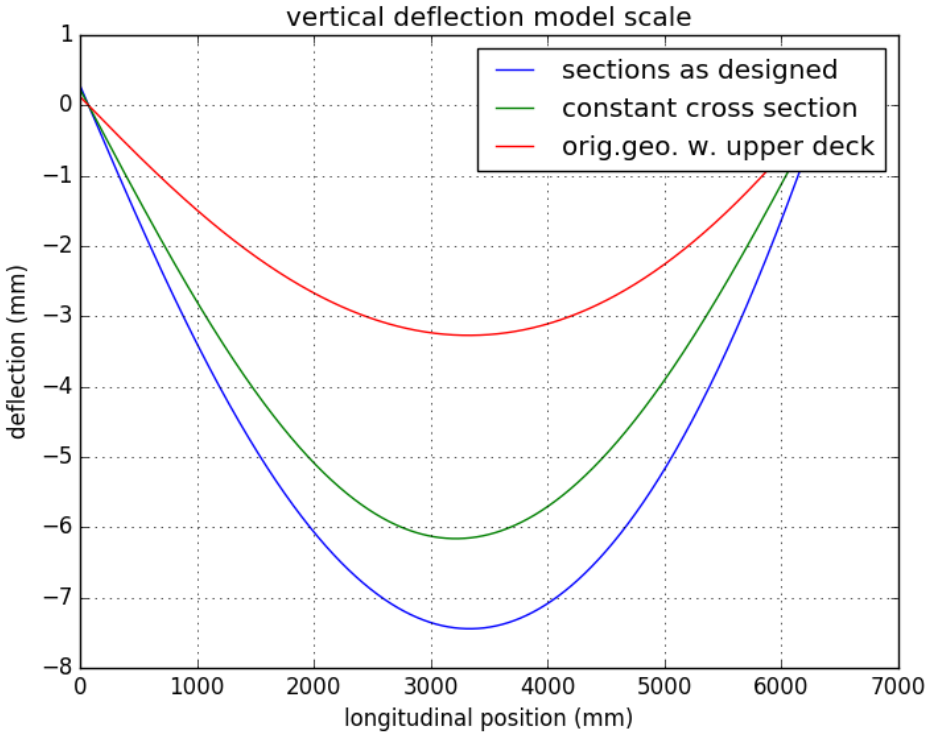

Figure 25 Vertical deflection in model scale

Figure 26 Stiffness coefficients in model scale

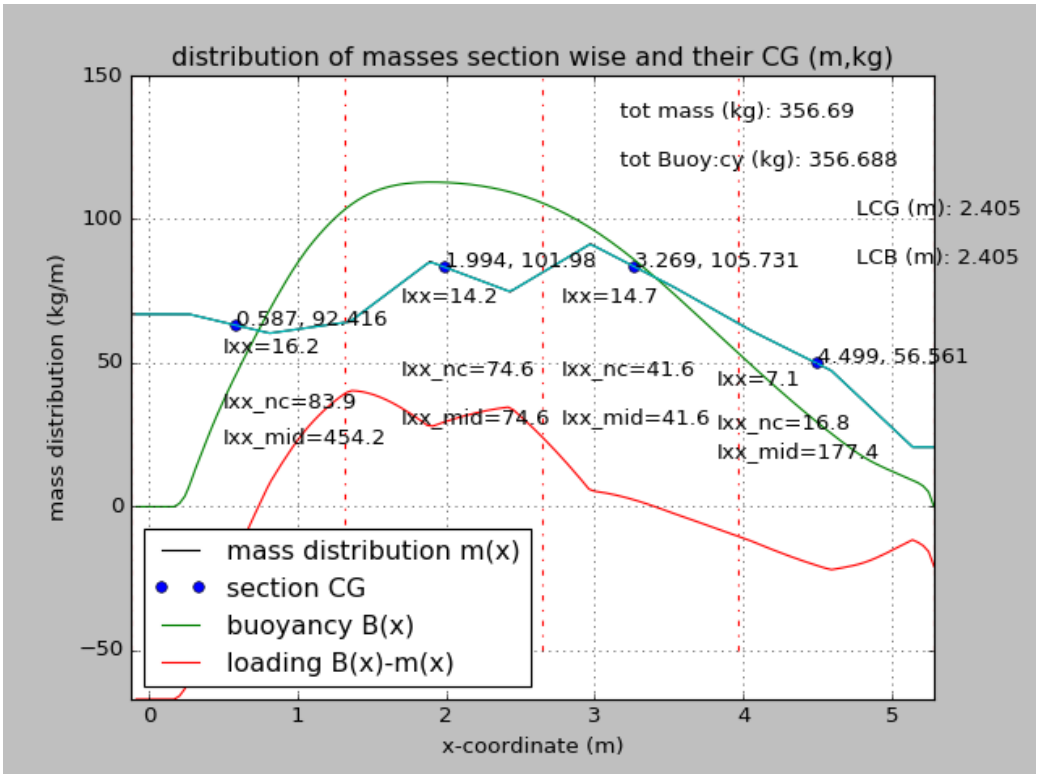

Figure 27. Scale model mass distribution, sectional masses, centre of gravity and radii of gyration.

6 Discussion, summary and conclusions

Some of the advantages, disantvatages and motivations for the chosen concept is presented and discussed in the subsections below.

Illustrations of the proposed model concept are shown in Figure 28 below.

The concept consist of a model built in four segments with hinges and adjustable springs at the hinges to be able to achieve the right static stiffness and 1st and 2nd global eigen frequencies.

In some mode detail, aluminium frames are attached to the hinges. Adjustable springs (the steel rods) are connected to the hinged side to provide correct static stiffness and eigenfrequencies. Force transducers are fitted to the unhinged side.

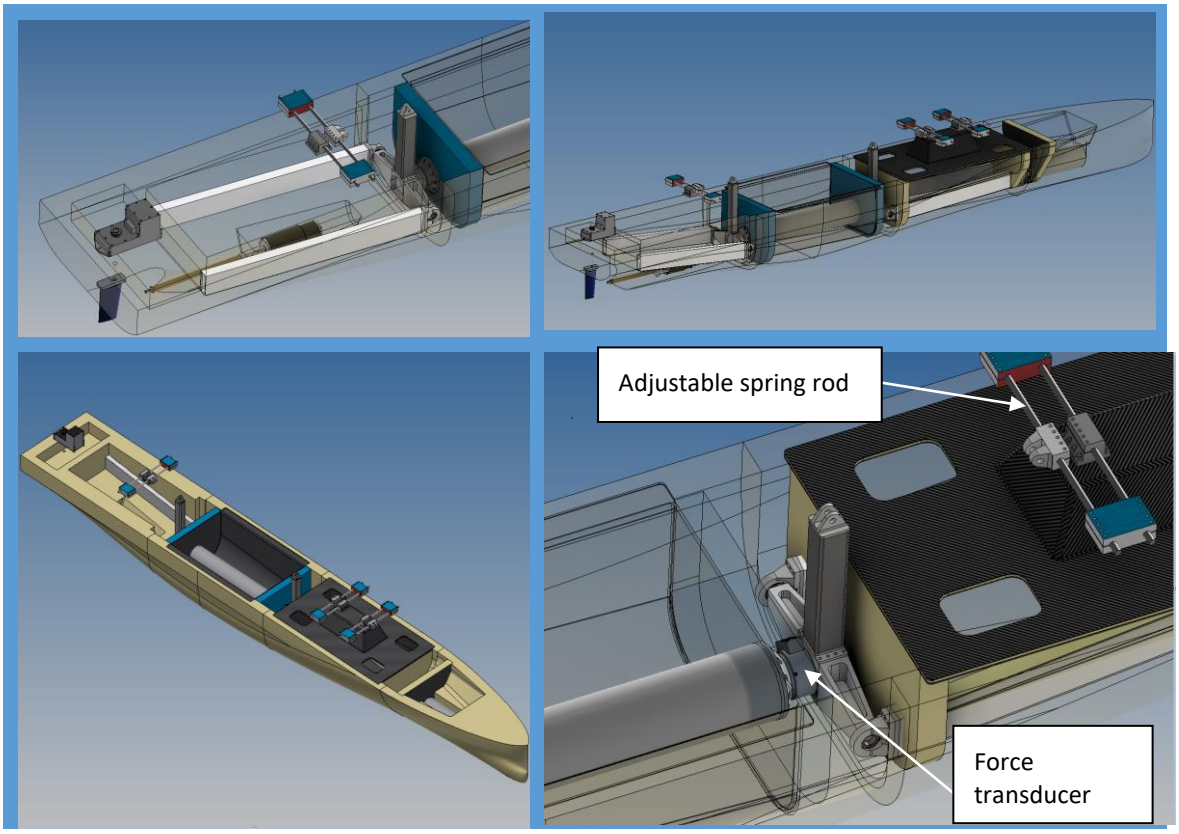

Figure 28. Illustration of model concept with four segments, hinges and adjustable springs in between

6.1 Discussion

With the current knowledge, model building technique and measurement technology at hand at SSPA Sweden a suitable model concept was put forward.

The current project propose a model built in four segments with hinges and adjustable springs at the hinges to be able to achieve the right static stiffness and 1st and 2nd global eigen frequencies. All three forces and all three moments are to be measured at the cuts. See Figure 28 for illustrations of model concept

It was considered to model structural dynamics in transverse bending. However, it was judged that the effect of structural dynamics due to lateral bending may be notable but that the design and construction of the model would be significantly more difficult. Further, it was also judged that the accuracy of measurements would be adversely affected and that it would be very uncertain to utilise such a model. The proposed model design already contain a number of novelties that need to be developed and evaluated to be able to introduce even further improved techniques:

- Six degree of freedom force (and moment) measurement integrated into one transducer
- Carbon fibre hull shell construction to be able to obtain the correct longitudinal mass distribution
- Pressure transducer set up to be able to utilise pressure reconstruction method to obtain pressure distribution on entire fore ship out of a few pressure gauges.
- Utilising optical measurements (Qualisys) to measure vertical deflection of the hull girder.

The above discussion hints also on some points of future research that may be proposed after the current set of projects:

- If and how the current setup can be extended to make a structural dynamic model of lateral bending.
- How important is modelling of correct shear centre?

6.2 Summary and conclusions

The targets for the current project was to put forward a model concept for testing structural dynamics in waves at SSPAs Marine Dynamic Laboratory (MDL). Hitherto a very limited number of model trials have been performed in wave basin with models capturing the most important structural dynamics with respect to fatigue life. Most of them have been purely research oriented. A few of them have given input to actual ship design. E.g. those described in ref. 3 and ref. 7.

The goal is to try out the model concept developed in the current project at a later stage, as described in *Figure 1* and thus be in the forefront of the current matter. Hence being able to provide leading services for ship owners and design firms for evolved and increasingly efficient and light hull structural design.

This is achieved by:

- Litterature study of research within the current matter
- Investigate possibilities and limitations of SSPAs facilities
- Gathering input from SSPAs project partners KTH, Chalmers and Stena Teknik AB
- Sum up the points above to find an optimal concept
- Document and present the model concept as CAD drawings, description of scaling principles and methods for determining model particulars

The concept proposed consist of a model with four rigid segments. The segments are connected by hinged joints with adjustable stiffness by the use of springs. The balance between accuracy and model complexity is achieved by modelling stiffness in vertical bending while keeping the other degrees of freedom fixed. Forces and moments are to be measured in all six degrees of freedom at each cut between the model segments.

A methodology for determining stiffness in joints is also put forward and described in the current report.

7 Detailed model design

Table *10 Position of fastening point for measurement arm from aft perpendicular, center line and baseline.*

Coordinate	Position (m)
X	2.327
Y	0
Z	0.355

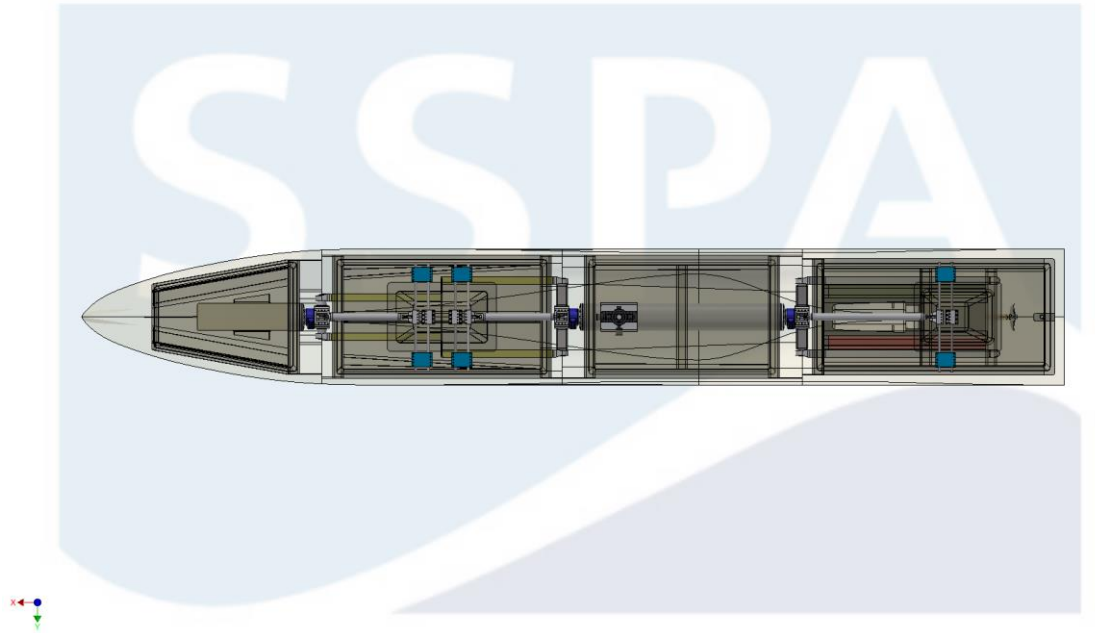

Figure 29. Overview of model design (from top)

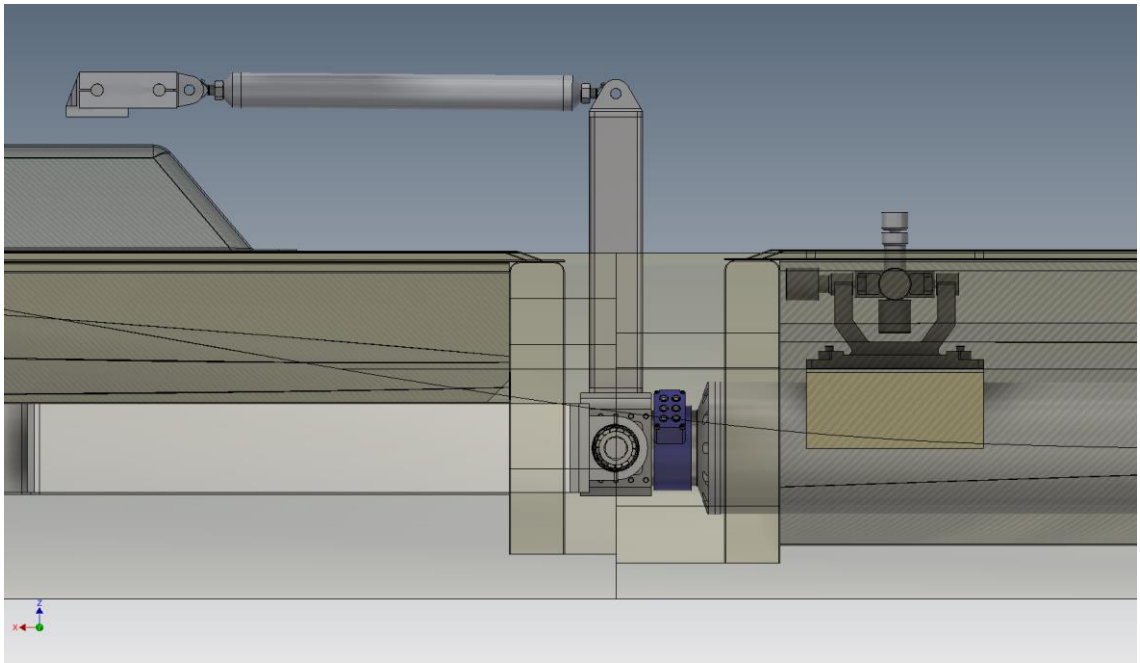

Figure 30. Detailed view of measurement transducer (in blue), hinged joint between segment 2 and 3 and fastener for measurement arm.

8 References

1. Ashar and Rodrigue, 2012. URL http://people.hofstra.edu/geotrans/eng/ch3en/conc3en/containerships.html
2. CLASSIFICATION NOTES, DET NORSKE VERITAS AS, No. 30.12, Fatigue and ultimate strength assessment of container ships including whipping and springing, JULY 2015.
3. Barhoumi M., Storhaug S. “Assessment of whipping and springing on a large container vessel”
4. Kapsenberg G.K., Veer van t. A.P.,” Whipping loads due to aft body slamming”, 24TH Symposium on Naval Hydrodynamics, Fukuoka, JAPAN, 8-13 July 2002
5. Dinsenbacher, A., Engle, A., Hermanski, G., 2010, Guidelines for Hydroelastic Model Design, Testing and Analysis of Loads and Responses, Report No. NSWCCD-65-TR-2010/12, Carderock Div, NSWC.
6. Md Emdadul Hoque “Dynamic Response of Ship Hull due to Slamming”, Msc thesis NTNU
7. Drummen I., “Experimental and Numerical Investigation of Nonlinear Wave-Induced Load Effects in Containerships considering Hydroelasticity”, Thesis for the degree of philosophiae doctor, Trondheim, June 2008, Norwegian University of Science and Technology Faculty of Engineering Science and Technology Department of Marine Technology.
8. Söderberg P. “The Swedish Coastal Wave Climate – Wave Statistics based on Measurements Carried out between 1978 and 1986”, SSPA No.104 1987, ISSN 0282-5805
9. https://www.stenateknik.com/projects/
10. Kim, J-H. and Kim, Y. (2014). Numerical analysis on springing and whipping using fully-coupled FSI models. Ocean Engineering, Vol. 91: pp. 28-50.
11. Mao, W., Ringsberg, J.W. and Rychlik, I. (2012a). What is the potential of using ship fatigue routing in terms of fatigue life extension? In: Proceedings of the Twenty-second International Offshore and Polar Engineering Conference (ISOPE2012) on Rhodes, Greece, June 17-22, 2012 (paper no. 1098-6189). Vol. 4 (2012), pp. 681-687.
12. Storhaug, G. (2014). The measured contribution of whipping and springing on the fatigue and extreme loading of container vessels. International Journal of Architecture and Ocean Engineering, Vol. 6: pp. 1096-1110.
13. Hong, S.Y. and Kim, B.W. (2014). Experimental investigations of higher-order springing and whipping-WILS project. International Journal of Architecture and Ocean Engineering, Vol. 6: pp. 1160-1181.

14. Mao, W., Li, Z., Ringsberg, J.W. and Rychlik, I. (2012b). Application of a ship-routing fatigue model to case studies of 2800 TEU and 4400 TEU container vessels. IMechE, Part M, Journal of Engineering for the Maritime Environment, Vol. 226: pp. 222-234.
15. https://github.com/rsmith-nl/beammech
16. Skype meetings with Gaute Storhaug, 2018-06-19 and 2017-06-15.

9 Appendix A – Ship data

Table A 1 Gross

		37	57	75	90	110	135	148	166	180	200
Cross sectional area of the longitudinal elements	m^2	1,77	2,02	2,13	2,21	2,16	2,14	2,09	1,93	1,35	1,03
Horizontal dist. from C.L. to vertical neutral axis, positive to port, Yn	m	0,00	0,00	0,00	0,00	0,00	0,00	0,00	0,00	0,00	0,00
Vertical distance fom B.L. to horizontal neutral axis, Zn	m	8,41	7,45	7,02	7,18	7,28	7,40	7,76	8,11	7,31	8,10
Vertical moment of inertia, Iy	m^4	41,90	56,10	61,83	65,65	64,28	62,04	57,30	50,64	34,59	26,74
Horizontal moment of inertia , Iz	m^4	124,35	143,89	156,42	157,72	152,48	146,14	136,18	109,96	73,22	43,94
Product of inertia about the neutral axes, Iyz	m^4	-0,001	0,00	0,00	-0,001	0,00	0,00	-0,001	0,00	-0,001	-0,001
Section Modulus, Bottom	m^3	4,98	7,53	8,81	9,15	8,83	8,38	7,39	6,25	4,73	3,30
Section Modulus, Strength deck at side (z = 21100mm)	m^3	6,17	7,24	7,56	8,18	8,12	7,96	7,70	7,14	4,38	3,77
Section Modulus, Equivalent deck line (z = 21100mm)	m^3	6,17	7,24	7,56	8,18	8,12	7,96	7,70	7,14	4,38	3,77
Section Modulus, at Side	m^3	8,98	10,39	11,29	11,39	11,01	10,54	9,83	7,94	5,33	3,55
First moment of the area above the neutral axis, S	m^3	3,61	4,63	5,05	5,29	5,18	5,04	4,73	4,27	2,95	2,27
I/S	m	11,61	12,12	12,24	12,41	12,41	12,32	12,13	11,86	11,71	11,75
Torsion constant, It	m^4	22	36	40	100	98	95	87	41	44	26

Table A 2 Net 50

		37	57	75	90	110	135	148	166	180	200
Cross sectional area of the longitudinal elements	cm^2	1,674	1,903	1,974	2,056	2,016	1,99	1,957	1,8366	1,267	0,968
Horizontal dist. from C.L. to vertical neutral axis, positive to port, Yn	m	0	0	0	0	0	0	0	0	0	0
Vertical distance fom B.L. to horizontal neutral axis, Zn	m	8,406	7,47	7,072	7,288	7,39	7,52	7,859	8,181	7,333	8,122
Vertical moment of inertia, Iy	m^4	39,19	52,29	57,17	61,54	60,25	58,08	53,76	47,796	32,15	24,86
Horizontal moment of inertia , Iz	m^4	117,8	136,4	144,1	146,6	141,7	135,8	127,2	105,43	69,35	41,57
Product of inertia about the neutral axes, Iyz	m^4	-0,001	0,001	0,001	-0,001	0	0,001	-0,001	0	-0,001	-0,001
Section Modulus, Bottom	m^3	4,662	7	8,084	8,444	8,153	7,723	6,84	5,842	4,385	3,06
Section Modulus, Strength deck at side (z = 21100mm)	m^3	5,768	6,764	7,034	7,777	7,715	7,562	7,324	6,81	4,087	3,512
Section Modulus, Equivalent deck line (z = 21100mm)	m^3	5,768	6,764	7,034	7,777	7,715	7,562	7,324	6,81	4,087	3,512

Section Modulus, at Side	m^3	8,506	9,849	10,4	10,58	10,23	9,797	9,182	7,612	5,044	3,361
First moment of the area above the neutral axis, S	m^3	3,388	4,33	4,667	4,94	4,835	4,698	4,42	4,037	2,754	2,121
I/S	m	11,57	12,08	12,25	12,46	12,46	12,36	12,16	11,84	11,68	11,72
Torsion constant, It	m^4	22	36	40	100	98	95	87	41	44	26

10 Appendix B - Testing practices

Scaling laws

Quantity	Prototype	Ideal Model	Practical Model
Length	L	L/λ	L/λ
Water Density	ρ	ρ/c	ρ/c
Time	t	$t/\lambda^{1/2}$	$t/\lambda^{1/2}$
Mass	m	$m/c\lambda^3$	$m/c\lambda^3$
Velocity	v	$v/\lambda^{1/2}$	$v/\lambda^{1/2}$
Acceleration	a	a	a
Force	F	$F/c\lambda^3$	$F/c\lambda^3$
Ship Displacement	Δ	$\Delta/c\lambda^3$	$\Delta/c\lambda^3$
Moment	M	$M/c\lambda^4$	$M/c\lambda^4$
Pressure	p	$p/c\lambda$	$p/c\lambda$
Frequency (flexural modes and Rigid body motions)	ω	$\omega\lambda^{1/2}$	$\omega\lambda^{1/2}$
Bending Rigidity	EI	$EI/c\lambda^5$	$EI/c\lambda^5$
Shear Rigidity	KAG	$KAG/c\lambda^3$	$KAG/c\lambda^3$
Modulus of Elasticity	E	$E/c\lambda$	E/e
Section Area			
Moment of Inertia	I	I/λ^4	$Ie/c\lambda^5$
Distance from neutral axis to outermost fiber for hull-girder (prototype) or strength bar (model)	y	y/λ	y/r
Section Modulus	Z	Z/λ^3	$Zer/c\lambda^5$
Flexure Stress	σ	$\sigma/c\lambda$	$\sigma\lambda/er$

Note:

λ is the ratio of prototype to model length

c is the ratio of prototype to model water density

e is the ratio of prototype to model modulus of elasticity

r is the ratio of distances from neutral axis to outermost fiber

From ref. 7.

Table 3.4: Measured inertial properties of the model. The numbering of the segments is as shown in Fig. B.1.

Description	Segm. I	Segm. II	Segm. III	Segm. IV	Model
M [kg]	82.1	277.9	327.9	153.3	841.2
LCG [m]	-2.26	-0.89	0.54	2.13	0.09
VCG [m]	0.44	0.25	0.23	0.35	0.28
I_{55} [kgm^2]	491.0	351.7	122.1	717.7	1682.4

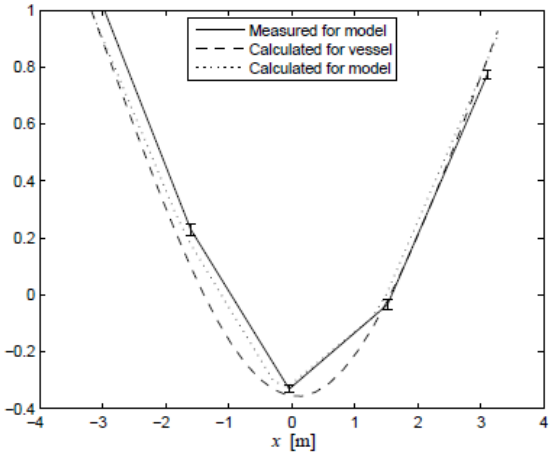

Figure 3.15: Normalised mode shapes of the two node vertical vibration mode. 'Calculated for vessel' refers to the wet mode for the objective (full scale) mass distribution and a continuous stiffness distribution. 'Calculated for model' refers to the wet mode for the measured mass distribution and a segmented stiffness distribution.

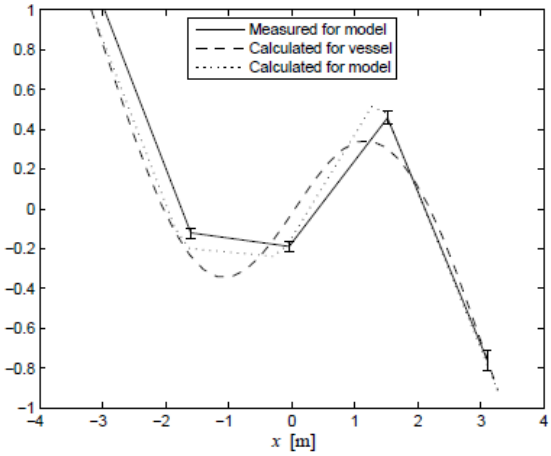

Figure 3.16: Normalised mode shapes of the three node vertical vibration mode. 'Calculated for vessel' refers to the wet mode for the objective (full scale) mass distribution and a continuous stiffness distribution. 'Calculated for model' refers to the wet mode for the measured mass distribution and a segmented stiffness distribution.

What is known before hand on forces and moments?

From ref 7

Full scale results from ref. 7. Scale, alfa =1:45 (in ref. 7) Lpp_s=294.01m ->Lpp_m)=6.53m

To obtain model scale moments the results shall be scaled by $1/alfa^4=1/4100625$. Forces are scaled to $alfa^3$.

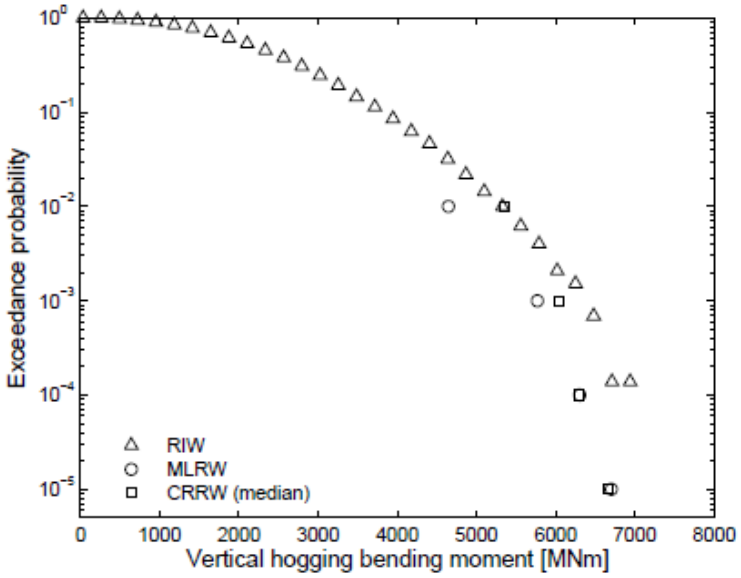

Fig. 8. Experimentally obtained probability distribution of the midships vertical hogging bending moment for a flexible hull. H_s=19m, T_p=15.89s and γ=4.75 (requested). RIW, MLRW and CRRW respectively denote random irregular wave, most likely response wave and conditional random response wave.

Approximation of Fz: My/(L/2)=>

Forces at Hs=19m

	Full scale	Model scale (L_m=6.53), alfa=45	Model scale (L_m=5.23) Alfa=56
My(p=$1e^{-3}$) [Nm]	$6e^9$	1463	610
Fz (approx.) [N]	$4.08e^7$	$4.48e^2$	$2.32e^2$

From ref 4

Full scale results from ref 4.

Lpp_s=233m, scale, alfa=1:49 =>Lpp_m=4.75

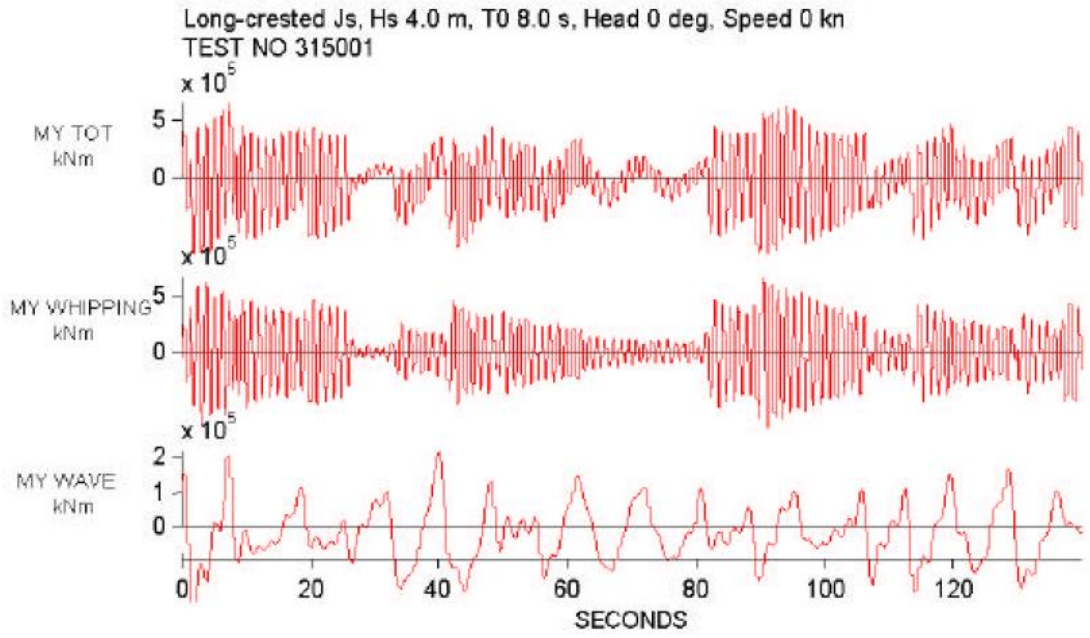

Figure 20 Time traces of the Vertical Bending Moment midships. Top: the total signal; Middle: the whipping component; bottom: wave frequent component.

Forces at Hs=4m

	Full scale	**Model scale (L_m=4.75), alfa=49**	**Model scale (L_m=5.23) Alfa=44.5**
My(max/1 series) [Nm]	$6e^{8}$	104	153
Fz (approx.) [N]	$5.15e^{6}$	43.8	58.4

Your Maritime Solution Partner SSPA

Trafikverket
781 89 Borlänge

Reference:
TRV 2017/41844 Ärende-ID 6459

REPORT
Date
2019-06-28
SSPA Report No:
RE40178202-00-01-A
Project Manager:
Olov Lundbäck
Author
Olov Lundbäck
+46 (730) 772 9177
olov.lundback@sspa.se

Model manufacturing and model tests

The current report is final report for one major part of the project “Dynamisk fartygsdimensionering”. The project as a whole has carried out a study consisting of the following parts:

1. Project management and co-ordination
2. Literature and concept study to put forward a model test methodology and conceptual design of a ship model for testing, analysis and evaluation of global and local structural responses
3. Detailed design for a model to be used for proof of concept of point 2 above
4. Test program and test methodology for proof of concept of point 2 and 3 above
5. Analytical structural analysis to support point 2,3 and 4 above
6. Numerical structural analysis to support point 2,3 and 4 above
7. Numerical hydrodynamic analysis to support point 2,3 and 4 above
8. Investigation of a novel method, in the current context, for pressure measurement and estimation of pressure distribution over large portions of a ship hull
9. Construction (building) of model for proof of concept of point 2 and 3 above
10. The actual performance of a model test series for proof of concept of point 2 to 9 above
11. Analysis of model tests
12. Comparison between model tests and analytical structural analysis
13. Comparison between model tests and numerical structural and hydro dynamical analysis

The current report contains final reporting of point 2, 3, 4, 5, 9, 10, 11, 12 and 13 above (Work package 1). Point 8 is reported in its own report (Work package 2). Point 6, 7 and 13 (Work package 3) is reported separately in one report, while point 1 and a project summary is presented in a summarizing wrap-up report.

SSPA Sweden AB

Joacim Linder
Vice president, Head of Department,
Maritime Consultants

SSPA Sweden AB

Olov Lundbäck
Work package manager, WP 1
Maritime Consultants

Revision History

Rev.	Publish Date	Description of changes	Signature
A	2019-06-28	Issued for Customer review	OLU

Summary and recommendations

The project as a whole was parted into three work packages:

1. Development of model concept, model testing techniques, -practices, detailed design and construction of model, evaluation techniques and supporting analytical methods. Senior advice for WP 3.
2. Pressure measurement and analysis.
3. Numerical analysis of hydrodynamics and structure.
4. Current report present work package 1 (WP 1).

The activities carried out in WP 1 led to the successful completion of the planned test series. Results of this test series give that the model concept works as intended, capturing all the most important physics. The actual model built and tested worked very well throughout the test series and gave, what seems as very accurate measurement of forces and moments, while measurement of deflections may be improved. However, forces and moments are the most important measured entities.

A lightweight model made of carbon fibre, divinycell and aluminium was designed and built. The lightweight design was necessary to provide possibility to attain the same mass distribute as the full-scale ship.

The structural properties of the model, such as stiffness, mass distribution and structural damping met the targets of the full-scale ship.

For models, where larger forces and moments are likely to occur (i.e. larger displacement and longer) one size larger transducers are likely to be needed or an alternative test setup.

A comparison between model tests and numerical computations have been performed in work package 2. A survey shows that numerical tools, off-shelf today does not offer a possibility to analysis the coupling between structural motions and hydrodynamics. Instead a quasi-static hydrodynamic numerical approach was utilised. Results show that, even for a slender ship, this approach is not accurate enough. However, the combination of model tests and numerical analysis with todays tools seem to be feasible.

For further method development, it is proposed to put forward a method to obtain a minimum test matrix to faithfully represent a ships life, in terms of structural dynamics and fatigue. It is also proposed to put forward numerical tools that can be used to simulate the coupled structural and hydrodynamics of a ship navigating in waves.

Table of Contents

1 Introduction

1.1 Project set up

A forerunner of the current project was funded by SSPAs funds to be able to make a conceptual design of the model tested during the current work. Figure 1 display basic schematics of the workflow. At part 1 SSPA performed the entire work. During part 2 in Figure 1, SSPA carried out project coordination, analytical study and the work related to model tests, KTH undertook an investigation of pressure measurement and method to estimate pressure distribution, while Chalmers performed numerical computations.

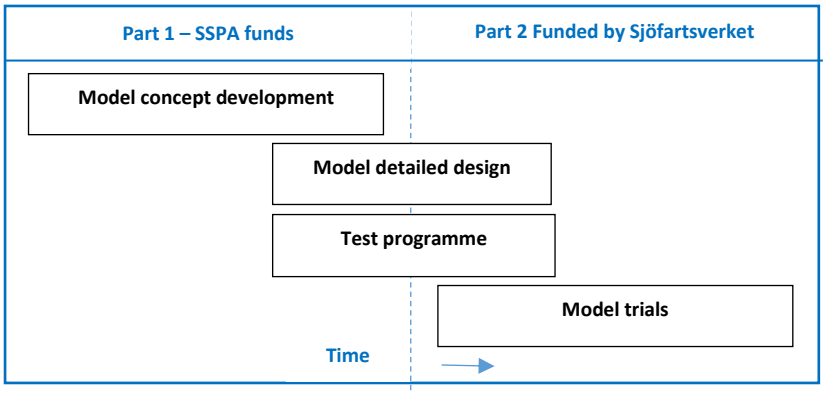

Figure 1 Schematic description of project set up and work flow

1.2 Whipping and springing

Whipping is the transient elastic vibration of the ship hull girder caused for example by slamming. Because of small damping ratio, the decay of whipping-induced responses is slow. Springing and whipping may therefore be difficult to distinguish when slamming occurs frequently.

Springing is the steady-state resonant vibration of the two-node flexural mode due to continuous wave loading. Linear springing is said to occur when the wave encounter frequency is equal to the natural frequency of the two-node flexural mode, nonlinear springing when it is a multiple of the encounter frequency that equals the two node natural frequency. Springing can also be related to the higher flexible modes. Due the high natural frequencies of these modes, they are, however, not very likely to be excited.

To accurately model whipping and springing it is needed to account for fluid structure interaction, noted by e.g. Storhaug, ref. [11]. This is not yet implemented in state-of-the-art ship motion simulation programs, ref [16] and [17]

1.3 Notes on hull structural dynamics and its impact on the marine industry

Traditionally, quasi static wave loads have been applied for analysis of structural strength and -design of ship hulls. This approach has been working well for many ship types and operational profiles. In practice it has also been, the only wide spread and established method for hull scantling due to wave loading. However stricter design rules, attributed to whipping and springing, appeared in the 1960'ies for inland water vessels. Evidence of shortcomings of quasi static load analysis for other ship types have been identified, if not

earlier, around year 2000. Then a large ore carrier operating in the north Atlantic was strengthened due to severe fatigue cracking, where half of the damage have been estimated to come from whipping/springing [11].

18th of January 2007 the UK-flagged MSC Napoli was subject to severe hull cracking due to extreme loads in the English Channel. Whipping is assumed to constitute a significant contribution of loading during the extreme event.

The accident investigation [12] states:

"The load and capacity assessments conducted by DNV and BV (Figure 26) show that, in the case of MSC Napoli, the design margin of safety was either insufficient when whipping is taken into account (BV), or non-existent (DNV). The analyses are supported by the fact that the vessel broke her back when within her seagoing limitations and, although the conditions were severe and had a low probability of occurrence, they were nevertheless equivalent to the current UR S11 design value.

Although it is implicit in UR S11 that the design of a ship ensures that her ultimate strength is in excess of the maximum loads expected, the scope of the excess or safety margin is not defined. In practice, it is generally based upon a classification society's experience, and does not explicitly take into account factors which increase bending moments such as whipping, or other variables such as inaccuracies in container weights and distribution. Given the importance of the design safety margin in ensuring an acceptable level of safety, a more methodical and objective approach is warranted."

Reference [12], further request research and updated design principles.

"In view of the potential increase in wave loading due to whipping effect, further research is required by classification societies to ensure that the effect is adequately accounted for in ship design and structural analyses, and that sufficient allowance is made for the effect when determining design margins."

After the wrecking of MSC Napoli, several classification societies undertook research and development within structural dynamics. This led to adjustment of scantling rules, however not by faithful representation of physics, for IACS member societies.

Figure 2. Photo from ref [12] showing some of the extent of the hull damage that led to scrapping of the container ship MSC Napoli after abandonment and beaching to prevent sinking.

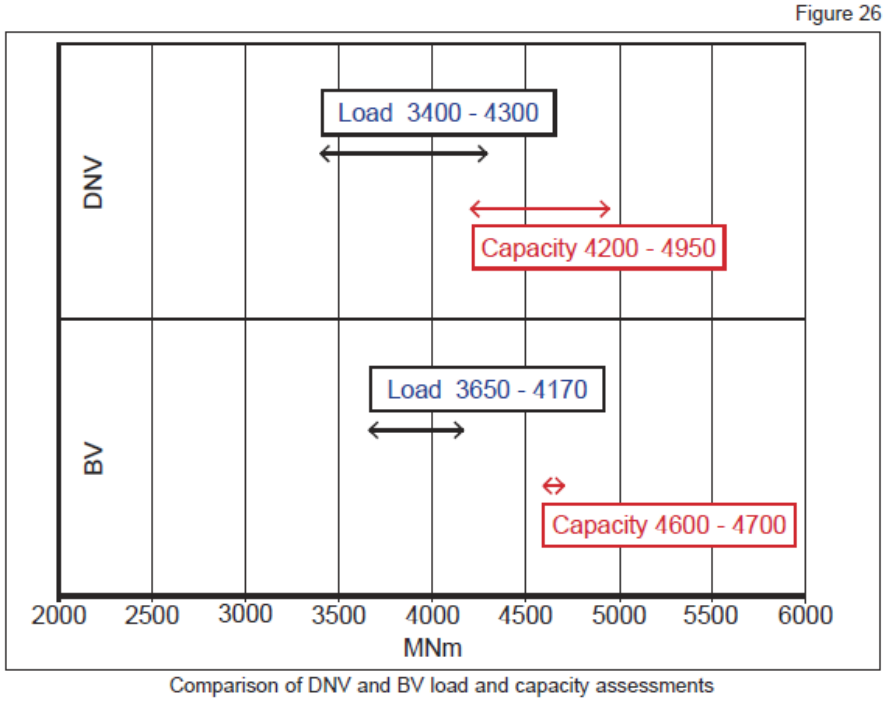

Figure 3. The accident investigations summary of the involved classification societies' analysis of loads and hull girder capacity at position of the crack in the hull of MSC Napoli. Figure 26 of ref. [12]. The graph does not include whipping effects.

1.4 Development within the maritime industry with bearing on structural dynamics

It is often noted that development and optimisation of ships as load carriers lead to increase in ship size and structures that are more and more light weight designs by their character.

Such a development leads to structures that are to carry more and more load per structural weight. In terms of structural dynamics, generally this means lower eigen frequencies. In general, this mean that the occurrence of wave encounter and wave impact that excite global and local structural eigen frequencies increase. Figure 4 illustrate the growth in size of container ships over the years.

During the 1970'ies The US Coast guard identified a need for more knowledge on structural dynamic loads for large ore carriers in service at the great lakes. In ref. [13], there is a presentation of research work performed jointly by US Coast Guard, National Research Laboratory (NRL), The American Bureau of Shipping (ABS), Webb Institute of Naval Architecture, the University of Michigan (UM) and Det norske Veritas (DnV)

Ref [13] reports:

"The American Bureau of Shipping and the US Coast Guard agreed upon of a set of interim rules for Great Lakes bulk carriers in March 1978. The requirements, which account for both the wave-induced and springing loads, are based on all the available research results of the past ten years. It still had several possible weak areas which the current research is attempting to either satisfy or strengthen."

Table 1. Measurements of max stresses on Stewart J. Cort

Storm	Date	Max Comb Stress (psi)	Max Springing Stress (psi)	Max Wave ind. Stress (psi)	Factor Total/ wave induced
1	02-maj	29400	16600	16000	1.77
2	08-nov	17677	7225	14800	1.19
		23600	5200	22400	1.05
3	10-dec	17300	6600	15500	1.12
		19100	7600	13330	1.43
4	13-dec	19200	10660	12700	1.51

Results of Table 1 are taken from [13]. The rightmost column shows that there is a significant contribution from structural dynamic loads. It can also clearly be seen that dynamic loads does not only contribute to high cycle fatigue but also to a significant accession of extreme loads.

Figure 4 Stewart J. Cort, which is still in service at the great lakes.

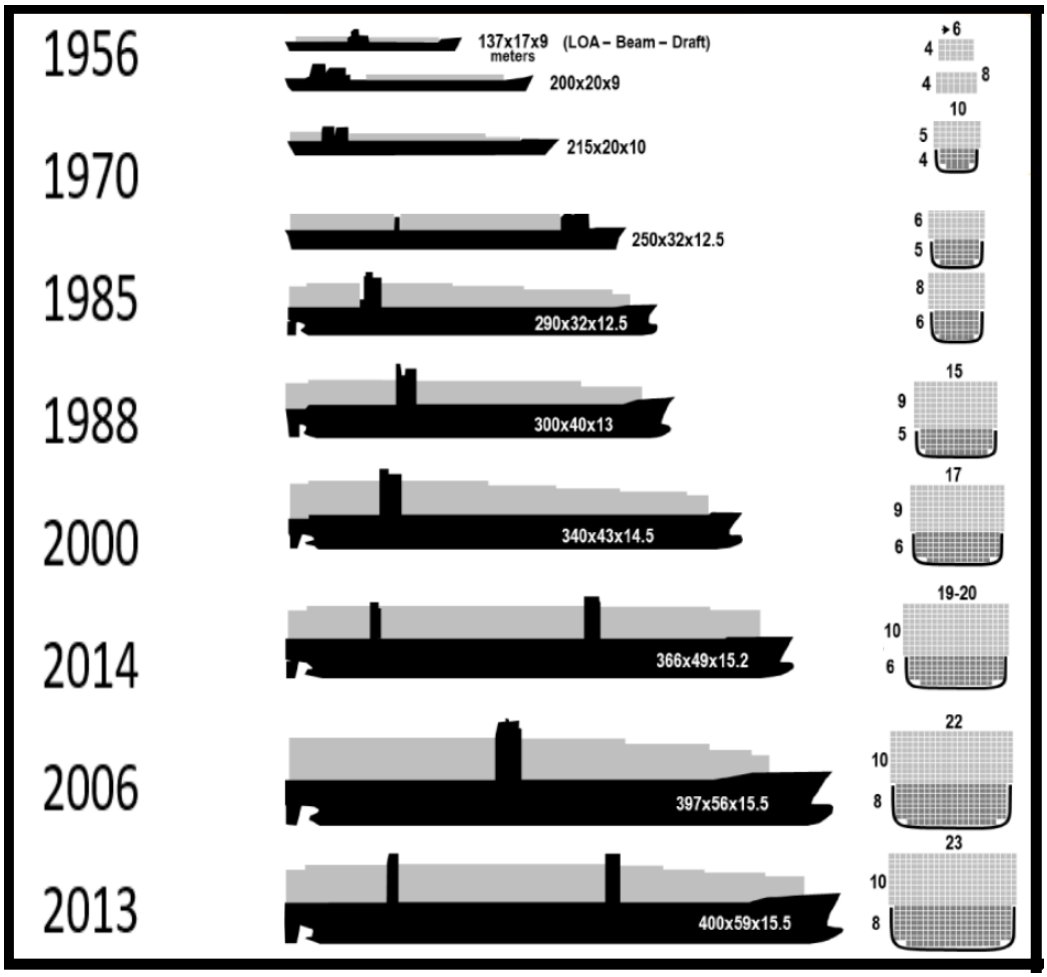

Figure 5. Illustration of size increase of container ships over the years.

1.5 Choice of ship and ship particulars

Stena Teknik AB, as a project partner, have been expressing a strong belief in lighter and more efficient ship structures in the years to come. They have also expressed a strong wish to investigate how a light structure could be incorporated in their future fleet. Their most recent testbed for innovations and increased efficiency within marine transport, Stena Electra, was hence chosen for the current project.

Stena Elektra is in an early phase in the design work. Many ship characteristics are still unknown, e.g. the vertical center of gravity (VCG or KG). The VCG value used throughout the current project is an estimation based on similar existing Stena Ships, Stena Electras transverse metacentric height (KM) and SSPAs manoeuvring database, shown as scatter plots in Figure 7. For these scatter plots it is worth to note that some ships are present with several loading conditions.

Figure 6. Rendered image of projected design for Stena Elektra.

Table 2 Comparison of main particulars for different Ro-ro ships

	Elektra, T=6.3	**Jutlandica, T=6.0**	**Germanica, T=6.0**	**Saga, T=6.8**	**Danica, T=6.3**	**Nautica, T=5.86**
Length between perpendiculars [m]	195.5	169.0	221.75	150.0	133.5	126.0
Beam [m]	26.46	27.8	28.7	28.4	28.5	24.0
Displacement [m^3]	17978	18400	28256	16595	15651	11081
Draught [m]	6.3	6.0	6.0	6.8	5.86	6.3
KG [m]	11.61[1]	12.5	11.87	13.4	13.0	10.0
GM [m]	2.1[1]	2.0	1.8	2.0	3.7	2.5
Note 1: Estimated values based on similar Stena Ships, Elektras KM-value of 13.71 and a cut out of SSPAs Manouvring database shown in Figure 7						

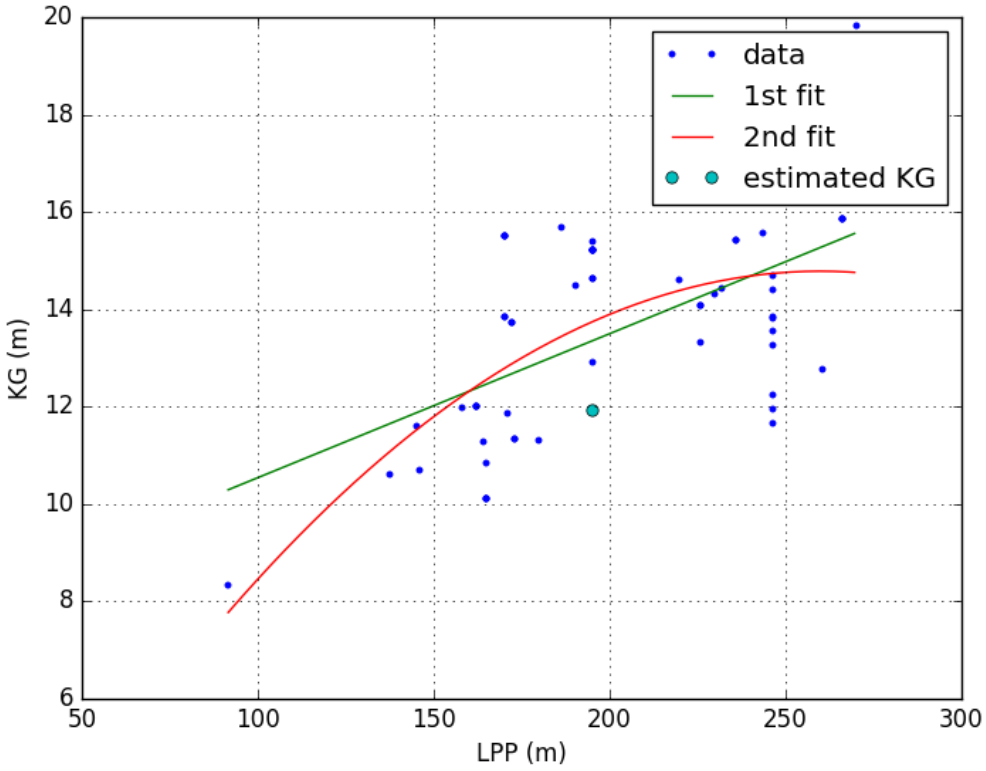

Figure 7. Scatter of VCG vs shiplength for similar ships in SSPAs manoeuvering database

2 Choice of model concept

Most of the work on choice of model concept has been performed in a forerunner of the current project. That forerunner was performed internally at SSPA. For the current latter part external partners were invited to participate. The current section summarize the work on choosing model concept. In Figure 8 below possible model types are described together with their respective advantages and disadvantages.

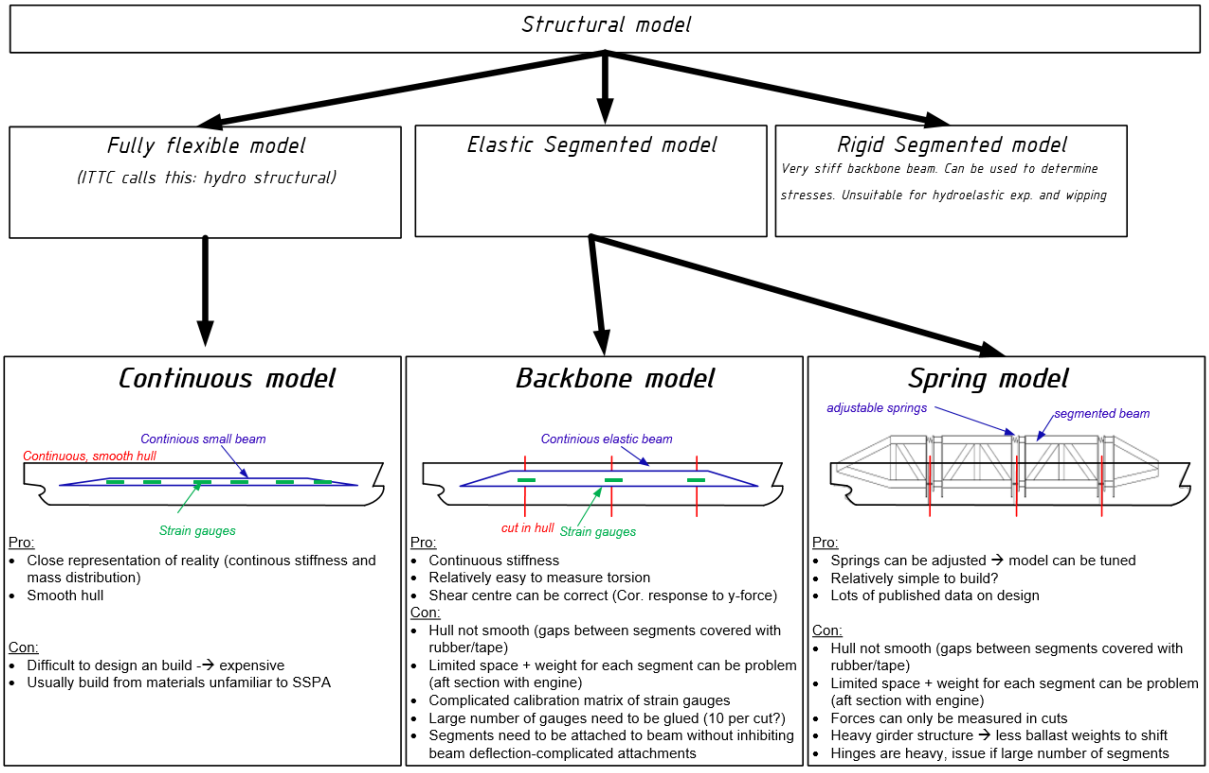

Figure 8. Illustration of main choices regarding model design.

2.1 Requirements for model concept

During the project, several requirements for the model concept have been identified. They can be summarised by the points below.

Must have:

1. Facilitate exact measurements of forces and moments for the most important degree of freedom
2. Provide a faithful representation of the lowest global eigen modes in the most important degree of freedom.
3. Measurement of motions with good accuracy in the most important degree of freedom
4. Exact measurements of forces and moments in all six degrees of freedom.
5. Economically feasible.

Good to have:

6. Measurement of motions at the other degrees of freedom
7. Provide a faithful representation of lowest eigenmodes at other degrees of freedom

2.2 Choice of model concept

When the concept types described in Figure 5 are weighted against the project requirements in section 2.1 above, the concept– spring model comes out as the best of the “must have – requirements” i.e. requirement 1-5.

This is especially true when it comes to exactness of measurements and fidelity in structural dynamics for the most important degree of freedom (vertical bending). For the “good to have – requirements” the spring model type is not a practical solution but on the other hand none of the other two model concept types fulfil all the “must have –requirements”. Hence the choice of model type is the spring model described in Figure 8.

3 Design of experiments and model set up

Four six component scales for measurement of forces and moments, on a model concept described by ref 1 and Figure 9, were purchased. Three of the scales were used at the tests and one scale was used for calibration purposes.

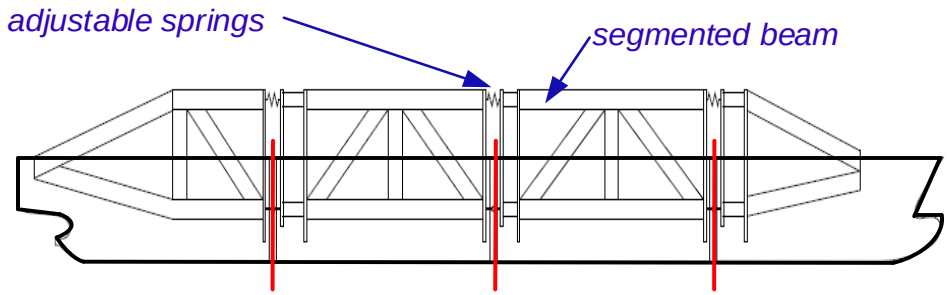

Figure 9. Illustration of model concept design

3.1 Design of model

The Concept ship Stena Electra is on an early project stage. For the current project there was no rudder design available. This led to a project specific rudder design. Calculation according to industry standards were performed. They gave the following values:

Input to rudder area calculation
Ship name: Stena Electra 40178202
Lpp: 195m, Bwl: 26.46m, T: 6.3m, displ: 17978m3
Cb= 0.55
Rudder recommendation DnV (Atot) old: 17.9 m2
Rudder recommendation DnV (Atot) new: 15.7 m2
Rudder recommendation SSPA (Atot): 28.5 m2

The Area recommendation according to SSPA (Norrbin) was chosen

A comparison of two ships of the same type in the same size range gave that the chosen value is reasonable.

Table 3. Comparison of different Ro-ro ships and their rudder area.

Ship name	Lpp (m)	B (m)	T (m)	Displ (m3)	No. rudders	Ar (m2)
Ship 23	158	25	5.8	14374	2	16.8
Ship 35	165	32.25	9.2	33079	1	36.3
Stena Electra	195	26.46	6.3	17978	1	28.5

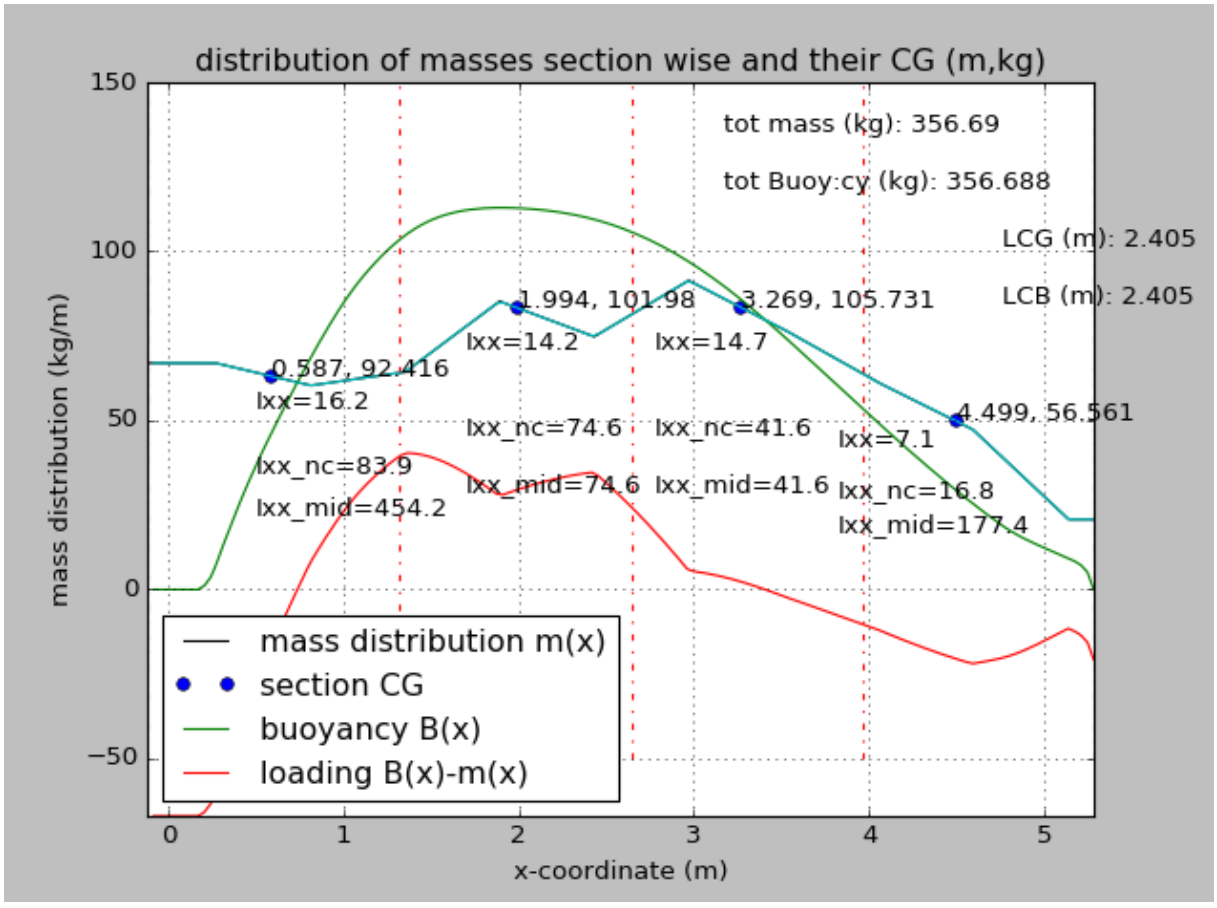

Figure 10. Buoyancy, mass –distribution and loading on Stena Electra in a preliminary design load case.

Table 4. Mass distribution in tabular form (model scale)

X (m)	-0.122	0.27	0.81	1.35	1.89	2.43	2.97	3.51	4.05	4.59	5.14	5.28
As run (fresh water) (kg/m)	66.97	66.97	60.34	64.29	85.26	74.77	91.41	77.05	61.31	47.47	20.73	20.73

X (m)	-0.122	0.27	0.81	1.35	1.89	2.43	2.97	3.51	4.05	4.59	5.14	5.28
Salt water values (kg/m)	68.47	68.47	61.69	65.73	87.17	76.45	93.46	78.78	62.69	48.54	21.2	21.2

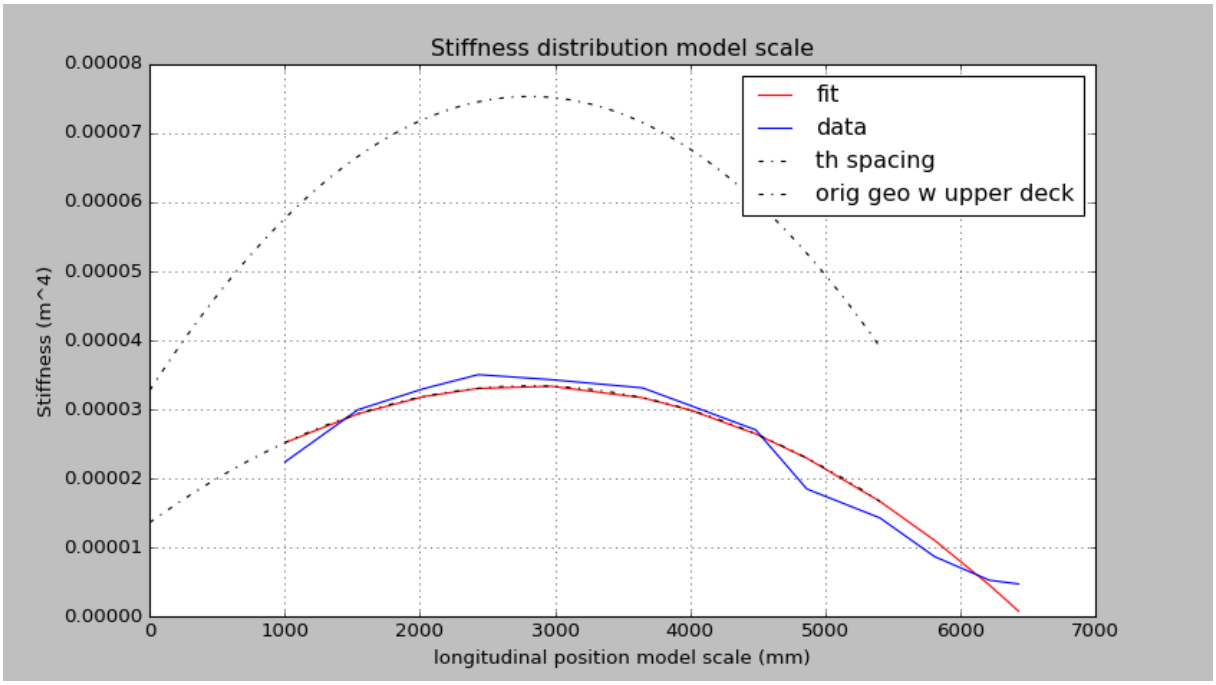

Figure 11. Fitted stiffness distribution used in simplified beam model ('th spacing').

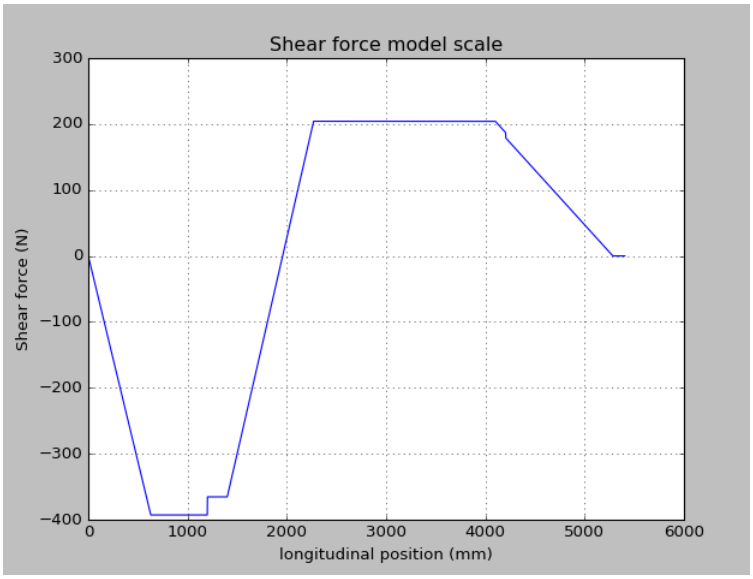

Figure 12. Shear force on the simplified beam model from the load case in Figure 10.

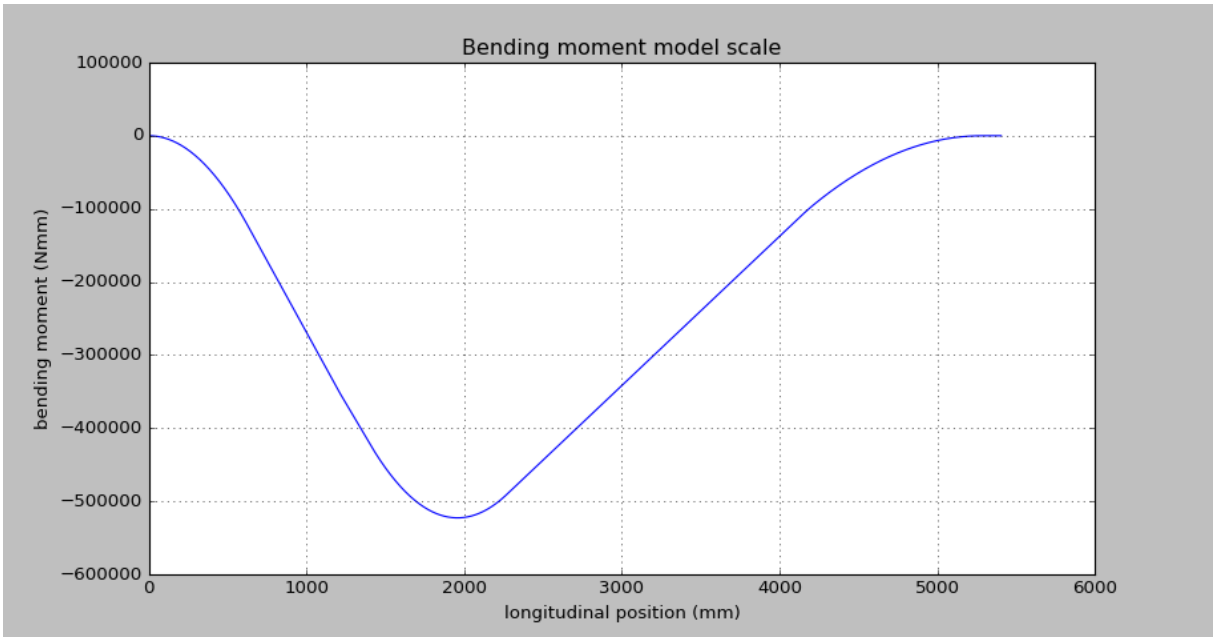

Figure 13. Bending moment on the simplified beam model from the load case in Figure 10.

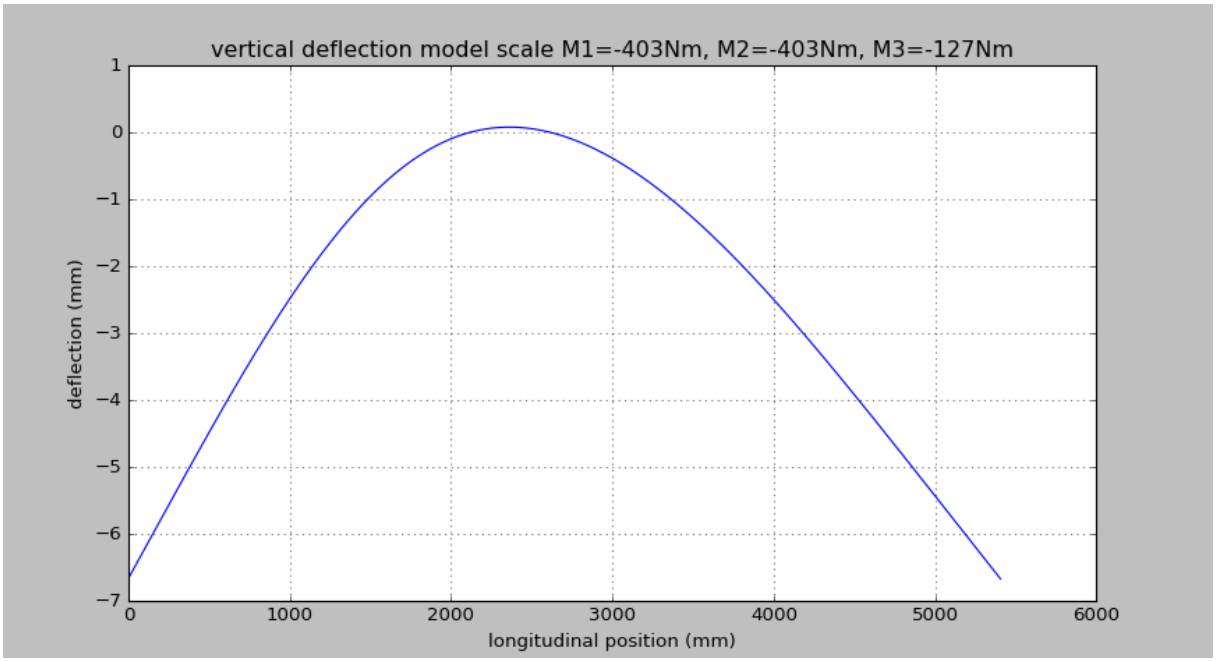

Figure 14. Deflection of simplified beam model.

3.2 Description of model design

Figure 15 illustrate the outcome of the extensive design work to obtain a model corresponding to project objectives, carried out at SSPA. In summary requirements on the model were:

1. Low structural damping, lower than or equal to 0.5%
2. Scaled stiffness virtually identical to full scale ship
3. Mass distribution equal to full scale ship
4. Very accurate measurement of internal forces and moments in the hull structure
5. Possibility to record structural motions with reasonable accuracy.

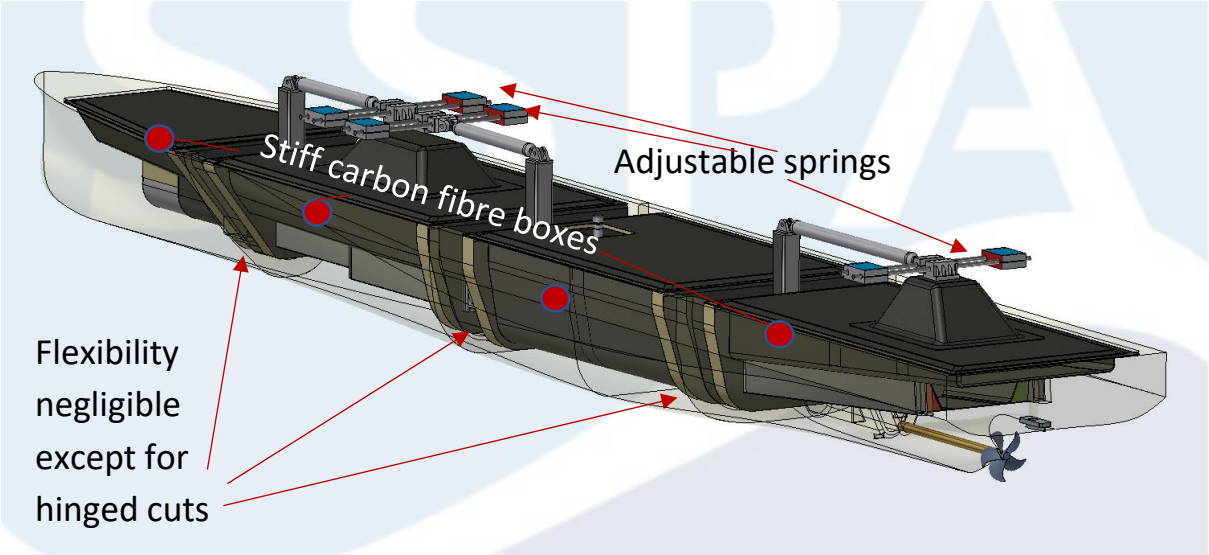

Figure 15. Model design and main features

It was considered to model structural dynamics in transverse bending. However, it was judged that the effect of structural dynamics due to lateral bending may be notable but that the design and construction of the model would be significantly more difficult. Further, it was also judged that the accuracy of measurements would be adversely affected and that it would be very uncertain to utilise such a model. The model design, nevertheless contains a number of novelties needed to be tested and evaluated:

- Six degree of freedom force (and moment) measurement integrated into one transducer
- Carbon fibre hull shell construction to be able to obtain the correct longitudinal mass distribution
- Utilising optical measurements measure vertical deflection of the hull girder.
- Low friction hinge

3.3 Set up of resonance test on land

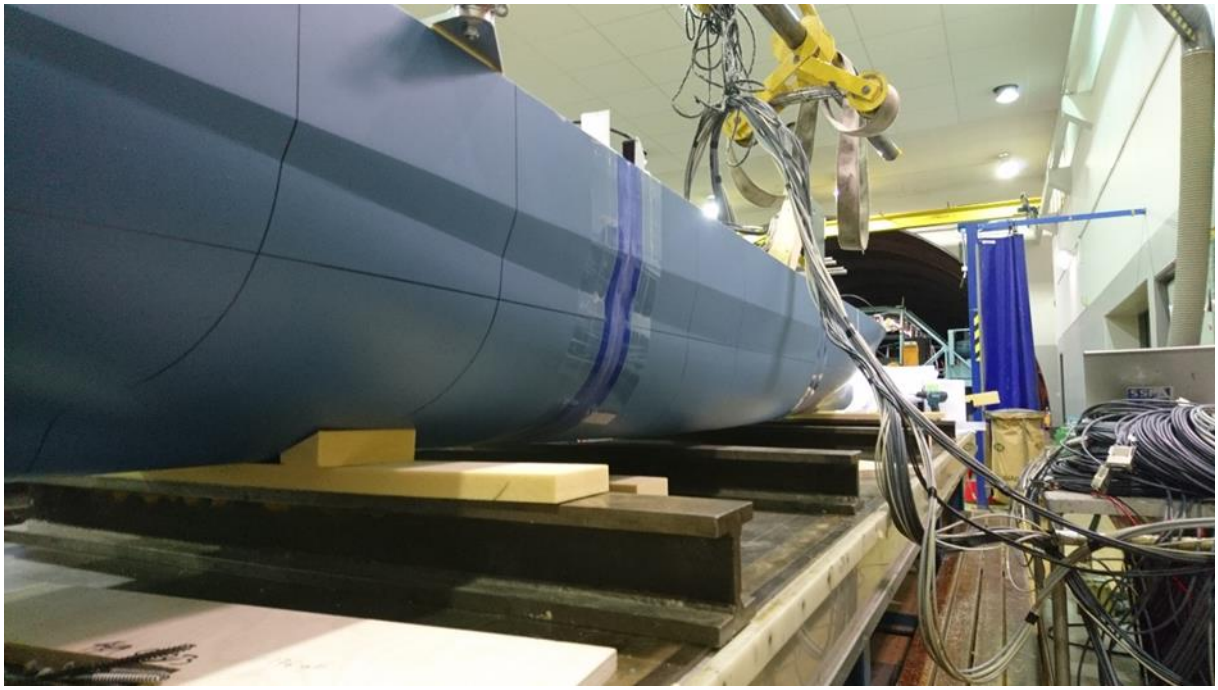

Figure 16. setup for resonance test. The supports in fore and aft are 1100mm from fore and aft respectively. Mid support is merely a safety measure to limit motions in case they would have become too high.

The resonance test was set up to be able to make a cross check, with static deflection test and measurement of mass distribution, that the stiffness and mass distribution is correct and to be able to compare resonance frequency in water with resonance frequency on land. The dry resonance frequency and the resonance frequency in water was compared to theoretical relation for their relative values.

Figure 16 display the setup for measuring resonance frequency on land.

4 Design of test programme

One part of the test programme is designed to excite the hull girder eigen-frequencies as much as possible.

Another part of the test programme is designed to provide as much non-linear excitations as possible. I.e. high and/ or steep waves.

Resonance frequency of full-scale ship in water is 0.87Hz, which correspond to 5.5rad/s or a period of 1.15s. The smallest sea states of Table 5 have a zero-crossing period of approximately 5.4s and a peak period of approximately 7.6s. According to eq. 3 the encountering (angular) peak frequency is approximately 3.9ad/s at 18kts. This is close enough to the structural resonance frequency of 5.5rad/s to have sufficient wave energy coinciding with the structural resonance frequency to excite some amount of springing. However, for a large springing contribution, the ship structure needs to have lower resonance frequency.

The equations below give relations between the wave period T, wave length, λ, wave frequency ω, course relative to waves μ and encountering wave frequency ω_e:

$$\boldsymbol{T = \frac{2 * \pi}{\omega}}$$	(1.)
$$\lambda = \frac{2 * \pi * g}{\omega^2}$$	(2.)
$$\omega_e = \omega - \frac{\omega^2 * U}{g} * \cos(\mu)$$	(3.)

Table 5. Average of wave heights and wave period including expected frequency of occurrence.

Sea State	Sign. wave height $H_{1/3}$ [m]		Wave period T_Z [s]	Expected frequency [%]
	range	mean value		
0-2	0-0.5			10.8
3	0.5-1.25	0.88	4.9	30.0
4	1.25-2.5	1.88	5.4	34.3
5	2.5-4.0	3.25	6.6	18.1
6	4.0-6.0	5.00	7.7	5.8
7	6.0-9.0	7.50	9.2	0.9
8	9.0-14	11.50		

Table 6. Sea states tested.

Sea state	Wave period 1	Wave period 2
4	Normal	Shortened
5	Normal	Shortened
6	Normal	-

Table 7 Wave conditions tested for each speed and course direction.

$H_{1/3}$ (m)	T_{p1} (s)	Tp_2 (s)
1.88	7.6	4.0
3.25	9.2	5.0
5.0	10.8	-

Two speeds were run for each sea state (5pcs) at each course direction (2pcs). In total this give 5*2*2 = 20 conditions. Ship structural dynamics is to a large extent triggered by non-linear phenomena. Hence it is required to run several conditions six times to gather a reasonable amount of statistics. In the current work. In average each run was repeated 4 times for this purpose, giving 80 test runs in waves in total. Added to this were preparation tests performed both in the towing tanks trim tank (to measure static moments) and in MDL to find resonance frequency in water plus the regular speed calibrations, roll decay tests, etc.

4.1 Test setup

Figure 17 show the model during outfitting, Figure 18 show the model during testing and Table 8 show full-scale main particulars of the ship model tested.

Table 8 Target values in full scale for tested model

Item	Values	Comment
Draught fore	6.3m	Due to variation in e.g. air pressure and temperature, the draught of hydrostatic equilibrium will vary in some extent
Draught aft	6.3m	Due to variation in e.g. air pressure and temperature, the draught of hydrostatic equilibrium will vary in some extent
Length between perpendiculars	195.50m	

Item	Values	Comment
Beam	27.70m	
Waterline length	187.68m	
Beam in waterline	26.46m	
Vertical center of gravity	11.61m	

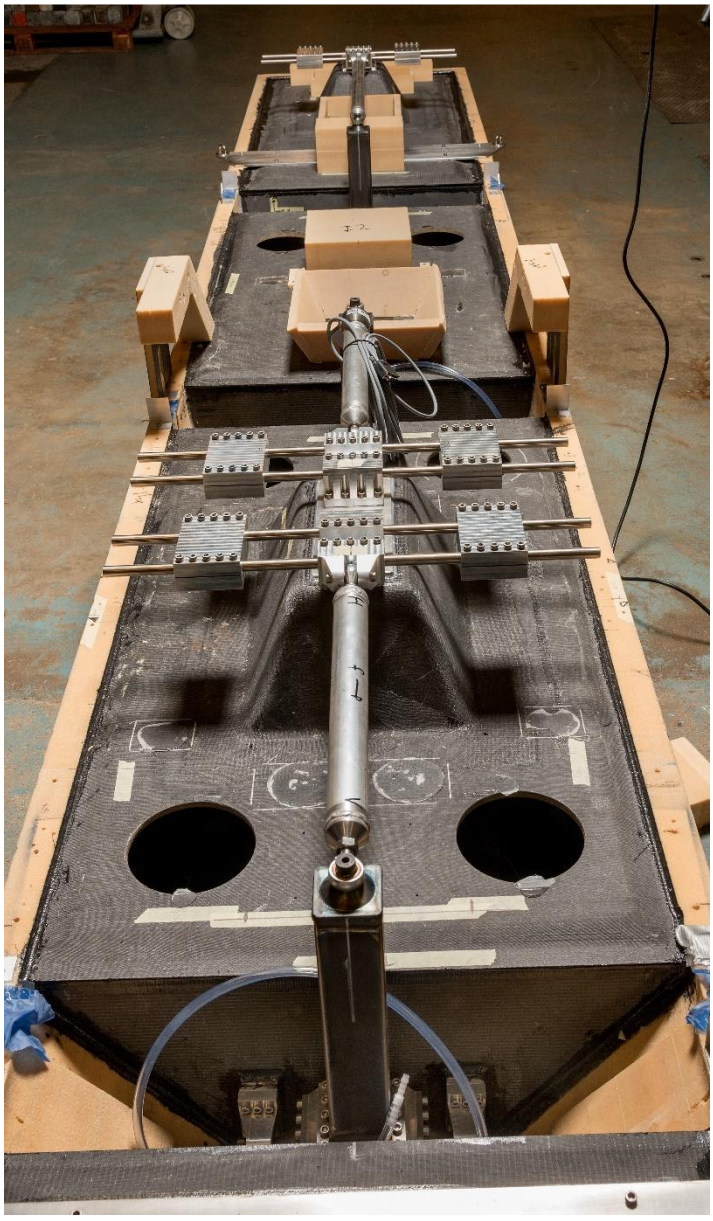

Figure 17 Ship model during outfitting

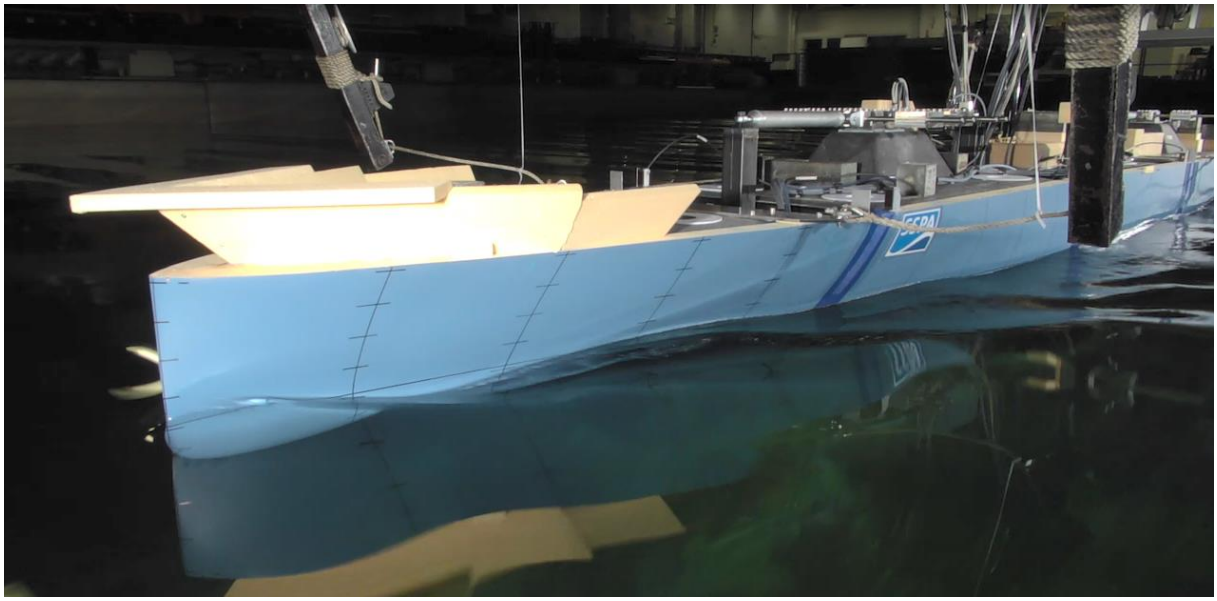

Figure 18. Ship model during testing

The ship model was parted into four cuts with a six component transducer measuring three forces and three moments at each cut. The model was fitted with adjustable stiffness at the hinge adjacent to each cut as illustrated in Figure 15, Figure 17 and Figure 18.

Table 9 shows a list of primary measured entities. Auxiliary entities regularly used to control the lab are not listed, such as propeller rpm to keep speed etc.

Table 9. List of measured primary entities.

Snitt 1	
Mätstorhet	**Givare**
Vertikalt böjmoment	6-komp-våg1, ch 1
Vertikal skjuvkraft	6-komp-våg1, ch 2
Horisontellt böjmoment	6-komp-våg1, ch 3
Horisontell sjuvkraft	6-komp-våg1, ch 4
Torsionsmoment	6-komp-våg1, ch 5
Vinkel snitt 1 BB	Avst/vinkelgivare 1 ch 6
Vinkel snitt 1 SB	Avst/vinkelgivare 2, ch 7

Snitt 2	
Vertikalt böjmoment	6-komp-våg2, ch8
Vertikal skjuvkraft	6-komp-våg2, ch9
Horisontellt böjmoment	6-komp-våg2, ch 10
Horisontell sjuvkraft	6-komp-våg 2, ch 11
Torsionsmoment	6-komp-våg1, ch 12
Vinkel snitt 2 BB	Avst/vinkelgivare 3, ch 13
Vinkel snitt 2 SB	Avst/vinkelgivare 4 ch 14

Snitt 3	
Vertikalt böjmoment	6-komp-våg3, ch 15

Vertikal skjuvkraft	6-komp-våg3, ch 16
Horisontellt böjmoment	6-komp-våg3, ch 17
Horisontell sjuvkraft	6-komp-våg3, ch 18
Torsionsmoment	6-komp-våg1, ch 19
Vinkel snitt 2 BB	Avst/vinkelgivare 5, ch 20
Vinkel snitt 2 SB	Avst/vinkelgivare 6, ch 21

Position	
x	mätarm, ch 22
y	mätarm, ch 23
z	mätarm, ch 24
roll	mätarm, ch 25
pitch	mätarm, ch 26
yaw	mätarm, ch 27

5 Results

The results of the current project are at present mainly used to evaluate the ability of the model and test setup concepts and design. This is shown in section 5.1-5.3 Techniques for evaluation of model trials on structural dynamics are also proposed. The latter is shown in section 5.4. Basic principles and data supporting the evaluation of the ability of the ship model and test setup is also shown in section 5.4. The entire test matrix is shown as statistics, power spectrum of midship forces and moments and fatigue cycle count of midship bending moment. However, techniques for determining a sufficient test matrix to establish fatigue life and fatigue damage and details of test evaluation are not addressed.

Results from tests in waves show that forces and moments span the entire measurement range of utilised force and moment transducers as intended. However, for models, where larger forces and moments are likely to occur (i.e. larger displacement and longer) one size larger transducers are likely to be needed or an alternative test setup.

5.1 Preparation tests

First test was a reference measurement to verify the loading in still water ensuring that the draught and the trim is correct. Figure 19 show the measured still water bending moment compared to theoretically calculated still water moment together with calculated shear force.

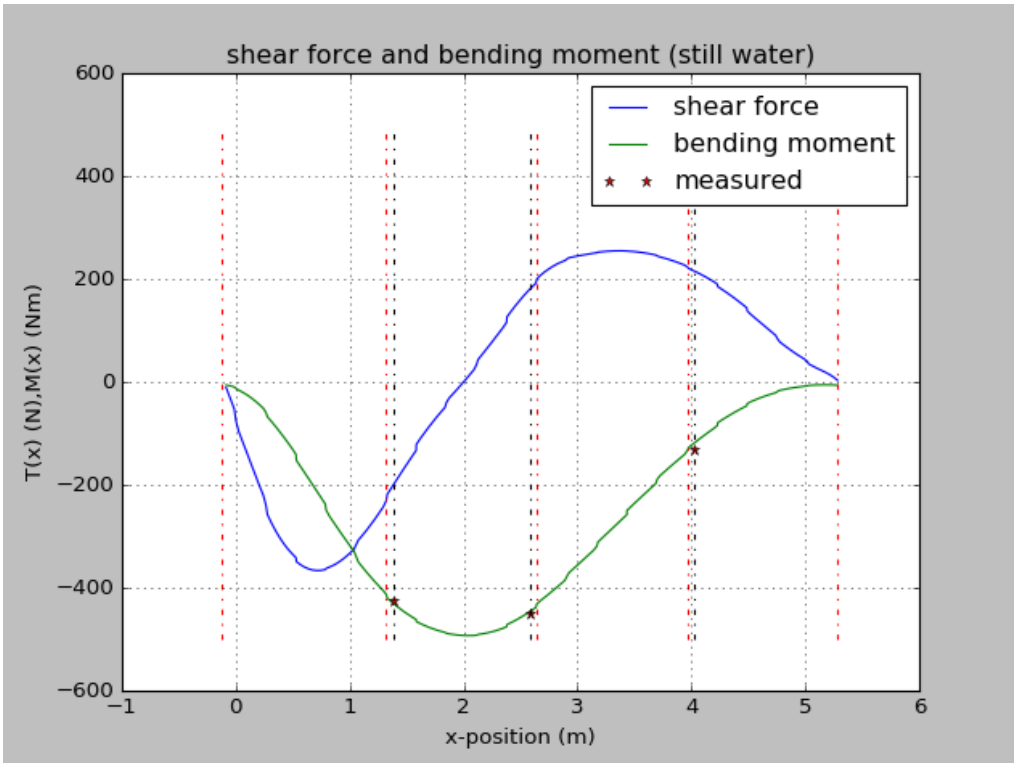

Figure 19. Calculated still water shear force and bending moment together with measured still water bending moment.

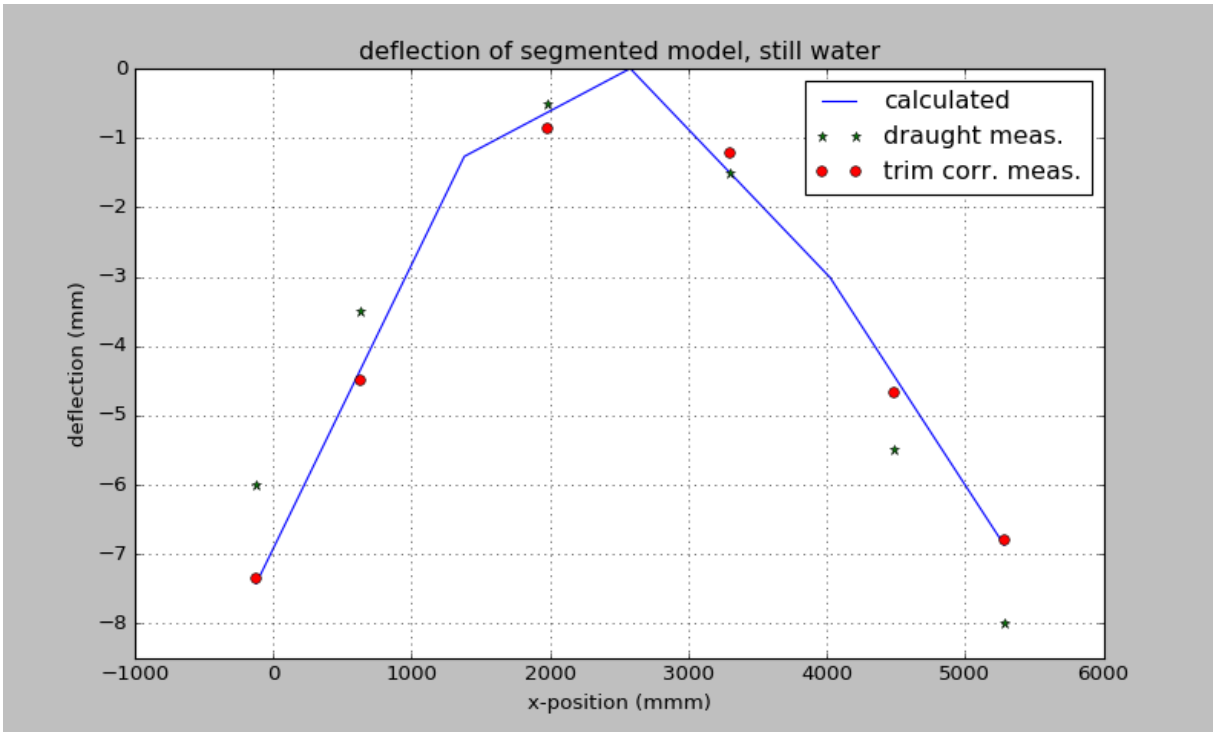

Figure 20. Deflection of segmented model in still water. Results from draught measurements.

5.2 Bending resonance tests on land

To get a measure of "dry" resonance frequency tests were performed with the model simply supported at two points. An impulse excitation was applied, the bending moments were recorded and analyzed.

In Table 10, a summary of the results of the tests of vertical bending resonance are presented. Spectrum plot and time history are presented in Figure 21-Figure 26. These figures show a frequency of largest peak at 7.39Hz in model scale. Moment measurement at all three cuts show two, more or less pronounced, smaller peaks at approximately 8.5Hz and 11.7Hz in model scale. The 7.39Hz peak is taken as the modal peak two node bending. This peak also correspond well to the very pronounced resonance peak in water.

The ratio between dry and wet eigen frequency is close to the theoretical ratio of √2, which is valid for a case with vertical added mass = displacement. For ship sections with a width to depth ratio between 2 and 8, the vertical added mass is close to the displacement at high frequency (ref 15 pp 299). A comparison between resonance frequency for two node bending can be seen in Table 11. Moment decay observed in the time series in Figure 22, Figure 24 and Figure 26 was used to calculate structural damping on land, which is shown in Figure 27.

Table 10 summary of results of resonance frequency test on land for two node bending

My/Cut	Resonance frequency model (Hz)	Resonance Period model (s)	Resonance frequency fullscale (Hz)	Resonance Period fullscale (s)
My/Aft	7.39	0.13	1.22	0.83
My/Mid	7.39	0.13	1.22	0.83
My/Fore	7.39	0.13	1.22	0.83

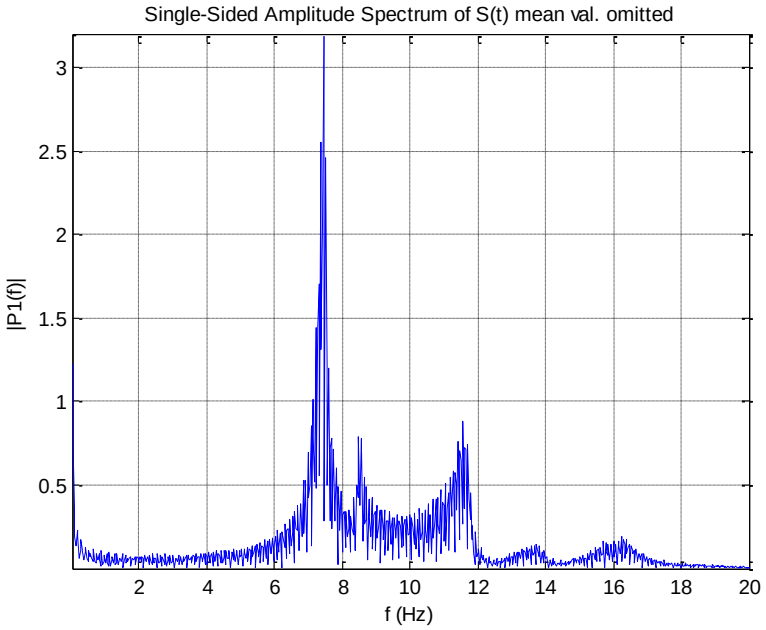

Figure 21 Single sided Fourier spectrum of Bending moment at aft cut

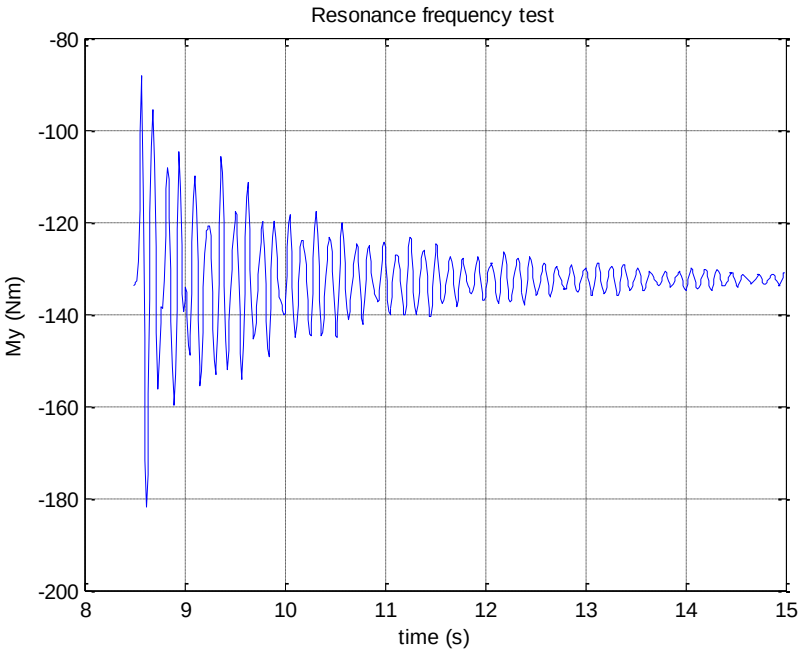

Figure 22 Time history of bending moment at aft cut

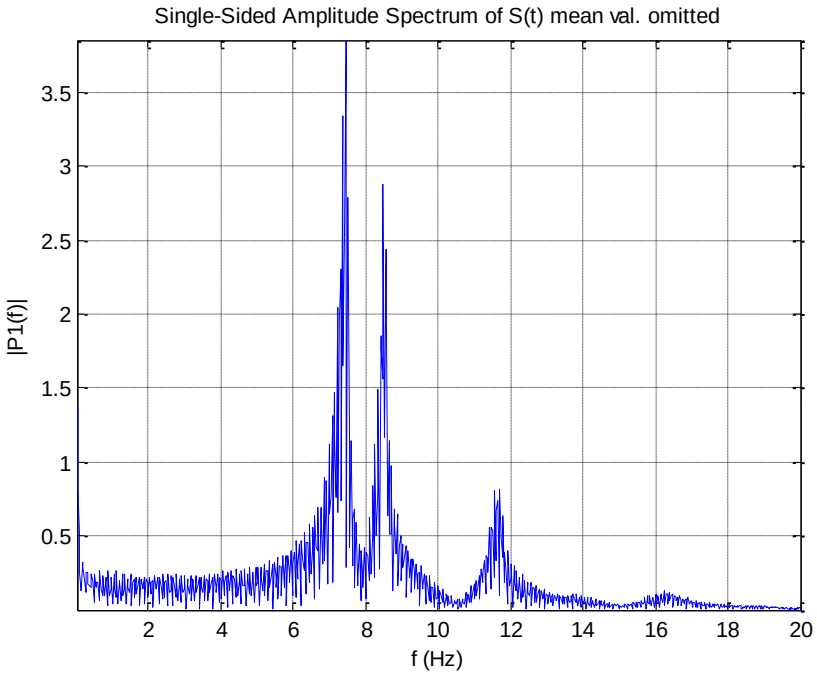

Figure 23 Single sided Fourier spectrum of Bending moment at mid cut

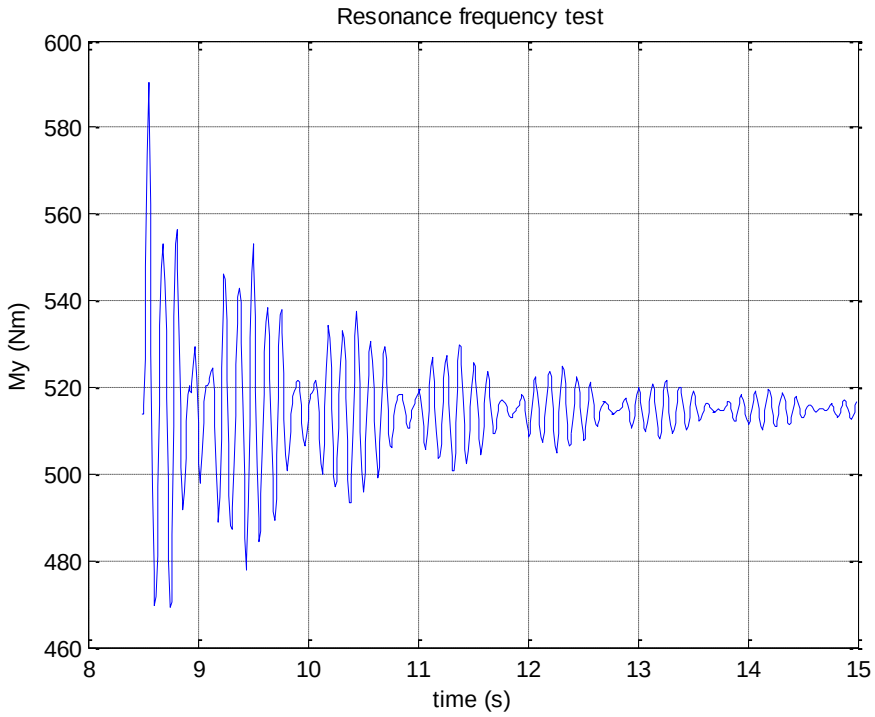

Figure 24 Time history of bending moment at mid cut

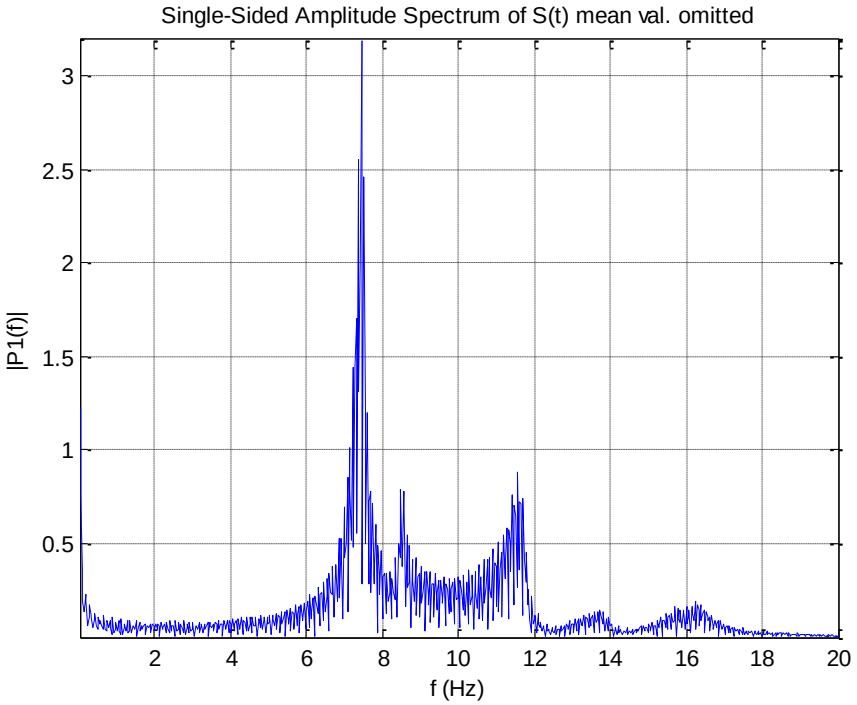

Figure 25 Single sided Fourier spectrum of Bending moment at fore cut

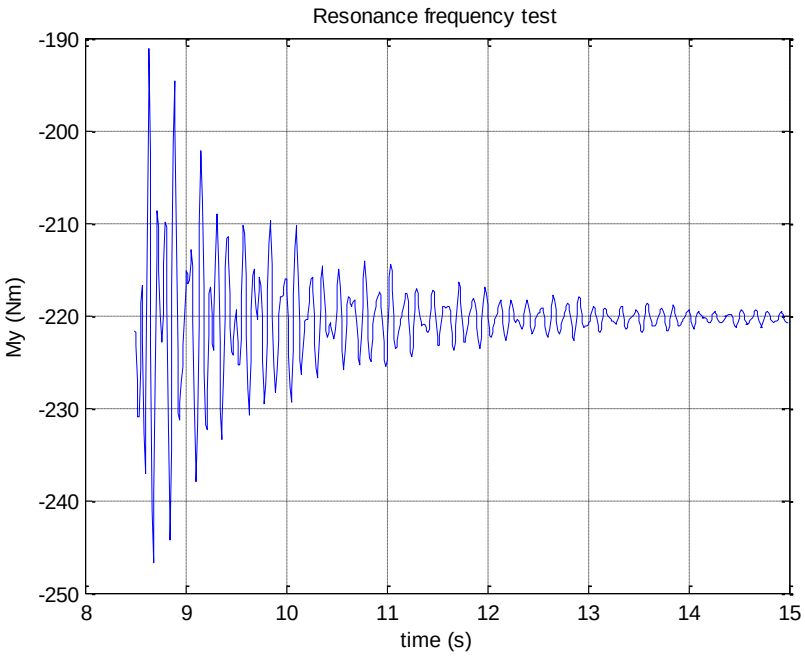

Figure 26 Time history of bending moment at fore cut

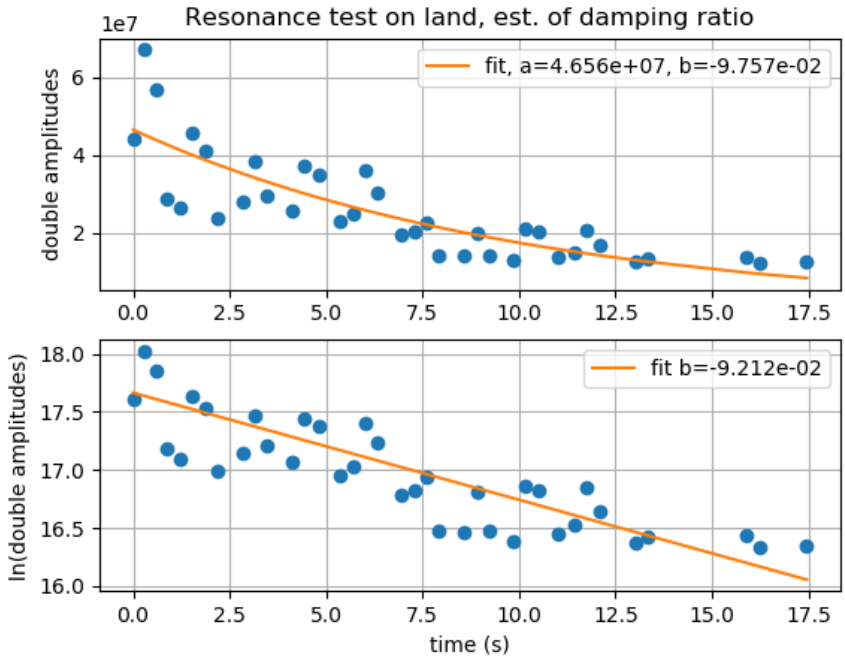

Figure 27 Estimation of structural damping in air, b=fraction of critical damping.

5.3 Bending resonance tests in water

Before tests in waves were performed, a series of bending resonance tests in still water were performed. A summary of these tests is shown in Table 11 with further details in Figure 28 - Figure 29. As mentioned in the section above the ratio between dry and wet eigenfrequencies are very close to what is given by theoretical calculations of spring mass system with small damping. Such calculations give a ratio of √(2). The ratio from current tests can be seen in the rightmost column of Table 11.

A time history of bending moment decay in mid cut is shown in Figure 28. This time series was bandpass filtered with a digital Fourier filter before computing the damping ratio shown in Figure 29.

Table 11 Bending resonance frequencies in water and comparison between resonance frequencies in water and on land

My/Cut	Resonance frequency model (Hz)	Resonance Period model (s)	Resonance frequency fullscale (Hz)	Resonance Period fullscale (s)	Ratio dry/wet freq. (-)
My/Aft	5.29	0.19	0.87	1.15	√(2.001)
My/Mid	5.29	0.19	0.87	1.15	√(2.001)
My/Fore	5.29	0.19	0.87	1.15	√(2.001)

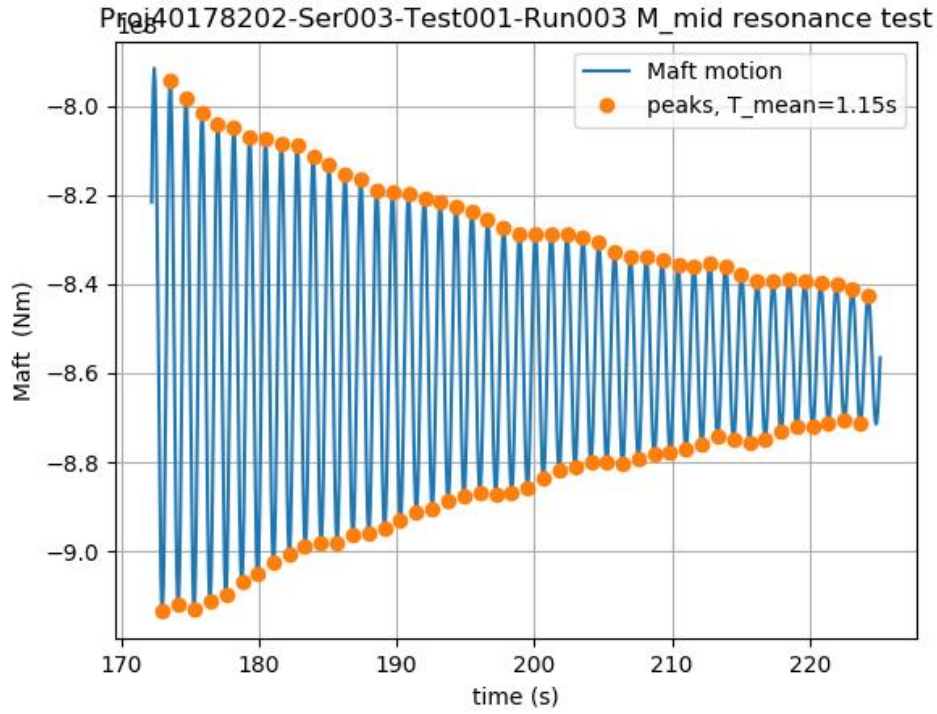

Figure 28. Time history of bending moment at mid cut.

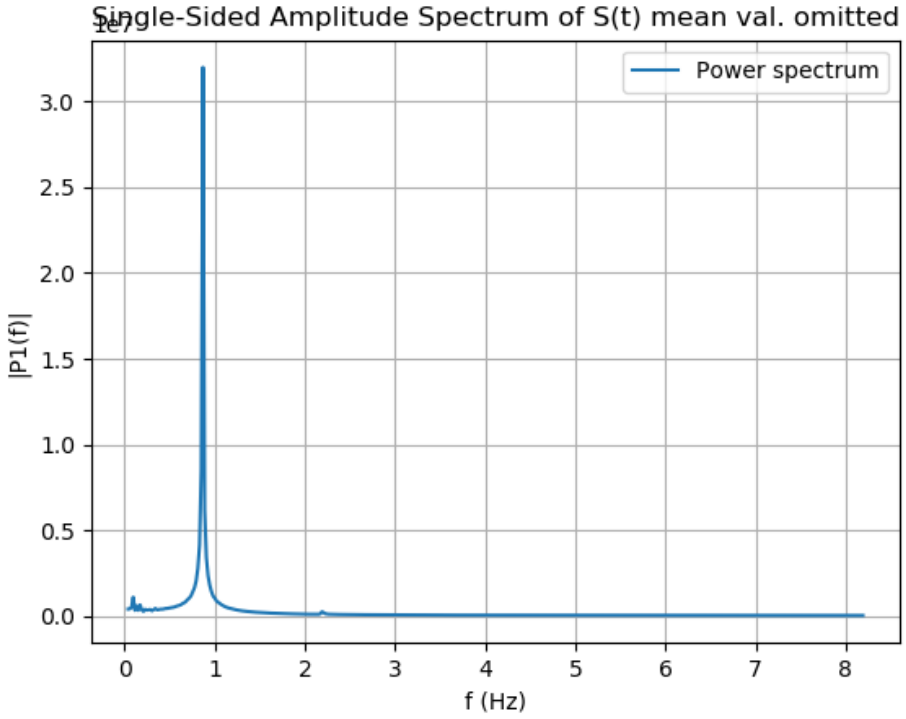

Figure 29. Frequency spectrum of the Moment resonance – decay – test with 0-frequency removed.

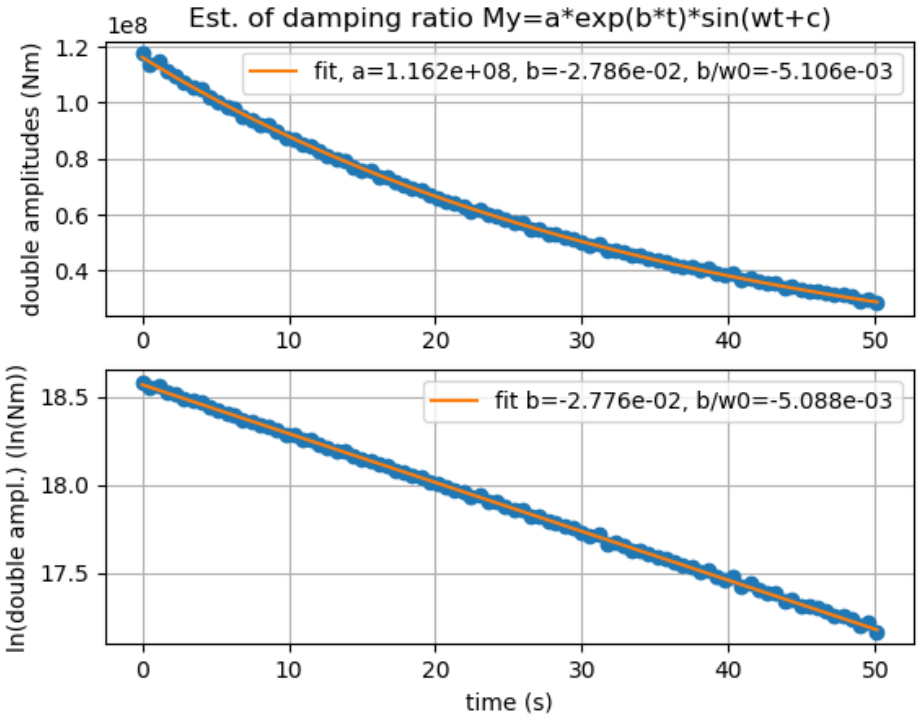

Figure 30. Estimation of structural damping in water, b=fraction of critical damping

5.4 Tests in waves

In Figure 31, an example of whipping recorded during the current project is shown. Until time=510s, the ship model encounter waves of equal height, then one wave period with large magnitude occur, triggering whipping, which can be seen as the ripple with same frequency as the structural resonance frequency. This oscillations with this frequency decays but persist throughout the measurement due to low structural damping.

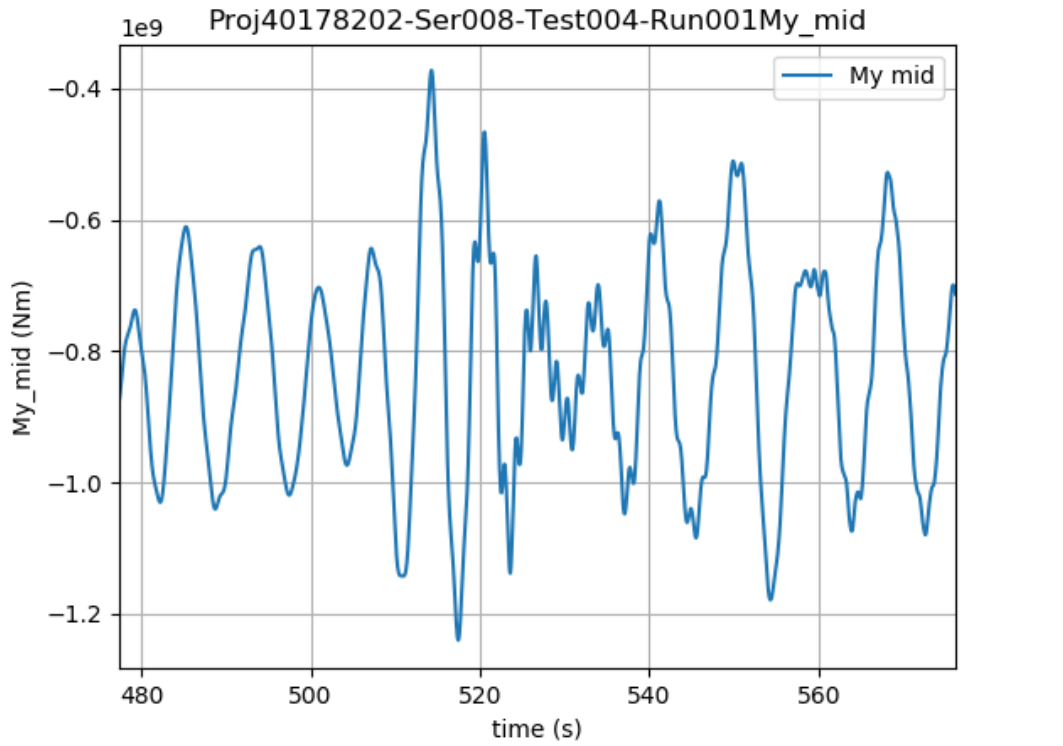

Figure 31. Time history of bending moment at test condition 1.

Figure 32 display a possible use of data from model trials with structural dynamic ship models, where midship bending moment have been used for fatigue cycle counting by the rainflow method. Cycle count have been performed for unfiltered bending moment and for low pass filtered and high pass filtered bending moment. Such data may at a later stage be compared to midship fatigue resistance to calculate fatigue life and fatigue damage.

Figure 33 display power spectrum of midship transverse force, vertical force, vertical bending moment and transversal bending moment. For the vertical bending moment the same results as in Figure 31 can be noted. I.e. a main effect of the wave frequency moment and a super posed smaller effect of whipping at the structures' resonance frequency (0.87Hz).

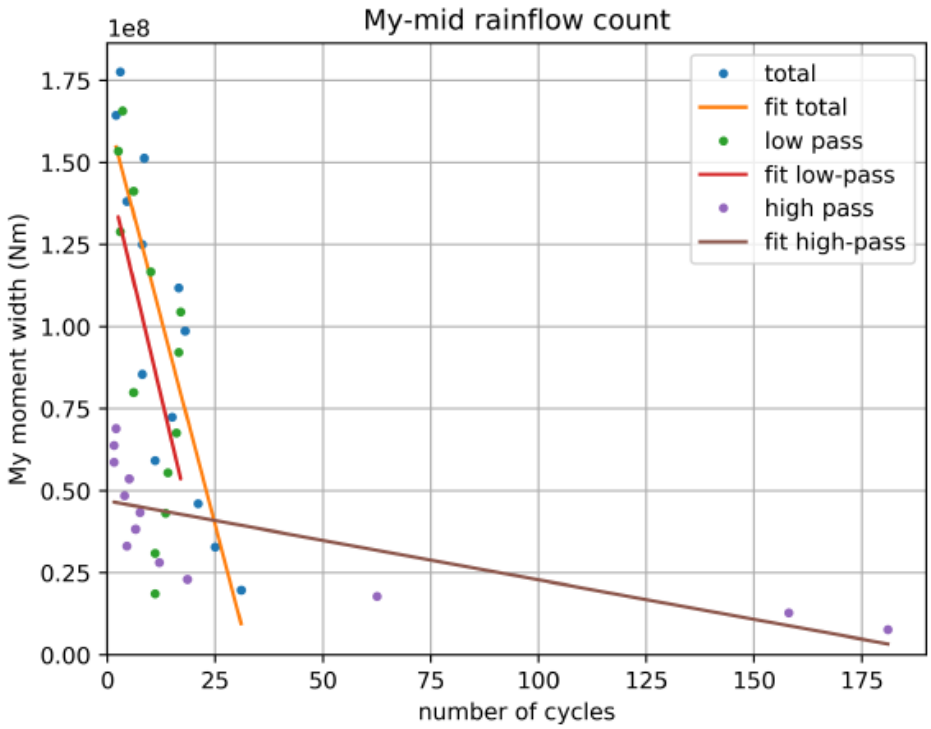

Figure 32. Fatigue cycle count of series 4 condition 1.

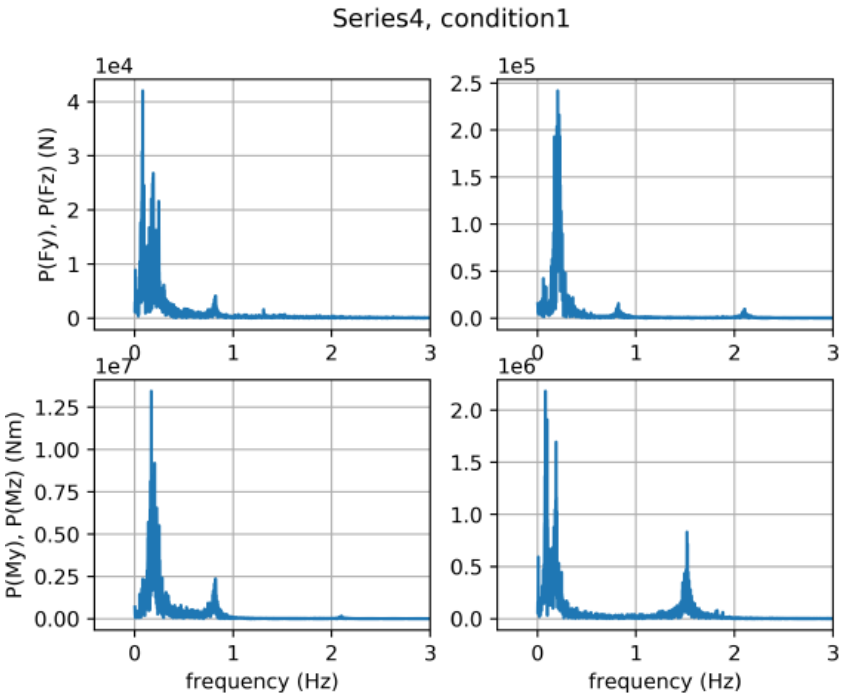

Figure 33. Power spectrum of midship transversal force, vertical force, vertical bending moment and transversal bending moment.

6 Discussion

With the current knowledge, model building technique and measurement technology at hand at SSPA Sweden a suitable model concept and detailed design was put forward.

The tested model was built in four segments with hinges and adjustable springs at the hinges to be able to achieve the right static stiffness and 1st and 2nd global eigen frequencies. All three forces and all three moments were measured at the cuts, along with angular deflection at the hinges.

It was considered to model structural dynamics in transverse bending. However, it was judged that the effect of structural dynamics due to lateral bending may be notable but that the design and construction of the model would be significantly more difficult. Further, it was also judged that the accuracy of measurements would be adversely affected and that it would be very uncertain to utilise such a model. The model design already contains a number of novelties needed to be tested and evaluated:

- Six degree of freedom force (and moment) measurement integrated into one transducer
- Carbon fibre hull shell construction to be able to obtain the correct longitudinal mass distribution
- Utilising optical measurements measure vertical deflection of the hull girder.
- Low friction hinge

Targets of the current project was to evaluate the model building concepts partly developed in an earlier project and find out how well it is possible to capture the structural dynamics, e.g. whipping and springing, and measure structural forces and moments at a model test.

The results of preparation tests shown in section 5.1 display very good agreement between measured and calculated hydrostatic bending moment, which indicate a very good measurement accuracy.

Springing occur when the peak period of the encountering wave spectrum is relatively close to the two-node bending eigenfrequency of the hull structure. However, whipping require a more impact like excitation (often at a encounter frequency apart from the structural eigenfrequency) and a low enough structural damping to occur. One of the major questions was, whether it is possible to get faithful representation of whipping from a model in four segments. Results displayed in Figure 31 indicate that whipping is well represented by the model built.

6.1 Further research

All indications from the current project points out that the model design, construction and test set-up is well suited for model testing of structural dynamics, which was the target of the current project. Nevertheless, some important questions remain un-addressed:

1. How to determine a sufficient test matrix to establish the fatigue life and fatigue damage of a ship?
2. How is a standardized test evaluation to be carried out?

3. How is an efficient numerical simulation of coupled hydro dynamics and structural dynamics to be carried out?
4. How can further ship types be gained from increased knowledge in ship structural dynamics?

To answer question 3 and to enable the use of simulations to help the solution of question 1 and 2 it is proposed to implement structural dynamics in a state-of-the-art simulation code, such as SSPAs Seaman software or similar.

It is believed that classification societies, universities and ship owners would have good use of having the questions above answered and participating in finding answers to them.

7 Conclusions

The model concept and design are well suited to capture, not only springing but also whipping. All results indicate that the measurement of forces and moments are measured with high accuracy and that all of the “must-have” project objectives are fulfilled. Results also show that the optical measurement of structural deflections may be improved.

The successful implementation of novel model design and testing technique further stress the importance of answering questions still remaining:

1. How to determine a sufficient test matrix to establish the fatigue life and fatigue damage of a ship?
2. How is a standardized test evaluation to be carried out?
3. How is an efficient numerical simulation of coupled hydro dynamics and structural dynamics to be carried out?
4. How can further ship types be gained from increased knowledge in ship structural dynamics?

8 Summary

The activities carried out in the current work package led to the successful completion of the planned test series. Results of this test series give that the model concept works as intended, capturing all the most important physics. The actual model built and tested worked very well throughout the test series and gave, what seems as very accurate measurement of forces and moments, while measurement of deflections may be improved. However, forces and moments are the most important measured entities.

A lightweight model made of carbon fibre, divinycell and aluminium was designed and built. The lightweight design was necessary to provide possibility to attain the same mass distribute as the full-scale ship.

The structural properties of the model, such as stiffness, mass distribution and structural damping met the targets of the full-scale ship.

The model concept and design are well suited to capture, not only springing but also whipping. All results indicate that the measurement of forces and moments are measured with high accuracy and that all of the “must-have” project objectives are fulfilled. Results also show that the optical measurement of structural deflections may be improved.

The successful implementation of novel model design and testing technique further stress the importance of answering questions still remaining:

1. How to determine a sufficient test matrix to establish the fatigue life and fatigue damage of a ship?
2. How is a standardized test evaluation to be carried out?
3. How is an efficient numerical simulation of coupled hydro dynamics and structural dynamics to be carried out?
4. How can further ship types be gained from increased knowledge in ship structural dynamics?

9 References

1. Lundbäck O., “Model for structural dynamics measurements – Outline specification for model design and construction”.
2. DNV-GL, “RULES FOR CLASSIFICATION, Ships, Edition July 2018, Part 1 General regulations, Chapter 2 Class notations”
3. DNV-GL, “RULES FOR CLASSIFICATION, Ships, Edition July 2018, Part 6 Additional class notations, Chapter 1 Structural strength and integrity”
4. DNV, “CLASSIFICATION NOTES, No. 34.1, CSA - DIRECT ANALYSIS OF SHIP STRUCTURES, JANUARY 2011”
5. DNV-GL, “RULES FOR CLASSIFICATION, Ships, Edition January 2018, Part 3 Hull, Chapter 9 Fatigue”
6. DNV-GL, “CLASS GUIDELINE, DNVGL-CG-0130 Edition January 2018, Wave loads”
7. Drummen I., “Experimental and Numerical Investigation of Nonlinear Wave-Induced Load Effects in Containerships considering Hydroelasticity”, Thesis for the degree of philosophiae doctor, Trondheim, June 2008, Norwegian University of Science and Technology Faculty of Engineering Science and Technology Department of Marine Technology.
8. DNV-GL, “CLASS GUIDELINE, DNVGL-CG-0153 Edition October 2015, Fatigue and ultimate strength assessment, of container ships including whipping and springing”
9. DNV-GL, “CLASS GUIDELINE, DNVGL-CG-0129 Edition October 2015, Fatigue assessment of ship structures”
10. Int. J. Nav. Archit. Ocean Eng. (2014) 6:1096~1110
11. Storhaug G., “The measured contribution of whipping and springing on the fatigue and extreme loading of container vessels”, http://dx.doi.org/10.2478/IJNAOE-2013-0233, ISSN: 2092-6782, eISSN: 2092-6790 SNAK, 2014
12. Marine Accident Investigation Branch (MAIB), “Report on the investigation of the structural failure of MSC Napoli English Channel on 18 January 2007”, Marine Accident Investigation Branch Carlton House Carlton Place Southampton United Kingdom SO15 2DZ Report No 9/2008 April 2008
13. Waldenland, D. A., Noll M. D., “Springing Research on a Great Lakes Ore Carrier”, U.S. Coast Guard, Report No. CG-D-13-81, April 1981.
14. Dinsenbacher, A., Engle, A., Hermanski, G., 2010, Guidelines for Hydroelastic Model Design, Testing and Analysis of Loads and Responses, Report No. NSWCCD-65-TR-2010/12, Carderock Div, NSWC.
15. Newman, J.N. “Marine Hydrodynamics”, 1977, Massachusetts Institute of Technology, ISBN 0-262-14026-8.
16. https://www.wamit.com/manual.htm
17. “Seaman Users Manual”, Wilske E. et. Al. v. 4.1 2016-12-01.

10 Appendix – Test results

Rapportering av KTH:s del i projektet Dynamisk fartygsdimensionering

Experimentell utvärdering av lokala slammingtryck

Anders Rosén, KTH Marina system, Stockholm 2018-12-12

Innehåll

Introduction

The overall goal of the project *Dynamisk fartygsdimensionering* has been to develop refined methods for characterizing dynamic loads on ship structures, involving numerical as well as experimental modelling of global and local loads. The KTH part of the project, which is reported in this document, was to develop an experimental setup for measuring local slamming loads on parts of a ship model and from corresponding measurements reconstruct the slamming pressure distribution to enable comparison with global loads measured with a backbone model setup developed by SSPA and numerical simulations performed by DNVGL and Chalmers. The plan for the local loads was to adapt and apply an experimental technique that has previously been applied successfully on high-speed craft. Through the here reported project it has however been clarified that application of this modelling technique on the here studied displacing ship would involve significant uncertainties which cannot be sorted out within the limited frames of this project. It was therefore decided to not go through with buying pressure sensors and building the related part of the experimental setup. It is of course unfortunate that this sub-project could not be performed as planned, still the project has contributed with further valuable understanding regarding the challenges involved in local slamming pressure measurements. This report describes the experimental technique that was planned to be used, background to and motifs for not going all the way with this sub-project, and recommendations for further research.

Experimental technique for local slamming pressure evaluation

The plan was to apply an experimental method that has previously been applied successfully for measuring and evaluating local slamming pressures on high-speed craft in full scale as well as model scale (e.g. Razola et al 2014, Rosén & Garme 2009, Rosén et al 2007, Rosén 2005). This method relies on pressure measurements made with small membrane area pressure transducers mounted on a number of sections along the ship hull as pictured in Figure 1.

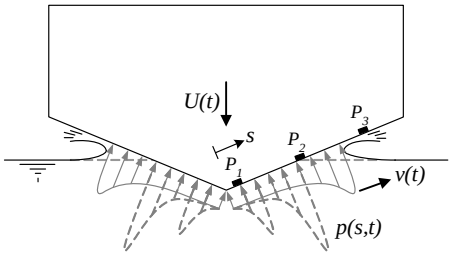

Figure 1: Schematic illustration of a cross section of a hull with pressure transducers (P1, P2, etc) mounted on a hull section.

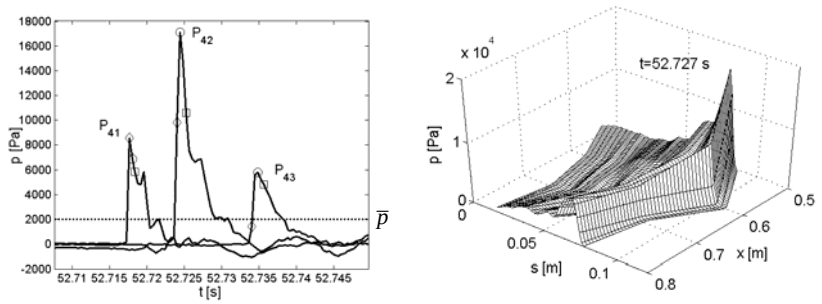

Figure 2: Example of measurements with three transducers on one section of a planing craft model (left) and the spacial pressure distribution at a particular moment during this impact event reconstructed based on measurements with three transducer equipped sections (right).

From discrete point measurements at a number of sections along the hull, the spatial pressure distribution can then be reconstructed as pictured in Figure 2 and as described in the following. Consider a hull section equipped with two pressure transducers, P_1 located in $s=S_1$ and P_2 in $s=S_2$, where $S_1<S_2$ and s is the transverse distance along the hull surface measured from the centre line. The time when the spray root passes a transducer is determined by the time when that transducer signal rises. The slamming pressure pulse velocity, v, is assumed stepwise constant and is given by the spacing between the transducers divided by the time between spray root passages. Each sample from a pressure transducer can be seen as a snap shot of one part of the passing pressure pulse. A sample from transducer P_1 at the time $t=t_k$ gives the pressure magnitude $p(S_1,t_k)=P_1(t_k)$ and the location $s(t_k)=S_1$ for one part of the pulse at the time of the sample. Having calculated the pulse velocity v, the location of this pulse part in all other times is given by $s(t)=S_1+v*(t-t_k)$. Knowing the spacing $\Delta S=S_2-S_1$ between P_1 and P_2, the time when this pulse part passes P_2 can be calculated as $t=t_k+\Delta S/v$. The pressure magnitude of the pulse part at this instant is related to the pressure measured by P_2, i.e. $p(S_2,t_k+\Delta S/v)=P_2(t_k+\Delta S/v)$, and its pressure magnitude in all other times is given by $p(s(t),t)=P_1(t_k)+dp*(t-t_k)$, where $dp=[P_2(t_k+\Delta S/v)-P_1(t_k)]/[\ t_k+\Delta S/v-\ t_k]$. All samples from P_1 and P_2 treated in this way gives the sectional pressure distribution, $p(s,t)$. If there are more than two transducers along a section, it is also possible to catch the rate of change of v and dp which increase the accuracy of the reconstruction. Further, if several sections are equipped with transducers, interpolation between the derived distributions on the different sections in each time step gives the complete pressure distribution, $\{p(s,t)|_{x=xa},\ p(s,t)|_{x=xb},\ p(s,t)|_{x=xc}\} \rightarrow \{p(x,s,t)\ ;\ x_a\leq x\leq x_c\}$ where x is the longitudinal coordinate. Forces can then easily be derived by integrating the reconstructed pressure distribution over the whole or parts of the pressure transducer equipped hull area.

In the present project the plan was to measure and reconstruct local slamming pressures in a way that enabled determination of forces and moments which could be compared with corresponding global loads measured with a backbone model setup developed by SSPA and numerical simulations performed by DNVGL and Chalmers. It was decided to build the model based on the geometry of Stena Elektra with four backbone segments as pictured in Figure 3. Several different pressure transducer setups were considered, for example with only two equipped sections on the second foremost segment as pictured in Figure 3, or two equipped sections in both the first and second hull segments, or several equipped sections in either the first or the second hull segment. Through the progress of designing the model it became obvious that space limitations would restrict the pressure transducer setup.

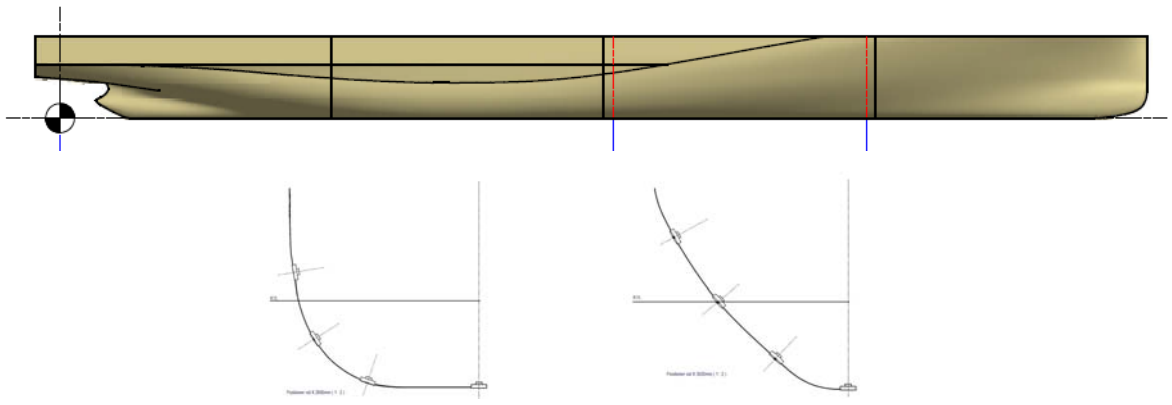

Figure 3: Profile view of the Stena Elektra based model showing the four backbone segments and a draft setup with four pressure transducers on two sections in the aft and fore ends of the second foremost hull segment.

As mentioned, previous applications of the here described pressure measuring and reconstruction technique has been on planing high-speed ships. In these applications the pressure transducers has been installed in parts of the v-shaped hull bottom which are submerged in the water while the ship is idling at zero speed and also at speed trough waves the transducers are only occasionally out of the water. Hereby the pressure transducers have been continuously cooled to maintain temperatures close to the water temperatures. However, in the here presented project several pressure transducers would have to be mounted well above the water surface, as pictured in Figure 3 and even higher, to enable capturing of the bow flare slamming at the most dramatic wave encounters where the largest global slamming loads were expected to occur. This rose questions regarding potential problems related to temperature variations of the pressure transducers and initiated a review of previous experiences from this type of measurements.

Temperature and acceleration effects on slamming pressure measurements

Slamming pressures have been studied experimentally for nearly a century, with early examples for example found in Thompson (1929) and Smiley (1952). Studies on experimental pressure measurements found in the literature concerns drop tests where different bodies (commonly wedges) are dropped vertically into the water, and also full scale and model scale experiments with high-speed craft, displacing ships, and various offshore structures. However, it can be concluded that the literature on slamming pressure measurements is rather limited and the issue of temperature effects is given almost no attention. In a literature survey on dynamic pressure measurement by Hjelmgren (2002) it is stated that more effort must be devoted to the influence of temperature, and also the influence of acceleration, on the behaviour of pressure transducers. The very few references found which considers temperature effects are here briefly reviewed.

A good overview of various challenges involved in dynamic pressure measurements at hull water impact is provided in van Nuffel et al (2013). Here three different categories of pressure sensors suitable for dynamic testing are described. The first category uses piezoelectric quartz crystals which generate an electric charge when being compressed due to an external applied pressure. The second type uses piezoresistive strain gauges placed on the membrane of the transducers. The third measuring principle is based on a variable capacitance between the sensor membrane and a metallic plate.

Bouvy & de Boer (2011) evaluates a selected set of pressure transducers with respect to various problematic phenomena. All pressure transducers investigated respond to a shock wise change in temperature when the sensing membrane immerses in the basin water. These observations are explained by the difference between the ambient air temperature and that of the basin water, where for example the lighting required for photographic purposes warms up the ship's hull. It is commented that the commonly used temperature compensation methods, e.g. using temperature depending resistors, only offer a slow response to these rapid phenomena. Other discussed problems are for example sensitivity to acceleration where inertia effects might influence the membrane at slamming impacts and thereby bias the measurements of the hydrodynamic pressure. The paper ends with: "The quest is going on: the ideal pressure transducer has still to be discovered".

van de Bunt & Bouvy (2011) presents a calibration method designed to deliver dynamic calibration for a high bandwidth pressure transducer used in sloshing tests at full scale. The pressure transducer sensing element is here mounted in a stainless-steel casing and protected from the external

environment by a thin coating of silicone elastomer to eliminate the temperature shock. It is however stated that temperature effects can be an issue at successive impacts.

van Nuffel et al (2013) states there is lack in experimental slamming pressure data and that this originates from the fact that accurate pressure measurements are difficult to perform. The paper investigates a number of parameters affecting the pressure recordings during water impact, for example it was observed that when submerging a pressure sensor adjusted to room temperature gently in colder water, the pressure increased although no physical load was applied to the sensor. The thermal nature of the phenomena is explained by considering the preloaded state of the piezoelectric crystal in the steel housing of the piezoelectric sensors. Furthermore, the thermal expansion coefficient of the crystal is about 20 times smaller than the thermal expansion coefficient of steel. It is recommended that pressure sensors using a preloaded piezocrystal should be adjusted to the water temperature before an experiment can be performed to prevent parasitic pressures in the pressure signals. Alternatively sensors based on other sensing technologies should be used.

Kværnes Øien (2015) reports negative pressures in the early phases of slamming and describes that the reason for the negative pressures is a temperature shock in the sensor. It is further described that when the sensors are switched on, an electric current travels through the sensor front and heats it up slightly, hereby even though the water and air are at equal temperature, the sensors will be warmer than the water due to this electrical heating when initially penetrating the water surface.

In an internal report by SSPA (2015) benchmark testing of two different types of piezoelectric pressure transducer, and an alternative transducer has been developed in house by SSPA based on a force transducer, is presented. Significant temperature shocks are found when the piezoelectric transducers with different temperatures than the water are slowly submerged in the water. The SSPA transducer is unaffected by temperature differences but instead shows significant inertia effects when subject to slamming. Since the temperature shocks for the piezoelectric transducers are of similar magnitudes as expected slamming pressures the use of these transducers for slamming purposes is very questionable unless the transducer temperatures can be kept constant. Similarly, it is questionable to use the SSPA transducer for slamming applications due to the inertia effects.

In phone and email correspondence between Anders Rosén/KTH and Göran Arnelo at Stig Wahlström Automatik (the Swedish agent for XP pressure transducers) Arnelo expressed that wave testing for ship models is a quite difficult application because the water is not always in contact with the sensing element and because the transducer is heated both by the running current and also by the spotlights which are generally used in model tests to enable video recordings. A suggestion was to lower the power and use only 3.3Vdc or 5Vdc instead of the normal 10Vdc, hereby lowering the thermal dissipation effect on the gages.

Similarly, in phone and email correspondence between Anders Rosén/KTH and Andreas Långström & Mats Turesson/SSPA, Långström and Turesson underlined the risk for adverse temperature effects due to the heating from video recording spotlights. Långström described that observations of these temperature effects was one reason for SSPA to develop their alternative in house transducers. The current version of the SSPA transducers were concluded to have too large measurement areas and too large inertia effects to be useful in the experimental setup for the present project. Rosén and Långström discussed the prospect of further developing the SSPA transducers and substantially reducing their size as an interesting option, which however would not be possible to fit within the frames of the present project.

Concluding remarks and recommendations

The here reported study has clarified that the experimental technique that was intended to be used for evaluating the local slamming pressure would involve significant uncertainties which could not be sorted out within the limited frames of this project. It was therefore decided to not go through with buying pressure transducers and building the related parts of the experimental setup. It is of course unfortunate that this sub-project could not be performed as planned, still the project has contributed with valuable further understanding regarding the challenges involved in local slamming pressure measurements. The need and potential for further research on slamming pressure measurements is obvious and the following is recommended for future studies:

- Systematic evaluation of and comparison between various pressure transducer technologies to clarify the characteristics of the adverse temperature and inertia effects.
- Systematic exploration of various means to mitigate adverse temperature effects, for example: minimization of the feeding power; elimination of video recording lights; silicon or other types of insulation of the pressure transducer membranes; and techniques for controlling the pressure transducer temperatures for example by water sprinkling or other type of cooling systems.
- Further development of the SSPA transducers for reducing the size of the measurement area and the inertia effects.

References

Bouvy, A. & de Boer J. (2011). Dynamic Behaviour of Pressure Transducers, Advanced Model Measurement Technology AMT'11, Newcastle, UK.

Hjelmgren J, (2002), Dynamic Measurement of Pressure - A Literature Survey, SP Technical Research Institute of Sweden, SP REPORT 2002:34

Kværnes Øien P (2015). Physical investigation of slamming loads on a 2D body, Master Thesis in Marine Technology, Norwegian University of Science and Technology, Department of Marine Technology.

Razola M, Rosén A, Garme K (2014). Experimental Evaluation of Slamming Pressure Models Used in Structural Design of High-Speed Craft, International Shipbuilding Progress, Vol.61, No.1-2, pp.17-39.

Rosén A, Garme K (2009). Model Experiment Addressing the Wave Loads on the Combat Craft Strb 2010 (23M), Report for the Swedish Defence Materiel Administration (FMV), KTH Royal Institute of Technology, Stockholm.

Rosén A, Garme K, Kuttenkeuler J (2007). Full-Scale Design Evaluation of the Visby Class Corvette, Proceedings of the 9th International Conference on Fast Sea Transportation (FAST'07), Shanghai, China.

Rosén A (2005). Impact Pressure Distribution Reconstruction from Discrete Point Measurements, International Shipbuilding Progress, Vol. 52, No.1.

Smiley R. F. (1952). Water-Pressure Distribution During Landings of a Prismatic Model Having an Angle of Dead Rise of 22.5° and Beam-Loading Coefficients of 0.48 and 0.97, NACA TN 2816.

SSPA (2015). Evaluation of MEAS pressure transducers for slamming. Internal SSPA report.

Thompson, F. L. (1929). Water-Pressure Distribution on Seaplane Float, NACA Report, No.290.

van de Bunt, E. & Bouvy, A. (2011). Dynamic Calibration of a Pressure Transducer, Advanced Model Measurement Technology AMT'11, Newcastle, UK.

van Nuffel D., Vepa K.S., de Baere I., Degrieck J., de Rouck J., van Paepegem W. (2013). Study on the Parameters Influencing the Accuracy and Reproducibility of Dynamic Pressure Measurements at the Surface of a Rigid Body during Water Impact, Experimental Mechanics 53:131-144.

CHALMERS
UNIVERSITY OF TECHNOLOGY

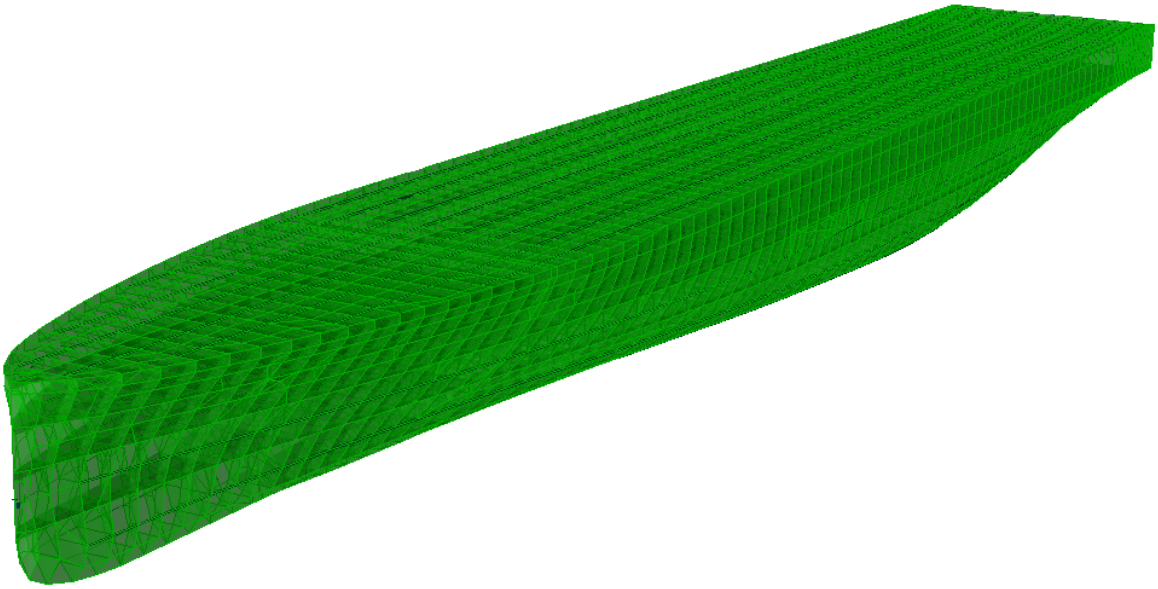

Numerical Simulation Assessment of a Ship Dynamic Behavior Against a SSPA Model Test

Master's thesis in the International Master´s Programme Naval Architecture and Ocean Engineering

JAVIER PELAYO LLOP SAYSON

Department of Mechanics and Maritime Sciences
CHALMERS UNIVERSITY OF TECHNOLOGY
Gothenburg, Sweden 2019
Master's Thesis 2019/78

MASTER'S THESIS IN THE INTERNATIONAL MASTER'S PROGRAMME IN NAVAL ARCHITECTURE AND OCEAN ENGINEERING

Numerical Simulation Assessment of a Ship Dynamic Behavior Against a SSPA Model Test

JAVIER PELAYO LLOP SAYSON

Department of Mechanics and Maritime Sciences

Division of Marine Technology

CHALMERS UNIVERSITY OF TECHNOLOGY

Göteborg, Sweden 2019

Numerical Simulation Assessment of a Ship Dynamic Behavior Against a SSPA Model Test
JAVIER PELAYO LLOP SAYSON

Master's Thesis 2019/78
Department of Mechanics and Maritime Sciences
Division of Marine Technology
Chalmers University of Technology
SE - 412 96 Göteborg
Sweden
Telephone: + 46 (0)31-772 1000

Cover: Hydrodynamic grid model using SESAM GeniE.

Printed by Chalmers Reproservice

Göteborg, Sweden 2019

Numerical Simulation Assessment of a Ship Dynamic Behavior Against a SSPA Model Test
Master's Thesis in the International Master's Programme in Naval Architecture and Ocean Engineering
JAVIER PELAYO LLOP SAYSON
Department of Mechanics and Maritime Sciences
Division of Marine Technology
Chalmers University of Technology

Abstract

Shipping carbon emission impact will increase in the upcoming years, achieving more than 3% of CO_2 world emissions by 2030. It is not unthinkable of incoming regulations limiting these emissions. To affront this challenge, significant changes in ship performance and construction are heavily needed to minimize energy consumption. For that reason, there is a stronger need for more efficient and simplified methods in the prediction and analysis of ship energy efficiency and dynamic behavior. This thesis emphasizes the analysis and assessment of a ship's dynamic response to different sea states.

The objective of this thesis is to compare a state-of-the-art simulation model with a segmented model test carried out at the SSPA wave basin. The simulation model is created for its use in DNV GL's SESAM package software which assumed a rigid body motions model. SESAM GeniE has been used for the model calibrations, whereas Wasim SESAM is used in the seakeeping simulations.

The assessment of the model consisted of the use of modal analysis for the structural behaviour and seakeeping analysis for the wave loads response. The wet vibration analysis gave an accurate result of the segmented model, concluding that the numerical model structure captures the behavior of the hammer test.

The seakeeping simulations have proven good predictions on shear and bending moments, where the mean value is within 7% of the experimental value. It is concluded that with the current methodology and software, there is a satisfactory accuracy in the use of rigid numerical model to capture the vertical load behavior of a segmented experimental model in moderate sea states.

Keywords: experiments, numerical simulation, seakeeping, segmented model, wave basin.

Table of contents

Preface

This thesis is part of the requirements for the master's degree in Naval Architecture and Ocean Engineering at Chalmers University of Technology, Göteborg, and has been carried out at the Division of Marine Technology, Department of Mechanics and Maritime Sciences, Chalmers University of Technology between January and June of 2019.

I want to acknowledge my examiner and supervisor Professor Jonas Ringsberg at the Division of Marine Technology on the Department of Mechanics and Maritime Sciences, Chalmers University of Technology for his knowledge, feedback, and encouragement. I also want to thank my co-supervisor Zhiyuan Li at Chalmers University of Technology for his support and guidance throughout all the thesis. I also like to give my gratitude to Olov Lundbäck from SSPA for his valuable time and feedback throughout the work.

Finally, I would send great gratitude to my family and friends for their endless support and love.

Göteborg, June 2019

Javier Pelayo Llop Sayson

Nomenclature

List of acronyms

BAU	Business as usual
CFD	Computational fluid dynamics
DOF	Degree of freedom
FE	Finite element
GHG	Greenhouse gas
HDF5	Hierarchical Data Format 5
IMO	International Maritime Organization
ITTC	International towing tank conference
JONSWAP	Joint North Sea Wave Project
MDL	Maritime Dynamics Laboratory
UN	United Nations

List of unit abbreviations

deg	degrees
kg	kilograms
Hz	hertz
m	meters
N	newton
s	seconds

Variables

Ship dimensions		*Unit*
B	Breath	m
D	Depth	m
T	Draft	m
L_{OA}	Length overall	m
L_{pp}	Length between perpendiculars	m
LCB	Longitudinal center of buoyancy	m
LCG	Longitudinal center of gravity	m
m	Mass	kg
VCG	Vertical center of gravity	m
B_{wl}	Waterline breath	m
L_{wl}	Waterline length	m

Wave properties		*Unit*
γ	Phase angle	deg
A	Wave Amplitude	m
β	Wave direction	deg
H_s	Wave height	m
k	Wave number	-
T_s	Wave period	s

Eigenanalysis		*Unit*
ω_n	Natural frequencies	Hz
Γ	Correction factor dependent on the geometry of the beam.	-

1 Introduction

The following chapter presents the introduction to the thesis work. A detailed description of the background and motivation of the thesis presents the problem intended to be solved in the work. A list of assumptions and limitations is presented under which this problem will be addressed. Finally, an outline of the thesis work is done to present the different subjects addressed in this thesis.

1.1 Background and motivation of study

Shipping currently accounts for nearly 3% of global CO_2 emissions; by 2020 those emissions will increase by 7%. In 2030, the average emissions by the shipping industry will increase by 29% and by 2050 the increase will be around 95% of the ones in 2020. Thus, the shipping industry could end up being responsible for 17% of the CO_2 global emissions in 2050 if they were left unregulated (Smith et al. 2015).

The International Maritime Organization (IMO) has established a series of baselines for the amount of fuel each type of ship burns for a specific cargo capacity. It is expected that by 2025 all new ships will be 30% more energy efficient than those built in 2014. This, together with the progressively increasing highest regulations concerning energy efficiency will imply that the new build vessels of the future will inevitably be lighter in weight.

The projections of the emissions in the different planned scenarios done by the Third IMO GHG Study (2015) are displayed in Figure 1.1. The study argues that the improvements in efficiency mitigate the emissions growth, but even the most significant improvements modelled do not result in a downward trend. The study also defends that the primary source of this rise is due to the increasing demand for maritime transport. Putting then more pressure in the role of the maritime industry with GHG emissions.

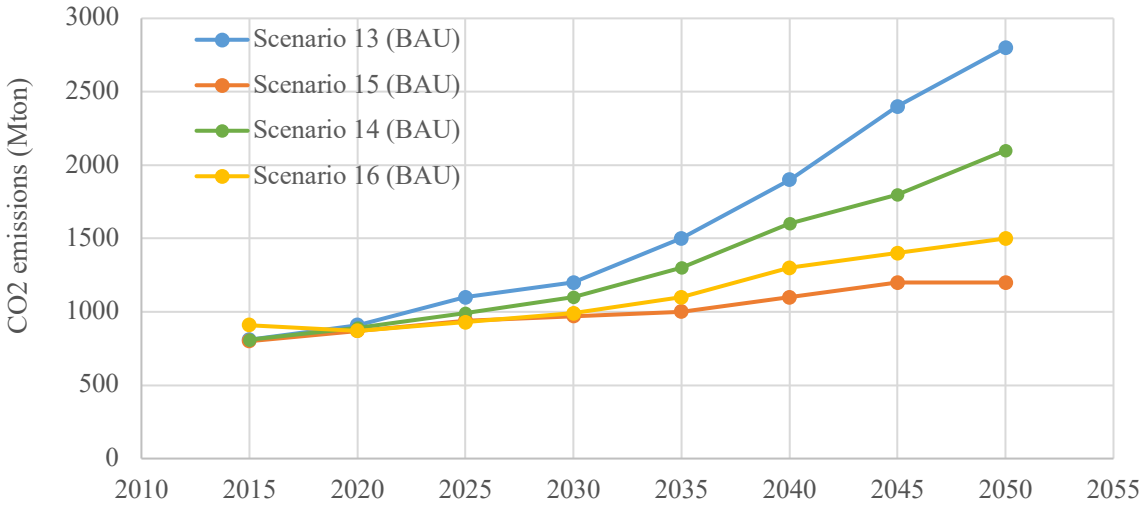

Figure 1.1: Emission projections for the BAU transport demand scenarios (Smith et al. 2015)

To avoid this situation the future vessels will need to move faster towards more sustainable transitions. The UN in their 2030 Agenda for Sustainable Development sets 17 Sustainable Development Goals; these goals integrate sustainable development in economic, social and environmental dimensions. (United Nations 2015). In the maritime industry, the IMO as the UN competent body gives advice and cooperation on how to move towards those goals. Of all the SDGs, the IMO takes a more interest concerning SDG 7 and SDG 13, concerning energy efficiency and the mitigation of climate change (IMO 2017). The IMO also promotes actions approaching the SDG 14 by the use of regulation of the carbon emission and marine geoengineering (IMO 2017).

Figure 1.2: The United Nation's 17 Sustainable Development Goals (United Nations 2019)

These challenges with the environment have motivated the urge for changes in shipbuilding. The intent of future designs is for increased energy efficiency, with the intent of complying with the environmental demands as well as for a more cost-effective vessel. One of the most popular developing methods to improve energy efficiency is by optimizing the hull design with a reduced weight. As a result of this optimization, the future new built vessels will have a more flexible hull, thus being more sensitive to waves. As a consequence, a hydroelasticity problem caused by the wave loads to the new, more efficient, vessel has to be addressed (Chen et al. 2017).

To ensure these optimizations do not compromise the structural integrity of the newbuilt vessel, new methods of hydrodynamic analysis have been developed. A more detailed experimental analysis that accounts for the new requirements can provide an insight into the dynamic load effect. Therefore, there is a tendency to simulate the complete vessel performance in waves instead of more focus-based single analysis in aspects such as rigid body response, slamming, sloshing or other areas of interest (Temarel et al. 2016).

At the same time, more simple methods of numerical analysis can give a faster and more robust solution, even if the applicability is limited due to the lack of critical physical phenomena not being considered. A more complete method has a more significant detail, but the solution

provided is more complex and time costly, making it not useful for some engineering applications. Additionally, in some cases it is not clear if the complex procedure can provide "better solutions" than a "simplified method".

Under this situation, the Swedish Maritime Administration granted a project research, on which the division of Maritime Technology of Chalmers collaborates with SSPA and Stena to develop methods for dynamic designs of ship. The vessel used for this study is the next generation of RoPax vessel, Stena Elektra. Still in the concept stage, Stena Elektra is designed to be powered fully electric operating between Göteborg and Frederikshavn (Stena Teknik 2019).

In the joint project, model tests are conducted in SSPA's towing tank, while the corresponding numerical simulations are carried out by Chalmers. In order to analyse better the behavior of the dynamic loads, SSPA carried out the experiments using a segmented or backbone model. Sophisticated numerical tools have been used to simulate the seakeeping characteristics and the dynamic structural responses of concept vessel. These have investigated together with the experimental data delivered by SSPA.

1.2 Objective and goals

The main objective of the thesis is to define under which circumstances can make a rigid body numerical model capture the behavior of a segmented backbone model. This is done by the use of a commercial tool and a state-of-the-art rigid body numerical model to simulate a sea basin experiment of a segmented backbone model.

An important goal is to understand under which sea state conditions and circumstances can make the simulation model capture the adequate motion and structural responses compared to a more flexible experimental model. This goal focuses on identifying where the limits are with the simulation model, under which conditions, and what needs to be adjusted and how in the simulation model.

Another goal of this thesis is to understand the methodology and behavior of the segmented model and to increase understanding and knowledge about dynamic loads on ship structures as well as the structural responses

The final goal is to define under which circumstances the numerical model data is similar to the experiment. Making it possible to deliver some recommendations on the use of a numerical dynamic model inside of the design process.

1.3 Assumptions and limitations

The main limitation of this thesis is the aim to predict the behavior of experiments done by a segmented backbone experimental model with a rigid numerical ship model. This will affect the comparison with the experimental data, because the more flexible segmented model is expected to be more sensitive to motions that will ultimately also affect the structure's responses.

This assumption is based on the main objective of this work, and it is related to the software used for the simulations concerning the different properties of the SESAM software package (DNV 2006). This software package has been widely used in the assessment of the experimental test, but the simulations are assuming the ship to be a rigid body against the segmented model used in the experiments.

The dry condition eigenanalysis is done by SESAM GeniE (DNV GL 2015a) setting the limitations to the ones of the software's code. In this analysis the model is treated as a beam being dependent on the properties of its supports. This could affect the numerical interpretation of the free vibration causing then uncertainties with experimental model value.

The seakeeping simulations with SESAM HydroD (DNV GL 2016) follow the use of potential flow. A Rankine Panel method is chosen to define the fluid grid, and the irregular waves are defined by the JONSWAP spectrum. Linear wave theory has been used for all simulations expecting good prediction for all sea states; a limiting criterion may appear in harshest sea states where moderate nonlinear effects start to be introduced.

The experiments done by SSPA are not included in the thesis. Some particulars concerning the model and the test that are relevant for the assessment and analysis of the numerical results are introduced in further chapters. However, there are experimental uncertainties that have not been investigated. These together with the model uncertainties may cause deviation of the results, but they have not been studied in detail.

1.4 Outline of thesis work

The outline of this thesis is divided into seven different chapters. Chapter 2 presents the methodology of the work, the workflow as well as a presentation of the software used, and procedures followed. Chapter 3 describes the experimental methods where the relevant subjects of the experiments are presented, such as the type of model and the types of tests produced. The presentation of the use of numerical methods for dynamic behavior as well as the definition of the main characteristics of the simulation model is presented in Chapter 4. Chapter 5 presents and discusses the results of the simulations and their comparison with the experimental results. A conclusion is made in Chapter 6 where the results are summarized, and the main finding of the results are discussed. Recommendations for further work are presented in Chapter 7.

2 Methodology

The methodology and the workflow of this thesis can be found in Figure 2.1; the main theoretical concepts involving the numerical simulations are studied for an increased understanding of the results. After a calibration of the numerical model is carried out to simulate the experimental model. Numerical analysis has been carried out for the comparison and later assessment of the hull structure natural frequencies, ship motions and wave loads.

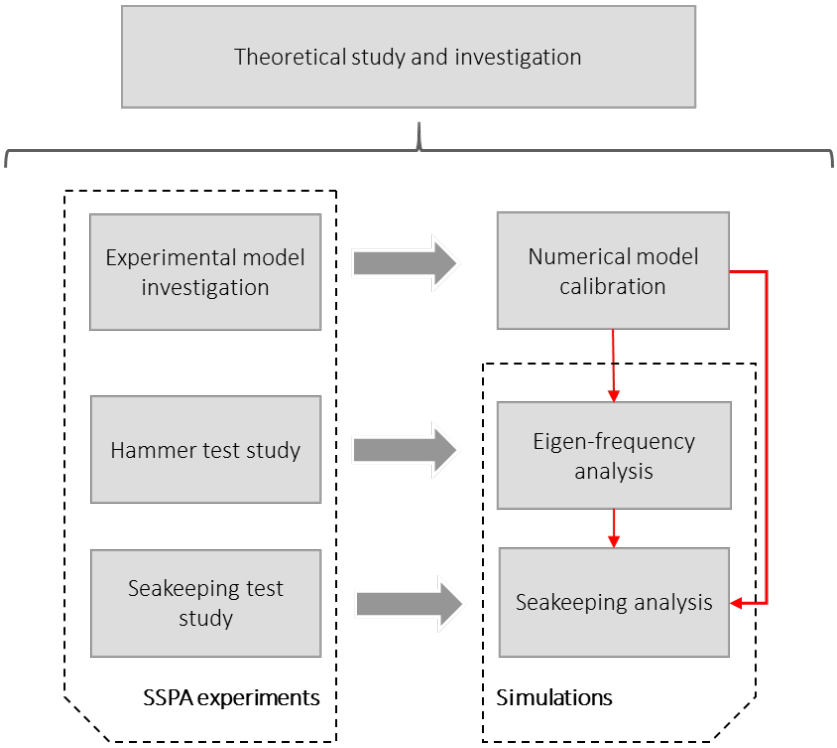

Figure 2.1: Chart describing the methodology applied in this thesis work

The theoretical study presented in this thesis is concerned with the limitations and assumptions of the thesis. An introduction to segmented models is presented as well as the main characteristics and properties in which this type of model functions. At the same time, the characteristics in which the simulations are defined are introduced. Concepts concerning the linearity of the waves, the panel method, and cross-section load calculation are presented. Also, the main particulars of the experimental test are presented in order to increase the understanding of the numerical analysis results.

The configurations of the numerical model are done using the package DNV GL SESAM. The eigenfrequency analysis is done using the FE-code Sestra inside DNV GL's SESAM GeniE (DNV GL 2015) while the hydrodynamic analysis is done with WASIM code inside HydroD (DNV GL 2016).

The scaling of the model test and experimental results are done following the ITTC Recommended Procedures and Guidelines (ITTC 2011). The dimensioning scale ratios for dynamic structural properties can be seen in Table 2.1.

A calibration of the numerical model is done to reproduce the test behavior. After, an eigenanalysis of the numerical model in FEM is implemented in dry and wet conditions in order to analyse the concerning model behavior and its later similarities with the experimental model.

Seakeeping simulations are also carried out following the main characteristics of the sea states, ship speeds, and wave direction according to the experiments. The ship motions for all these conditions are measured, as well as the cross-sectional forces and motions. These results are compared with the experimental data. These data are compiled in a series of HDF5 format files and data models that store the measured data of each one of the experiments runs. Each one of these hierarchical files contain all the relevant data for each experimental run, such as the moments, forces, wave spectrum and wave motions.

For the discussion and results, the extraction and statistical analysis of the results is done using MATLAB (Mathworks 2016). After, the conclusion to the thesis is presented. Finally, some recommendations for the use of the numerical model simulations as well as some proposed future work after the thesis.

Table 2.1: Ideal and Practical Scaling Ratios (Dinsenbacher et al. 2010)

Quantity	Prototype	Ideal Model	Practical Model
Length	L	L/λ	L/λ
Water density	ρ	ρ/c	ρ/c
Time	t	$t/\lambda^{1/2}$	$t/\lambda^{1/2}$
Mass	m	$m/c\lambda^3$	$m/c\lambda^3$
Velocity	v	$v/\lambda^{1/2}$	$v/\lambda^{1/2}$
Acceleration	a	a	a
Force	F	$F/c\lambda^3$	$F/c\lambda^3$
Ship Displacement	Δ	$\Delta/c\lambda^3$	$\Delta/c\lambda^3$
Moment	M	$M/c\lambda^4$	$M/c\lambda^4$
Pressure	P	$P/c\lambda$	$P/c\lambda$
Frequency (flexural modes and rigid body motions)	w	$w\lambda^{1/2}$	$w\lambda^{1/2}$
Bending Rigidity	EI	$EI/c\lambda^5$	$EI/c\lambda^5$
Shear Rigidity	KAG	$KAG/c\lambda^3$	$KAG/c\lambda^3$
Modulus of Elasticity	E	$E/c\lambda$	E/e
Section Area			
Moment of Inertia	I	I/λ^4	$Ie/c\lambda^5$
Distance from neutral axis to outermost fiber for hull-girder (prototype) or strength bar (model)	y	y/λ	y/r
Section modulus	Z	Z/λ^3	$Zer/c\lambda^5$
Flexure Stress	σ	$\sigma/c\lambda$	$\sigma\lambda/er$

Note:
λ is the ratio of prototype to model length
c is the ratio of prototype to water density
e is the ratio of prototype to modulus of elasticity
r is the ratio of distances from the neutral axis to the outermost fiber

3 Description of physical ship model tests

In this chapter, the main characteristics of the experiments are presented. The particulars of the experimental model used are displayed as well as the main properties of a segmented model. The experiments carried out in the SSPA wave basin are also explained in order to provide knowledge for better numerical analysis and assessment of results presented later in the thesis. These experiments are the wave calibration, manoeuvring, hammer test, and seakeeping test.

3.1 Segmented models

The main particularity of the segmented model is that it can approach the hull interaction with waves as a hydro-elastic problem. On the other hand, the more general approach is to determine the ship loads and motions working on the assumption that the ship behaves as a rigid body (Jiao et al. 2019). This general assumption is not reliable enough for light weight vessels, high speed vessel or large ships where the wave loads and ship vibrations are considered as a hydro elastic problem. This hydro-elastic approach is proven to be better for fluid-structure interactions where the structure vibration and deformations are more accurate (Jiao et al. 2019).

The segmented model is characterized by dividing the ship's model in several segments that are fixed by a beam or interface, also known as "backbone" (Figure 3.1). Segmented models transfer the wave forces on the hull to the backbone producing a better reading of the results, due to the hydro elasticity of the whole segmented model. Making their use ideal for seakeeping experiments, allowing them to investigate better hydro-elastic responses.

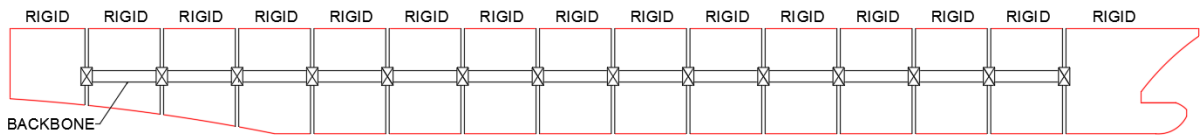

Figure 3.1: Sketch of a segmented body disposition

The segmented body simulates the model as a combination of smaller individual rigid segments and not as a whole rigid model, due to that it allows the segments to move individually in the six DOF (Figure 3.2). This allows it to be more prone to read the wave loads and their consequent phenomena, such as whipping and springing (Marón and Kapsenberg 2014). While the number of segments of the ship is determined by the desired detail of the results, the following rule of thumb can be made, the more modes shapes the higher number of segments (Marón and Kapsenberg 2014).

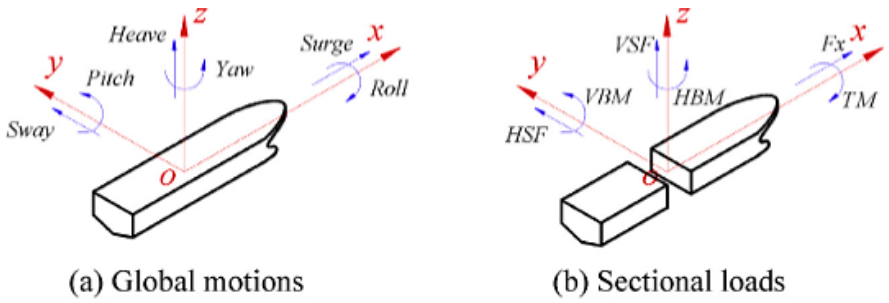

Figure 3.2: Definition of global motions and loads (Jiao et al. 2019)

The use of experimental models and their consequent numerical analysis has been widely used since 1980 (Davies et al. 2018). Since then, the segmented models have been mainly focused on the study of large containerships and bulk cargo vessels, due to their more sensible behavior towards horizontal wave loads, therefore having also higher probabilities on whipping and springing.

These effects are a consequence of the dynamic interaction between ship and wave both in dynamic mode. The impact of the waves into a moving ship usually does not suppose a greater effect into the hull structure, but in rough weather when slamming occurs (produced by the sudden impact of the bow when it breaks away from the water) it can excite the structure producing whipping. Whipping is, as a consequence of slamming, a two-node vibration of the hull on fundamental frequency that can produce high stresses and large loads in the area of impact.

Springing, which is also a result of the interaction between the structure and the waves, is the resonance between the frequencies of the waves encounter and the natural frequency of the ship. Slamming, as well as whipping, can be avoided by reducing the speed or changing the course of the vessel. Unfortunately, it is more difficult to predict springing due to all the different wave frequencies that can be found in several sea states. That is why a proper investigation of the structure natural frequencies in the model is really important for the ship's behavior.

For most of the segmented models the space between the cuts of each segment is usually between 5 to 10 mm. The use of rubber for the model construction is not recommended because of its disturbance in high damping (Storhaug 2014). For investigation, the model has to share the same neutral axis as the real ship. The elasticity of the model depends on a high degree on the stiffness of the backbone. From the rigidity of the backbone, a segmented model can be divided into two types: elastic and rigid (ITTC 2011).

1. **Rigid Segmented model**. This type of segmented model is characterized by having a much more rigid backbone. In this model there is no variation on the wave peaks at measured and natural structural frequencies making them larger than the wave frequency (ITTC 2011). Load data can evaluate either from each segment or directly from the bending moment from the beam. For the eigenanalysis, the model can be assumed to be rigid making it able to use its loading results as an input for an analysis of the structure. (ITTC 2011).

2. **Elastic Segmented model**. This type of segmented model is characterized by having an elastic backbone, allowing to read the different data at different points of the model. A rigid internal structure can be used in these types of models in which the rigidity of the model segments can be instrumented (ITTC 2011).

Segmented models are made to reproduce the vibrations in the most realistic way, generally for vertically in two nodes modes. Depending on the purpose of the study such as in the investigation of a refinement the model's material is made and by matching the natural frequencies, using an open section beam, the analysis can be done (Hong et al. 2011). The mass distribution of the model should be following the same mass properties as the ship under study. For fatigue analysis, where the whipping and springing are analysed, it is recommended to have three flexible joints in the model (Storhaug 2014).

For the experimental test, the model can be moved either self-propelled or towed externally. In the case of being towed, the towing forces cannot interfere with the experiments. The springs supporting the model should give real values for surge and model speed and at the same time not compromise the direction (Storhaug 2014).

3.2 Experimental model of the case study vessel

The model is an elastic segmented model divided into four different segments (Figure 3.3), which ensures a proper reading of the data and at the same time, makes it more economically viable. Each segment had a stiff carbon fiber box that with the use of adjustable springs on the top of the model could change the flexibility of the model.

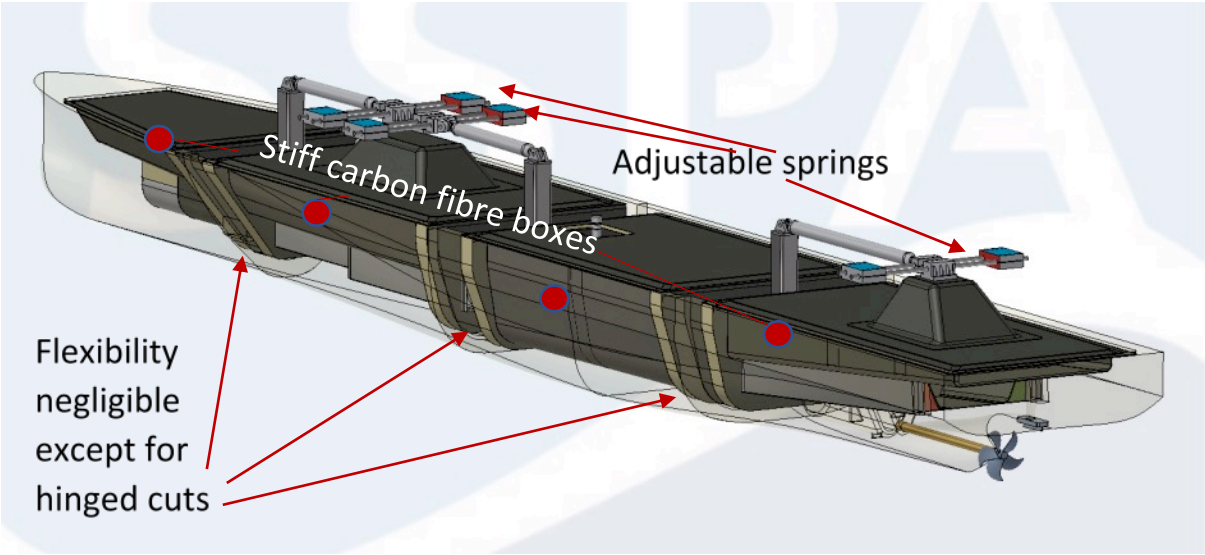

Figure 3.3: Experimental model set up

The main particulars model and their respective scaled value for the full-size vessel are displayed in Table 3.1. These characteristics and properties of the model are scaled to full size to be fitted for the numerical simulation in order to ensure that the properties of the experiment stay the same in the computational simulations, following the ITTC scale recommendation shown in Table 2.1.

Table 3.1: Model characteristics

Model	Experimental	Numerical
Length between perpendiculars, Lpp [m]	5.284	195.5
Waterline length, Lwl [m]	5.072	187.68
Depth, T [m]	0.409	15.12
Beam, B [m]	0.749	27.74
Beam in waterline, Bwl [m]	0.715	26.46
Draught fore [m]	0.17	6.3
Draught aft [m]	0.17	6.3
Displacement, Δ [kg]	356.69	18 477 075
LCB, LCG [m]	2.405	88.985
VCG [m]	0.314	11.61
Water density [kg/m3]	998	1025
Water ratio density		0.97
Scale factor		37

For the reading of the data, the coordinate system for the experiment follows x- horizontal, y- transversal, z- vertical; being the positive direction looking at the fore-ship and into the bottom. The center of gravity is set at the aft perpendicular at ground level. The measuring cross-section is located at the aft, fore, and mid-section of the model at 6.29 meters from the ship base. In this work only the midsection data has been analysed, being the measuring point coordinates located at (88.895, 0, 6.29) meters.

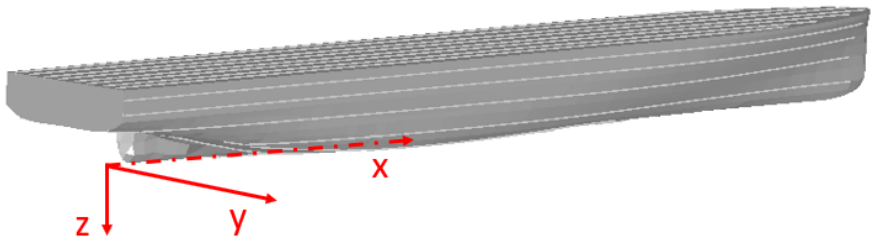

Figure 3.4: Coordinate system

3.2.1 Rigidity of the segmented model

A segmented model such as the one used can predict the eigenfrequencies by adjusting the mass distribution and effective stiffness. This gives the model four degrees of freedom for each segment (the three direction displacements (x, y, z plus the horizontal rotation of the hull segment). Therefore, the model is able to reproduce the flexural dynamics of the real vessel (Vakilabadi et al. 2014).

The weight distribution of the model as presented by SSPA is in Figure 3.5. There, the center of gravity and moments of inertia of each segment are set in order to the full size vessel in full operation. The stiffness of the model was set to reach a target stiffness of 2442 Nm/deg for all

three cuts of the model. These results can be seen in Table 3.2, whereas the total stiffness distribution in the model is displayed in Figure 3.6.

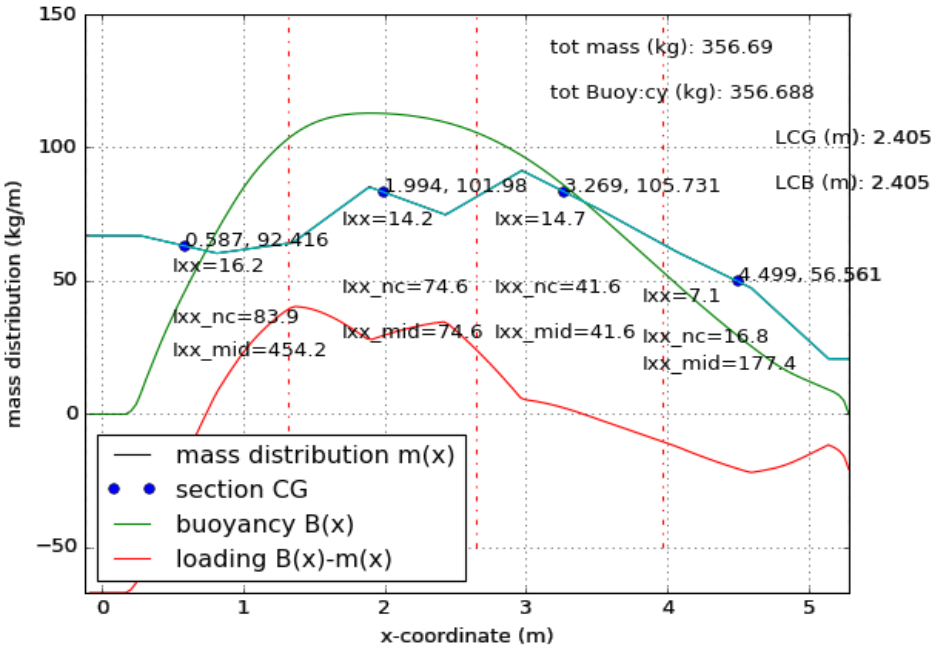

Figure 3.5: Graph over mass distribution, buoyancy distribution (model scale)

Table 3.2: Achieved values of cut stiffness

Cut	Stiffness (Nm/deg)
Aft	2452
Mid	2522
Fore	2397

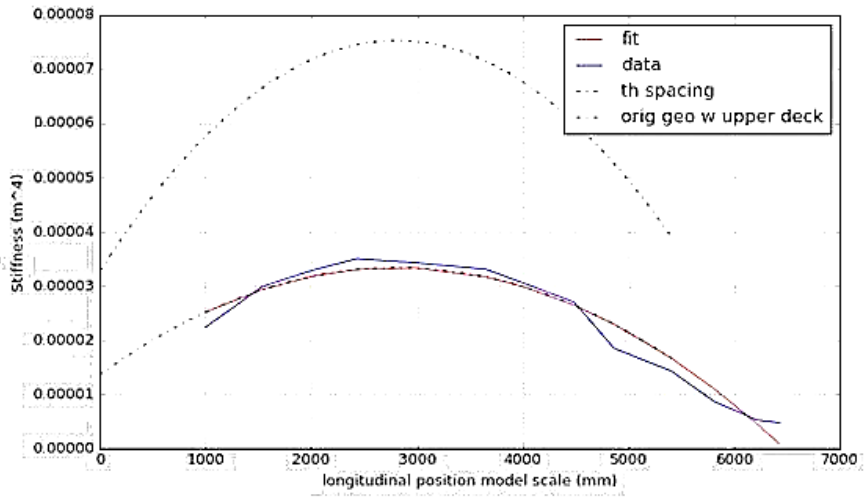

Figure 3.6: Stiffness distribution model scale

3.3 Setup and design of the experiments

To understand the hydrodynamic behavior the structural integrity of the vessel under dynamic loads, SSPA carried out the experiments under a segmented or backbone experimental model. This will make it possible to provide data for analysis in the following areas of interest (ITTC 2011):

1. Primary design loads
2. Slamming, whipping and springing loads
3. Validation of computational methods
4. Frequency domain application to lifetime designs
5. Application to extreme loads – stochastic analysis
6. Fatigue analysis and design
7. Safe operating envelope

The focus of this project lays in the validation of the computational methods, giving later some recommendations for the use of the model for the rest of the areas of interest.

The SSPA different experiments can be summarized in Table 3.4; these experiments consist of a series of different types that go from the wave basin and model calibration to the seakeeping experiments. These different test types carried out with the model are:

1) **Wave calibration**: For the preparation of the tank a wave calibration is needed in order to set the different sea states for other test types. For each different run, the wave height and wave period has been measured to ensure their quality.

2) **Manoeuvring**: Preparation test done in order to calculate the GM and to do the model speed calibration for all the different speeds.

3) **Hammer test**: Test that consists of hitting the model with a hammer to see the resonance frequency of the model structure. This type of test was carried out in dry and wet conditions.

4) **Seakeeping**: These tests are carried out using the JONSWAP spectrum in the wave basin, they were done with following seas and bow seas (180 and 150 degrees) at different speeds in order to increase the number of wave encounters and increase the chance of slamming.

The wave calibration and manoeuvring form part of the set up for the preparation of the wave basin for the seakeeping test these two tests are not relevant to the simulations but are essential for the preparation of the experiment. The wave calibration is the set-up of each of the different sea states in the basin for a period of time, ensuring the wave behavior for the next experiments. The calibration of the waves had a duration of 10 minutes per sea states; the different sea states can be shown in Table 3.3. On the other hand, the manoeuvring test consists of the calibration of the model speed in the wave basin in order to ensure the behavior of the model for further experiments.

The seakeeping test are then divided into different series, each one representing one of the different five sea states. These sea conditions are representative of the area of the operation of the real vessel. The last two seakeeping series are neglect due to their lack of providing any relevant information. In S009 there was no performance of the model, while S010 failed to provide any added data concerning the aft-body slamming in following seas.

Table 3.3: Test series sea states

Series	Sea state	Hs [m]	Tp [s]
S004	4 long crested seas	1.88	7.56
S005	4 short crested seas	1.88	4
S006	5 long crested seas	3.25	9.24
S007	5 long crested seas	3.25	5
S008	6 long crested seas	5	10.78

The waves generated for all the seakeeping tests are irregular; this type of wave is suited to determine unknown resonances, response amplitude operator and statistical data provided from the time series data. The selection of short crested seas for S005 and S007 helps to provide a higher loading impacting the model. The calmer sea states, from series S004 to S006, are expected to behave well inside the linear wave theory, while the in rougher sea states, for series S007 and S008, the behavior is expected to be within the border of nonlinearity.

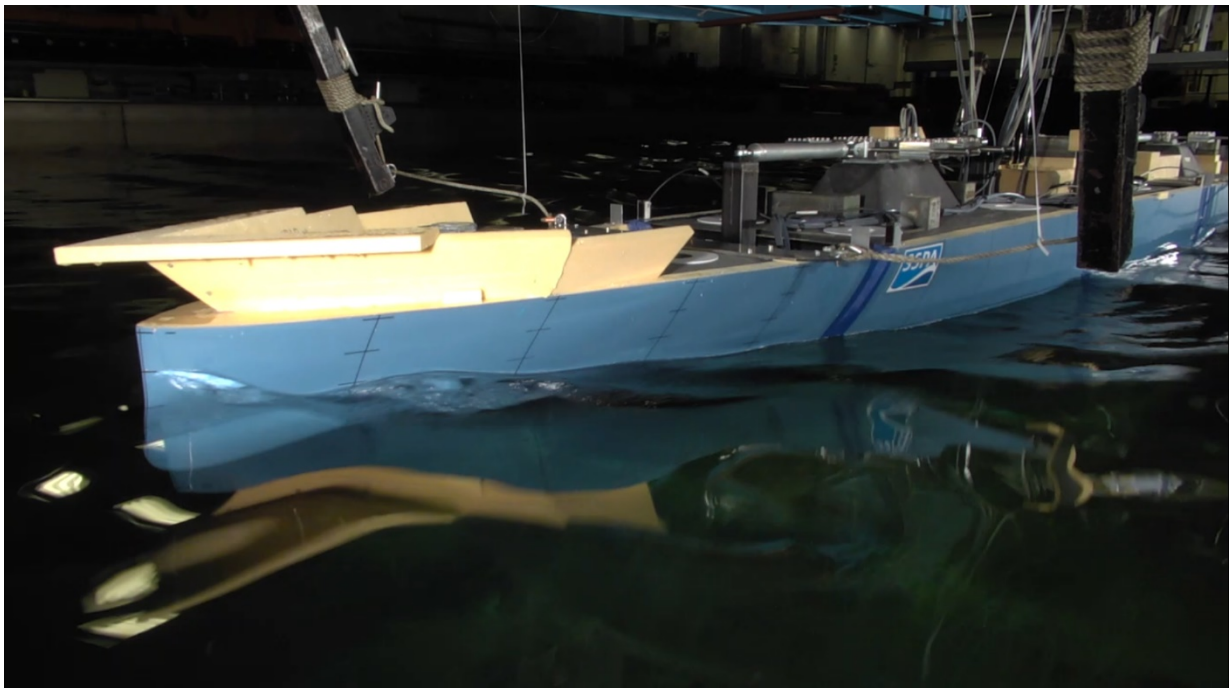

Figure 3.7: Seakeeping test run in SSPA MDL wave basin

To make the comparison with the numerical simulations, a compilation of relevant data from different model tests has been assembled for each simulated condition. That way, the resultant

assembled test data for each condition has had more experimental time to compare against the numerical simulations. The total experimental time for each simulation condition that has been compared against the simulation are presented in Table 4.3. The experiments test selected and compiled for each condition that have been compiled for the assessment of this thesis can be found in the appendix.

Table 3.4: Experiments run set up

Series	Test type	Number of tests	Sea states	Wave direction [deg]	Model speed [m/s]	Ship speed [kts]
S000	Wave calibration	5	--	--	--	--
S001	Manoeuvring	10	--	--	--	--
S003	Hammer test and control	--	--	--	--	--
S004	Seakeeping	28	4 long crested seas	150; 180	1.269; 1.522; 1.776	15; 18; 21
S005	Seakeeping	9	4 short crested seas	180	1.522	18
S006	Seakeeping	23	5 long crested seas	150; 180	1.269; 1.522	15; 18
S007	Seakeeping	9	5 long crested seas	180	1.522	18
S008	Seakeeping	11	6 long crested seas	150; 180	1.015; 1.269	12; 15
S009	Seakeeping	--	--	--	--	--
S010	Seakeeping	--	--	--	--	--

4 Description of the numerical simulation model

The aim of this chapter is to describe the theoretical basis for the software and models. Theoretical concepts regarding the assumptions and limitations for the wave grid and the calculation of forces and motion give later a large understanding of the numerical results against the experiment data. Later, the set up for the simulation are presented, showing the main defining characteristics for the seakeeping simulation.

4.1 Wave definition

The wave definition has been done using the Wasim interface inside SESAM HydroD (DNV GL 2016). Showing that the waves can be described as the sum of harmonics defined as (DNV 2006):

$$\eta(x,y,t) = A\,cos[(kcos\beta)x + (ksin\beta)y - \omega t + \gamma] \tag{1}$$

Which can also be expressed in complex form as;

$$\eta(x,y,t) = A\,\exp\,[i\big((kcos\beta)x + (ksin\beta)y - \omega t + \gamma\big)] \tag{2}$$

The use of wave amplitude and phase angle as parameters in the sum of harmonics allows to define all types of sea states. At the same time, Wasim allows the possibility of using infinite depth, which would allow the term:

$$k = \frac{\omega^2}{g} \tag{3}$$

The wave grid in Wasim is done using the Rankine Panel method; one of the advantages of this method is its adaptability to work with different types of boundary condition problems (Aichun et al. 2016). This method describes a boundary value problem governed by the Laplace equation in irrotational and potential flow:

$$\nabla^2\phi = 0 \tag{4}$$

At the same time, these conditions have to be applied to the free surface (S_f), body surface (S_b), the bottom (S_0) and the surrounding surface at infinity (S_∞) (Beck 1994). For the wetted surface and the bottom, there is a kinematic condition:

$$\frac{\mathrm{d}\Phi}{dn} = V_B \cdot n \text{ on } S_B \tag{5}$$

$$\frac{\mathrm{d}\Phi}{dn} = V_0 \cdot n \text{ on } S_0 \tag{6}$$

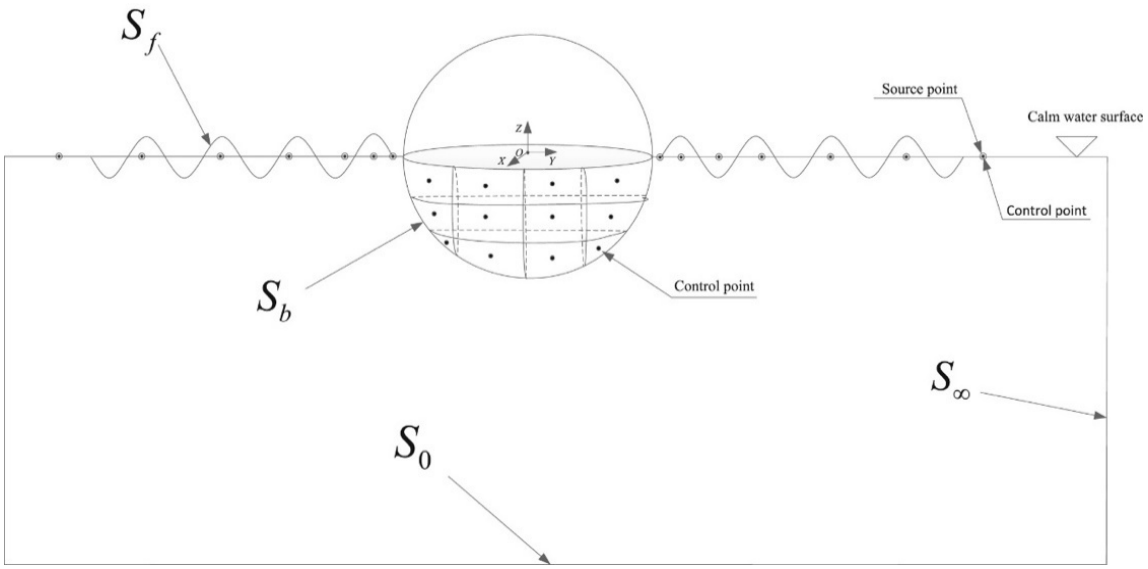

Table 4.1: Three-dimensional numerical model sketch (Aichun et al. 2016)

Where *n* is the normal vector, V_B is the velocity of a point in the surface and V_0 is the velocity of the bottom. For an infinite depth, V_0 will tend to zero. This way the all the fluid conditions interacting with the model can be described as it is seen in Figure 3.1. This gives two main advantages for the Rankine Panel method comparing it with other Panel methods such as the Green Panel method, these are:

1. Easy handling of the free surface conditions.
2. No use of irregular frequencies.

On the other hand, as a consequence of the problem description of the flow, the Rankine Panel method must consider the following boundary conditions (Bertram 2012):

1. There is no water flow considered along the ship surface.
2. Kutta conditions, the fluid pressure is the same at both sides of the edge of the hull.
3. Transom condition, the transom is considered to be dry.
4. Kinematic free surface condition, in the free surfaces there is no flow of water.
5. Dynamic free surface condition, the atmospheric pressure is considered in the free surface.
6. The effects of the ship on the water are neglected away from the ship analysis area.
7. Radiation conditions, the waves created by the ship disturbance move away from the ship.
8. Open boundary condition, the waves created leave the computational domain not returning after.
9. The forces on the ship produce ship motion.

4.2 Hydrodynamic interaction with the hull

The wave loads due to dynamic behavior are due to the difference between the forces of inertia and the forces due to hydrodynamic pressure on the hull surface (Fonseca and Guedes Soares 2004). This can be expressed as:

$$F_i(t) = I_i(t) - R_i(t) - D_i(t) - K_i(t) - H_i(t) - G_i(t) \quad (7)$$

$$M_j(t) = I_j(t) - R_j(t) - D_j(t) - K_j(t) - H_j(t) - G_j(t) \quad (8)$$

The subjects i j represents the associated ship motion to the different load components; being surge, sway and heave for forces and roll, pitch, and yaw for moments. The load components are the radiation (R) the diffraction (D), the Froude-Krylov force (K_k) and the restoring hydrostatic force (H_k).

For linear formulation in WASIM, the components for hydrostatic and Froude-Krylov forces calculated by the pressure integration of the mean wetted surface producing unrealistic distribution of stress in the splash zone, implying that the sea pressure above that value (Li et al. 2014).

The exciting forces due to the incident waves can be divided into two components: Froude-Krylov force and diffraction forces.

- **The diffraction force** is produced by the effect of the wave field while the vessel is moving. It is expressed as the advancement of the ship at a certain speed (considered constant for this thesis) while the ship goes through the waves and it is restrained by the mean position.
- **The Froude-Krylov force** is related to potential wave incident, is a result of the integration of the associated pressure over the hull wetted surface. In irregular waves, the wave field pressure is calculated through the harmonic superposition that defines the waves. As mentioned before, the linearity defines the wave pressure up to the mean of the waterline, thus making the hydrostatic pressure on the free surface negligible.

The hydrostatic forces are a result of the integration of the hydrostatic pressure on the wetted surface. For the linear method, this force is only computed under the undisturbed wave profile. In this case, the hydrostatic force components can be expressed as the standard linear of restoring force coefficients, as for heave and pitch (Singh and Sen 2007):

$$H_3 = \rho g AWP \xi_3 \quad (9)$$

$$H_5 = \rho g \nabla GML \xi_5 \quad (10)$$

The radiation restoring force corresponds to the correction to the ship hydrodynamic forces due to the flow acting in the hull. The radiation force is related to that way to the restoring coefficients, being a collection of these with the memory functions representing the vessel properties moving at a certain speed.

The green water forces are the vertical forces related to the effect of green water on the deck. This one occurs when the relative motions are larger than the freeboard. The water force is proportional to the height of the water on the deck, which is the difference of the motions with the freeboard of the vessel.

4.3 Setup of numerical simulations

The numerical model of Stena Elektra has been designed by DNV GL for Chalmers following the hull design of Stena; this model has been specially designed for its use with the DNV GL SESAM software pack. The dimensions of the model follow the properties of the real size ship (Table 3.1).

The panel resolution of the model follows an aspect ratio of 0.03, which has been recommended by DNV GL. A convergence analysis has proven that this aspect ratio works for drafts between 6 and 7 meters. On the other hand, the use of a higher draft or ratio will degenerate into mesh errors.

The numerical simulation model is used to simulate the experiments presented in Table 3.4. To achieve that mass distribution, the simulated ship has to reproduce the experimental model geometric properties (See Figure 3.5). A calibration of the ship's weight is needed to reproduce as much as possible the same geometrical properties as the experimental model.

The computational methods need more detail and control in their calculations. Higher measurement and control of variables will help in the analysis against the model forces (ITTC 2011). For advanced numerical tools, motion control is needed as a requirement for an accurate prediction of ship motions (Lin et al. 2004).

A ship motion control has been set up in the simulation to keep the desired course of the model. These springs are attached to the bow and stern of the vessel to decouple the surge from saw and yaw (Figure 4.1). Both stiffness and damping are defined for the springs. In Wasim, the user does not specify the damping and stiffness coefficients directly. Damping is a fraction of the critical damping; that is why the stiffness is implicitly given by the specifying natural period in the modes control (DNV GL 2015b).

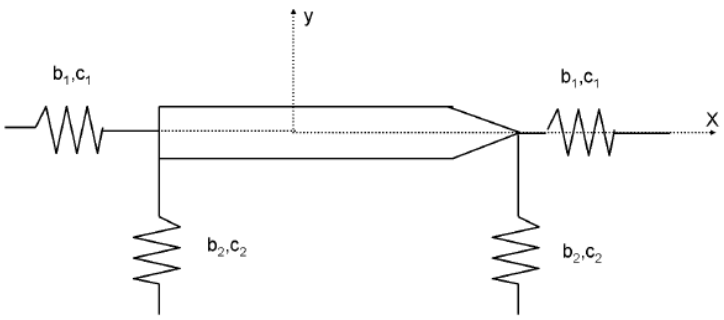

Figure 4.1: Motion spring in bow and stern (DNV GL 2015b)

The natural periods specified should be much longer than the natural period in roll in order to avoid interferences with the roll motion. Typical values range from 60-120s for conventional ships and 30-60s for high speed vessels. Notice that depending on the increase of this value may also affect the transient period of the simulation; the stiffness will be computed by assuming that the modes are uncoupled. Thus, the actual natural periods may differ from the periods given by the user (DNV 2006). These motion controls used in the simulation can be seen in Table 4.2.

Table 4.2: Motion control on the bow and stern

	Eigenperiods			Damping coefficients		
	Surge	Sway	Yaw	Surge	Sway	Yaw
For moderate speeds	100s	70s	70s	0.05	0.05	0.05
For high speed (21kts)	75s	45s	45s	0.45	0.45	0.45

To verify the hull structure of the numerical method, the eigenvalues of the numerical model will be analysed and compared with the experiment to ensure the behavior of the structure for hydro elastic behavior. This eigenfrequency analysis is carried out using the Wadam for floating and fix structures inside SESAM HydroD (DNV GL 2016) to find the resonance frequencies of the numerical model. This frequency is later compared with the results of the hammer test experiments.

Once the modal analysis has verified the model, the five different sea states are simulated using the Wasim code under the HydroD (DNV GL 2016). This software is meant for hydrodynamic analyses of fixed and floating vessels with or without forward speed, and at the same time, it also computes the motions and local pressure on the ship under study.

The conditions for the different sea states and seakeeping tests, shown before Table 3.4 and in Table 3.3, have been compiled in 16 different simulation runs to analyse. These are found in Table 4.3, where the relevant data describing each sea condition is found.

Table 4.3: Simulation conditions

Condition	Sea state	Speed (kts)	Wave direction (deg)	Significant wave height (m)	Wave period (s)	Relevant time for analysis [scaled] (s)
1	S004	15	180	1.88	7.56	681.939
2	S004	15	150	1.88	7.56	423.117
3	S004	18	180	1.88	7.56	552.437
4	S004	18	150	1.88	7.56	341.000
5	S004	21	180	1.88	7.56	115.000
6	S004	21	150	1.88	7.56	130.000
7	S005	18	180	1.88	4.00	200.000
8	S006	18	180	3.25	9.24	584.979
9	S006	18	150	3.25	9.24	340.148
10	S006	15	180	3.25	9.24	467.521
11	S006	15	150	3.25	9.24	441.122
12	S007	18	180	3.25	5.00	250.000
13	S008	12	180	5.00	10.78	980.116
14	S008	12	150	5.00	10.78	568.130
15	S008	15	180	5.00	10.78	475.307
16	S008	15	150	5.00	10.78	425.855

5 Results and discussion

The following chapter addresses the results of this thesis; a discussion of the assessment of the numerical results against the experimental data is also introduced. This chapter is divided into the calibration of the model, the frequency analysis and the different sections concerning the seakeeping simulations. The seakeeping simulations results are starts with the incident waves, and later the motions and loads are introduced.

5.1 Calibration of the numerical model

A series of masses were added in the experiment model that represented the ship in full load condition. These weights were distributed along the model resulting in the properties expressed in Figure 3.5. To reproduce those main characteristics, a calibration of the simulation model has been done using Sesam GeniE (DNV GL 2015a).

This calibration sets the mass points along the model, to represent the mass characteristics of the experiment, as well as the ones as in real scaled ship. For each segment, a mass point is added on the upper deck and in a lower deck aiming to reproduce the same VCG as well as the same LCG.

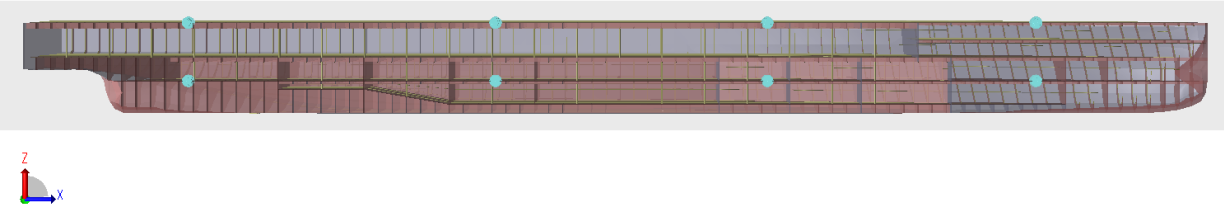

Figure 5.1: Numerical model analysis set up

The calibrated set-up of the mass points distributions of the model is presented in Figure 5.1 and Table 5.1. This distribution does not reproduce accurately the characteristics of each segment of the experimental model. Due that the mass point's distribution along the ship length does not follow the properties for their respective model segment. On the other hand, the calibration has achieved to reproduce the real size ship properties presented in Table 5.2.

Table 5.1: Mass component properties [kg]

	LCG=21.719m	LCG=75m	LCG=121m	LCG=166.463m
Upper deck (VCG= 5.40m)	1 089 915	1 202 709	1 246 946.56	667 056.44
Lower deck (VCG= 15.20m)	2 778 441	3 065 978	3 178 750.14	1 700 478.45
Hull weight [COG (87, 0, 8.121) m]				3 546 716.30

Table 5.2: Numerical model properties

Weight [tones]	18 477
COG [m]	(88.895, -5.29e-06, 11.613)
Ixx [m^4]	6.469 e +008
Iyy [m^4]	4.5901e +010
Izz [m^4]	4.5682e +010

5.2 Frequency analysis

5.2.1 Hammer test

The ITTC recommended guidelines (Dinsenbacher et al. 2010) were used as the procedure to do the resonance test. Two hammer tests were carried out for dry and wet conditions to find the natural frequencies of the structure.

For the dry condition, the model was supported at two points at 1100 mm (or 40.7 meters scaled) from the fore and aft of the model as can be seen in Figure 5.2. A third support was placed in the middle of the model to avoid any big high motions on the structure. For the wet condition, the model was made to resonate in the wave basin supported only by the water in free vibration.

The results on dry conditions and wet conditions are presented in Table 5.1. While the impulsive excitation was applied, the bending moments and shear forces were recorded by measuring cells between the segment cuts. The Fourier spectrum and the bending moment throughout time graphs are presented in Figure 5.3 and Figure 5.4.

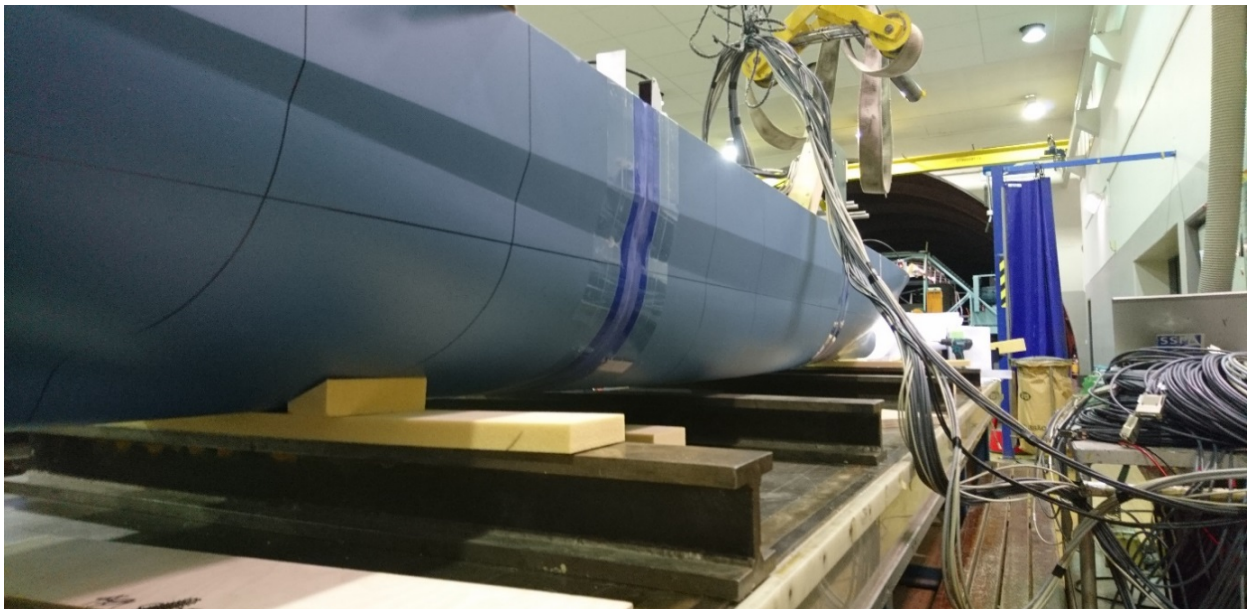

Figure 5.2: Picture of set up for resonance test

Table 5.1: Summary of results of resonance frequency test for two node bending

	Wet conditions		Dry conditions	
My/Cut	Resonance frequency model (Hz)	Resonance frequency full scale (Hz)	Resonance frequency model (Hz)	Resonance frequency full scale (Hz)
My/Aft	5.29	0.87	7.39	1.22
My/Mid	5.29	0.87	7.39	1.22
My/Fore	5.29	0.87	7.39	1.22

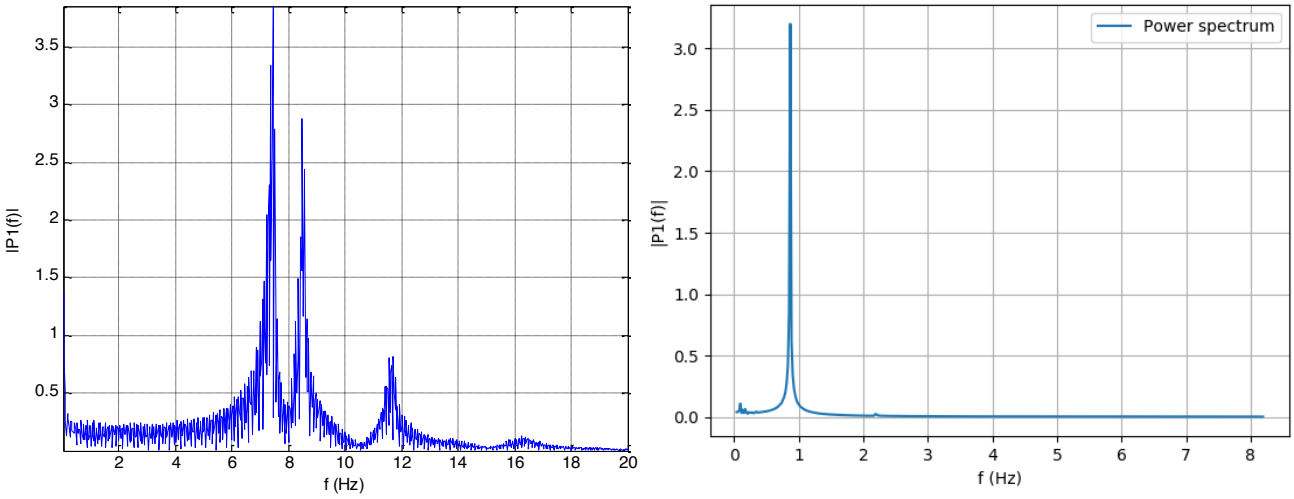

Figure 5.3: Single sided Fourier spectrum of bending moment at mid cut for (left) wet and (right) dry test conditions

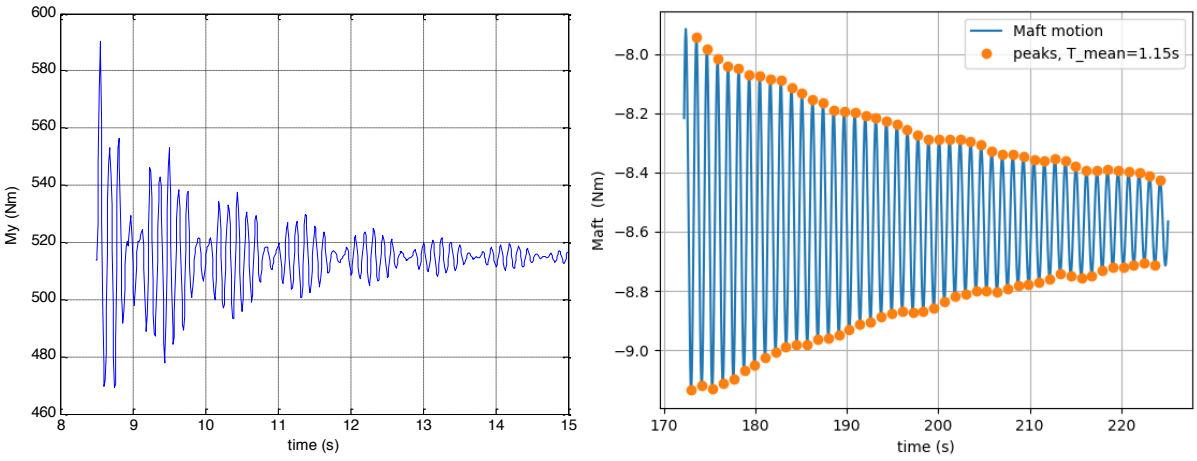

Figure 5.4: Time history of bending moment at mid cut for (left) dry and (right) wet test conditions

5.2.2 Eigenfrequency analysis

The numerical eigenvalue analysis set-up simulates the mass distribution of the model (Figure 3.5). This distribution is reproduced in the FE model in GeniE (DNV GL 2015a) as it has been presented in Section 5.1.

The eigenfrequency analysis for wet conditions has been simulated with the Wadam code inside HydroD (DNV GL 2016). Wadam is an analysis program for the computation of wave-structure interaction for fixed and floating structures. The Wadam code allows to extract the natural frequency from the wet condition in free vibration for a rigid body motion.

The result extracted from the code gave 0.79 Hz as the natural frequency of the model, showing a good performance in the model calibration with a difference of 9.1%. As expected, the numerical eigenfrequency is lower than the one the hammer test, showing the apparent effect of the rigid body. Under vibration, the behavior of the segmented model in the water environment affects each one of the segments producing a higher frequency reading.

The discrete mass distribution presented in Section 5.1, proves to be an effective and practical simplification to the real distribution in the experiment. A better mass distribution as well could improve the result obtained. Another cause of deviation for the simulation is the rigidity of the numerical model. Other factors due to the uncertainties of the experiment could have also affected the divergence of results.

For the calculation of the dry condition, the eigenfrequency has been computed with the GeniE (DNV GL 2015a) under its Sestra code. For the computation of the eigenanalysis, Sestra treats the model as a beam making it dependent on the geometry, mass distribution and supports, as boundary conditions. The treatment of the numerical model as a beam is a cause of uncertainty in the calculation as it does not allow a free vibration analysis.

For the frequency analysis, two support arrangements in the analysis setup are presented; their configuration is in Table 5.2 and Figure 5.5 and Figure 5.6. The first one introduces the supports at the edges of the model aiming to reproduce the vibration of the whole vessel fixed in the edges, giving a resultant frequency of 0.33 Hz for the first vertical mode. The second configuration aimed to reproduce the behavior of the hammer test experiment having the supports at 40.7 meters from aft and fore resulting in 0.72 Hz.

Table 5.2: Boundary condition of the supports

Arrangement		Position [m]	x	y	z	rx	ry	rz
1	Support 1	(-4.5, 0, 7.4)	free	fixed	fixed	free	free	free
	Support 2	(195.5, 0, 7.3)	free	free	fixed	free	free	free
2	Support 1	(36, 0, 0)	fixed	fixed	fixed	free	free	free
	Support 2	(154.4, 0, 0)	free	fixed	fixed	free	free	free

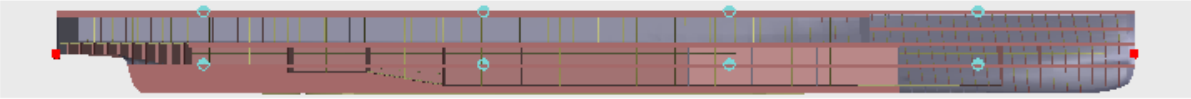

Figure 5.5: Dry eigenanalysis arrangement for layout 1

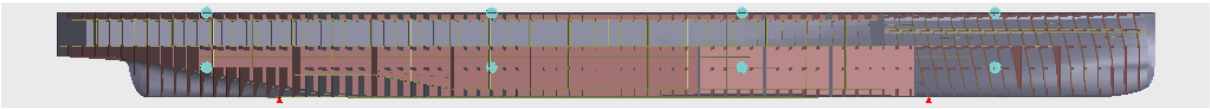

Figure 5.6: Dry eigenanalysis arrangement for layout 2

Due to the large difference of results with the hammer test (1.22 Hz), none of the simulations performed are satisfactory in the dry vibration analysis. Uncertainties on the setup or in the treatment as a supported beam by code could be a reason for these results. A problem in the nature of the rigid body against the segmented model could be a reason for some discrepancies in the vibration, but due to the high difference presented, this option is disregarded. Other factors that could also affect the computation could be the size of the numerical model, but it is unlikely due to the nature of the software. In the end, the numerical simulations failed to provide a valid result in water conditions.

To provide a more representative result in the dry condition analysis, the Immersed beam formula is introduced (Equation 12). This approximation work on the assumption that the fluid where the beam is immersed is incompressible (Sader 1998), assumption already been made by the panel method, see Section 4.1.

For a dry environment, the eigenfrequencies have been overestimated by the numerical results, inconsistencies that are uncertain for the conditions of this analysis. This divergence in the results could be due to the misuse of the software properties in frequency analysis. For that, the use of an approximation is introduced for the assessment of this value. This consist of

$$w_{fluid} = \frac{w_{vacuum}}{\sqrt{1 + \frac{\pi}{4}\frac{b}{h}\frac{\rho_{fluid}}{\rho_{beam}}\Gamma}} \tag{12}$$

where (Veryst Engineering 2019):

1) Γ: is the correction factor dependent on the geometry of the beam.
2) ρ_{fluid}/ρ_{beam}: is the density ratio
3) b is the aspect ratio

For practical use in water, the equation can be summarized in the following:

$$\frac{w_{air}}{\sqrt{2}} = 1.015 w_{water} \approx w_{water}\ (1\%\ or\ 2\%\ deviation) \tag{13}$$

This simplified version of the immersed beam vibration formula (Equation 13) that has been proven to work correctly in the correlation with the experimental results. The formula used comes from its extended version in Equation 12, where the value of the coefficient for the different frequencies are the result of the properties of the ship cross-section and environment conditions.

The calculated results presented show a slightly similar results with a natural frequency of 1.13 Hz in dry conditions and an error of 7.3% from the experimental test. The resultant frequency of the analysis can be found in Table 5.3. Hence, under these circumstances, the agreement between the experimental and the numerical model is considered to be satisfactory.

Table 5.3: Results eigenfrequency analysis

	Numerical [Hz]	Experimental [Hz]	Difference
Wet condition (simulated)	**0.79**	0.87	9.1%
Dry condition (approximation)	**1.13**	1.22	7.3%

5.3 Seakeeping simulations

A total of 16 seakeeping simulations have been carried out following the properties of Table 4.3. These simulations done in HydroD (DNV GL 2016) follow the weight distribution presented in this work as well as the main conditions expressed in Section 4.3.

For the seakeeping test carried in SSPAs MDL wave tank, a draft of 6.3 meters was fixed for all simulations to reproduce the desired draft desired behavior of Stena´s design. An offset on the seakeeping experiments has been found as a result of that draft. To simulate it, in the seakeeping simulation, the draft has also been fixed at 6.3 meters.

The simulations are carried out with the JONSWAP spectrum to define the wave profile. The simulation follows the linear wave theory with irregular waves. A standard of 2000 wave components have been selected for each simulation. The time for each simulation is of 30 min (1800sec) with time steps of 0.1 sec, a transient period of 100 sec for each simulation has been selected in order to produce a smoother transition at the start of the simulation.

The simulations have been carried out on time domain in Wasim and later analysed against the scaled experimental data in MATLAB (Mathworks 2016). The statistical analysis and conversion to the encounter spectrum are done using the WAFO toolbox (Brodtkorb et al. 2000). The main particulars for each simulation can be found in the appendix.

The sea motions of the numerical simulation have been recorded accordantly to the experimental model. For the simulation, the motions are measured in the midsection at draft height. The motion simulated follows the control spring motion presented in Section 4.3. The cross-section loads are measured in the aft, mid and fore section of the model.

5.3.1 Incident waves

The incident wave height has been analysed in order to ensure a good estimation of the wave impact on the model. This estimation has been done by setting the incident wave height on the time domain in the spectra. This way a good fit of the incidental wave will ensure the quality of the incident irregular waves (Zhu et al. 2011a). A display of the wave spectra for different simulation conditions is shown in Figure 5.7. Where it can be observed that both results show a good definition of the JONSWAP spectra profile. In calmer sea states at low speed the incident waves of experiment and simulation stay similar; at lower speeds the incident of waves on the hull decreases. As the sea state becomes higher the numerical incident wave surpasses the experimental prediction. This could be due to the linearity of the waves and its assumption of not considering the wave effect of the water flowing thorough the hull. The linearity of the numerical result is also compromised at high-speed such as it can be seen in S004. There, the spectrum starts to overestimate the experimental result.

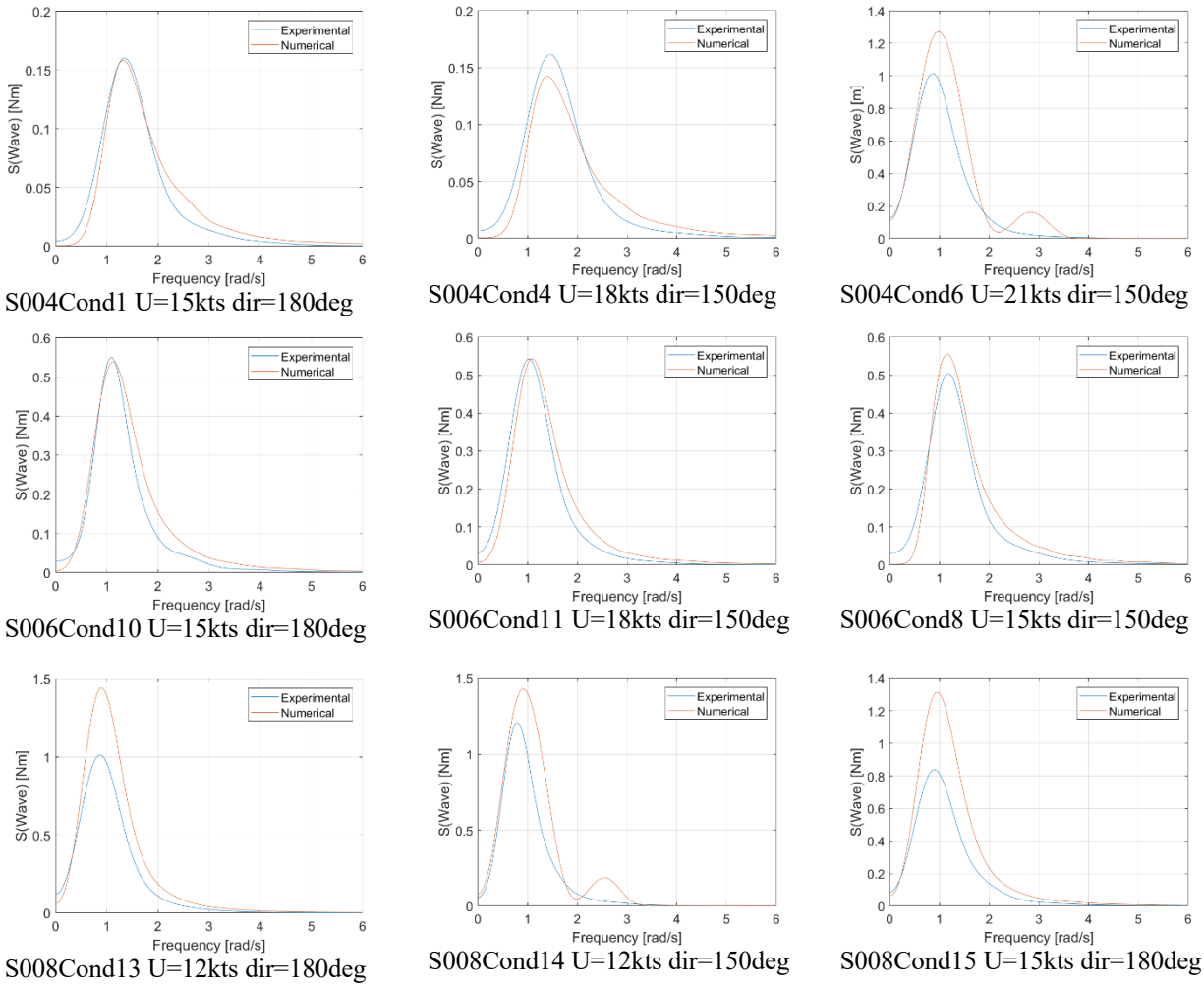

Figure 5.7: Incident wave spectra for the three non-crested sea states for different heading angle and speed.

In short crested waves, the spectra show more discrepancies than the other sea states between the experiment and the simulation. Even if the energy spectra are similar, the fact that the peak

of the numerical spectrum is found at a higher frequency is indicative of greater discrepancies in the other motions.

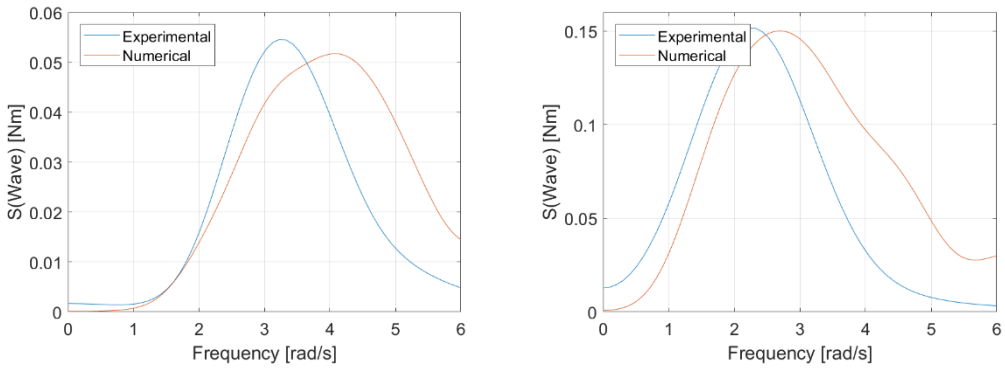

S005Cond7 U=15kts dir=150deg S007Cond12U=18kts dir=180deg

Figure 5.8: Incident wave spectra for short crested sea states

These performances of waves are indicative of the simulation set for the wave grid, as well as how the motions and loads will be predicted in the different conditions. Even though the area beneath the graph shows that the simulations have higher wave energy, they are still similar. At the same time, the spectrum peak of the numerical simulation is set at a higher frequency. Nevertheless, it can be said that the definition of JONSWAP waves in the simulations achieves to give an accurate description of the sea states, especially in lower seas.

5.3.2 Heave motions

All the global motions responses have been measured at the mid-section at draft height. In the motion analysis for heave, the overall results seem to be accurate. The major divergences are found as the sea states become higher. It is observed that the heave values do not move around zero, even in the lower sea state conditions. For a consequence of the draft offset in the setup of the seakeeping tests for both experiment and simulation.

In Figure 5.9, different seas states at the same speed are showcased. From there the peak values for heave in the simulations shown in the time domain are higher than the experimental ones. At the same time, the standard deviation is also higher in the numerical simulation increasing with each sea state, and this is clearly shown on S008Cond13. As the sea state becomes higher, the amplitude of the numerical result increases showing a more uniform response than in the experiment test. These effects can also be seen in the spectrum where the numerical responses show higher energy.

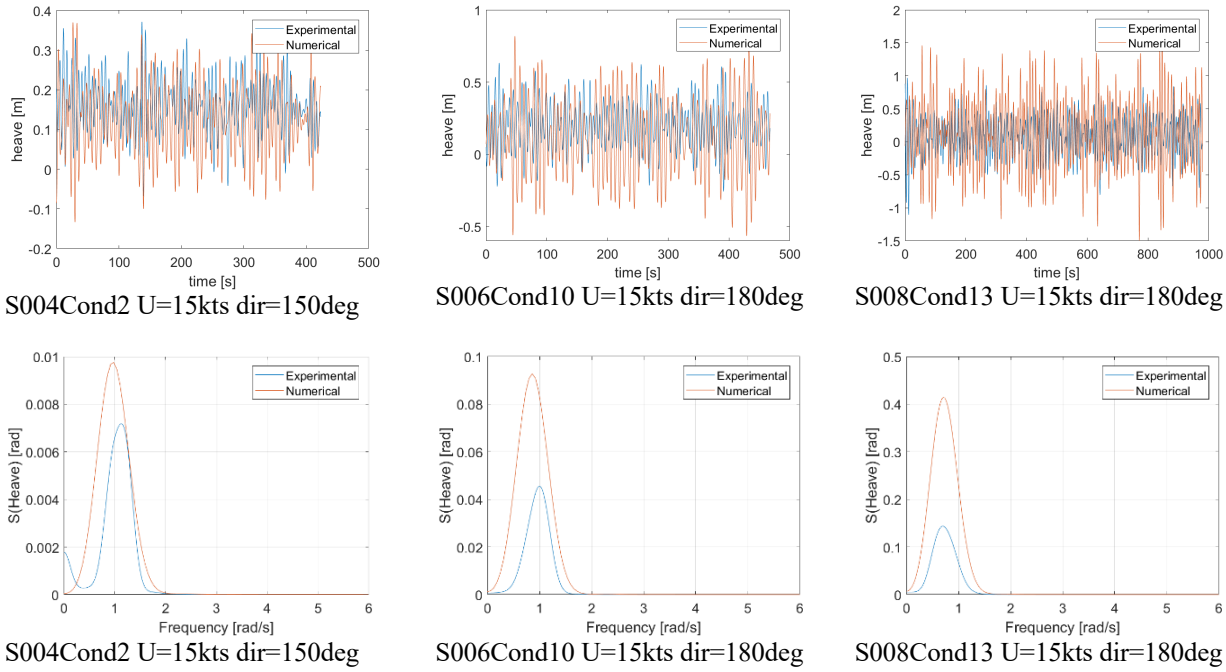

Figure 5.9: Heave motion in the time domain for non-crested seas

At lower speed, the heave mean value of the experiment and simulations remains very similar, with a mean difference of 13% between each other. This difference increases with the ship speed, showing a clear difference at high speeds, the simulated mean value is at 0.12m against the 0.26m of the experimental. The standard deviation does not vary a lot with the speed showing similar patterns between numerical and experimental. This can be seen in similarities of the spectrum for the three speeds, as shown in Figure 5.10.

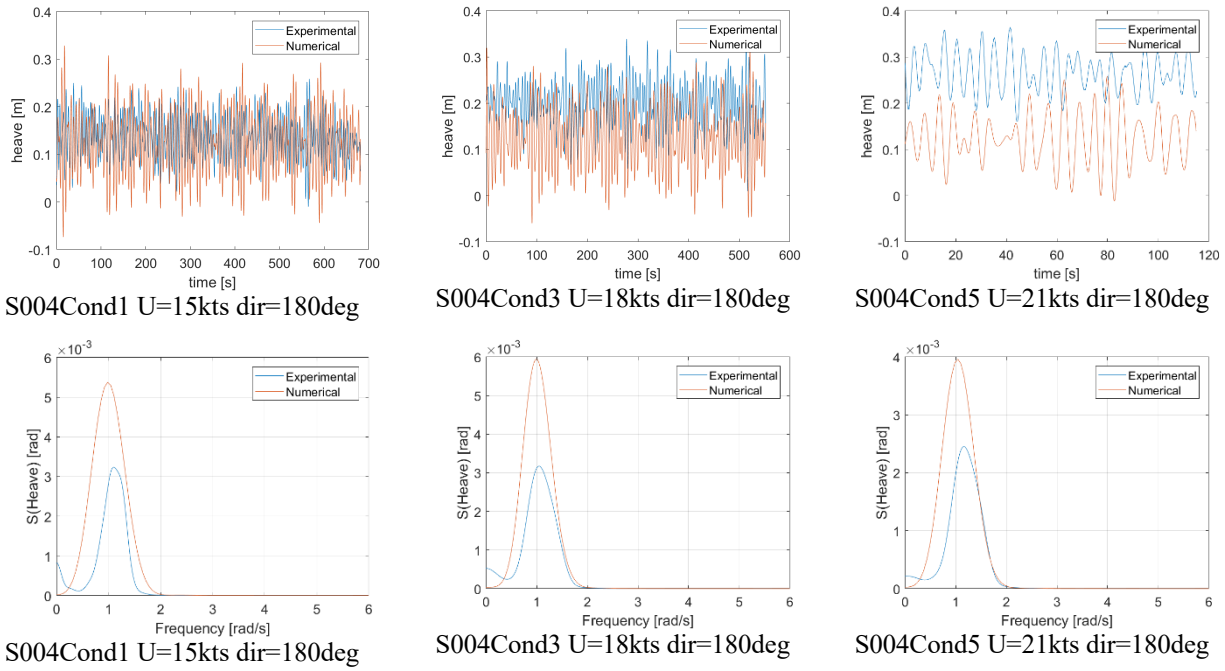

Figure 5.10: Heave response in S004 for different speeds

5.3.3 Pitch motions

The resulting pitch motions present similar differences with the heave responses between experimental and numerical tests. The numerical standard deviation is larger than the one in the experiments; this difference increases with the vessel speed. These results in an overestimation of the spectra energy in by the simulation as it is shown in Figure 5.12.

The increase of the sea state does not particularly affect much in the accuracy of the result were in differences between the most sea states stay similar, as it can be seen in S004 and S006 where the standard deviation differences with the experiment is around a 95%.

On the other hand, some inconsistencies are shown in the short-crested seas predictions, especially concerning the difference of the mean value, as it is shown in S007Cond12. This effect is slightly higher in the experiment, producing that the peak in the spectra is at a lower spectrum frequency.

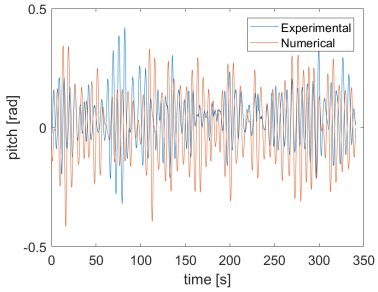

S004Cond4 U=18kts dir=150deg

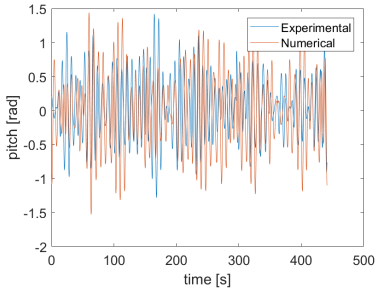

S006Cond11 U=15kts dir=180deg

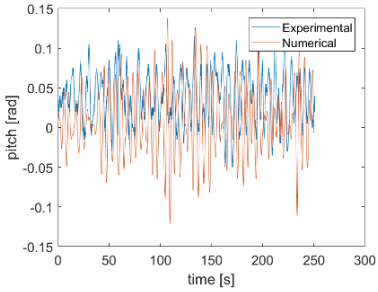

S007Cond12 U=18kts dir=180deg

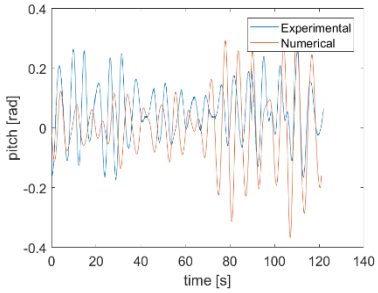

S004Cond6 U=21kts dir=150deg

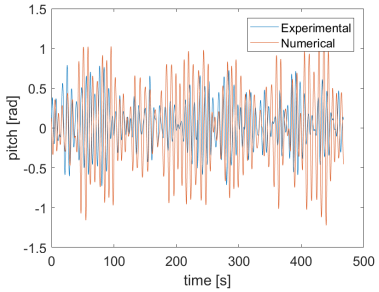

S006Cond9 U=18kts dir=180deg

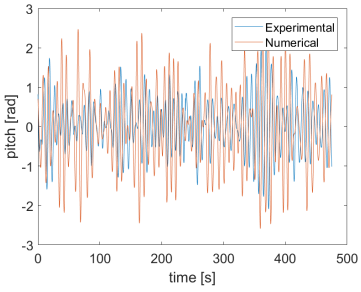

S008Cond13 U=12kts dir=150deg

Figure 5.11: Pitch response in time domain

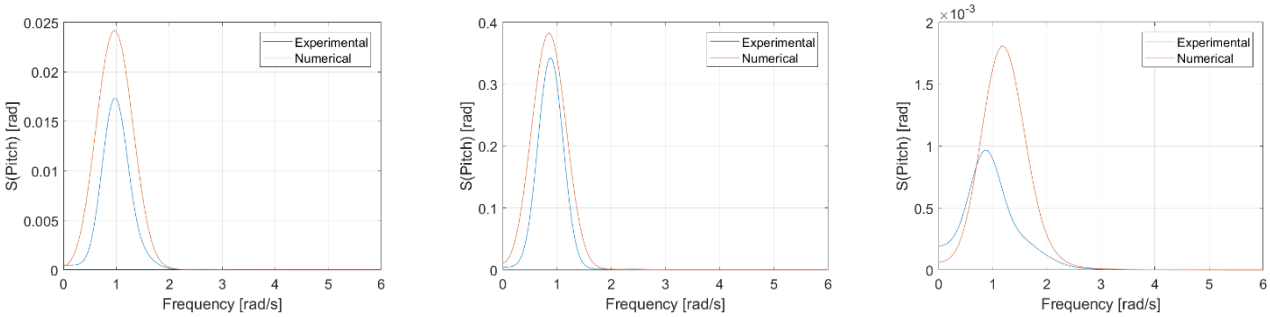

S004Cond4 U=18kts dir=150deg | S006Cond11 U=15kts dir=180deg | S007Cond12 U=18kts dir=180deg

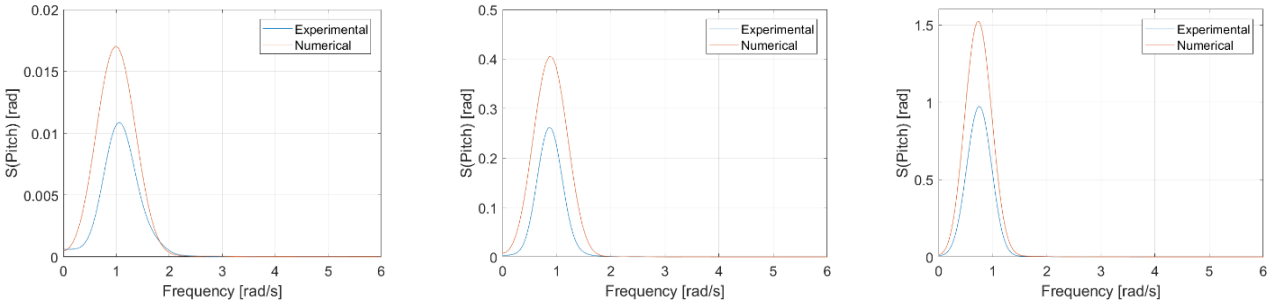

S004Cond6 U=21kts dir=150deg | S006Cond9 U=18kts dir=180deg | S008Cond13 U=12kts dir=150deg

Figure 5.12: Pitch response in the spectrum

5.3.4 Roll motions

The roll motion for oblique seas is also presented in Figure 5.13, showing similarities in the motion response. The numerical values move through similar mean values. The standard deviation of the numerical motion on time domain surpasses the one in the experiments as the sea state changes.

These divergences due to the absence of roll damping in the numerical simulations. The roll damping is a resultant of the decrease of the roll angle amplitude due to the loss of energy. In this case, the roll damping is mainly produced by the viscous friction and the wave radiation, effects in which due to the simulation set up (concerning with the Rankine panel method) have been neglected.

Another factor to consider is the scatter of the experimental data. On the other hand, the numerical result can be divided into sections; the values along the time domain follow a more predictable pattern. In this case, the rigidity of the numerical model could be a reason for this predictable trend. However, a more flexible experimental model could have had an unpredictable motion response by the waves affecting individually each one of the segments.

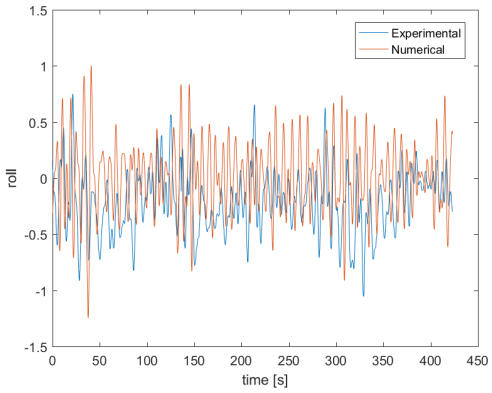

S004Cond2 U=15kts dir=150deg

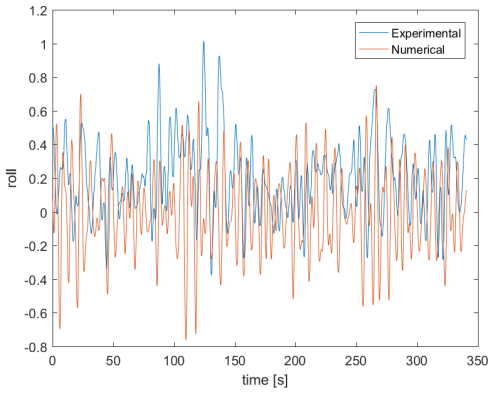

S004Cond4 U=18kts dir=150deg

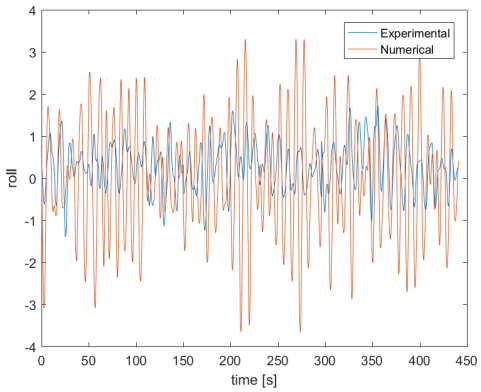

S006Cond11 U=15kts dir =180deg

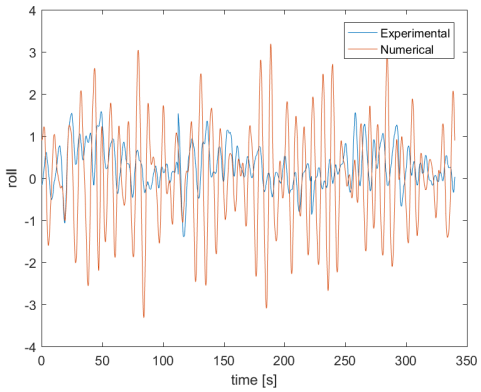

S006Cond9 U=18kts dir=150deg

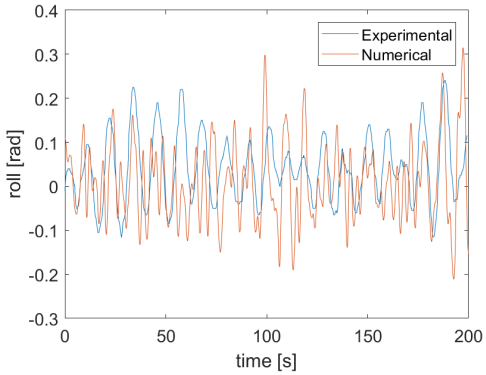

S005Cond7 U=15kts dir =180deg

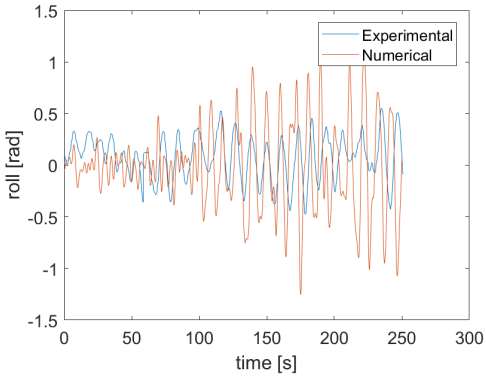

S007Cond12 U=18kts dir=180deg

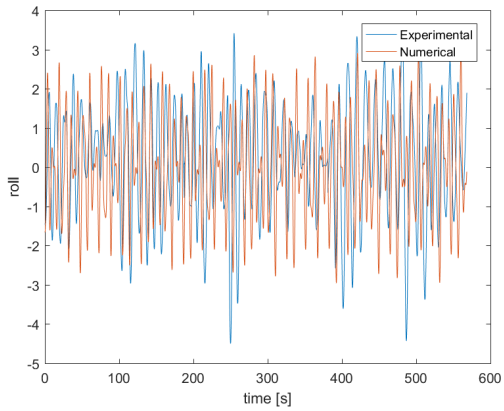

S008Cond14 U=12kts dir=150deg

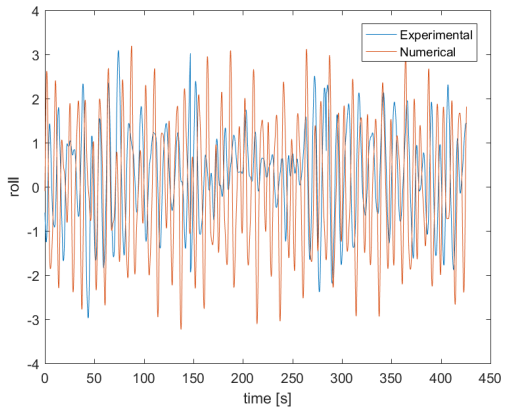

S008Cond16 U=15kts dir=150deg

Figure 5.13: Roll motion in time domain

5.3.5 Shear forces

The cross-section shear force at the midsection for the different sea states is also evaluated, the results in spectra and time domain can be seen in Figure 5.14 and Figure 5.15. The negative values of the shear force on the mid-section indicates that both models are under a sagging condition.

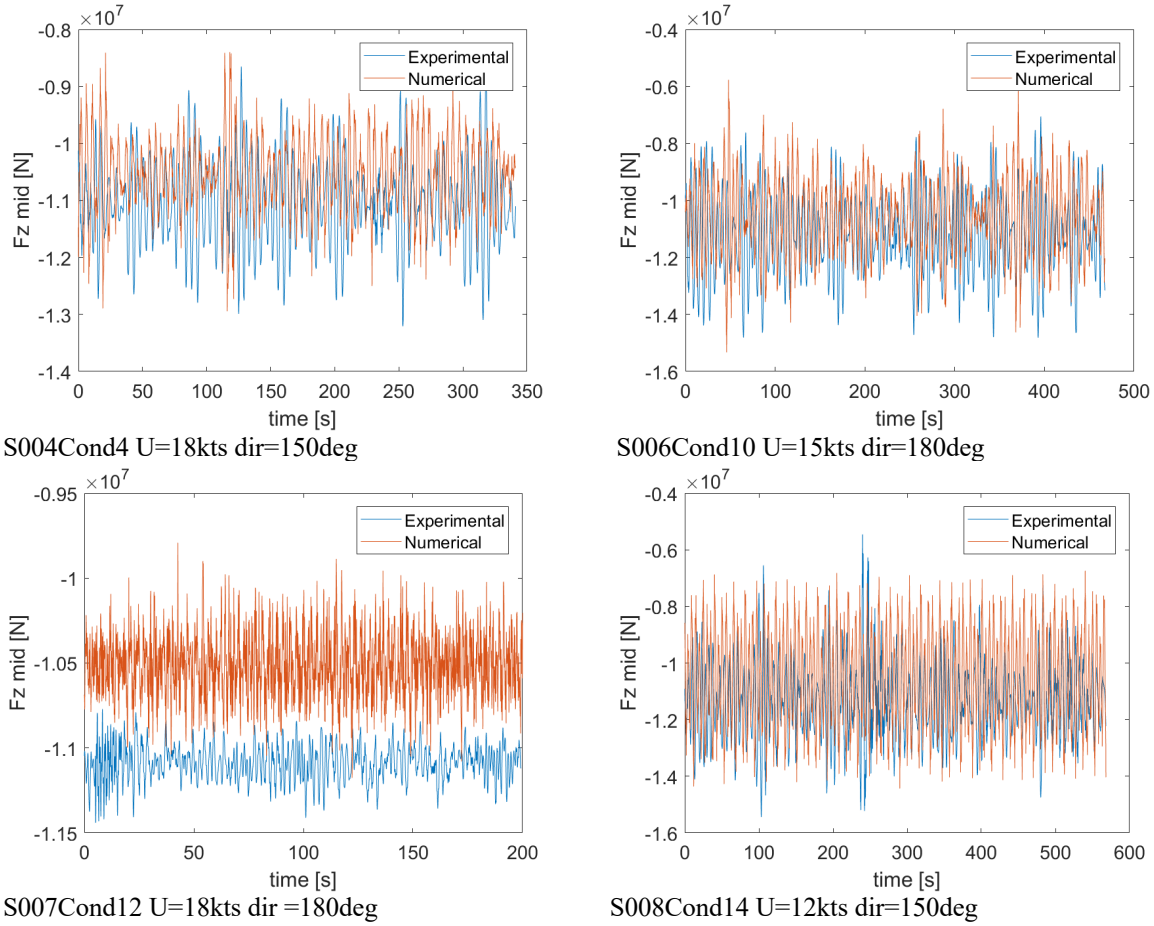

Figure 5.14: Shear forces for mid-section in the time domain

Due to the rigidity of the model and the use of linear wave theory, the simulated shear forces show symmetries around the mean value in all sea states; these are shown as the waves become higher as in S008. On the other hand, in the experimental reading there is no that much symmetry as in the simulation. Even in the calm S004, where there are should not be nonlinearities, a less predictable trend is seen, where the experimental peaks exceed the numerical results. An explanation for this could be the wave load effect on each segment of the experimental model. The freedom of each segment to respond individually to the vertical wave loads in the much more flexible experimental model results in a less stable reading of data, in contrast with the rigid model used in the simulations.

The numerical model proves to capture accurately the shear force behavior in terms of mean values where the difference for all sea states is within 7% of the experimental model. These relatively small differences in the mean value could be due to different factors. There is a

possibility that there are some discrepancies due to scaling and model geometry on the measurement cross-section from both models. Differences due to draft position could cause a difference in the mean value of the force.

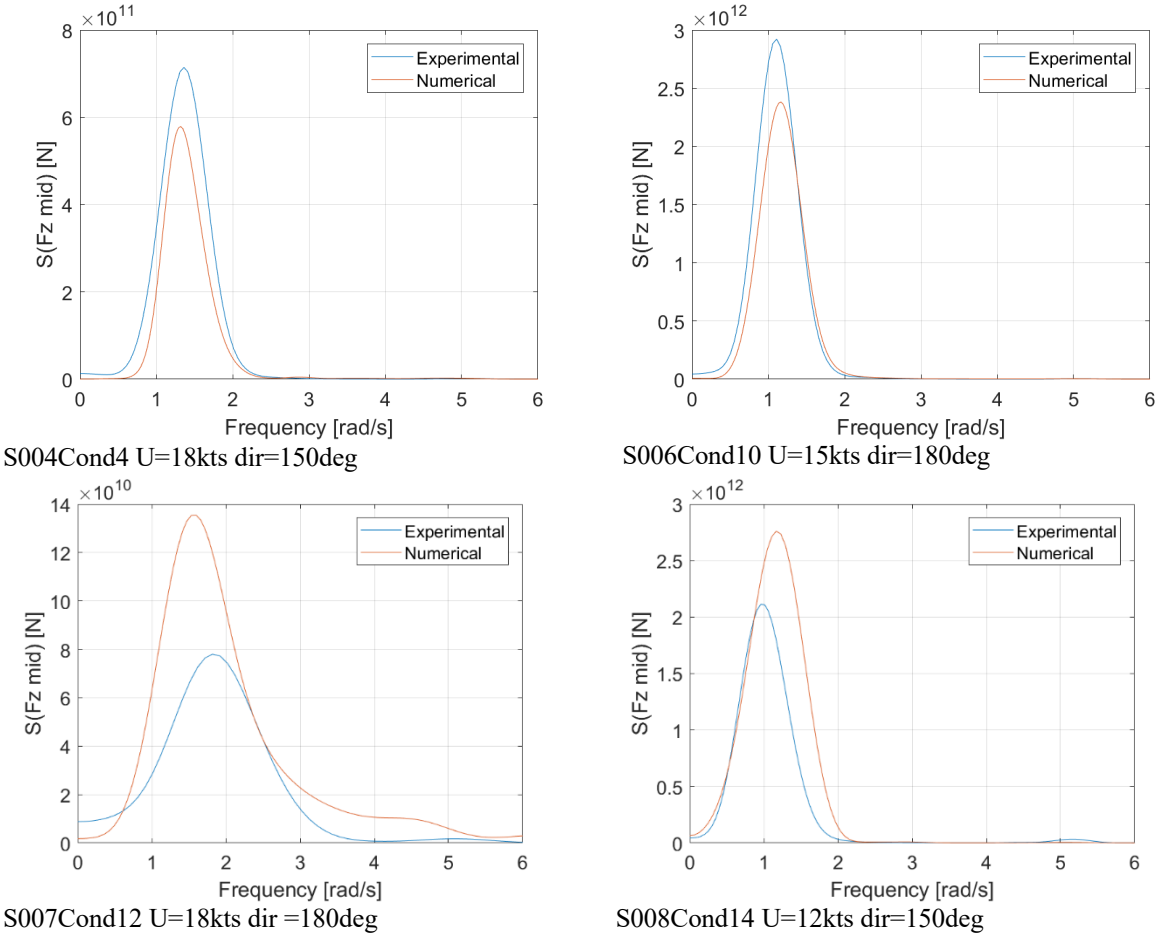

Figure 5.15: Shear forces for mid-section in frequency domain

At the same time, the standard deviation stays within an error of around 20% of the model test. In S007 the small shear force amplitude of short crested seas causes the numerical result not overlapping the experimental data. By S008 the numerical amplitude overestimates the experimental shear values presenting a very uniform trend and showing that the rigidity of the numerical model compromises the accuracy of the prediction. Other factors affecting the results are due to the nonlinear effects of the sea state being introduced into the experiment in the wave basin as the sea state gets higher.

The vessel speed also affects the shear force; as the speed increases the load does the same. This increase of the shear force becomes underestimated by the numerical simulations as the ship speed increases as can be seen in Figure 5.16. The increased speed affects the accuracy of mean values producing an underestimation of its prediction. At the same time with the speed increase, an underestimation of the standard deviation also occurs, as is seen in S004Cond5.

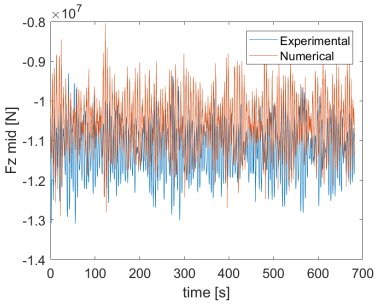

S004Cond1 U=15kts dir=180deg

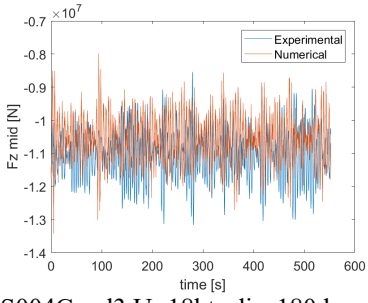

S004Cond3 U=18kts dir=180deg

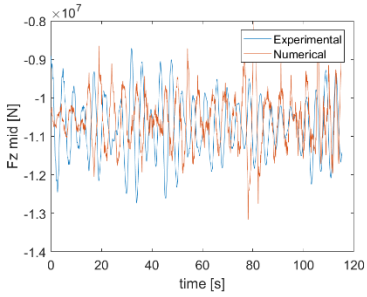

S004Cond5 U=21kts dir=180deg

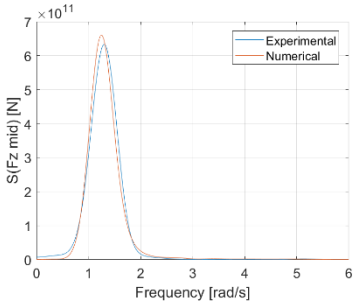

S004Cond1 U=15kts dir=180deg

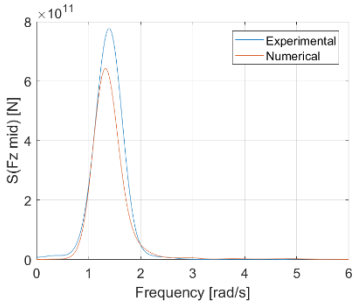

S004Cond3 U=18kts dir=180deg

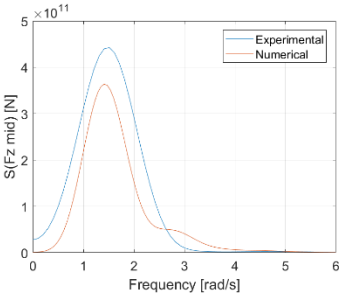

S004Cond5 U=21kts dir=180deg

Figure 5.16: Shear force through different speeds

From a general perspective, the numerical prediction of the shear forces is accurate due to the differences in mean and standard deviation between models, shown in Table 5.4. It is clearly stated that two main parameters are the ones affecting the accuracy of the prediction: the increase of sea state and the increase of speed. It is on the combination of these two factors where the numerical prediction starts to be compromised (as seen in S007Cond12). On S008, we see that even with the high seas, the prediction is not compromised due to low and moderate speeds used there.

Table 5.4: Mean and standard deviation numerical difference of the experimental data for Shear forces

Fz	Mid	Mean error	Standard deviation error
S004	Cond1	0%	0%
S004	Cond2	-6%	-21%
S004	Cond3	-5%	-9%
S004	Cond4	-5%	-16%
S004	Cond5	-2%	-15%
S004	Cond6	-5%	-16%
S005	Cond7	-5%	-12%
S006	Cond8	-5%	-15%
S006	Cond9	-4%	-7%
S006	Cond10	-6%	-9%
S006	Cond11	-6%	-11%
S007	Cond12	-5%	36%
S008	Cond13	-7%	2%
S008	Cond14	-7%	23%
S008	Cond15	-6%	16%
S008	Cond16	-6%	17%

5.3.6 Vertical bending moments

The vertical bending moments at the midsection for the different sea states are presented in Figure 5.17 for the time domain and in Figure 5.18 for the frequency domain. The numerical vertical bending moments follow a good relation with the experimental model.

From the time domain result, the numerical moments show higher peaks in most of the sea states. Similarly, the shear forces both models follow a steady symmetry around their respective mean values, showing great similarities in the prediction. This symmetry starts to be compromised with the vessel at higher speeds and in higher sea states, where some wave linearity starts to be introduced.

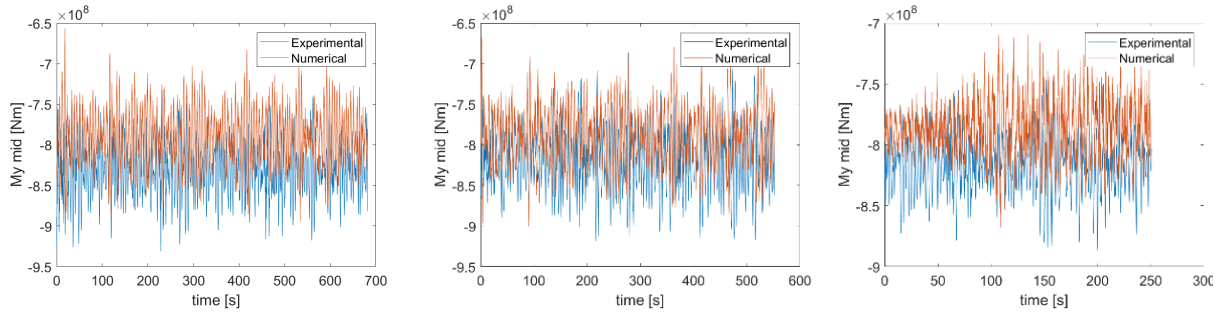

S004Cond1 U=15kts dir=180deg | S004Cond3 U=18kts dir=180deg | S007Cond12U=15kts Dir=180deg

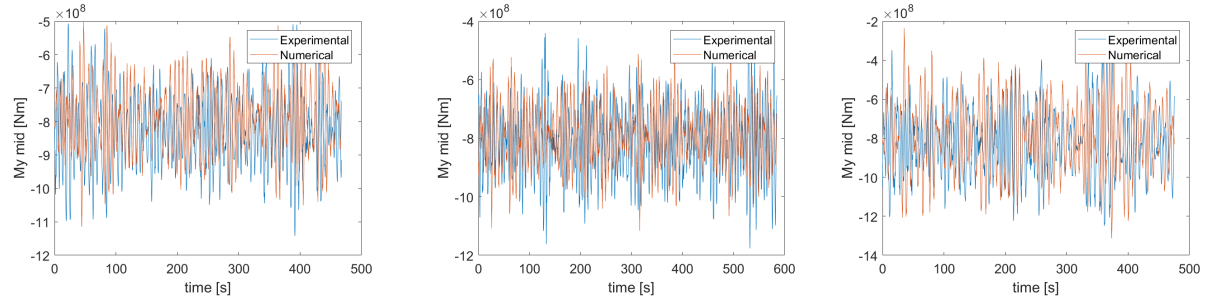

S006Cond10 U=15kts dir=180deg | S008Cond8 U=18kts dir=180deg | S008Cond15 U=15kts dir=180deg

Figure 5.17: Vertical bending moment for Mid-section in time domain

The frequency domain graphs also show good agreements with the experimental results; the spectra area also shows agreements, showing similarities between both models. In Table 5.5, the difference from the experimental bending moments are showed cased. The nonlinearities do not seem to dramatically affect the predictions showing small differences in standard deviation. However, some indication can start to be seen at the higher sea states as well as at high speeds. It can be said that the simulation is able to predict accurately the segmented model behavior for all sea states.

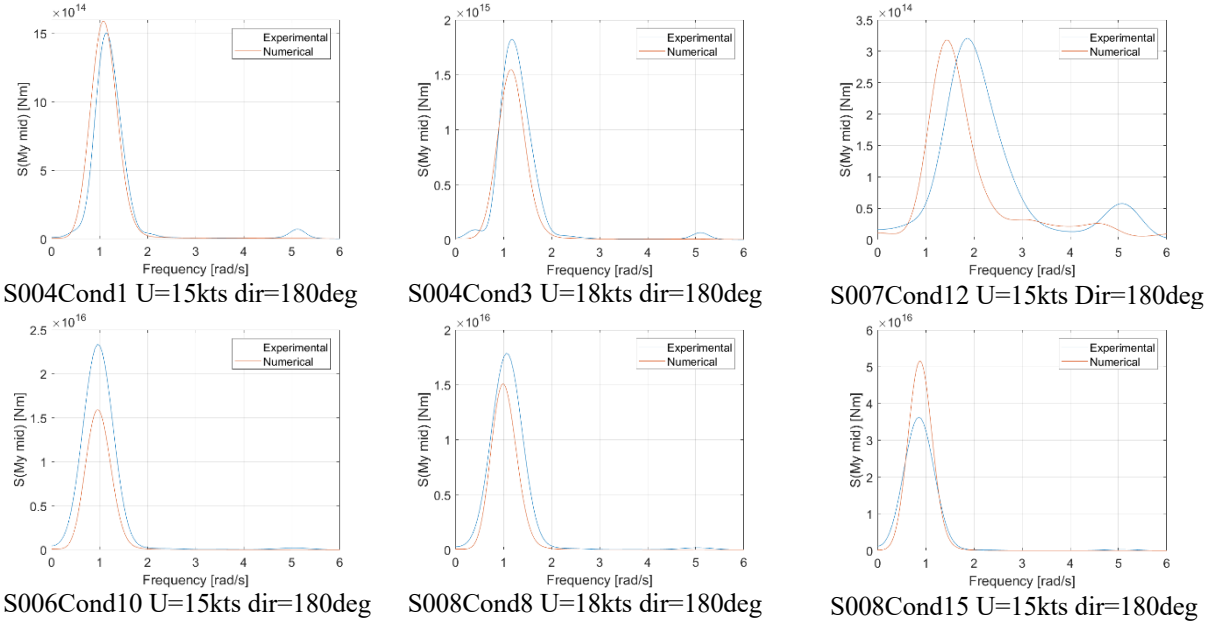

S004Cond1 U=15kts dir=180deg | S004Cond3 U=18kts dir=180deg | S007Cond12 U=15kts Dir=180deg

S006Cond10 U=15kts dir=180deg | S008Cond8 U=18kts dir=180deg | S008Cond15 U=15kts dir=180deg

Figure 5.18: Vertical bending moment for Mid-section in frequency domain for heading seas

Table 5.5: Mean and standard deviation numerical difference of the experimental data for Vertical Bending moment

My	Mid	Mean error	Standard deviation error
S004	Cond1	0%	2%
S004	Cond2	-5%	-18%
S004	Cond3	-3%	-9%
S004	Cond4	-3%	-20%
S004	Cond5	-1%	-11%
S004	Cond6	-3%	-20%
S005	Cond7	-4%	-8%
S006	Cond8	-3%	-17%
S006	Cond9	-3%	-14%
S006	Cond10	-4%	-7%
S006	Cond11	-5%	-25%
S007	Cond12	-4%	6%
S008	Cond13	-5%	-7%
S008	Cond14	-5%	-3%
S008	Cond15	-4%	6%
S008	Cond16	-3%	-7%

5.3.7 Torsional bending moments

The simulated torsional bending moments on oblique seas are shown in Figure 5.19 with the experimental data. As expected, the numerical torsional results show wide discrepancies due to the rigid nature of the numerical model. Usually, the use of experimental model tests is more suited for torsion providing more detail readings, against the numerical prediction that are usually more focused on vertical prediction (Zhu et al. 2011b).

This is seen in the results presented where, due to the nature of the models, the results do not show the same symmetric behavior as in the previous vertical moment. The experimental

maximum and minimum peaks are higher, nearly all sea states. The more scatter behavior of the experimental data due to the flexible behavior of the segments is seen in all sea states, being especially pronounced on S008Cond16 against the linear numerical trend. At this high sea states, the numerical symmetry of the moments, show larger discrepancies between the models' rigidity.

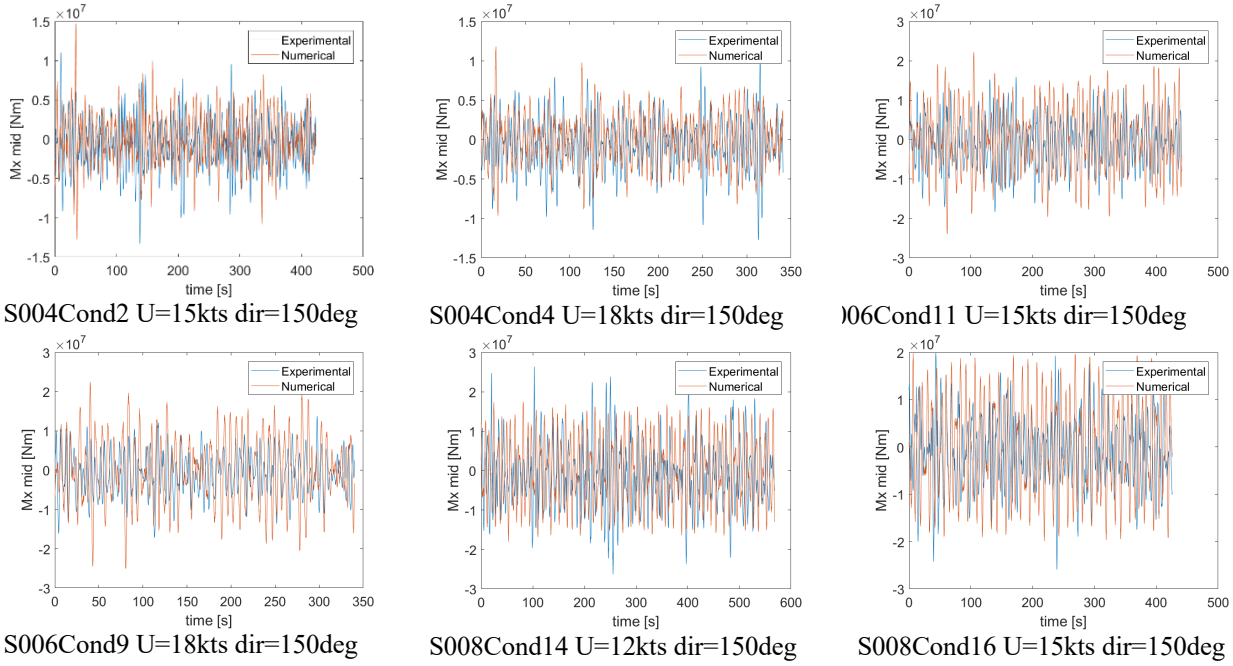

Figure 5.19: Torsional bending moment in mid-section for oblique seas

The spectra show the effect of the speed vessel in the prediction accuracy. There is an overestimation of the numerical simulations as the speed. On the other hand, in the lowest sea state, the numerical accuracy is high, showing agreements in the spectrum.

As an overall view of the torsional moment results, the numerical values cannot be used as an adequate prediction of the experimental behavior. A numerical difference in mean values of around 100% is in all sea states. This difference could be due to geometric and scaling uncertainties, but they cannot be taken as proper reference. It is only in the standard deviation results cases as in the lowest sea state S004 and in slowest speed S008Cond14 where there is some accuracy of the simulation. In these, the numerical model could be used as a reference to understand the magnitude of the motion.

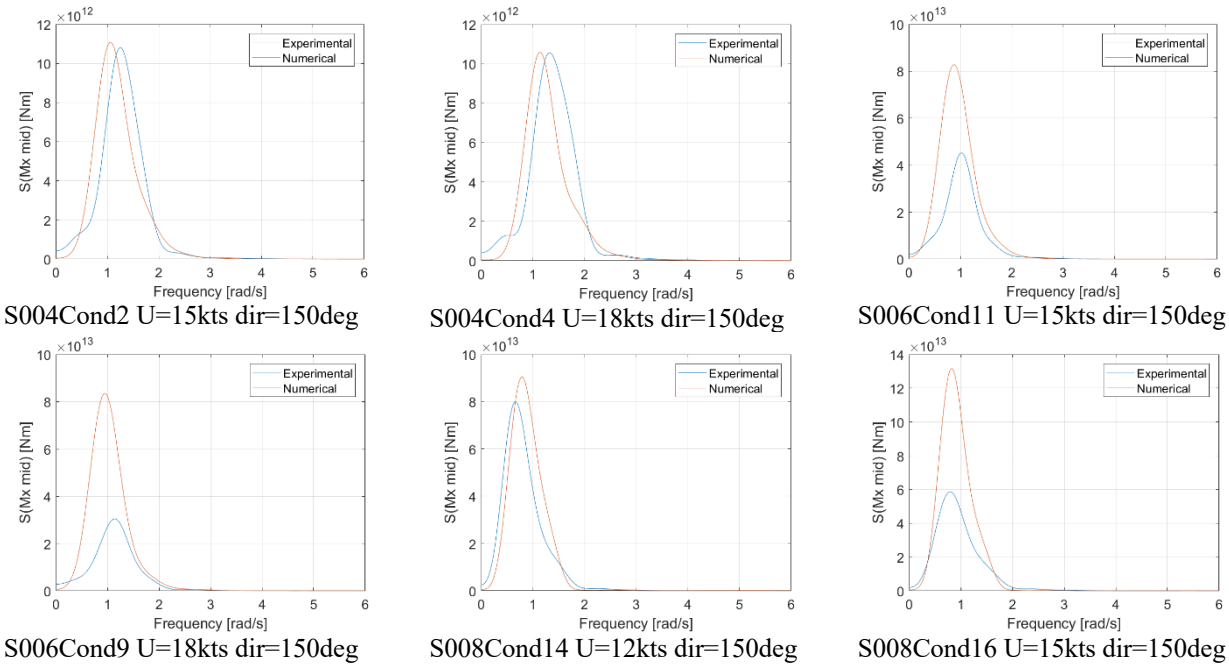

Figure 5.20: Torsional bending moment in mid-section for oblique seas

Table 5.6: Mean and standard deviation error for torsional bending moments

Mx	Mid	Mean error	Standard deviation error
S004	Cond2	-99%	2%
S004	Cond4	-102%	-4%
S004	Cond6	-102%	-4%
S006	Cond9	-95%	55%
S006	Cond11	-103%	39%
S008	Cond14	-101%	5%
S008	Cond16	-100%	35%

5.3.8 Discussion of results

The numerical seakeeping simulation has taken the experimental results as a reference in its analysis. Uncertainties due to the numerical simplifications in the discrete mass distribution and hull shape could be a reason for inconsistencies, since there will always be differences between the segmented and numerical models (Zhu et al. 2011a). As observed, the accuracy of the simulation set up of the draft could be a factor of discrepancy in the results. Some differences in the mean values of heave motion and shear forces could be partly to the result an uncertainty in the real position of draft, fixed for the experiment. A misrepresentation in the scaling of the real position of the cross-section could also add to the geometric uncertainty.

The rigidity of the model compromises the prediction of the numerical results, as it can be seen in the roll motion. The flexibility of the segmented model, characterized by its stiffness in the different segments, shows a more sensible reading of the data due to the response of each segment to the waves. Whereas the numerical model provides a more predictable pattern that ends, due to its rigidity, overestimating the real standard deviation of the experiment.

The use of linear wave theory by the simulations starts compromising the results on higher sea states and at higher speeds, where there is a rougher interaction between hull and wave. In these cases, nonlinearities are also introduced, producing higher differences with the simulation results. Other effects not considered in the simulations as roll damping are also factors on the accuracy of the numerical results.

The characteristics of the set up for the seakeeping analysis are described in previous chapters, as well as for the main characteristics for the Rankine panel grid and the properties of the motion springs used for the simulations. Considering the software, the interpretation of the JONSWAP definition by Wasim reproduces with discrepancies the induced waves of the short-crested sea states. This effect is later reflected in the motion and loads.

Even though in some conditions there are some deviations, between the models, the simulated results can be considered to be close to the one measured on the experiment working as a good predicament of the segmented model behavior. The simulated shear forces and vertical bending moments for all sea states are within 7% of mean error from the experimental values. At the same time, the prediction at short vessel speed is accurate showing that this at under slow velocities even in high seas such as in S008Cond13 and S008Cond14; there are good agreements.

The seakeeping numerical simulations work well for the motions and loads presented. The set-up choice used in the analysis show good agreements in the prediction of the motions and loads presented, especially in lower sea states and at low speed. Regarding the torsional moment, even if there is a clear need for more accuracy the response can work as an initial indicator. For a better analysis of higher sea states at higher vessel speeds, it would be recommended to introduce roll damping as well as small nonlinearities in the simulation.

6 Conclusions

This work has focused on the assessment of the simulations of a rigid numerical model against the experimental segmented model test. The goal has been to understand where limits are with the simulations, and under which conditions can the simulation reproduces the experimental behavior. The thesis work used insights from literature and the experiment to understand and prepare the numerical simulation and its following assessment analysis.

The eigenfrequency simulation result agrees well with the hammer test result in wet conditions. The rigid model with a discrete mass distribution along the hull has proven to be in good agreement with the experimental test; with a natural frequency of 0.79 Hz, having the model is an 8% of difference to the experimental value. The discrepancy between the model's frequencies could be due to several sources, such as the simplified mass distribution and the rigidity of the model. Other sources of divergence could also be due to uncertainties in the hammer test experiment. However, the simulated dry frequency differs significantly from the experimental eigenfrequency. An indicative frequency of 1.13 Hz, calculated through an approximation, has been presented.

For the seakeeping simulations, good agreements have been found with the different sea states on the analysis. This correlation was found for all shear forces and bending moments in all sea states. This is due to the ability of the numerical model to read vertical loads in comparison with the heave motion, where the effect of a vertical offset could have affected the predictions. These similarities in the prediction were particularly found on lower sea states at lower speeds where the difference between models was minimal, due to the linearity of the waves and also the effects caused by the segmented model.

More discrepancies in the results were found at higher waves, and with higher speeds. Some limitations were found concerning the accuracy due to the linearity of the waves to define short crested conditions, which showed higher deviations in the prediction of the loads. However, it cannot be concluded that nonlinearity is the only factor of divergence. Other factors, such as the rigidity of the model, uncertainties in the experiment and mass distributions could have also affected the results. More significant differences are found in the torsional moments for which the rigid body model behaves much differently in comparison with the segmented model. Thus, the numerical model is not recommended for a torsion analysis; it is mainly applicable for analysing the vertical responses.

In summary, a numerical rigid model simulation is able to present a segmented model test behavior and to give accurate vertical responses. Comparing the numerical values with the experiment data one concludes that the numerical model achieves to capture the load response, especially in terms of vertical forces and moments. The model at the same time is limited by the linearity of the simulations starting to compromise the predictions at conditions higher seas and speed. The use of the model as the one in this thesis is a path to ensure a more straightforward analysis in an elaborated experimental model, helping shipbuilding focus on hull optimization. This model focuses on lightweight construction in combination with other mathematical approach to ship design the industry will response to the sustainability requirements of society.

7 Future work

In the current work, several different simplifications where made related to the numerical simulation set up to overcome specific difficulties and to facilitate the method. The use of linear wave theory proved to capture the vertical forces and moments, but it becomes less accurate at higher sea states with higher vessel speed. A more sophisticated numerical model that accounts more nonlinearities as well as other effects such as roll damping could give more convincing results when a rigid model is utilized.

The use of the SESAM software package helped the workflow in terms of compatibility between the programs used for the thesis. On the other hand, in the eigenanalysis, more sophisticated software such as ABAQUS is expected to be useful to compare with the GeniE results, by providing the use of free vibration as well as a more detailed mass distribution.

A fatigue assessment of dynamic loads could also add to the understanding of the ship dynamics' structural behavior into the long-term vessel operation. It would be interesting to know how the rigid body model could capture the dynamic effects such as springing or whipping. This study could be especially helpful in the investigation of the impacts of sea conditions such as the presented in this thesis.

9 References

Aichun, F.; Wei, B.; You, Y.; Zhi-Min, C.; Price W.G. (2016). A Rankine source method solution of a finite depth, wave-body interaction problem. *Journal of Fluids and Structures* 62 p. 14-32.

Appa Rao, T.V.S.R.; Iyer, N.R.; Rajasankar, J.; Palani, G.S. (2000). Dynamic Response Analysis of Ship Hull Structures. *Marine Technology* 37(3) p. 117-128.

Beck, R.F. (1994) Time-domain computations for floating bodies. *Applied Ocean Research* 16 p. 267-282.

Bertram, V. (2012). Practical Ship Hydrodynamics. 2nd. Oxford: Elsevier Ltd.

Brodtkorb, P.A.; Johannesson, P.; Lindgren, G.; Rychlik, I.; Rydén, J.; Sjö, E. (2000). WAFO - a Matlab toolbox for analysis of random waves and loads. *Proceedings of the 10th International Offshore and Polar Engineering Conference* in Seattle, WA, United States.

Chen, Z.; Jiao, J.; Li, H. (2017). Time-domain numerical and segmented ship model experimentalanalyses of hydroelastic responses of a large container ship in oblique regular waves. *Applied Ocean Research* 67 p. 78-93.

Davies, E.A.J.; Woodward, J.B.; Vance, J.E.; Stilwell, J.J. (2018). Encyclopædia Britannica. https://www.britannica.com/technology/ship (accessed May 22, 2019).

Dinsenbacher, A.; Engle, A.; Hermanski, G. (2010). Guidelines for Hydroelastic Model Design, Testing and Analysis of Loads and Responses. *Report No. NSWCCD-65-TR2010/12* (Report No. NSWCCD-65-TR2010/1), no. Carderock Div, NSWC.

DNV GL. (2015). Genie V7.2-07. *DNV GL - Software*.

DNV GL. (2016). HydroD V.4.9-02. *DNV GL Software SESAM*.

DNV GL. (2015). SESAM USER MANUAL. WASIM Wave Loads on Vessels with Forward Speed. *DNV GL - Software*.

DNV. (2006). SESAM User Manual Wasim. 5th. Horvik: Det Norske Veritas.

Fonseca, N.; Soares, C.G. (2004). Experimental Investigation of the Nonlinear Effects on the Statistics of Vertical Motions and Loads of a Containership in Irregular Waves. *Journal of Ship Research*. 48 (2) p. 148-167.

Groenenboom, P.; Cartwright, B.; McGuckin, D. (2009). Numerical Simulation Of Ships In High Seas Using A Coupled SPH-FE Approach. *Fremantle: The Royal Institution of Naval Architects*.

Hong, S.Y; Kim, B.W.; Nam; B.W. (2011). Experimental study on torsion springing and whipping of a large container ship. *Proceedings of the International Offshore and Polar Engineering Conference* (*21st International Offshore and Polar Engineering Conference)* in Maui, HI; United States p. 486-494.

IMO. (2017) IMO and Sustainable Development. http://www.imo.org/en/MediaCentre/HotTopics/Documents/IMO%20SDG%20Brochure.pdf (accessed April 1, 2019).

ITTC. (2011) ITTC – Recommended Procedures and Guidelines: Global Loads Seakeeping Procedure. 26th ITTC Seakeeping Committee.

Jiao, J.; Chen, C.; Ren; H. (2019) A comprehensive study on ship motion and load responses in short-crested irregular waves. *International Journal of Naval Architecture and Ocean Engineering* 11(1) p. 364 - 379.

Jung-Hyun, K.; Kim, Y.; Yuck, R-H.; Lee, D-Y. (2015). Comparison of slamming and whipping loads by fully coupled hydroelastic analysis and experimental measurement. *Journal of Fluids and Structures* 52 p. 145-165.

Li, Z.; Mao, W.; Ringsberg, J.W.; Johnson, E.; Storhaug, G. (2014). A comparative study of fatigue assessments of container shipstructures using various direct calculation approaches. *Ocean Engineering* 82(15) p. 65-74.

Lin, W-M.; Weems, K.M.; Liut D.A. (2004). Design and Assessment of Ship Motion Control Systems with Advanced Numerical Simulation Tools. *Habitability of Combat and Transport Vehicles: Noise, Vibration and Motion (RTO-MP-AVT-110).* in Prague, Czech Republic, 2004.

Marón, A.; Kapsenberg, G. (2014). Design of a ship model for hydro-elastic experiments in waves. *International Journal of Naval Architecture and Ocean Engineering* 5(4) p. 1130-1147.

Mathworks. (2016) Matlab R2016b. Mathworks, Inc.

Norwood, M.N.; Dow, R.S. (2013) Dynamic analysis of ship structures. *Ships and Offshore Structures* 8(3-4) p. 270-288.

Perez, T. (2015). Ship Motion Control: Course Keeping and Roll Stabilisation Using Rudders and Fins. *First. Trondheim: Springer*.

Sader, J.E. (1998). Frequency response of cantilever beams immersed in viscous fluids with applications to the atomic force microscope. *Journal of Applied Physics* 84(1) p. 64-76.

Singh, S.P.; Sen, D. (2007). A comparative linear and nonlinear ship motion study using 3-D time domain methods. *Ocean Engineering* 34(13) p. 1863-1881.

Stena Teknik. (2019). Take A Glimpse At Our Projects. https://www.stenateknik.com/projects/ (accessed April 4, 2019).

Storhaug, G. (2014). The measured contribution of whipping and springing on the fatigue and extreme loading of container vessels. *International Journal of Naval Architecture and Ocean Engineering* 6(4) p. 1096-1110.

Temarel, P.; Bai, W.; Bruns, A.; Derbanne, Q.; Dessi, D.; Dhavalikar, S.; Fonseca, N.; Fukasawa, T.; Gu, X.; Nestegard, A.; Papanikolaou, A.; Song, K.H.; Wang, S. (2016). Prediction of wave-induced loads on ships: Progress and challenges. *Ocean Engineering* 116 p. 274-308.

United Nations. (2015). Resolution adopted by the General Assembly on 25 September 2015. October 21, 2015. http://www.un.org/ga/search/view_doc.asp?symbol=A/RES/70/1&Lang=E (accessed April 1, 2019).

United Nations.(2019). Sustainable Development Goals: 17 Goals to Transform Our World. https://www.un.org/sustainabledevelopment/ (accessed April 2, 2019).

Vakilabadi, K.A.; Khedmati, M.A.; Sayyari, A. (2014). Analysis of the flexural mode response of a novel trimaran by segmented model test."*Latin American Journal of Solids and Structures* 14(11) p. 2573-2588.

Veryst Engineering. (2019). Immersed Beam Vibration. https://www.veryst.com/project/immersed-beam-vibration (accessed March 2019-03-20, 2019).

Zhu, S.; Wu, MK.; Moan, T. (2011). Experimental and Numerical Study of Wave-Induced Load Effects of Open Ships in Oblique Seas. *Journal of Ship Research* 55(2) p. 100-123.

Zhu, S.; Wu, MK.; Moan, T. (2011) Experimental Investigation of Hull Girder Vibrations of a Flexible Backbone Model in Bending and Torsion. *Applied Ocean Research*, p. 252-272.

A. Statistical data of the numerical and experimental results

In this appendix lists, tables regarding the results for each seakeeping running condition from the experiment and simulations are presented. Showing the maximum, minimum, mean and standard deviation for all sea state conditions. At the same time the numerical difference in results with the experiments is also presented. The seakeeping wave basin test runs used for comparison in the thesis are also showcased. The order followed is the same as the one presented in Table 4.3.

A.1 S004

A.1.1 Condition 1

The experimental tests compared against are:

- Ser004-Test001-Run001
- Ser004-Test001-Run002
- Ser004-Test002-Run001

Table A.1 Properties for S004Cond1

Sea state	S004
Speed (Kts)	15
Wave direction (deg)	180
Significant wave height (m)	1,88
Wave period (s)	7,56

Table A.2: Statistical data of the experiment for S004Cond1

S004Cond1	Min	Mean	Max	Standard deviation
Wave elevation (m)	-1,62	0,00	1,32	0,43
Surge (m)	-0,08	0,08	0,48	0,10
Sway (m)	-0,17	0,01	0,25	0,07
Heave (m)	-0,01	0,14	0,26	0,04
Roll (deg)	-0,45	0,06	0,53	0,19
Pitch (deg)	-0,17	0,04	0,21	0,06
Yaw (deg)	0,00	0,00	0,26	0,08
Mid cut Fx (N)	7,98E+06	8,30E+06	8,64E+06	1,08E+05
Mid cut Fy (N)	-2,75E+06	-2,44E+06	-2,12E+06	1,03E+05
Mid cut Fz (N)	-1,31E+07	-1,13E+07	-9,30E+06	6,39E+05
Mid cut Mx (Nm)	-3,31E+06	-4,43E+04	2,93E+06	9,21E+05
Mid cut My (Nm)	-9,31E+08	-8,31E+08	-7,34E+08	3,21E+07
Mid cut Mz (Nm)	-3,31E+06	-4,43E+04	2,93E+06	9,21E+05

Table A.3: Statistical data of the simulation for S004Cond1

S004Cond1	Min	Mean	Max	Standard deviation	Mean difference	Std. deviation difference
Wave elevation (m)	-1,34	0,00	1,13	0,42	-0,14	-0,03
Surge (m)	-0,06	0,11	0,48	0,11	0,40	0,07
Sway (m)	-0,15	0,01	0,12	0,05	0,30	-0,21
Heave (m)	0,02	0,14	0,25	0,04	0,03	0,00
Roll (deg)	-0,45	0,06	0,53	0,19	0,01	0,03
Pitch (deg)	-0,15	0,04	0,21	0,06	-0,01	0,00
Yaw (deg)	0,00	0,00	0,20	0,07	0,86	-0,12
Mid cut Fx (N)	7,98E+06	8,30E+06	8,63E+06	1,10E+05	3,41E-04	1,71E-02
Mid cut Fy (N)	-2,75E+06	-2,44E+06	-2,12E+06	1,07E+05	-1,19E-04	4,03E-02
Mid cut Fz (N)	-1,31E+07	-1,13E+07	-9,30E+06	6,41E+05	-1,52E-04	3,09E-03
Mid cut Mx (Nm)	-3,31E+06	-4,70E+04	2,93E+06	9,61E+05	5,97E-02	4,28E-02
Mid cut My (Nm)	-9,31E+08	-8,31E+08	-7,34E+08	3,27E+07	-3,76E-04	1,89E-02
Mid cut Mz (Nm)	-3,31E+06	-4,70E+04	2,93E+06	9,61E+05	5,97E-02	4,28E-02

A.1.2 Condition 2

The experimental tests compared against are:

- `Ser004-Test003-Run001`
- `Ser004-Test004-Run002`
- `Ser004-Test005-Run001`

Table A.4: Properties for S004Cond2

Sea state	S004
Speed (Kts)	15
Wave direction (deg)	150
Significant wave height (m)	1,88
Wave period (s)	7,56

Table A.5: Statistical data of the experiment for S004Cond2

S004Cond2	Min	Mean	Max	Standard deviation
Wave elevation (m)	-1,62	0,02	1,56	0,46
Surge (m)	-0,39	0,01	0,31	0,17
Sway (m)	-0,37	0,05	0,48	0,26
Heave (m)	-0,07	0,16	0,37	0,07
Roll (deg)	-1,06	-0,21	0,75	0,27
Pitch (deg)	-0,31	0,04	0,36	0,11
Yaw (deg)	-0,01	-0,01	0,45	0,25
Mid cut Fx (N)	7,76E+06	8,29E+06	8,90E+06	1,53E+05
Mid cut Fy (N)	-4,08E+06	-2,41E+06	-9,96E+05	3,93E+05
Mid cut Fz (N)	-1,37E+07	-1,13E+07	-8,17E+06	7,68E+05
Mid cut Mx (Nm)	-1,33E+07	-7,33E+05	1,11E+07	3,08E+06
Mid cut My (Nm)	-9,93E+08	-8,31E+08	-6,18E+08	4,85E+07
Mid cut Mz (Nm)	-1,33E+07	-7,33E+05	1,11E+07	3,08E+06

Table A.6: Statistical data of the simulation for S004Cond2

S004Cond2	Min	Mean	Max	Standard deviation	Mean difference	Std. deviation difference
Wave elevation (m)	-1,52	0,00	1,55	0,47	-0,98	0,04
Surge (m)	-0,40	-0,28	-0,17	0,05	-29,43	-0,71
Sway (m)	-0,27	-0,03	0,17	0,11	-1,54	-0,58
Heave (m)	-0,13	0,12	0,37	0,09	-0,25	0,29
Roll (deg)	-1,25	0,00	1,00	0,31	-1,01	0,14
Pitch (deg)	-0,46	0,00	0,39	0,15	-0,96	0,40
Yaw (deg)	0,00	0,00	0,05	0,02	-1,35	-0,91
Mid cut Fx (N)	3,72E+06	4,27E+06	4,84E+06	1,81E+05	-4,85E-01	1,82E-01
Mid cut Fy (N)	-1,15E+06	-6,92E+02	1,03E+06	3,31E+05	-1,00E+00	-1,56E-01
Mid cut Fz (N)	-1,30E+07	-1,06E+07	-8,15E+06	6,05E+05	-6,27E-02	-2,11E-01
Mid cut Mx (Nm)	-1,28E+07	-8,19E+03	1,47E+07	3,14E+06	-9,89E-01	2,21E-02
Mid cut My (Nm)	-9,01E+08	-7,90E+08	-4,87E+10	3,98E+07	-5,05E-02	-1,79E-01
Mid cut Mz (Nm)	-4,20E+07	-7,24E+04	3,79E+07	1,37E+07	-9,01E-01	3,44E+00

A.1.3 Condition 3

The experimental tests compared against are:

- `Ser004-Test006-Run001`
- `Ser004-Test008-Run002`
- `Ser004-Test010-Run001`

Table A.7: Properties for S004Cond3

Sea state	S004
Speed (Kts)	18
Wave direction (deg)	180
Significant wave height (m)	1,88
Wave period (s)	7,56

Table A.8: Statistical data of the experiment for S004Cond3

S004Cond1	Min	Mean	Max	Standard deviation
Wave elevation (m)	-1,63	0,01	1,64	0,48
Surge (m)	-0,26	0,00	0,21	0,09
Sway (m)	-0,16	0,00	0,18	0,06
Heave (m)	0,01	0,20	0,34	0,05
Roll (deg)	-0,38	0,04	0,47	0,14
Pitch (deg)	-0,18	0,04	0,27	0,07
Yaw (deg)	0,00	0,00	0,23	0,10
Mid cut Fx (N)	8,08E+06	8,47E+06	8,84E+06	1,24E+05
Mid cut Fy (N)	-2,79E+06	-2,43E+06	-2,06E+06	1,01E+05
Mid cut Fz (N)	-1,32E+07	-1,11E+07	-8,54E+06	7,19E+05
Mid cut Mx (Nm)	-3,40E+06	7,30E+03	3,13E+06	8,63E+05
Mid cut My (Nm)	-9,19E+08	-8,17E+08	-6,86E+08	3,75E+07
Mid cut Mz (Nm)	-3,40E+06	7,30E+03	3,13E+06	8,63E+05

Table A.9: Statistical data of the simulation for S004Cond3

S004Cond3	Min	Mean	Max	Standard deviation	Mean difference	Std. deviation difference
Wave elevation (m)	-1,73	0,00	1,53	0,47	-1,02	-0,02
Surge (m)	0,03	0,16	0,31	0,06	-45,48	-0,38
Sway (m)	0,00	0,00	0,00	0,00	-1,00	-1,00
Heave (m)	-0,06	0,12	0,32	0,06	-0,38	0,34
Roll (deg)	0,00	0,00	0,00	0,00	-1,00	-1,00
Pitch (deg)	-0,30	0,00	0,27	0,10	-0,94	0,48
Yaw (deg)	0,00	0,00	0,00	0,00	-1,00	-1,00
Mid cut Fx (N)	3,78E+06	4,27E+06	4,71E+06	1,46E+05	-4,96E-01	1,75E-01
Mid cut Fy (N)	-1,72E+01	1,13E-02	2,07E+01	4,02E+00	-1,00E+00	-1,00E+00
Mid cut Fz (N)	-1,34E+07	-1,06E+07	-7,97E+06	6,55E+05	-4,51E-02	-8,89E-02
Mid cut Mx (Nm)	3,09E+03	3,75E+03	4,43E+03	2,09E+02	-4,86E-01	-1,00E+00
Mid cut My (Nm)	-9,01E+08	-7,89E+08	-6,68E+08	3,40E+07	-3,37E-02	-9,31E-02
Mid cut Mz (Nm)	-7,51E+02	1,33E+01	7,88E+02	2,20E+02	-9,98E-01	-1,00E+00

A.1.4 Condition 4

The experimental tests compared against are:

- `Ser004-Test015-Run001`
- `Ser004-Test016-Run002`
- `Ser004-Test017-Run001`

Table A.10: Properties for S004Cond4

Sea state	S004
Speed (Kts)	18
Wave direction (deg)	150
Significant wave height (m)	1,88
Wave period (s)	7,56

Table A.11: Statistical data of the experiment for S004Cond4

S004Cond1	Min	Mean	Max	Standard deviation
Wave elevation (m)	-2,19	0,00	1,46	0,48
Surge (m)	-0,22	-0,01	0,20	0,09
Sway (m)	-0,33	0,06	0,43	0,14
Heave (m)	0,05	0,22	0,42	0,06
Roll (deg)	-0,38	0,20	1,02	0,22
Pitch (deg)	-0,32	0,04	0,42	0,11
Yaw (deg)	-0,02	-0,02	0,53	0,20
Mid cut Fx (N)	8,01E+06	8,45E+06	8,99E+06	1,69E+05
Mid cut Fy (N)	-3,58E+06	-2,39E+06	-1,13E+06	3,79E+05
Mid cut Fz (N)	-1,32E+07	-1,11E+07	-8,65E+06	7,40E+05
Mid cut Mx (Nm)	-1,27E+07	-7,15E+05	1,07E+07	3,18E+06
Mid cut My (Nm)	-9,59E+08	-8,17E+08	-6,81E+08	5,05E+07
Mid cut Mz (Nm)	-1,27E+07	-7,15E+05	1,07E+07	3,18E+06

Table A.12: Statistical data of the simulation for S004Cond4

S004Cond4	Min	Mean	Max	Standard deviation	Mean difference	Std. deviation difference
Wave elevation (m)	-1,62	0,00	1,48	0,47	-1,57	-0,01
Surge (m)	0,20	0,28	0,35	0,03	-31,83	-0,67
Sway (m)	-0,11	0,00	0,09	0,03	-1,06	-0,78
Heave (m)	-0,13	0,12	0,38	0,09	-0,43	0,37
Roll (deg)	-0,76	0,00	0,75	0,25	-1,00	0,10
Pitch (deg)	-0,42	0,00	0,34	0,14	-0,96	0,35
Yaw (deg)	0,00	0,00	0,02	0,00	-1,04	-0,98
Mid cut Fx (N)	3,57E+06	4,27E+06	4,83E+06	1,86E+05	-4,95E-01	1,06E-01
Mid cut Fy (N)	-1,00E+06	1,51E+03	9,10E+05	3,31E+05	-1,00E+00	-1,27E-01
Mid cut Fz (N)	-1,29E+07	-1,06E+07	-8,40E+06	6,18E+05	-4,54E-02	-1,65E-01
Mid cut Mx (Nm)	-9,66E+06	1,61E+04	1,18E+07	3,06E+06	-1,02E+00	-3,93E-02
Mid cut My (Nm)	-9,17E+08	-7,89E+08	-6,51E+08	4,03E+07	-3,36E-02	-2,01E-01
Mid cut Mz (Nm)	-4,30E+07	2,25E+04	4,57E+07	1,40E+07	-1,03E+00	3,39E+00

A.1.5 Condition 5

The experimental tests compared against are:

- `Ser004-Test015-Run024`
- `Ser004-Test016-Run025`

Table A.13: Properties for S004Cond5

Sea state	S004
Speed (Kts)	21
Wave direction (deg)	180
Significant wave height (m)	1,88
Wave period (s)	7,56

Table A.14: Statistical data of the experiment for S004Cond5

S004Cond5	Min	Mean	Max	Standard deviation
Wave elevation (m)	-1,42	0,02	1,10	0,47
Surge (m)	-0,19	-0,07	0,02	0,06
Sway (m)	-0,18	0,01	0,15	0,09
Heave (m)	0,16	0,27	0,36	0,04
Roll (deg)	-0,26	0,01	0,22	0,10
Pitch (deg)	-0,11	0,05	0,20	0,06
Fore cut Mz (Nm)	-9,10E+04	-6,19E+04	-2,91E+04	9,49E+03
Mid cut Fx (N)	8,37E+06	8,69E+06	9,03E+06	1,28E+05
Mid cut Fy (N)	-2,65E+06	-2,40E+06	-2,20E+06	8,25E+04
Mid cut Fz (N)	-1,27E+07	-1,07E+07	-8,71E+06	7,97E+05
Mid cut Mx (Nm)	-2,34E+06	1,77E+04	1,75E+06	7,17E+05
Mid cut My (Nm)	-9,23E+08	-8,01E+08	-6,89E+08	4,05E+07

Table A.15: Statistical data of the simulation for S004Cond5

S004Cond5	Min	Mean	Max	Standard deviation	Mean difference	Std. deviation difference
Wave elevation (m)	-1,41	0,00	1,64	0,43	-0,95	-0,07
Surge (m)	-0,13	-0,10	-0,06	0,02	0,38	-0,74
Sway (m)	0,00	0,00	0,00	0,00	-1,00	-1,00
Heave (m)	-0,01	0,12	0,26	0,06	-0,53	0,32
Roll (deg)	0,00	0,00	0,00	0,00	-1,00	-1,00
Pitch (deg)	-0,19	0,00	0,19	0,09	-0,97	0,47
Fore cut Mz (Nm)	-1,21E+00	-7,83E-03	1,08E+00	3,68E-01	-1,00E+00	-1,00E+00
Mid cut Fx (N)	3,81E+06	4,27E+06	4,68E+06	1,47E+05	-5,09E-01	1,49E-01
Mid cut Fy (N)	-1,23E+01	4,64E-03	1,33E+01	4,10E+00	-1,00E+00	-1,00E+00
Mid cut Fz (N)	-1,32E+07	-1,06E+07	-8,02E+06	6,78E+05	-1,69E-02	-1,49E-01
Mid cut Mx (Nm)	-4,30E+03	3,75E+03	-3,09E+03	2,01E+02	-7,88E-01	-1,00E+00
Mid cut My (Nm)	-8,92E+08	-7,89E+08	-6,79E+08	3,61E+07	-1,43E-02	-1,08E-01

A.1.6 Condition 6

The experimental tests compared against are:

- `Ser004-Test026-Run001`
- `Ser004-Test027-Run001`
- `Ser004-Test028-Run001`

Table A.16: Properties for S004Cond6

Sea state	S004
Speed (Kts)	21
Wave direction (deg)	150
Significant wave height (m)	1,88
Wave period (s)	7,56

Table A.17: Statistical data of the experiment for S004Cond6

S004Cond6	Min	Mean	Max	Standard deviation
Wave elevation (m)	-2,19	0,00	1,46	0,48
Surge (m)	-0,22	-0,01	0,20	0,09
Sway (m)	-0,33	0,06	0,43	0,14
Heave (m)	0,05	0,22	0,42	0,06
Roll (deg)	-0,38	0,20	1,02	0,22
Pitch (deg)	-0,32	0,04	0,42	0,11
Fore cut Mz (Nm)	-2,20E+05	-8,32E+04	3,14E+04	3,01E+04
Mid cut Fx (N)	8,01E+06	8,45E+06	8,99E+06	1,69E+05
Mid cut Fy (N)	-3,58E+06	-2,39E+06	-1,13E+06	3,79E+05
Mid cut Fz (N)	-1,32E+07	-1,11E+07	-8,65E+06	7,40E+05
Mid cut Mx (Nm)	-1,27E+07	-7,15E+05	1,07E+07	3,18E+06
Mid cut My (Nm)	-9,59E+08	-8,17E+08	-6,81E+08	5,05E+07

Table A.18: Statistical data of the simulation for S004Cond6

S004Cond6	Min	Mean	Max	Standard deviation	Mean difference	Std. deviation difference
Wave elevation (m)	-1,62	0,00	1,48	0,47	-1,57	-0,01
Surge (m)	0,20	0,28	0,35	0,03	-31,83	-0,67
Sway (m)	-0,11	0,00	0,09	0,03	-1,06	-0,78
Heave (m)	-0,13	0,12	0,38	0,09	-0,43	0,37
Roll (deg)	-0,76	0,00	0,75	0,25	-1,00	0,10
Pitch (deg)	-0,42	0,00	0,34	0,14	-0,96	0,35
Fore cut Mz (Nm)	-3,53E+01	6,59E-02	4,27E+01	1,23E+01	-1,00E+00	-1,00E+00
Mid cut Fx (N)	3,57E+06	4,27E+06	4,83E+06	1,86E+05	-4,95E-01	1,06E-01
Mid cut Fy (N)	-1,00E+06	1,51E+03	9,10E+05	3,31E+05	-1,00E+00	-1,27E-01
Mid cut Fz (N)	-1,29E+07	-1,06E+07	-8,40E+06	6,18E+05	-4,54E-02	-1,65E-01
Mid cut Mx (Nm)	-9,66E+06	1,61E+04	1,18E+07	3,06E+06	-1,02E+00	-3,93E-02
Mid cut My (Nm)	-9,17E+08	-7,89E+08	-6,51E+08	4,03E+07	-3,36E-02	-2,01E-01

A.2 S005
A.2.1 Condition 7

The experimental tests compared against are:

- Ser005-Test001-Run001
- Ser005-Test002-Run001
- Ser005-Test007-Run001

Table A.19: Properties for S005Cond7

Sea state	S005
Speed (Kts)	18
Wave direction (deg)	180
Significant wave height (m)	1,88
Wave period (s)	4

Table A.20: Statistical data of the experiment for S005Cond7

S005Cond7	Min	Mean	Max	Standard deviation
Wave elevation (m)	-1,9099	0,063881	1,410456	0,37
Surge (m)	-0,24959	-0,00838	0,102388	0,05
Sway (m)	-0,13875	0,000631	0,190165	0,06
Heave (m)	0,209872	0,243279	0,26789	0,01
Roll (deg)	-0,115	0,040087	0,24	0,08
Pitch (deg)	0	0,03612	0,065	0,01
Yaw (deg)	0,003494	0,003494	0,22	0,13
Mid cut Fx (N)	8,31E+06	8,50E+06	8,66E+06	5,07E+04
Mid cut Fy (N)	-2,58E+06	-2,44E+06	-2,33E+06	3,95E+04
Mid cut Fz (N)	-1,14E+07	-1,11E+07	-1,08E+07	1,03E+05
Mid cut Mx (Nm)	-1,65E+06	-1,39E+05	1,25E+06	4,21E+05
Mid cut My (Nm)	-8,56E+08	-8,18E+08	-7,76E+08	1,15E+07
Mid cut Mz (Nm)	-1,65E+06	-1,39E+05	1,25E+06	4,21E+05

Table A.21: Statistical data of the simulation for S005Cond7

S005Cond7	Min	Mean	Max	Standard deviation	Mean difference	Std. deviation difference
Wave elevation (m)	-1,48	0,00	1,65	0,46	-0,99	0,27
Surge (m)	1,10	3,11	5,33	1,26	-372,45	23,07
Sway (m)	-0,11	0,03	0,16	0,06	39,52	0,08
Heave (m)	0,21	0,22	0,24	0,01	-0,08	-0,27
Roll (deg)	-0,21	0,01	0,31	0,09	-0,76	0,17
Pitch (deg)	-0,04	0,00	0,03	0,01	-1,09	0,04
Yaw (deg)	-0,01	-0,01	0,02	0,01	-4,18	-0,91
Mid cut Fx (N)	4,06E+06	4,26E+06	4,47E+06	6,34E+04	-0,50	0,25
Mid cut Fy (N)	-4,00E+05	-2,72E+03	5,73E+05	1,54E+05	-1,00	2,88
Mid cut Fz (N)	-1,12E+07	-1,05E+07	-9,79E+06	1,94E+05	-0,05	0,88
Mid cut Mx (Nm)	-5,20E+06	-3,39E+04	5,69E+06	1,43E+06	-0,76	2,39
Mid cut My (Nm)	-8,25E+08	-7,89E+08	-7,49E+08	1,06E+07	-0,04	-0,08
Mid cut Mz (Nm)	-2,41E+07	-5,45E+04	2,58E+07	7,98E+06	-0,61	17,96

A.3 S006

A.3.1 Condition 8

The experimental tests compared against are:

- Ser006-Test002-Run001
- Ser006-Test009-Run001
- Ser006-Test010-Run001

Table A.22: Properties for S006Cond8

Sea state	S006
Speed (Kts)	18
Wave direction (deg)	150
Significant wave height (m)	3,25
Wave period (s)	9,24

Table A.23: Statistical data of the experiment for S006Cond8

S006Cond8	Min	Mean	Max	Standard deviation
Wave elevation (m)	-3,24359	0,072949	2,277077	0,77
Surge (m)	-0,749	-0,0009	0,370811	0,22
Sway (m)	-0,44142	-0,01185	0,390555	0,13
Heave (m)	-0,26842	0,250548	0,703848	0,17
Roll (deg)	-0,87	0,03425	0,945	0,30
Pitch (deg)	-0,83	0,052067	0,985	0,30
Yaw (deg)	0,013258	0,013258	0,52	0,16
Mid cut Fx (N)	7,53E+06	8,61E+06	1,03E+07	4,20E+05
Mid cut Fy (N)	-3,09E+06	-2,43E+06	-1,63E+06	2,35E+05
Mid cut Fz (N)	-1,50E+07	-1,11E+07	-6,79E+06	1,53E+06
Mid cut Mx (Nm)	-4,56E+06	-8,21E+04	4,83E+06	1,57E+06
Mid cut My (Nm)	-1,18E+09	-8,12E+08	-4,41E+08	1,21E+08
Mid cut Mz (Nm)	-4,56E+06	-8,21E+04	4,83E+06	1,57E+06

Table A.24: Statistical data of the simulation for S006Cond8

S006Cond8	Min	Mean	Max	Standard deviation	Mean difference	Std. deviation difference
Wave elevation (m)	-2,84	0,00	3,02	0,82	-0,97	0,06
Surge (m)	-0,04	0,28	0,63	0,12	-311,12	-0,45
Sway (m)	0,00	0,00	0,00	0,00	-1,00	-1,00
Heave (m)	-0,67	0,12	0,96	0,29	-0,51	0,69
Roll (deg)	0,00	0,00	0,00	0,00	-1,00	-1,00
Pitch (deg)	-1,41	0,00	1,36	0,49	-0,94	0,63
Yaw (deg)	0,00	0,00	0,00	0,00	-1,00	-1,00
Mid cut Fx (N)	2,88E+06	4,27E+06	5,71E+06	4,86E+05	-0,50	0,16
Mid cut Fy (N)	-2,85E+01	-2,88E-02	3,54E+01	8,59E+00	-1,00	-1,00
Mid cut Fz (N)	-1,58E+07	-1,06E+07	-6,39E+06	1,30E+06	-0,05	-0,15
Mid cut Mx (Nm)	-1,29E+03	-3,75E+03	6,31E+03	8,18E+02	-0,95	-1,00
Mid cut My (Nm)	-1,12E+09	-7,90E+08	-5,00E+08	9,96E+07	-0,03	-0,17
Mid cut Mz (Nm)	-1,90E+03	-1,15E+00	2,39E+03	6,10E+02	-1,00	-1,00

A.3.2 Condition 9

The experimental tests compared against are:

- Ser006-Test016-Run001
- Ser006-Test020-Run001
- Ser006-Test020-Run001

Table A.25: Properties for S006Cond9

Sea state	S006
Speed (Kts)	18
Wave direction (deg)	150
Significant wave height (m)	3,25
Wave period (s)	9,24

Table A.26: Statistical data of the experiment for S006Cond9

S006Cond9	Min	Mean	Max	Standard deviation
Wave elevation (m)	-2,49997	0,056267	1,936718	0,73
Surge (m)	-0,72395	0,165184	0,884315	0,36
Sway (m)	-0,92923	0,025314	1,367124	0,50
Heave (m)	-0,32311	0,245451	0,779939	0,20
Roll (deg)	-1,395	0,27333	1,585	0,49
Pitch (deg)	-1,015	0,059751	1,19	0,39
Yaw (deg)	-0,02539	-0,02539	1,25	0,48
Mid cut Fx (N)	7,60E+06	8,64E+06	9,97E+06	4,20E+05
Mid cut Fy (N)	-3,87E+06	-2,37E+06	-3,37E+05	6,32E+05
Mid cut Fz (N)	-1,42E+07	-1,11E+07	-7,64E+06	1,16E+06
Mid cut Mx (Nm)	-1,72E+07	-1,00E+06	1,37E+07	5,21E+06
Mid cut My (Nm)	-1,13E+09	-8,11E+08	-4,88E+08	1,16E+08
Mid cut Mz (Nm)	-1,72E+07	-1,00E+06	1,37E+07	5,21E+06

Table A.27: Statistical data of the simulation for S006Cond9

S006Cond9	Min	Mean	Max	Standard deviation	Mean difference	Std. deviation difference
Wave elevation (m)	-3,17	0,00	2,29	0,81	-0,97	0,11
Surge (m)	-0,15	0,26	0,77	0,17	0,60	-0,52
Sway (m)	-2,46	-0,05	1,79	1,06	-2,81	1,10
Heave (m)	-0,78	0,12	0,97	0,34	-0,50	0,72
Roll (deg)	-3,32	0,01	3,19	1,21	-0,96	1,47
Pitch (deg)	-1,39	0,00	1,38	0,56	-0,93	0,43
Yaw (deg)	0,01	0,01	0,56	0,23	-1,24	-0,52
Mid cut Fx (N)	2,55E+06	4,27E+06	5,73E+06	5,30E+05	-0,51	0,26
Mid cut Fy (N)	-1,91E+06	-2,52E+03	1,91E+06	6,77E+05	-1,00	0,07
Mid cut Fz (N)	-1,51E+07	-1,06E+07	-5,50E+06	1,09E+06	-0,04	-0,07
Mid cut Mx (Nm)	-2,51E+07	-4,66E+04	2,25E+07	8,09E+06	-0,95	0,55
Mid cut My (Nm)	-1,14E+09	-7,89E+08	-4,96E+08	1,00E+08	-0,03	-0,14
Mid cut Mz (Nm)	-8,64E+07	-3,87E+04	7,76E+07	3,01E+07	-0,96	4,79

A.3.3 Condition 10

The experimental tests compared against are:

- Ser006-Test006-Run001
- Ser006-Test007-Run001
- Ser006-Test020-Run001

Table A.28: Properties for S006Cond10

Sea state	S006
Speed (Kts)	15
Wave direction (deg)	180
Significant wave height (m)	3,25
Wave period (s)	9,24

Table A.29: Statistical data of the experiment for S006Cond10

S006Cond10	Min	Mean	Max	Standard deviation
Wave elevation (m)	-3,73193	0,057716	2,115221	0,75
Surge (m)	-0,47209	0,10784	0,497125	0,16
Sway (m)	-0,34889	-0,00823	0,357029	0,12
Heave (m)	-0,25853	0,201113	0,632527	0,16
Roll (deg)	-1,275	0,065571	1,445	0,46
Pitch (deg)	-0,73	0,049966	0,79	0,28
Yaw (deg)	0,003194	0,003194	0,265	0,12
Mid cut Fx (N)	7,49E+06	8,43E+06	9,61E+06	3,60E+05
Mid cut Fy (N)	-3,06E+06	-2,44E+06	-1,64E+06	2,52E+05
Mid cut Fz (N)	-1,48E+07	-1,12E+07	-7,06E+06	1,41E+06
Mid cut Mx (Nm)	-7,02E+06	-1,41E+05	7,86E+06	2,06E+06
Mid cut My (Nm)	-1,14E+09	-8,26E+08	-5,08E+08	1,09E+08
Mid cut Mz (Nm)	-7,02E+06	-1,41E+05	7,86E+06	2,06E+06

Table A.30: Statistical data of the simulation for S006Cond10

S006Cond10	Min	Mean	Max	Standard deviation	Mean difference	Std. deviation difference
Wave elevation (m)	-2,58	0,00	2,69	0,83	-0,97	0,10
Surge (m)	-0,04	0,28	0,65	0,13	1,58	-0,21
Sway (m)	0,00	0,00	0,00	0,00	-1,00	-1,00
Heave (m)	-0,57	0,12	0,82	0,26	-0,39	0,67
Roll (deg)	0,00	0,00	0,00	0,00	-1,00	-1,00
Pitch (deg)	-1,22	0,00	1,27	0,48	-0,96	0,70
Yaw (deg)	0,00	0,00	0,00	0,00	-1,00	-1,00
Mid cut Fx (N)	2,93E+06	4,27E+06	5,48E+06	4,56E+05	-0,49	0,27
Mid cut Fy (N)	-2,41E+01	3,86E-02	3,29E+01	9,08E+00	-1,00	-1,00
Mid cut Fz (N)	-1,53E+07	-1,06E+07	-5,77E+06	1,29E+06	-0,06	-0,09
Mid cut Mx (Nm)	-1,86E+03	-3,75E+03	5,74E+03	7,51E+02	-0,97	-1,00
Mid cut My (Nm)	-5,02E+08	-7,90E+08	-1,11E+09	1,02E+08	-0,04	-0,07
Mid cut Mz (Nm)	-1,91E+03	9,26E+00	2,06E+03	6,56E+02	-1,00	-1,00

A.3.4 Condition 11

The experimental tests compared against are:

- Ser006-Test003-Run002
- Ser005-Test004-Run002
- Ser005-Test005-Run001

Table A.31: Properties for S006Cond11

Sea state	S006
Speed (Kts)	15
Wave direction (deg)	150
Significant wave height (m)	3,25
Wave period (s)	9,24

Table A.32: Statistical data of the experiment for S006Cond11

S006Cond11	Min	Mean	Max	Standard deviation
Wave elevation (m)	-2,4787	0,039449	2,274302	0,79
Surge (m)	-1,09664	0,029133	0,725007	0,43
Sway (m)	-0,79264	0,073059	1,223466	0,46
Heave (m)	-0,4786	0,180948	0,822205	0,21
Roll (deg)	-1,39	0,289697	1,725	0,56
Pitch (deg)	-1,28	0,061485	1,42	0,45
Yaw (deg)	0,002305	0,002305	0,98	0,44
Mid cut Fx (N)	7,38E+06	8,43E+06	1,02E+07	4,50E+05
Mid cut Fy (N)	-4,63E+06	-2,41E+06	7,07E+03	7,33E+05
Mid cut Fz (N)	-1,50E+07	-1,13E+07	-7,12E+06	1,29E+06
Mid cut Mx (Nm)	-1,84E+07	-1,02E+06	1,59E+07	5,80E+06
Mid cut My (Nm)	-1,19E+09	-8,27E+08	-4,21E+08	1,36E+08
Mid cut Mz (Nm)	-1,84E+07	-1,02E+06	1,59E+07	5,80E+06

Table A.33: Statistical data of the simulation for S006Cond11

S006Cond11	Min	Mean	Max	Standard deviation	Mean difference	Std. deviation difference
Wave elevation (m)	-2,59	0,00	2,33	0,82	-0,95	0,04
Surge (m)	-0,05	0,27	0,65	0,13	8,40	-0,69
Sway (m)	-2,78	-0,20	1,63	1,06	-3,77	1,32
Heave (m)	-0,85	0,12	0,92	0,31	-0,32	0,49
Roll (deg)	-3,67	-0,02	3,30	1,36	-1,06	1,45
Pitch (deg)	-1,53	0,00	1,44	0,55	-0,99	0,23
Yaw (deg)	0,00	0,00	0,42	0,25	-1,25	-0,42
Mid cut Fx (N)	2,50E+06	4,27E+06	5,71E+06	5,04E+05	-0,49	0,12
Mid cut Fy (N)	-1,78E+06	-1,83E+02	1,78E+06	6,52E+05	-1,00	-0,11
Mid cut Fz (N)	-1,43E+07	-1,06E+07	-6,42E+06	1,08E+06	-0,06	-0,16
Mid cut Mx (Nm)	-2,40E+07	3,48E+04	2,22E+07	8,07E+06	-1,03	0,39
Mid cut My (Nm)	-1,15E+09	-7,89E+08	-4,85E+08	1,02E+08	-0,05	-0,25
Mid cut Mz (Nm)	-7,60E+07	1,75E+05	7,88E+07	2,80E+07	-1,17	3,83

A.4 S007

A.4.1 Condition 12

The experimental tests compared against are:

- Ser007-Test002-Run001
- Ser007-Test003-Run001
- Ser007-Test004-Run001

Table A.34: Properties for S007Cond12

Sea state	S007
Speed (Kts)	18
Wave direction (deg)	180
Significant wave height (m)	3,25
Wave period (s)	5

Table A.35: Statistical data of the experiment for S007Cond12

S007Cond12	Min	Mean	Max	Standard deviation
Wave elevation (m)	-2,29742	0,080143	2,513848	0,61
Surge (m)	-0,4014	-0,02541	0,237543	0,14
Sway (m)	-0,32136	-0,04231	0,280658	0,14
Heave (m)	0,164576	0,255713	0,332554	0,03
Roll (deg)	-0,475	0,075896	0,55	0,22
Pitch (deg)	-0,05	0,039297	0,125	0,03
Yaw (deg)	0,031508	0,031508	0,325	0,14
Mid cut Fx (N)	8,19E+06	8,52E+06	8,86E+06	8,88E+04
Mid cut Fy (N)	-2,89E+06	-2,42E+06	-2,06E+06	1,32E+05
Mid cut Fz (N)	-1,25E+07	-1,11E+07	-9,73E+06	3,54E+05
Mid cut Mx (Nm)	-3,91E+06	-1,74E+05	3,85E+06	1,40E+06
Mid cut My (Nm)	-8,87E+08	-8,16E+08	-7,46E+08	2,26E+07
Mid cut Mz (Nm)	-3,91E+06	-1,74E+05	3,85E+06	1,40E+06

Table A.36: Statistical data of the simulation for S007Cond12

S007Cond12	Min	Mean	Max	Standard deviation	Mean difference	Std. deviation difference
Wave elevation (m)	-2,54	0,00	3,03	0,74	-1,00	0,21
Surge (m)	0,42	1,15	1,59	0,36	-46,35	1,48
Sway (m)	-0,58	0,11	0,59	0,25	-3,58	0,78
Heave (m)	0,12	0,23	0,35	0,03	-0,11	0,32
Roll (deg)	-1,25	-0,02	1,06	0,41	-1,22	0,90
Pitch (deg)	-0,12	0,01	0,14	0,04	-0,77	0,36
Yaw (deg)	0,00	0,00	0,10	0,04	-1,01	-0,70
Mid cut Fx (N)	3,87E+06	4,25E+06	4,74E+06	1,16E+05	-0,50	0,30
Mid cut Fy (N)	-1,22E+06	-1,73E+03	1,33E+06	3,80E+05	-1,00	1,87
Mid cut Fz (N)	-1,24E+07	-1,05E+07	-8,52E+06	4,81E+05	-0,05	0,36
Mid cut Mx (Nm)	-1,13E+07	-6,34E+03	1,11E+07	3,45E+06	-0,96	1,47
Mid cut My (Nm)	-8,68E+08	-7,87E+08	-7,09E+08	2,33E+07	-0,04	0,03
Mid cut Mz (Nm)	-4,15E+07	1,41E+05	4,69E+07	1,43E+07	-1,81	9,21

A.5 S008

A.5.1 Condition 13

The experimental tests compared against are:

- Ser008-Test001-Run001
- Ser008-Test001-Run002
- Ser008-Test002-Run001

Table A.37: Properties for S008Cond13

Sea state	S008
Speed (Kts)	12
Wave direction (deg)	180
Significant wave height (m)	10,78
Wave period (s)	5

Table A.38: Statistical data of the experiment for S008Cond13

S008Cond13	Min	Mean	Max	Standard deviation
Wave elevation (m)	-4,886188587	-0,000440005	4,623520111	1,05
Surge (m)	-3,527043941	-0,072384064	1,350497768	0,65
Sway (m)	-0,504131399	0,000428228	0,699478278	0,17
Heave (m)	-1,105700269	0,078216529	0,968433559	0,28
Roll (deg)	-2,83	0,061005833	2,44	0,91
Pitch (deg)	-3,32	0,056951477	3,18	0,75
Yaw (deg)	-0,001393956	-0,001393956	0,695	0,18
Mid cut Fx (N)	6,07E+06	8,40E+06	1,31E+07	5,82E+05
Mid cut Fy (N)	-4,57E+06	-2,46E+06	-6,01E+05	4,19E+05
Mid cut Fz (N)	-1,76E+07	-1,14E+07	-2,56E+06	1,79E+06
Mid cut Mx (Nm)	-8,71E+06	-1,38E+05	1,03E+07	3,41E+06
Mid cut My (Nm)	-1,51E+09	-8,33E+08	7,55E+07	1,91E+08
Mid cut Mz (Nm)	-8,71E+06	-1,38E+05	1,03E+07	3,41E+06

Table A.39: Statistical data of the simulation for S008Cond13

S008Cond13	Min	Mean	Max	Standard deviation	Mean difference	Std. deviation difference
Wave elevation (m)	-3,78	0,00	3,56	1,25	6,60	0,19
Surge (m)	-0,87	0,29	1,37	0,38	-5,04	-0,41
Sway (m)	0,00	0,00	0,00	0,00	-1,00	-1,00
Heave (m)	-1,50	0,12	1,66	0,52	0,59	0,82
Roll (deg)	0,00	0,00	0,00	0,00	-1,00	-1,00
Pitch (deg)	-3,03	0,00	3,17	0,97	-1,00	0,30
Yaw (deg)	0,00	0,00	0,00	0,00	-1,00	-1,00
Mid cut Fx (N)	1,9E+06	4,3E+06	6,8E+06	7,48E+05	-0,49	0,28
Mid cut Fy (N)	-8,0E+01	-1,2E-01	8,2E+01	2,72E+01	-1,00	-1,00
Mid cut Fz (N)	-1,7E+07	-1,1E+07	-3,6E+06	1,83E+06	-0,07	0,02
Mid cut Mx (Nm)	-7,6E+02	3,7E+03	7,9E+03	1,32E+03	-1,03	-1,00
Mid cut My (Nm)	-1,4E+09	-7,9E+08	-2,1E+08	1,79E+08	-0,05	-0,07
Mid cut Mz (Nm)	-6,4E+03	-2,1E+00	5,9E+03	2,20E+03	-1,00	-1,00

A.5.2 Condition 14

The experimental tests compared against are:

- Ser008-Test003-Run001
- Ser008-Test004-Run001
- Ser008-Test005-Run001

Table A.40: Properties for S008Cond14

Sea state	S008
Speed (Kts)	12
Wave direction (deg)	150
Significant wave height (m)	10,78
Wave period (s)	5

Table A.41: Statistical data of the experiment for S008Cond14

S008Cond14	Min	Mean	Max	Standard deviation
Wave elevation (m)	-4,637393	-0,02781	3,494231	1,05
Surge (m)	-1,788602	0,112856	1,362791	0,63
Sway (m)	-1,146859	0,038615	1,712174	0,59
Heave (m)	-1,257244	0,06205	1,258971	0,40
Roll (deg)	-4,5	0,244239	3,555	1,47
Pitch (deg)	-3,18	0,062342	3,165	0,91
Yaw (deg)	-0,020823	-0,02082	2,055	0,58
Mid cut Fx (N)	6,44E+06	8,39E+06	1,15E+07	5,60E+05
Mid cut Fy (N)	-6,94E+06	-2,44E+06	1,08E+05	9,58E+05
Mid cut Fz (N)	-1,54E+07	-1,14E+07	-5,46E+06	1,31E+06
Mid cut Mx (Nm)	-2,63E+07	-1,19E+06	2,64E+07	7,79E+06
Mid cut My (Nm)	-1,45E+09	-8,31E+08	1,26E+07	1,81E+08
Mid cut Mz (Nm)	-2,63E+07	-1,19E+06	2,64E+07	7,79E+06

Table A.42: Statistical data of the simulation for S008Cond14

S008Cond14	Min	Mean	Max	Standard deviation	Mean difference	Std. deviation difference
Wave elevation (m)	-3,23	0,01	3,15	1,25	-1,19	0,19
Surge (m)	-0,50	0,29	1,05	0,34	1,56	-0,46
Sway (m)	-2,17	-0,04	1,77	0,65	-2,02	0,10
Heave (m)	-1,13	0,12	1,35	0,60	0,93	0,52
Roll (deg)	-2,96	0,00	2,91	1,28	-1,00	-0,13
Pitch (deg)	-2,00	0,01	2,02	1,15	-0,86	0,27
Yaw (deg)	0,03	0,03	0,77	0,26	-2,56	-0,55
Mid cut Fx (N)	2,6E+06	4,3E+06	5,9E+06	8,04E+05	-0,49	0,43
Mid cut Fy (N)	-1,8E+06	-2,1E+03	1,8E+06	8,04E+05	-1,00	-0,16
Mid cut Fz (N)	-1,4E+07	-1,1E+07	-6,7E+06	1,61E+06	-0,07	0,23
Mid cut Mx (Nm)	-1,8E+07	8,2E+03	1,7E+07	8,15E+06	-1,01	0,05
Mid cut My (Nm)	-1,2E+09	-7,9E+08	-4,2E+08	1,76E+08	-0,05	-0,03
Mid cut Mz (Nm)	-7,3E+07	-1,3E+05	6,9E+07	3,10E+07	-0,89	2,98

A.5.3 Condition 15

The experimental tests compared against are:

- Ser008-Test006-Run001
- Ser008-Test007-Run001

Table A.43: Properties for S008Cond15

Sea state	S008
Speed (Kts)	15
Wave direction (deg)	180
Significant wave height (m)	10,78
Wave period (s)	5

Table A.44: Statistical data of the experiment for S008Cond15

S008Cond15	Min	Mean	Max	Standard deviation
Wave elevation (m)	-3,053983478	-0,006511853	2,890278125	0,99
Surge (m)	-1,86897387	0,032752299	0,918541805	0,53
Sway (m)	-0,418435856	-0,008232846	0,34170971	0,11
Heave (m)	-0,716216622	0,116539405	0,842315376	0,30
Roll (deg)	-1,18	0,043712257	1,515	0,40
Pitch (deg)	-2,09	0,054220189	2,055	0,67
Yaw (deg)	0,006242963	0,006242963	0,355	0,15
Mid cut Fx (N)	7,16E+06	8,52E+06	1,03E+07	5,70E+05
Mid cut Fy (N)	-3,29E+06	-2,44E+06	-1,50E+06	2,98E+05
Mid cut Fz (N)	-1,54E+07	-1,13E+07	-6,01E+06	1,59E+06
Mid cut Mx (Nm)	-6,09E+06	-7,43E+04	6,39E+06	1,83E+06
Mid cut My (Nm)	-1,25E+09	-8,23E+08	-2,94E+08	1,69E+08
Mid cut Mz (Nm)	-6,09E+06	-7,43E+04	6,39E+06	1,83E+06

Table A.45: Statistical data of the simulation for S008Cond15

S008Cond15	Min	Mean	Max	Standard deviation	Mean difference	Std. deviation difference
Wave elevation (m)	-3,85	0,00	3,98	1,25	-0,70	0,26
Surge (m)	-0,68	0,29	1,06	0,31	7,75	-0,41
Sway (m)	0,00	0,00	0,00	0,00	-1,00	-1,00
Heave (m)	-1,42	0,12	1,61	0,58	0,06	0,90
Roll (deg)	0,00	0,00	0,00	0,00	-1,00	-1,00
Pitch (deg)	-2,59	0,00	2,54	1,02	-0,99	0,52
Yaw (deg)	0,00	0,00	0,00	0,00	-1,00	-1,00
Mid cut Fx (N)	1,9E+06	4,3E+06	6,5E+06	8,32E+05	-0,50	0,46
Mid cut Fy (N)	-6,8E+01	1,8E-01	7,6E+01	2,27E+01	-1,00	-1,00
Mid cut Fz (N)	-1,7E+07	-1,1E+07	-3,7E+06	1,85E+06	-0,06	0,16
Mid cut Mx (Nm)	-3,7E+02	3,8E+03	7,9E+03	1,46E+03	-1,05	-1,00
Mid cut My (Nm)	-1,3E+09	-7,9E+08	-2,4E+08	1,80E+08	-0,04	0,06
Mid cut Mz (Nm)	-5,8E+03	8,5E+00	5,4E+03	1,89E+03	-1,00	-1,00

A.5.4 Condition 16

The experimental tests compared against are:

- Ser008-Test008-Run001
- Ser008-Test009-Run001
- Ser008-Test010-Run001

Table A.46: Properties for S008Cond16

Sea state	S008
Speed (Kts)	15
Wave direction (deg)	150
Significant wave height (m)	10,78
Wave period (s)	5

Table A.47: Statistical data of the simulation for S008Cond16

S006Cond16	Min	Mean	Max	Standard deviation
Wave elevation (m)	-4,33403	-0,02526	3,279656	1,07
Surge (m)	-1,896738	0,072105	1,361832	0,70
Sway (m)	-0,925173	0,027112	1,029323	0,49
Heave (m)	-1,22484	0,097213	1,421339	0,39
Roll (deg)	-2,975	0,26816	3,09	1,05
Pitch (deg)	-3,025	0,060519	3,16	0,93
Yaw (deg)	0,0136194	0,013619	1,355	0,50
Mid cut Fx (N)	6,65E+06	8,57E+06	1,21E+07	6,48E+05
Mid cut Fy (N)	-5,97E+06	-2,42E+06	6,47E+05	9,45E+05
Mid cut Fz (N)	-1,62E+07	-1,12E+07	-4,84E+06	1,41E+06
Mid cut Mx (Nm)	-2,59E+07	-1,21E+06	1,99E+07	7,14E+06
Mid cut My (Nm)	-1,35E+09	-8,18E+08	2,24E+07	1,92E+08
Mid cut Mz (Nm)	-2,59E+07	-1,21E+06	1,99E+07	7,14E+06

Table A.48: Statistical data of the simulation for S008Cond16

S006Cond16	Min	Mean	Max	Standard deviation	Mean difference	Std. deviation difference
Wave elevation (m)	-3,15	0,00	3,16	1,25	-1,19	0,17
Surge (m)	-1,14	0,25	1,58	0,48	2,47	-0,31
Sway (m)	-1,37	0,04	1,49	0,57	0,33	0,15
Heave (m)	-1,23	0,12	1,49	0,69	0,21	0,75
Roll (deg)	-3,24	0,00	3,19	1,42	-0,99	0,35
Pitch (deg)	-2,18	0,01	2,18	1,23	-0,85	0,33
Yaw (deg)	0,01	0,01	0,68	0,25	-0,15	-0,50
Mid cut Fx (N)	2,5E+06	4,3E+06	6,1E+06	9,03E+05	-0,50	0,39
Mid cut Fy (N)	-1,8E+06	-3,5E+02	1,8E+06	8,58E+05	-1,00	-0,09
Mid cut Fz (N)	-1,5E+07	-1,1E+07	-6,6E+06	1,65E+06	-0,06	0,17
Mid cut Mx (Nm)	-2,0E+07	3,7E+03	2,0E+07	9,60E+06	-1,00	0,35
Mid cut My (Nm)	-1,2E+09	-7,9E+08	-4,1E+08	1,79E+08	-0,03	-0,07
Mid cut Mz (Nm)	-6,8E+07	2,6E+04	6,9E+07	3,01E+07	-1,02	3,21